Universidade de Trás-os-Montes e Alto Douro (UTAD)

Efficient tools to simulate main crops in Portugal for decision support systems

PhD Thesis

Agricultural Production Chains - From Fork to Farm

Chenyao Yang

Supervisor: Professor Doctor João Carlos Andrade Santos

Co-supervisors: Professor Doctor Wim Van Ieperen

Doctor Helder Fraga

VILA REAL, 2019

Universidade de Trás-os-Montes e Alto Douro (UTAD)

Efficient tools to simulate main crops in Portugal for decision support systems

PhD Thesis

Agricultural Production Chains - From Fork to Farm

Chenyao Yang

Supervisor: Professor Doctor João Carlos Andrade Santos

Co-supervisors: Professor Doctor Wim Van Ieperen

Doctor Helder Fraga

Jury Members:

President**:**

Doutora Ana Maria Araújo de Beja Neves Nazaré Pereira (UTAD);

Vowels**:**

Doutor Alfredo Moreira Caseiro Rocha, Professor Associado com Agregação (UA);
Doutor Aureliano Natálio Coelho Malheiro, Professor Auxiliar (UTAD);
Doutor Hernâni Varanda Gerós, Professor Associado com Agregação (UMinho);
Doutor João Carlos Andrade dos Santos, Professor Auxiliar com Agregação (UTAD);
Doutor José Paulo de Melo e Abreu, Professor Associado com Agregação (ISA);
Doutor Marco Moriondo, Investigador do Italian National Research Counicil (CNR).

VILA REAL, 2019

Declaração

Esta Tese foi expressamente elaborada para cumprimentos dos requisitos necessários à candidatura ao grau de Doutor em Cadeias de Produção Agrícola - da mesa ao campo pela Universidade de Trás-os-Montes e Alto Douro.

Declaro para os devidos fins que a Tese de Doutoramento atende as normas técnicas e científicas exigidas pelos regulamentos em vigor da Universidade de Trás-os-Montes e Alto Douro. As doutrinas apresentadas no presente trabalho são da exclusiva e inteira responsabilidade do autor.

The PhD works are supported by European Investment Funds under FEDER/COMPETE/POCI – Operational Competitiveness and Internationalization Program (POCI-01-0145-FEDER-006958), and by National Funds of FCT – Portuguese Foundation for Science and Technology (UID/AGR/04033/2013). I also acknowledge the granted FCT fellowship (PD/BD/113617/2015) under the Doctoral Program "Agricultural Production Chains − from fork to farm" (PD/00122/2012).


It's a long road,
but it's worth it.

ACKNOWLEDGEMENTS

It felt as if a blink of eye in four years of time with intense training, working and living in a foreign country away from home. It is indeed a significant challenge for me to undertake the PhD works at beginning, as there are insufficient experience, limited resources and a big knowledge gap in this research topic. In particular, it is a brave decision to jump into this new field of research for me, who previously held a background of molecular biology in master degree. But when I looked back at the time of delivering my applications to this International PhD program four years ago, I still appreciate being given this opportunity to improve myself and empower my career as long aspiring to be a scientific researcher. At some point of time, it just occurred to me I really have passions for this topic, in particular for crop system modelling. Over these four years of PhD works, I feel fortunate for not being lonely in this path. I want to have my genuine thanks to many who have generously helped me in both life and works:

To my supervisor and tutor Professor João Carlos Andrade Santos, for his guidance of works, concerns in my personal life, for always being supportive, available and dedicated. His advices, transmitted knowledge, encouragement for explorations, all contribute to the success of the works;

To my co-supervisor Professor Wim Van Ieperen, for his valuable insights, guidance of works, and expert opinions in crop modelling, which all contribute to the success of works. Also, special thanks for his great assistance in arranging my wonderful stay in Wageningen University;

To my co-supervisor Helder Fraga, for being a friend in life, his detailed instructions in crop modelling, and for his experience and advices in designing research directions, which all contribute to the success of works. I also appreciate his many novel and inspiring ideas during the course;

To the secretaries of the doctoral program, Mrs. Lígia Pinto and Mrs. Lídia Nobrega, and Miss Ana Moura, who always respond to my requests quickly and efficiently arrange the logistic matters, as well as providing great assistance in dealing with the bureaucratic issues and procedures;

To Universidade de Trás-os-Montes e Alto Douro (UTAD) and Wageningen University (WUR);

To the Professor Amelia M. L. Dias da Silva, who kindly help me and my family´s settlement, and for her dedications in running this doctoral program in the beginning and ensure a smooth transition afterwards;

To the Professor Eduardo Rosa, for being the director of this doctoral program most of the time, who is very committed to monitoring our progress and organizing the program. I am inspired by his insistence on research quality and on importance of state-of-the-art literature reviewing;

To the Professor Henrique Trindade, for his useful inputs from an agronomic expert point of view;

To the STICS founders, forum and team members, for their technical assistance and shared advices;

To my friend Myriam Taghouti, who always act selflessly and give me and my family great support and help, for her toughness and positivity in life;

To my friend Ratnajit Mukherjee, for his essential support in computer programming that greatly facilitate my works. I am very grateful by his detailed guidance to the "New World";

To my team members and friends Andre Fonseca, Ricardo Costa and Mónica Santos, who share the same values and principles in research, having fun, respect and help each other;

To my colleagues and friends António Fernandes, Ana Abraão, André Lemos, Chenhe Zhang, Daniela Terêncio, Ermelinda Silva, Ivo Pavia, Iva Prgomet, Liren Shu, Lisa Martins, Luis Rocha, Miguel Oliveira, Nikola Grcic, Richard Gonçalves, Shweta Singh, Weina Hou for their companies;

Lastly, I want to express my most important and enormous gratitude to my beloved wife (Manyou Yu) and kid (Krystal Isabella Yu Yang), as well as beloved father (Junpin Yang) and mother (Jinyu Chen) for their infinite loves, tolerance, great support and cares, continuous encouragements. Language is pale to describe how much I love all of you. Without them, it would be impossible to accomplish the works and complete the PhD thesis.

ABSTRACT

Agricultural systems are inherently vulnerable to climate variability and climate change is expected to increase this vulnerability. Various studies warn the anthropogenic-driven global warming with elevated CO_2 concentration and altered regional precipitation pattern, are expected to negatively affect local crop productivity and thus exacerbate food insecurities in many regions worldwide, particularly for Mediterranean basin. Mediterranean basin is one of the most prominent climate change "hotspot" due to ongoing and projected changes in both climate means and variabilities, comprising a robust climate change signal of an overall warming and drying trend, accompanied by more frequent occurrence of severe drought and extreme high temperatures. Specifically, these projected changes are expected to be more pronounced in southern Europe, such as in Portugal, where annual mean temperature has increased at a rate more than double the global warming rate in the past decades, along with the observed decreases in precipitation and its enhanced inter-annual variability.

Therefore, it is urgently needed to carry out the assessment of climate change impacts on agricultural production and explore suitable adaptation strategies, whereas the related studies so far remain scarce in Portugal. We had chosen three important cropping systems for Portuguese agriculture, i.e. irrigated maize, rainfed wheat and perennial forage grassland, while representative study sites in their current principal growing regions were identified accordingly. The overall methodology follows combined use of climate and crop models, where the spatially-downscaled bias-corrected climate change projections from climate models were utilized to drive crop model simulations at study sites, which were prior calibrated using local observed weather, soil and management data. For employed process-based crop models, both STICS and AquaCrop were applied for the irrigated maize production, whereas the other two cropping systems were only analyzed using STICS model. It was noteworthy one major strength from current studies consisted in, on top of projected mean climate changes, we had consistently incorporated the effects of potential changes in climate variability and its associated extreme weather events into the simulated impacts (e.g. yield changes) for a more reliable assessment.

The results indicate threats and risks of future climate change are substantially high for agriculture production in Portugal. Because an overall negative climate change impact from the mid until the end of 21st century is obtained for all three important cropping systems, corresponding to moderate-to-severe yield losses with increased inter-annual variabilities. Yield losses are greater

in magnitude with higher year-to-year variability, in the second half of the century than in the first half, and in a high emission pathway than in a low emission scenario. The CO_2 fertilization effect is unlikely to compensate these yield reductions, where it brings more yield increment for C3 species (wheat and defined grass mixture) than for C4 (maize). Specifically, majority of negative impacts are derived from the shortened growth duration for irrigated maize under a warmer climate, and from intensified drought and heat stresses during a sensitive period (grain-filling) for rainfed wheat or during an unfavorable summer period for perennial grassland. These aspects correspond to the vulnerabilities of cropping systems facing climate change. It is interesting to note though higher temperature is clearly detrimental to irrigated maize production, it facilitates advanced phenology of perennial grass shifting towards the favorable cool and wet winter period for enhanced production or it may also help rainfed wheat crop to mature earlier to avoid excessive terminal stresses. Yet the magnitude of climate change impacts on agricultural productivity remains uncertain, varying with analyzed cropping systems, locations and management practices, applied climate models (including downscaling approaches) and crop models (including partial or full calibration), selected time periods and emission pathways.

Adaptation strategies provide potential to mitigate these negative impacts, and development of appropriate and risk-focused adaptation policy should address previously identified vulnerabilities and prioritize available options for an integrated and comprehensive strategy. For annual cereal crops, increased irrigation amount at various levels has been firstly tested for irrigated maize cropping system under climate change, taking into account crop water demand and projected seasonal rainfall distribution. Though increased irrigation is able to mitigate yield reductions and maintain current yield levels, crop WUE considerably declines as a result of diminished yield responsiveness to seasonal water input with shorter growth duration. In view of increasing risks of water scarcity and decreasing portion of fresh water available for agriculture in the Mediterranean basin, solely increased irrigation supply might not be a feasible strategy, whereas the adaptive response for maize should be prioritized to promote water-saving techniques and maximize WUE for stabilizing yields (marginal reductions allowed). Combining optimized irrigation strategy (e.g. deficit irrigation) and installed efficient facilities (e.g. drip irrigation system) with other adaptation options, including introducing longer cycle cultivars and advanced sowing dates to counterbalance the shortened growing duration, is recommend, but should be further rigorously examined.

For the rainfed wheat cropping system, adaptation priority should address the exacerbated risks of drought and heat stresses during the sensitive anthesis and grain-filling periods. The terminal stress escaping strategy is proposed by firstly testing early flowering cultivars (also known as short-cycle genotypes), where the trade-off between lower risk of exposure to terminal stress and higher risk of reduced yield potential tends to be positive, leading to net yield gains. Still, this option needs to be combined with other adaptation opportunities including early sowing date, wheat cultivars with less or no vernalization requirement (e.g. using spring wheat) and supplementary irrigation during the sensitive stage. Early sowing is expected to achieve the same stress escaping goals by anticipation of growth cycle. But winter warming during early sowing window could potentially slow vernalization fulfillment, with limited benefits to advance the susceptible stages. Using early-flowering spring wheat cultivars (the earliness threshold must be carefully defined) thus can help advocating early sowing practice that potentially make use of more autumn-winter rainfall. Nevertheless, the proposed stress escaping strategy is found to be comparatively more useful to avoid enhanced terminal heat stress (>38^{o} last over a short period) than prolonged terminal drought stress, where the latter can be alleviated with optimized supplemental irrigation.

Adaptation strategy for perennial forage grassland should take advantage of opportunity and tackle the challenge, both arising from climate change. Benefiting from advanced phenology towards winter and early spring with alleviated cold stress and enriched ambient CO_2 concentration, adaptation measures should focus on maximizing growth potential during this favorable period. These include optimized resource use (balanced early fertilization strategy with limited N leaching) and using grass-legume mixture for flexible forage utilization and better exploiting the stimulated CO_2 responsiveness. In contrast, to cope with the challenge of exacerbated risks of summer heat and drought stresses, future breeding programs should ensure a diversification (intra- and interspecific variations) of available germplasms in phenology (fit new seasonal climate pattern), heat tolerance and dehydration tolerance for principal forage species. Specifically, continuous improvement of drought persistence and summer dormancy traits should gain more importance for rainfed Mediterranean grassland. Moreover, these drought survival traits should be integrated into plant materials with deeper root system to enhance water uptake (e.g. more of tall fescue), but it may raise forage quality issues that remain unassessed. Besides, we also hypothesize it is possible to adapt to summer drought from a management perspective without the needs to improve and diversify the species and variety mixture. The findings suggest that provided minimum soil

moisture is guaranteed by supplemental irrigation to ensure adequate drought survival rate and standing density, breeding efforts should be more motivated towards heat tolerance, particularly in southern Portugal. Meanwhile, this measure is likely to result in a considerable increase in irrigation need, rendering a similar water-restriction issue facing irrigated maize.

Crop yield projections and explored adaptation strategies are essential to assess the regional food security prospects and provide crucial information to support planning and implementing suitable adaptation strategies for farmers and policymakers in Portugal and in Mediterranean basin that is known to be susceptible to climate change. Despite the uncertainties in the magnitude of yield impacts and quantitative effectiveness of adaptations, the proposed and recommended adaptation strategies can represent promising opportunities to maintain or increase production in future climate while minimize environment impacts. Future research efforts should be directed towards using multi-model ensembles (both crop and climate models) to quantify the uncertainties and make the estimations more robust and reliable, but sustained and extensive international cooperation is required. Moreover, stronger link of field experimentation with crop modelling is essential for a more mechanistic understanding of crop response to climate change, as well as the integration of crop model into economic modelling for complex farm-level assessment. These shall all contribute to appropriate manage the climate risks and comprehensively improve the resilience of cropping system.

Keywords: Cropping systems, Crop modelling, Climate change projections, Mediterranean conditions, Impact and vulnerability assessments, Adaptation explorations.

RESUMO

Os sistemas agrícolas são inerentemente vulneráveis à variabilidade climática e espera-se que a mudança climática aumente essa vulnerabilidade. Vários estudos alertam para o facto de que o aquecimento global de causas antropogénicas, a elevada concentração atmosférica de CO_2 e padrões de precipitação regional alterados deverão afetar negativamente a produtividade local das culturas e, assim, exacerbar inseguranças alimentares em muitas regiões do mundo, particularmente na bacia do Mediterrâneo. A bacia do Mediterrâneo é um dos mais proeminentes "hotspots" das alterações climáticas, devido às mudanças climáticas em curso e projetadas, tanto na média como na variabilidade, compreendendo um sinal robusto de mudanças climáticas com uma tendência geral de aquecimento e secura, acompanhada pela ocorrência mais frequente de secas severas ou extremas e temperaturas muito altas. Especificamente, espera-se que estas mudanças projetadas sejam mais pronunciadas no sul da Europa, como em Portugal, onde a temperatura média anual aumentou a uma taxa de mais do dobro da taxa de aquecimento global nas últimas décadas, juntamente com os decréscimos observados na precipitação e maior variabilidade interanual.

Por conseguinte, é necessário avaliar os impactos das alterações climáticas na produção agrícola e explorar estratégias de adaptação adequadas, enquanto os estudos efetuados até agora permanecem escassos em Portugal. Escolhemos três importantes sistemas de cultivo para a agricultura portuguesa, nomeadamente o milho de regadio, trigo de sequeiro e pastagens forrageiras perenes, sendo os locais de estudo escolhidos representativos das suas principais regiões de crescimento. A metodologia geral segue o uso combinado de modelos de clima e de culturas, onde as projeções climáticas de elevada resolução espacial e corrigidas de viés foram utilizadas como forçamentos das simulações de modelos de culturas, tendo sido estes previamente calibrados usando dados meteorológicos, de solo e de práticas agrícolas locais. Para a produção de milho de regadio foram utilizados os modelos de culturas dinâmicos STICS e AquaCrop, enquanto os outros dois sistemas de cultivo foram analisados apenas com o modelo STICS. É importante salientar que os resultados do presente estudo incorporaram nos impactos simulados os efeitos das alterações não apenas na média, mas também na variabilidade climática e seus extremos (por exemplo, mudanças de produção), o que permite uma avaliação mais rigorosa. Os resultados indicam que as ameaças e os riscos das alterações climáticas são elevados para a produção agrícola em Portugal, dado que se

verifica um impacto global negativo para os três sistemas de cultivo estudados, correspondendo a perdas de rendimento moderadas a severas, com elevadas variabilidades inter anuais. As perdas de rendimento são maiores, com maior variabilidade interanual na segunda metade do século do que na primeira metade, e para um cenário de emissão elevada do que num cenário de baixa emissão. É improvável que o efeito da fertilização com CO_2 compense estas reduções de rendimento, com um maior rendimento para as espécies C3 (trigo e pastagem) do que para a C4 (milho). Mais especificamente, a maioria dos impactos negativos resulta do encurtamento do período de crescimento do milho de regadio sob um clima mais quente, e da intensificação do stresse hídrico e térmico durante o período sensível para o trigo de sequeiro ou para as pastagens perenes. Esses aspetos correspondem às vulnerabilidades dos sistemas de cultivo face às alterações climáticas. É interessante notar que temperaturas mais altas são claramente prejudiciais à produção de milho de regadio, mas facilitando a antecipação da fenologia das pastagens perenes, melhorando a produção durante para o período favorável de inverno fresco e húmido. Estas novas condições também podem ajudar o trigo de sequeiro a amadurecer mais cedo, evitando valores excessivos de stresse. No entanto, a magnitude dos impactos da mudança climática na produtividade agrícola permanece incerta, dependendo do sistema de cultivo, local e práticas culturais, modelos climáticos aplicados (incluindo abordagens de downscaling) e modelos de culturas (incluindo calibração parcial ou total), períodos de tempo selecionados e cenários de emissão.

As estratégias de adaptação fornecem potencial para mitigar esses impactos negativos. O desenvolvimento de medidas de adaptação apropriadas e focadas no risco deve ter em conta as vulnerabilidades previamente identificadas e priorizar as opções disponíveis para uma estratégia integrada e abrangente. Para as culturas anuais de cereais, o aumento dos volumes de rega em vários níveis foi primeiramente testado para o sistema de cultivo de milho de regadio em cenários de alterações climáticas, tendo em consideração as necessidades de água da cultura e a projeção da distribuição sazonal de precipitação. Embora o aumento da rega seja capaz de mitigar as reduções de rendimento e manter os níveis atuais, a WUE da cultura decresce consideravelmente como resultado da menor resposta ao fornecimento de água devido ao encurtamento da época de crescimento. Devido ao risco crescente de escassez de água e à redução da água disponível para a agricultura na bacia do Mediterrâneo, o aumento do recurso à rega pode não ser uma estratégia viável, devendo ser priorizadas estratégias de gestão de água e maximização da WUE com vista à estabilização dos rendimentos (reduções marginais permitidas). Combinar estratégias de irrigação

otimizadas (por exemplo, irrigação deficitária) e instalações eficientes (por exemplo, sistema de rega gota a gota) com outras opções de adaptação, incluindo a introdução de variedades de ciclo mais longo e datas de sementeira mais precoces de forma a contrabalançar o encurtamento do período de crescimento é recomendável. Para o sistema de cultivo do trigo de sequeiro, a prioridade de adaptação deve abordar os riscos exacerbados stresse térmico e hídrico durante os períodos sensíveis de antese e enchimento de grãos. A estratégia para evitar o stresse terminal é proposta testando primeiramente variedades de floração precoce (também conhecidas como genótipos de ciclo curto), onde o trade-off entre menor risco de exposição ao stresse terminal e maior risco de redução do potencial produtivo tende a ser positivo, levando a ganhos líquidos de rendimento. Ainda assim, esta opção precisa ser combinada com outras estratégias de adaptação, incluindo a data de semeadura antecipada, cultivares de trigo com menor ou nenhum requisito de vernalização (por exemplo, usando trigo de primavera) e irrigação suplementar durante o período mais sensível. Uma sementeira mais precoce deverá permitir evitar o stresse terminal por antecipação do ciclo de crescimento. No entanto, o aquecimento de inverno durante a janela de sementeira precoce poderá potencialmente abrandar a vernalização, com benefícios limitados no avanço das fases suscetíveis. A utilização de variedades de trigo de primavera com floração precoce (o limiar de antecipação deve ser cuidadosamente definido) advogam sementeira precoce, o que permite a utilização da precipitação de outono-inverno. No entanto, a estratégia proposta para evitar o stresse é comparativamente mais útil para evitar o aumento do stresse térmico terminal (> 38ºC por um período curto) do que o stresse prolongado por seca, onde este último pode ser aliviado com rega suplementar otimizada. A estratégia de adaptação para pastagens forrageiras perenes deve aproveitar a oportunidade e enfrentar o desafio, ambos decorrentes da mudança climática. Beneficiando-se de fenologia avançada em relação ao inverno e início da primavera, com menor stresse por frio e maior concentração atmosférica de CO_2, as medidas de adaptação devem-se concentrar na maximização do potencial de crescimento durante este período favorável. Estes incluem o uso otimizado de recursos (estratégia balançada de fertilização precoce com limitação da lixiviação de N) e o uso de mistura de gramíneas e leguminosas para utilização de forragens flexíveis e melhor exploração da resposta estimulada de CO_2. Em contraste, para lidar com o desafio dos riscos exacerbados de calor no verão e stresse hídrico, futuros programas de melhoramento devem garantir uma diversificação (intra e inter varietal) dos germoplasmas disponíveis em fenologia (ajuste ao novo padrão climático sazonal), tolerância ao calor e tolerância

à desidratação para espécies forrageiras. Concretamente, a melhoria contínua das características de persistência à seca e de dormência de verão devem ganhar mais importância para as pastagens mediterrâneas de sequeiro. Além disso, estas características de sobrevivência à seca devem ser integrados em materiais vegetais com sistema radicular mais profundo para aumentar a absorção de água (por exemplo, festuca mais alta), mas isso pode resultar em problemas de qualidade da forragem que ainda permanecem por avaliação. Além disso, também formulamos a hipótese de que é possível a adaptação à seca de verão a partir de uma perspetiva de gestão sem a necessidade de melhorar e diversificar a mistura de espécies e variedades. Os resultados sugerem que, desde que a humidade mínima do solo seja garantida pela rega suplementar para garantir a taxa adequada de sobrevivência à seca e a densidade de planta, os esforços de melhoramento devem ser mais motivados para a tolerância ao calor, particularmente no sul de Portugal. Ao mesmo tempo, esta medida provavelmente resultará num aumento considerável na necessidade de rega, tornando-se num problema similar de restrição de água enfrentado pelo milho de regadio.

As projeções de colheira e as estratégias de adaptação exploradas são essenciais para avaliar as perspetivas regionais de segurança alimentar e fornecer informações cruciais para apoiar o planeamento e a implementação de estratégias adequadas de adaptação para agricultores e decisores políticos em Portugal e na bacia do Mediterrâneo. Apesar das incertezas na magnitude dos impactos na produção e na eficácia quantitativa das adaptações, as estratégias de adaptação propostas e recomendadas podem representar oportunidades promissoras para manter ou aumentar a produção no clima futuro, minimizando ao mesmo tempo os impactos ambientais. Esforços de investigação futuros devem ser direcionados para o uso de ensembles de modelos (tanto modelos agrícolas quanto climáticos) para melhor quantificar as incertezas e tornar as estimativas mais robustas e confiáveis. Não obstante, é necessária uma cooperação internacional vasta e sustentável. Além disso, uma forte ligação entre a experimentação de campo e a modelação de culturas é essencial para uma compreensão mais mecanicista da resposta da cultura às alterações climáticas, bem como a integração dos modelos de cultura na modelação económica. Todos estes devem contribuir para gerir adequadamente os riscos climáticos e melhorar a resiliência dos sistemas de cultivo.

Palavra Chave: Sistemas de cultivo, Modelação de culturas, Projeções de mudanças climáticas, Condições do Mediterrâneo, Avaliações de impacto e vulnerabilidade, Estratégias de adaptação.

LIST OF PUBLICATIONS DERIVED FROM THE THESIS

Scientific Articles

1. Yang, C., Fraga, H., van Ieperen, W. and Santos, J.A., 2017. Assessment of irrigated maize yield response to climate change scenarios in Portugal. Agricultural Water Management, 184: 178-190. https://doi.org/10.1016/j.agwat.2017.02.004

2. Yang, C., Fraga, H., van Ieperen, W. and Santos, J.A., 2018. Modelling climate change impacts on early and late harvest grassland systems in Portugal. Crop and Pasture Science, 69(8): 821-836. https://doi.org/10.1071/CP17428

3. Yang, C., Fraga, H., van Ieperen, W., Trindade, H. and Santos, J.A., 2019. Effects of climate change and adaptation options on winter wheat yield under rainfed Mediterranean conditions in southern Portugal. Climatic Change, 154(1): 159-178. https://doi.org/10.1007/s10584-019-02419-4

4. Yang, C., Fraga, H., van Ieperen, W. and Santos, J.A. Assessing the impacts of recent-past climatic constraints on potential wheat yield and adaptation options under Mediterranean climate in southern Portugal (submitted)

Invited Speaker

Yang, C., Santos, M., Fraga, H., van Ieperen, W and Santos, J.A., 2019. Climate change projections for precipitation in Portugal and potential impacts on grassland and forage systems. In workshop on "Efficient use of water on dairy farming" under project of Eurodairy (https://eurodairy.eu/), 18–19 June, 2018, Póvoa de Varzim, Portugal.

Oral communication in international conference

Yang, C., Fraga, H., van Ieperen, W., and Santos, J.A., 2019. Modelling grapevine phenology and productivity under different growing environments across Europe. In kick-off seminars and workshops on European project "Climate Change Impact Mitigation For European Viticulture" (Clim4Vitis), 18–20 February, 2019, UTAD, Vila Real, Portugal (https://clim4vitis.eu/).

Panel communications in conferences

Yang, C., Fraga, H., van Ieperen, W., and Santos, J.A., 2016. Assessment of optimal N fertilizer use on Portuguese maize yield using the STICS crop model. In 24th International Symposium of the International Scientific Centre of Fertilizers, Plant nutrition and Fertilizer issues for specialty crop, Abstract Book, pp. 63–64, 6–8 September, Coimbra, Portugal, 2016. https://doi.org/10.5073/berjki.2016.185.000

Santos, JA., **Yang**, C., Fraga, H., Costa, R., 2017. Alterações climáticas e potenciais implicações na agricultura Portuguesa: estudo de caso para as pastagens e forragens. In XXXVIII Spring Meeting of the Portuguese Society of Pastures and Forages, Abstract Book, 27–28 April, 2017, Castelo Branco, Portugal. ISBN 978-989-20-7439-9

Poster communications in conferences

International

Yang, C., Fraga, H., van Ieperen, W., and Santos, J.A., 2017. Analysis of maize yield under climate change scenarios using STICS. In the 2nd Agriculture and Climate Change Conference, Abstract Book, 26–28 March, 2017, Sitges, Spain. https://www.elsevier.com/__data/assets/pdf_file/0006/277926/Poster-Programme.pdf

Yang, C., Fraga, H., van Ieperen, W., and Santos, J.A., 2017. Modelling irrigated maize yield response to climate change scenarios in Portugal. In European Meteorological Society (EMS) Annual Meeting, Abstract Book, Vol. 14, EMS2017-488, 2017, Dublin, Ireland. https://meetingorganizer.copernicus.org/EMS2017/EMS2017-488.pdf

Yang, C., Fraga, H., van Ieperen, W., and Santos, J.A., 2017. Modelling the impact of climate change scenario on permanent irrigated grassland between high and low irrigation input farming system in Portugal. In the 2nd World Symposium on Climate Change Adaptation (WSCCA-2017), Conference Proceedings, 6–8 September, Coimbra, Portugal. https://www.haw-hamburg.de/fileadmin/user_upload/FakLS/07Forschung/FTZ-ALS/Veranstaltungen/_PDF/Livro_ABSTRACTS_FINAL.pdf

Yang, C., Fraga, H., van Ieperen, W., and Santos, J.A., 2019. Modelling impacts of climate change on irrigated grassland productivity with contrasting growth duration under Mediterranean climate. In the 3rd Agriculture and Climate Change Conference, Abstract Book, 24–26 March, 2019, Budapest, Hungary. https://www.elsevier.com/events/conferences/agriculture-and-climate-change-conference/programme

National

Yang, C., Fraga, H., van Ieperen, W., and Santos, J.A., 2018. Climate change impacts on permanent irrigated grassland in Portugal. In Encontro Ciência 2018, Conference proceedings, 2–4 July, 2018, Lisbon, Portugal.

TABLE OF CONTENTS

INDEX OF FIGURES AND TABLES

CHAPTER 1

CHAPTER 2

CHAPTER 3

CHAPTER 4

CHAPTER 5

LIST OF ABBREVIATIONS

A

AgriChains – Agricultural Production Chains – from fork to farm

AquaCrop – Agricultural crop-water productivity model

AgMIP – Agricultural Model Intercomparison and Improvement Project

AR5 – Fifth Assessment Report of Intergovernmental panel on climate change

AR4 – Fourth Assessment Report of Intergovernmental panel on climate change

B

BA – Bias Adjustment

BC – Bias Correction

C

CA – Climate Anomaly

CC – Correlation Coefficient

CCS – Climate Change Scenarios

CM SAF – Satellite Application Facility on Climate Monitoring

CMIP3 – Coupled Model Intercomparison Project phase three

CMIP4 – Coupled Model Intercomparison Project phase four

CMIP5 – Coupled Model Intercomparison Project phase five

CV – Coefficient of Variation

D

DC – Delta Change

DCMs – Dynamic Crop Models

DMY – Dry Matter Yield

DSS – Decision Support System

DSSAT – Decision Support System for Agrotechnology Transfer

DWP – Daily Water Productivity

E

ECA&D – European Climate Assessment & Dataset

ED – Ensemble Delta technique

E-OBS – European-wide ensemble version of daily gridded observational dataset

ERA-interim – Re-analysis dataset of European Centre for Medium-Range Weather Forecasts

ES – Early Spring cut grassland system

ESMs – Earth System Models

ESD – Empirical Statistical Downscaling

ET – Actual Evapotranspiration

EU-SoilHydroGrids – European-wide Soil Hydraulic Database

EURO-CORDEX – European branch of the global Coordinated Regional Downscaling Experiment

EUR11 – EURO-CORDEX climate model simulations at 12.5 km

EUR44 – EURO-CORDEX climate model simulations at 50 km

F

FAO – Food Agricultural Organization

FACE – Free Air CO2 Enrichment

G

GCMs – Global Climate Models

GDD – Growing Degree Days

GHG – Greenhouse Gas

GTOPO30 – 30-arc second Digital Elevation Model developed by U.S Geological Survey

GCMs – coupled Global Climate Models and Regional Climate Models chains

H

HI – Harvest Index

HWSD – Harmonized World Soil Database

I

INE – Instituto Nacional de Estatística

INRA – French National Institute for Agricultural Research

IPCC – Intergovernmental Panel on Climate Change

IP – Iberian Peninsula

ISIMIP – Inter-Sectoral Impact Model Intercomparison Project

ISOP – Information and Objective Follow-up of Pastures

L

LAI – Leaf Area Index

LS – Late Summer cut grassland system

M

MAE – Mean Absolute Error

MACSUR – Modelling European Agriculture with Climate Change for Food Security

MESAN – Mesoscale re-analysis dataset

N

NOAA – National Oceanic and Atmospheric Administration

P

PET – Potential Evapotranspiration

R

RCMs – Regional Climate Models

RCPs – Representative Concentration Pathways

RF – Radiative Forcing

nRMSE – normalized Root Means Square Error

RUE – Radiation Use Efficiency

S

SCMs – Statistical Crop Models

SD – Standard Deviation

SIAM – Scenarios, Impacts and Adaptation measures

SMHI-RCA4 – Rossby Centre climate model from Swedish Meteorological and Hydrological Institute

SRES – Special Report on Emission Scenarios

STICS – Simulateur mulTIdisciplinaire pour les Cultures Standard

T

TAW – Total Available Water

U

USDA ST – Soil Taxonomy developed by United States Department of Agriculture

W

WCRP – World Climate Research Program

WGCM – Working Group on Coupled Modelling

WMO – World Meteorological Organization

WP – Water Productivity

WUE – Water Use Efficiency

CHAPTER 1

General Introduction

1.1 Context introduction and importance of problems

One of the millennium development goals established by Food Agricultural Organization (FAO) is to eradicate extreme poverty and hunger, as the number of hungry people still remains unacceptably high despite recent efforts to restrict this figure below 1 billion (UNICEF, 2004). Even if hunger is primarily a question of insufficient access to food due to poverty, there is a global consensus that crop production needs to increase considerably by about 60% in the middle of 21st century to satisfy the food demand for agricultural products, due to population and consumption growth, economic development and rapid urbanization (Alexandratos and Bruinsma, 2012; Godfray et al., 2010). As in the past, crop production increases were mainly achieved by productivity gains with moderate changes in cropping areas or livestock numbers (Godfray et al., 2010). For instance, crop yield improvement should account for more than 80% of total crop output increase in the next decade, according to OECD/FAO agricultural outlook 2016–2025 (OECD/FAO, 2016). However, in the context of foreseen global climate change in the upcoming decades, i.e. anthropogenic-driven greenhouse gas emissions with elevated atmospheric CO_2 level, rising temperature, altered local precipitation pattern (IPCC, 2013), it is becoming increasingly difficult to maintain or increase crop yields without any changes in current cropping systems.

A robust and coherent global pattern is discernible of climate change impacts on crop productivity that could have consequences on two dimensions of food security, i.e. availability and stability (Wheeler and von Braun, 2013). A comprehensive meta-analysis of global climate change impacts indicated a great risk of mean yield reductions for staple crops (maize, wheat and rice) in tropical and temperate regions by a projected moderate warming of 2°C, being more consistent from 2030s onwards, up to 25% of aggregated yield losses (Challinor et al., 2014). Besides decreases in mean yields, increased inter-annual yield variabilities, associated with increased climate variabilities and extreme events, are expected to negatively affect future year-to-year stability of food crop supply, amplifying marketing price and fluctuations (Asseng et al., 2014; Challinor et al., 2014). A notable example was the 2003 summer heat wave, characterized by an increase in mean temperature and much larger temperature variability, which considerably reduced cereal production by about 23 million tons in Europe, with huge economic impacts on the food supply chains (Schär et al., 2004). This situation concretely demonstrated how climate variability and associated extreme events may have significant impacts on agriculture production.

1.2 Vulnerability and research gaps in Portugal

It is likely that climate change and variability have more impacts on cropping systems and exacerbate food insecurities in current vulnerable regions, such as the Mediterranean region (Prosperi et al., 2014). Projections from a wide range of global and regional climate models confirm a robust climate change signal of an overall warming and drying trend for the Mediterranean basin, accompanied by greater frequency and intensity of extreme events (Giorgi and Lionello, 2008). Despite being identified as one of the most prominent "hot-spot" for climate change impacts (Giorgi and Lionello, 2008), relatively fewer studies have been conducted to evaluate climate change impacts in the Mediterranean region compared to the counterpart temperate region. Studies are even more scarce for Portugal, a southern European country within Mediterranean basin, which currently calls for the strong needs for research assessments on climate change impacts and risks, to identify vulnerabilities of various agro-ecosystems and exploration of policy guidelines for planning efficient, integrated and target adaptation strategies (Carvalho et al., 2014). Resultantly, the findings obtained are not only relevant in Portugal, but also have broader implications for regions with similar Mediterranean-type climates.

Scenarios, Impacts and Adaptation measures (SIAM, http://cciam.fc.ul.pt/prj/siam/) was a pioneering project for climate change impact assessments in Portugal over 1999–2006 (Santos and Miranda, 2006). It revealed that future climate change may reduce yields of rainfed wheat and irrigated maize in Portuguese major producing regions by 25% and 29% respectively, highlighting the need for development and planning of adaptation strategies (e.g. early sowing dates and introducing cultivars with better heat and drought tolerance) (Santos and Miranda, 2006). However, one major limitation from the SIAM project arises from the fact that their climate projections are directly based on the coarse horizontal resolution (200–300 km) of Global Climate Model (GCM) simulations that are normally not appropriate for direct use in impact models, i.e. crop models are typically operated at 1 ha scale (Yang et al., 2019; Yang et al., 2010). Moreover, the trajectories of future Greenhouse Gas (GHG) emissions are dependent on demographic changes, technologic trends, social-economic development and policy influences, thus adding uncertainty to the climate change projections (Asseng et al., 2013). Climate change scenarios adopted by SIAM are based on limited sets of social-economic scenarios (Carvalho et al., 2014; Santos and Miranda, 2006), such as A1 and A1B from the Special Report on Emission Scenarios (SRES), where these scenarios do not include possible future policy interventions and thus not encompass full ranges of potential

outcomes (Nakicenovic et al., 2000). Besides, the crop models are implemented without adequate calibrations and performance evaluations, as well as lack of appropriately incorporating local agronomic characteristics (Santos and Miranda, 2006). Moreover, quantitative effectiveness of adaptation strategies explored has not been evaluated in their simulations, only providing qualitative suggestions based on interpretations of projected yield impacts that are inherently uncertain (Santos and Miranda, 2006).

1.3 Framework of PhD program

In the framework of a novel doctoral program in the field of agriculture science (Agricultural Production Chains – from fork to farm, AgriChains), my PhD research was carried out to extend and improve estimations of agricultural impacts of and adaptation responses to climate change, attempting to address the challenge issues and fill the research gaps in climate change risk assessment studies in Portugal. The resulting development of decision support systems (DSS) will allow for planning, guiding and implementing climate change adaptation strategies for the Portuguese agriculture, taking into account potential climate variability and change scenarios. This approach is plainly justified within the framework of the AgriChains doctoral program. In fact, it corresponds to one of its main topics (cf. approved proposal by FCT): "Climate changes and adaptation measures". Moreover, it is aimed to provide practical information to farmers and policy-makers, in order to bridge scientific knowledge to real economy.

1.4 Overall methodologies

We have firstly identified three crop production systems that are socially, culturally and economically important in Portugal, namely irrigated maize, perennial grassland and rainfed wheat crops, which are chosen as the subjects in our climate impact studies (Yang et al., 2018; Yang et al., 2019; Yang et al., 2017). The corresponding representative study sites in the major producing regions of Portugal have been identified. The overall methodologies follow the combined use of climate models and crop models. Climate models generate a wide range of plausible projections of future climate conditions at study sites, at which crop responses are simulated by process-based crop models, resulting in the variations and changes of important agronomic outputs (e.g. growth duration, grain yield, aerial biomass) relative to the reference (baseline) period. These variations and changes are primarily interpreted as impacts of climate change, for which quantitative

effectiveness of field-level adaptation strategies are proposed and tested by modifying cultivar traits or adjusting management inputs that are both available as an integral part of crop models (Challinor et al., 2014; Ruiz-Ramos et al., 2018). Climate models are appropriate tools for analyzing climate change, while crop growth and yield formation processes are simulated by dynamic crop models that quantify the impacts of complex interactions among Genotypes × Management × Environment (G × M × E) on a daily time-step (Asseng et al., 2014; Challinor et al., 2014). Moreover, use of crop models allows to isolate the impacts of climatic and non-climatic factors on crop yields while keep other factors constant, which are difficult to determine in field experiment or long-term yield trends, e.g. trend of time-series regional yield statistics is a result of numerous interplaying factors, thus being difficult to isolate their individual contribution to yield, such as the case of temperature or precipitation (Asseng et al., 2011; Lobell et al., 2005).

Over the course of my PhD, I mainly focused on using the STICS crop model, which has been developed by INRA (French National Institute for Agricultural Research) since 1996 (Brisson et al., 2003; Brisson et al., 2009; Brisson et al., 1998; Brisson et al., 2002). The model is initially parameterized for cereal crops, such as maize and wheat (Brisson et al., 1998; Brisson et al., 2002), but later being adapted to various other crops, such as perennial grassland (Ruget et al., 2009). The robustness of model, with its standard set of parameters, has been sufficiently tested and examined, showing satisfactory performance for a wide range of agro-climatic conditions, including situations under Mediterranean-type climate (Coucheney et al., 2015). AquaCrop, a water-driven crop model developed by FAO (Steduto et al., 2009), which is relevant for studying the relations between crop yield and water productivity under climate change, is also employed in my thesis works for one occasion (Yang et al., 2017).

In **Chapter 2**, we will provide state-of-the-art literature reviews on modelling climate change impacts on crop growth and yield, including detailed information on the social-economic importance of these identified production systems in Portugal, as well as current state of knowledge concerning climate change projections and model-based evaluation of impacts and adaptation options (including a brief overview of the STICS crop model). In short, projected climate change impacts on crop growth and productivity, based on the combined use of crop and climate models, are known to vary with different locations and regions, characteristics of selected cropping systems, GHG emission scenarios and future time periods chosen (Asseng et al., 2013; Challinor et al., 2014; Islam et al., 2012; Rötter et al., 2018; Wang et al., 2018). Therefore,

assessments of climate change impacts and exploration of adaptation strategies should be carried out in a specified local context. Appropriate assimilations of local crop growing conditions into crop models, including observed climate data, dominant soil types and representative farming practices (e.g. common cultivars, planting dates, resource investments, among others) before feeding climate projections data, are essential for a more relevant and reliable analysis.

1.5 Objectives and tasks

The overall objectives of my PhD thesis research are **1**) to explore food security prospects for farmers and stakeholders by providing crucial information and insights on yield projections of three main crop production systems in Portugal (i.e. irrigated grain maize, rainfed winter wheat and perennial grassland); **2**) to aid in developing, planning and enacting climate change adaptation strategies for Portuguese major producing regions of these crops, based on rigorously examined various levels of adaptation options in the modelling processes; **3**) to bring added value to enhance the resilience of agri-food chains where key inputs are available to bio-economic or farming system models for more integrated and comprehensive risk assessment and management; **4**) to improve our understandings of crop physiological and growth response to climate change.

In line with these objectives, the following research tasks have been carried out:

1) Analysis of performance of two dynamic crop models (STICS and AquaCrop) in simulating irrigated maize yields at regional scale by comparing to statistic data in the Portuguese major producing region (Ribatejo) (**Chapter 3)**.

2) Analysis of the response of several important outputs of the irrigated maize system (i.e. yield, growth duration, seasonal water input and water use efficiency) to project climate change in Ribatejo, based on the previous two crop models, and propose irrigation-based adaptation strategies, by analyzing water-yield relations under different climate change scenarios (**Chapter 3)**.

3) Evaluation of STICS model performance in simulating local grain yields of winter wheat, using 5-year published yield data at one representative site within a major wheat growing region in Portugal (Alentejo) (**Chapter 4)**.

4) Assessment of winter wheat yield response to projected climate change using STICS model, and estimate the quantitative effectiveness of using early flowering cultivars and early sowing

dates as potentially suitable regional adaptation options for wheat production in Alentejo (**Chapter 4)**.

5) Comparison of forage Dry Matter Yield (DMY) of Mediterranean perennial grassland simulated by STICS with observations, and estimate potential climate change impacts on DMY under contrasting grassland growth duration and irrigation water supply (**Chapter 5)**.

6) Explorations of recommendable adaptive responses to the impacts of foreseeable enhanced extreme weather events in summer (June–August) derived from climate change projections, by separating the effects of severe water deficits on DMY from effects of heat stress using STICS model at grassland sites throughout Portugal (**Chapter 5)**.

The current PhD thesis is organized in 7 chapters, with **Chapter 6** of General Discussion and **Chapter 7** of Concluding Remarks and Future Outlooks. A diagram overview is provided below in **Fig. 1**.

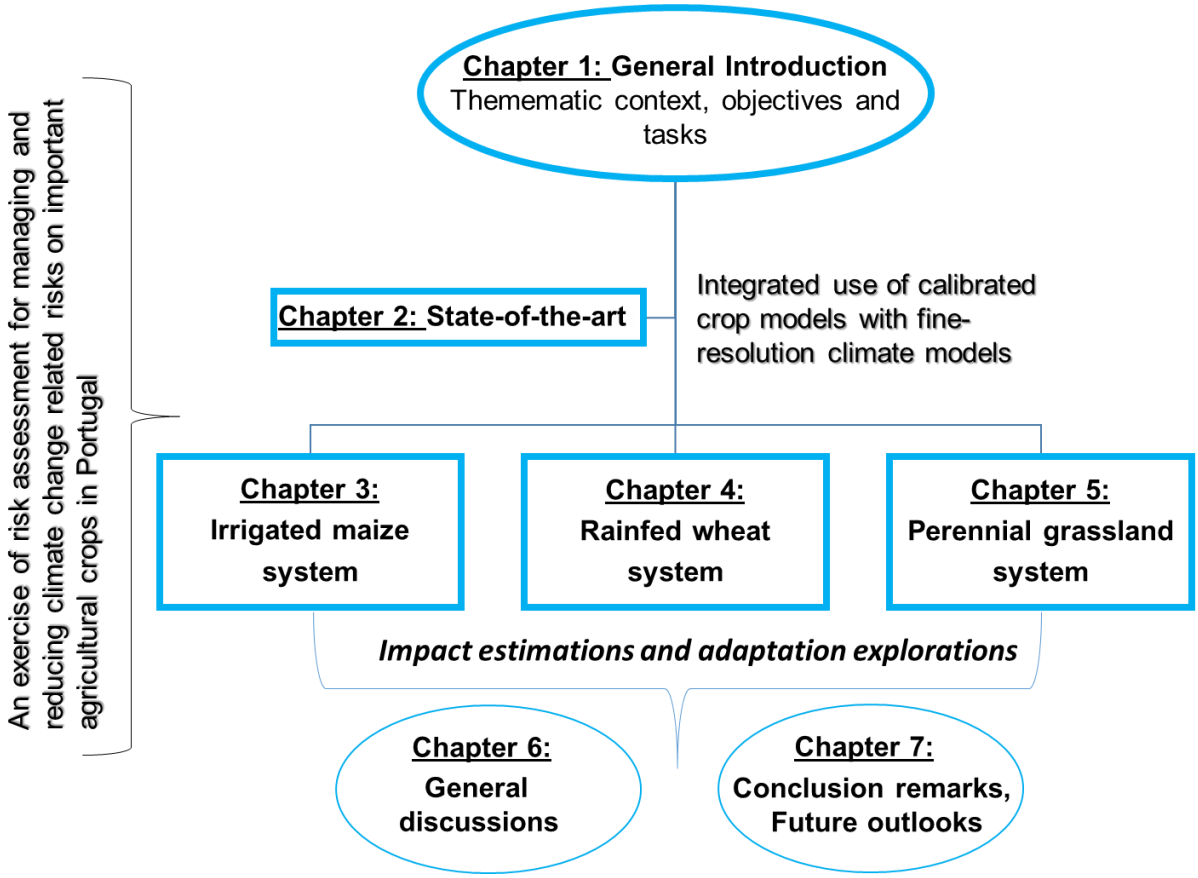

Figure 1. An overview of present PhD thesis structure

References

Alexandratos, N. and Bruinsma, J., 2012. World agriculture towards 2030/2050: the 2012 revision, ESA Working paper No. 12-03, Rome, FAO.

Asseng, S. et al., 2014. Rising temperatures reduce global wheat production. Nature Climate Change, 5: 143.

Asseng, S. et al., 2013. Uncertainty in simulating wheat yields under climate change. Nature Climate Change, 3(9): 827-832.

Asseng, S., Foster, I. and Turner, N.C., 2011. The impact of temperature variability on wheat yields. Global Change Biol, 17(2): 997-1012.

Brisson, N. et al., 2003. An overview of the crop model stics. European Journal of Agronomy, 18(3): 309-332.

Brisson, N., Launay, M., Mary, B. and Beaudoin, N., 2009. Conceptual basis, formalisations and parameterization of the STICS crop model. Editions Quae, Versailles, France, 297 pp.

Brisson, N. et al., 1998. STICS: a generic model for the simulation of crops and their water and nitrogen balances. I. Theory and parameterization applied to wheat and corn. Agronomie, 18(5-6): 311-346.

Brisson, N. et al., 2002. STICS: a generic model for simulating crops and their water and nitrogen balances. II. Model validation for wheat and maize. Agronomie, 22(1): 69-92.

Carvalho, A., Schmidt, L., Santos, F.D. and Delicado, A., 2014. Climate change research and policy in Portugal. Wiley Interdisciplinary Reviews: Climate Change, 5(2): 199-217.

Challinor, A.J. et al., 2014. A meta-analysis of crop yield under climate change and adaptation. Nature Climate Change, 4: 287.

Coucheney, E. et al., 2015. Accuracy, robustness and behavior of the STICS soil–crop model for plant, water and nitrogen outputs: Evaluation over a wide range of agro-environmental conditions in France. Environ Modell Softw, 64: 177-190.

Giorgi, F. and Lionello, P., 2008. Climate change projections for the Mediterranean region. Global Planet Change, 63(2): 90-104.

Godfray, H.C.J. et al., 2010. Food Security: The Challenge of Feeding 9 Billion People. Science, 327(5967): 812-818.

IPCC, 2013. The physical science basis. Contribution of working group I to the fifth assessment report of the intergovernmental panel on climate change [Stocker, T.F., D. Qin, G.-K.

Plattner, M. Tignor, S.K. Allen, J. Boschung, A. Nauels, Y. Xia, V. Bex and P.M. Midgley (eds.)]. Cambridge University Press, Cambridge, United Kingdom and New York, NY, USA, 1-1535 pp.

Islam, A. et al., 2012. Modeling the impacts of climate change on irrigated corn production in the Central Great Plains. Agricultural Water Management, 110: 94-108.

Lobell, D.B. et al., 2005. Analysis of wheat yield and climatic trends in Mexico. Field Crops Research, 94(2): 250-256.

Nakicenovic, N. et al., 2000. Special report on emissions scenarios (SRES), a special report of Working Group III of the intergovernmental panel on climate change. Cambridge University Press.

OECD/FAO, 2016. OECD-FAO Agricultural Outlook 2016-2025 OECD. Publishing Paris, pp. 137.

Prosperi, P., Allen, T., Padilla, M., Peri, I. and Cogill, B., 2014. Sustainability and Food & Nutrition Security:A Vulnerability Assessment Framework for the Mediterranean Region. SAGE Open, 4(2): 2158244014539169.

Rötter, R.P., Hoffmann, M.P., Koch, M. and Müller, C., 2018. Progress in modelling agricultural impacts of and adaptations to climate change. Curr Opin Plant Biol, 45: 255-261.

Ruget, F., Satger, S., Volaire, F. and Lelievre, F., 2009. Modeling Tiller Density, Growth, and Yield of Mediterranean Perennial Grasslands with STICS. Crop Sci, 49(6): 2379-2385.

Ruiz-Ramos, M. et al., 2018. Adaptation response surfaces for managing wheat under perturbed climate and CO2 in a Mediterranean environment. Agr Syst, 159: 260-274.

Santos, F.D. and Miranda, P., 2006. Climate Change in Portugal: Scenarios, Impacts and Adaptation Measures - SIAM II Project. Gradiva, Lisbon.

Schär, C. et al., 2004. The role of increasing temperature variability in European summer heatwaves. Nature, 427(6972): 332-336.

Steduto, P., Hsiao, T.C., Raes, D. and Fereres, E., 2009. AquaCrop—The FAO crop model to simulate yield response to water: I. Concepts and underlying principles. Agron J, 101(3): 426-437.

UNICEF, 2004. Millennium Development Goals: 1. Eradicate extreme poverty and hunger.

Wang, B., Liu, D.L., Waters, C. and Yu, Q., 2018. Quantifying sources of uncertainty in projected wheat yield changes under climate change in eastern Australia. Climatic Change, 151(2): 259-273.

Wheeler, T. and von Braun, J., 2013. Climate Change Impacts on Global Food Security. Science, 341(6145): 508-513.

Yang, C., Fraga, H., van Ieperen, W. and Santos, J.A., 2018. Modelling climate change impacts on early and late harvest grassland systems in Portugal. Crop and Pasture Science, 69(8): 821-836.

Yang, C., Fraga, H., van Ieperen, W., Trindade, H. and Santos, J.A., 2019. Effects of climate change and adaptation options on winter wheat yield under rainfed Mediterranean conditions in southern Portugal. Climatic Change, 154(1): 159-178.

Yang, C.Y., Fraga, H., Van Ieperen, W. and Santos, J.A., 2017. Assessment of irrigated maize yield response to climate change scenarios in Portugal. Agricultural Water Management, 184: 178-190.

Yang, W. et al., 2010. Distribution-based scaling to improve usability of regional climate model projections for hydrological climate change impacts studies. Hydrology Research, 41(3-4): 211-229.

CHAPTER 2

State-of-the-art

2.1 Crop production and challenge under climate change

2.1.1 Importance of crop production in Portugal

The European Union is one of the world´s largest and most productive supplier for food, standing for 20% of global cereal production, with crop productivity 60% higher than the world average (Olesen et al., 2011). In Portugal, where the agricultural area represents about 40% of the whole territory, with a remarkable economical volume (approximate 4,640 million euros), the inter-annual crop yield variability has played a determinant role on food price and security, as well as land use competitions with non-food sectors (Charlier and de Gasperi, 2007).

Fodder crop production (including perennial and annual grassland) stands for the largest proportion of total crop production in Portugal (**Fig. 1**). There are around 2.5 million hectares of grassland in Portugal, accounting for 25% of territory area, with its main distribution in the northwest, center and south regions (Jongen et al., 2011). In the northwest, large areas are devoted to intensive dairy farms, which contributes to more than 50% of national milk production (Trindade, 2015). Success of these dairy farms are largely dependent on self-sufficient forage supply from none-grazing permanent grassland (Trindade, 2015). In the center region, grassland utilization generally focuses on integrated livestock production, e.g. in Quinta da Franca covering around 500 ha, in which irrigated pasture provides an essential forage source (Pereira et al., 2004). For the south, where grassland is the main vegetation cover, semi-natural grassland with higher

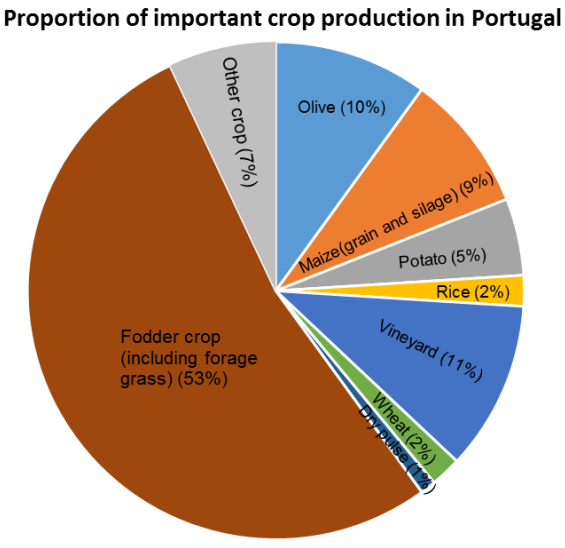

Figure 1 Proportion of various crop production systems in Portugal (INE, 2015).

conservation value (Aires et al., 2008), is critical to sustain extensive animal grazing, but being gradually replaced by sown biodiverse permanent pasture (Teixeira et al., 2011). Given the important role of forage production, climate conditions may exert strong control on farmer's livelihood. For instance, in the dry year of 2004-2005, animal stocking rate in several pasture farms significantly decreased as a result of drought induced forage deficiency (Teixeira et al., 2011). Perennial crops are inherently vulnerable to climate changes, owing to the all-around-the-year exposure to fluctuations in local weather conditions that also vary from place to place. Evaluations of climate change impacts and development of adaptation measures for perennial grassland are most needed.

It is also evident from **Fig. 1** that maize (*Zea mays L.*) is the most important cereal crop in Portugal grown for grain and silage production. The most important growing area is located in the Ribatejo region, having approximately ~30,000 ha of maize fields (ca. 35% of the total maize area in Portugal) (Yang et al., 2017). The Ribatejo climate, characterized by very dry summers, does not naturally provide optimal conditions for a high water-demanding crop like maize, with a spring-summer growing season. Hence, almost all of the maize cultivated area (94%) is currently irrigated (INE, 2015). Within the region, the Sorraia Valley is another example of intensive irrigated maize growing area, in which irrigated maize cultivation area accounts for about 25.6–44.9% of the total area irrigated during 2004–2014 (Ramos et al., 2017). In a larger context, the agricultural sector is by far the largest water consumer, where approximately 80% of water consumption has been allocated to irrigation in the Mediterranean region (Araus, 2004). However, water availability for agricultural purposes is rapidly declining due to increasing competition from non-food sectors, as well as driven by projected warming and drying trends (Challinor et al., 2014; Giorgi and Lionello, 2008; Hamdy et al., 1995; Iglesias et al., 2007). Given the fact that irrigation practice plays a critical role in increasing crop productivity and improving production stability, scarcity of water resource with poor field management is expected to significantly hinder sustainable development of maize production. Therefore, sustainable methods to increase crop Water Use Efficiency (WUE) are gaining importance in arid and semi-arid regions such as the Mediterranean basin (Geerts and Raes, 2009). In recent years, the research focus has shifted to limiting factors of cropping systems (e.g. water availability) for sustainable intensification, instead of solely maximizing crop productions. Adaptation strategies based on optimized water management, such as deficit irrigation that contribute to maximize WUE on crops grown in drought-prone area, enable water

saving practices while helping to stabilize crop yields (Geerts and Raes, 2009; Zhang and Oweis, 1999).

Another import cereal crop in Portugal is wheat (mainly winter wheat) that are culturally, socially and economically important in Portugal, but insufficient domestic productions lead to the dependency on imports for satisfying internal demand (Almeida et al., 2016) (**Fig. 1)**. The main wheat growing areas are situated in the Alentejo region in southern Portugal, representing about 80% of total growing areas and account for >75% of national wheat production (INE, 2019). In Alentejo, the prevalence of dryland farming systems leads to wheat cultivation under rainfed conditions (Valverde et al., 2015). Approximately, 95% of wheat growing areas in Alentejo are devoted to bread wheat production (Gouveia and Trigo, 2008). The typical Mediterranean climate of this region causes a high evaporative demand in late spring (ca. April–June) when precipitation is low, thus considerably enhancing the risks of occurrence of severe water deficit during the most susceptible growth stage of winter wheat, i.e., flowering and post-anthesis grain filling period (Costa et al., 2013; Páscoa et al., 2017). It is clear that climate-related risks for wheat production are substantially high in this region. A previous analysis revealed that climatic water deficits in May and June in this region, largely coinciding with the grain filling and ripening stages, may impose strong limitations on wheat yields (Páscoa et al., 2017). Over the last decades, it was found that regional wheat growing areas had declined drastically from an average of 211,104 ha (331,007 t), during 1986–1995, to of 47,394 ha (84,227 t), during 2006–2015 (INE, 2019). The reason for this increasingly low adoption, in addition to policy modifications, can be largely explained by the observed climate trend towards a more arid climate in Alentejo, aggravating the existing climatic constraints, with serious concerns over yield returns and economic viability (Páscoa et al., 2017; Valverde et al., 2015). More investments and efforts are required by farmers to offset the negative impacts on yield. Therefore, it is important to quantify and understand to what extent the two main abiotic stresses (drought/heat) have limited wheat yield, and how adaptation options can help overcoming these limitations.

Other important annual crop species, like rice and potato and dry pulses (**Fig. 1**), also play an important role in Portuguese agri-food production, with annual production reaching ~600,000 ton in total (INE, 2015). For fruit crop, grapevine contributes to more than 11% of total production (**Fig. 1**) (INE, 2015), making Portugal the 11th highest wine producing and exporting country in

the world. The commercial vineyards were distributed across 12 viticulture regions in mainland Portugal, representing 227,000 ha (Fraga et al., 2016).

2.1.2 Observed yield stagnations in Europe and Portugal

The growing trends of food consumption, due to rapidly increasing population, economic growth and urbanization, are predicted to boost land use and water resource competition, creating marked impacts on various socioeconomic sectors (Alexandratos and Bruinsma, 2012; Godfray et al., 2010). In such a context, maintaining crop production under changing climates to satisfy increasing consumption demand is the greatest challenge we face as a species. During the last century, increased crop yields were brought about mainly through Green Revolution, i.e. breeding for increased harvest index and disease resistance, as well as by using more irrigation and agrochemicals (Evenson and Gollin, 2003). While genetic gains continue, the multiple challenges of climate change and growing global population demand new approaches to produce nutritious, high yielding, climate resilient crops. For instance, it is shown that the continuous genetic progress on cereal grain yields has been partly counteracted by climate warming since 1990, resulting in yield stagnations in many European countries (Brisson et al., 2010). This particularly holds true for Portugal, which displays the lowest level of wheat yield with the slowest increasing rate (FAO, 2003; Porter and Semenov, 2005) (**Fig. 2**).

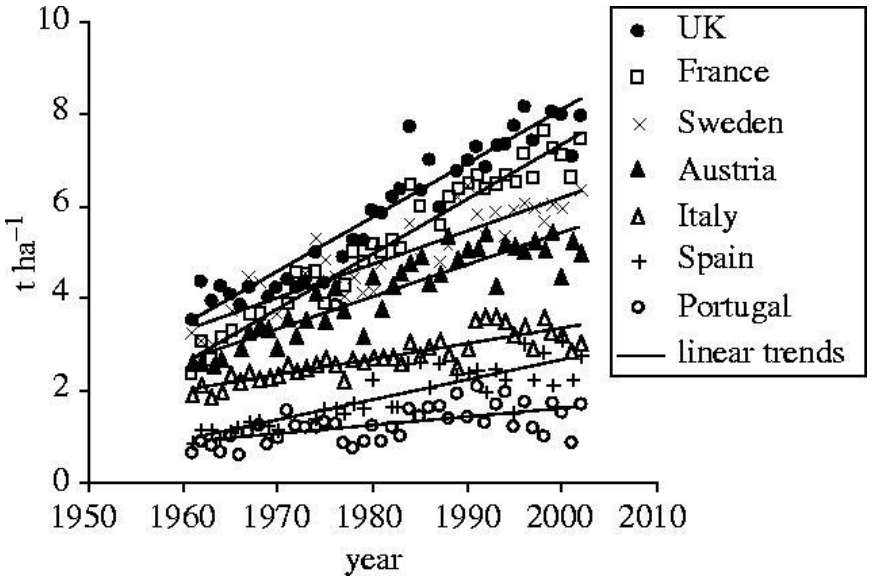

Figure 2 Observed wheat grain yields in selected European countries (FAO, 2003; Porter and Semenov, 2005).

2.1.3 Crop response to climate change and variability

The agricultural sector is intrinsically vulnerable to climate change, as crops are commonly subject to several forcing factors, being climate variability among the most important driver on crop yield variation. Climatic variability plays a major role in producing meteorological conditions that deviate substantially from mean conditions, known as climate anomalies, accompanied by the occurrences of extreme weather events. A number of modelling studies, centred on the effects of elevated atmospheric CO_2 level in conjunction with changes in average climatic conditions (e.g. annual mean temperature and precipitation) on crop production, were conceptually incomplete, likely causing an underestimation of climate impacts (Asseng et al., 2013; Kassie et al., 2015; Tubiello et al., 2000). This is because crop is generally subject to a combination of several growth-limiting factors (e.g. water and nutrients shortage and heat stress) and respond non-linearly to changes in growing conditions, exhibiting discontinuous threshold response (Porter and Semenov, 2005; Semenov and Porter, 1995). Therefore, increased climate variability, on top of changes in mean climate conditions, can assume a greater role as climatic constraints in limiting crop yields. For example, the nation-level cereal productions across the globe were reduced by an average of 9–10% during 1964–2007, resulting from the impacts of historical extreme drought and heat stresses (Lesk et al., 2016). Likewise, the 2003 European summer heat wave, characterized by an increase in mean temperature and much larger temperature variability, considerably reduced cereal production by about 23 million tons in Europe, with huge economic impacts on the food supply chains (Schär et al., 2004).

It is repetitively stressed that along with projected mean climate changes (such as annual mean temperature and precipitation), changes in climate variability and associated frequency and intensity of extreme weather events, such as severe drought and heat stress, should also be explicitly included in climate change impact analysis (Lesk et al., 2016; Moriondo et al., 2011). It is later confirmed by IPCC (2013) that climates may become more extreme if the variance of the climate distribution is larger. As an illustrative example from a statistic point of view, the postulated temperature distribution changes were presented by Porter and Semenov (2005) in relation to the effects of increase in mean and variance on the frequency of occurrence of extreme temperature events, i.e. heat stress or frost damages (**Fig. 3**). **Figure 3** below indicates (i) increasing mean temperature moves the distribution towards warmer weather (**Fig. 3a**); (ii) increasing temperature variance results in the tendency towards more frequent occurrence of

extreme weather events, such as heat stress (**Fig. 3b**); (iii) increases in both mean and variance of temperature cause warmer and more frequent heat stress (**Fig. 3c**).

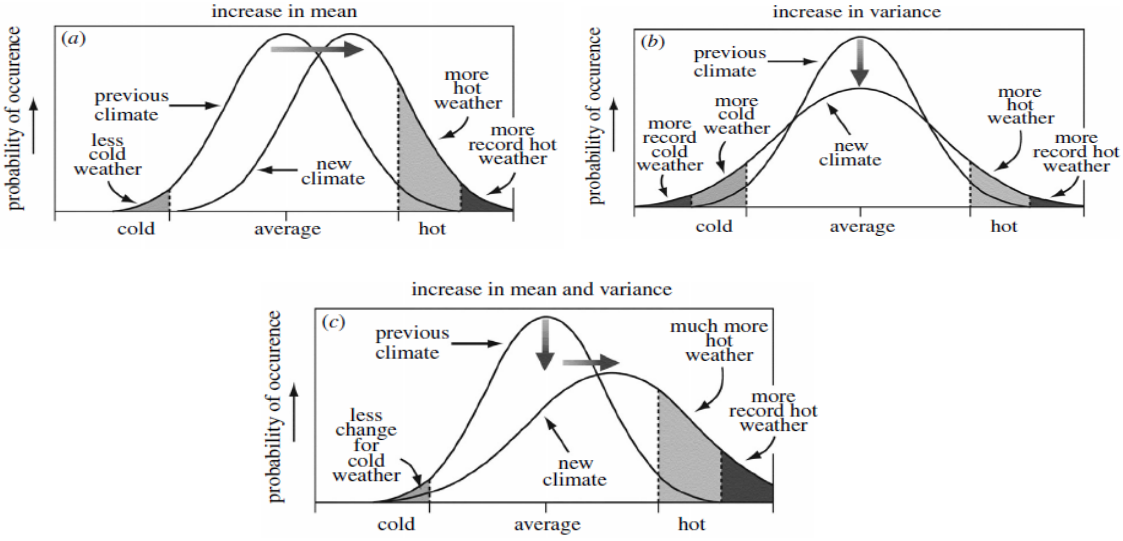

Figure 3 Postulated temperature distribution changes via increases in ***(a)*** mean temperature, ***(b)*** temperature variance and (***c***) in both mean and variance of temperature (Porter and Semenov, 2005).

2.2 Climate changes and climate model projections

2.2.1 Concepts of climate systems, variabilities and changes

According to the World Meteorological Organization (WMO), climate can be defined as the statistical description in terms of mean and variability of relevant quantities over a period of time (typically 30 years) (WMO, 1983). Therefore, climate is the statistical description of weather at a given location, including the likelihood for a range of weather phenomena and states (Arguez and Vose, 2011). For this reason, climate sometimes refers to the average weather. Weather at individual locations is further subject to larger-scale complex interactions between components within the earth climate system, of which comprising the atmosphere, biosphere, land surface, hydrosphere and cryosphere (WMO, 1983). The chaotic processes occurring within the climate system, mainly due to the non-linear interactions between its components, constitute the internal climate variability, which is more pronounced at shorter temporal and smaller spatial scales (Frankcombe et al., 2015; Hawkins and Sutton, 2011). Moreover, the climate system might be forced by external factors beyond internal processes, including natural variations in solar radiation and volcanic eruptions, as well as human-induced alterations to atmospheric composition and land use, a process known as the external climate variability (Frankcombe et al., 2015). Strictly

speaking, the term "climate variability" refers to variations in the mean or any other statistical properties of the climate state, on all temporal and spatial scales, which is often used to measure the deviations of climate statistics over a given period of time (e.g. month, season or year) from the long-term statistics for the same calendar period, namely Climate Anomaly (CA) (WMO, 1983). In contrast, climatic change, according to WMO and its usage by the Intergovernmental Panel on Climate Change (IPCC), is defined as the statistically significant variations in the mean state of climate or its variability, persisting for a long period of time (decades or longer) (IPCC, 2013). It refers to any changes in climate system, caused by either internal variability or external variability. In essence, the conceptual differences between climate variability and climate change consist in the fact that the former looks at changes at smaller timeframes (month, season or year), whereas climate change considers changes for a much larger scale (decades or longer) (WMO, 1983). From a practical viewpoint, the difference can also be interpreted as if the anomalous conditions persist as compared before, i.e. rare events occur more frequently. Care should be taken when attributing individual events to anthropogenic-driven climate change, because a sequence of consecutive anomalous events can even be within the bounds of natural climate variability (Deser et al., 2012). Only a persistent series of unusual events, in the context of broad changes in regional climate parameters, can suggest a potential change in climate has occurred (Deser et al., 2012; IPCC, 2013).

2.2.2 Observed global warming and associated Greenhouse gas emissions (GHG)

This sub-section is based on the Summary for Policymakers chapter that is contained in the synthesis report of the Fifth Assessment Report (AR5) of IPCC, which synthesizes the contributing IPCC working group reports and providing an overview of the state of knowledge concerning the science of climate change (IPCC, 2014). The evidences of human influence on the earth climate system have grown since the IPCC Fourth Assessment Report (AR4), and recent anthropogenic emissions are the highest in history: surface temperature of Northern Hemisphere barely changes in the last 1400 years, except over the recent 30-year period (1983–2012), with widespread impacts on human and natural ecosystems (IPCC, 2013). The observed climate warming is unequivocal, as the global average combining ocean and surface temperatures shows a robust multi-decadal warming of 0.85°C [0.65–1.06°C] over 1880–2012, accompanied by great decadal and inter-annual variability (**Fig. 4a**). This warming occurs despite nearly 60% of total emissions have

already been removed from the atmosphere, either through various natural sinks involved in the carbon cycle (e.g. uptake by plants and immobilization by soil microorganisms) or via energy absorptions in the ocean (IPCC, 2013). Ocean warming dominates the energy increases in our climate system, storing about 30% of emitted anthropogenic CO_2 and accounting for more than 90% of total energy uptake between 1971 and 2010 (IPCC, 2013). This eventually creates ocean acidification, which represents a significant challenge for future sustainable development goals (Harrould-Kolieb and Herr, 2012; IPCC, 2014). The atmosphere and ocean warming have likely affected the global hydrological cycle, causing the retreat of glaciers, increased surface melting of arctic ice sheet and greatly contributing to the sea level increase. Over the period from 1901 to 2010, global mean sea level rose by 0.19 [0.17 to 0.21] m (**Fig. 4b**). The sea level rising rate since the mid-19th century has been larger than the mean rate during the previous two millennia (IPCC, 2013).

More than half of globally averaged surface temperature increase can be explained by the anthropogenic increased GHG emission since the mid-20th century (IPCC, 2014). The GHG emissions have since driven large increases in the atmospheric concentrations of CO_2, CH_4 and N_2O, of which 78% are derived from CO_2 emissions by fossil fuel burnt, cement production and other industrial process, as well as from forestry and other land cover and land use changes (**Fig. 4c, d**). The anthropogenic forced CO_2 emission, mainly driven by population and economic growth, have produced an approximate 40% increase in the atmospheric concentration of CO_2, from about 280 ppm in 1850 to nearly 400 ppm in 2010 (**Fig. 4c**). To attribute human activities to observed climate warming, the recent IPCC Special Report, as part of the IPCC AR6 on the impacts of 1.5°C global warming, provides an estimation of 1°C [0.8–1.2°C] warming that is caused by anthropogenic forcing since the pre-industrial era. The warming rate is likely to continue until reaching 1.5°C between 2030 and 2052 (IPCC, 2018).

2.2.3 CMIP5 simulation experiments and framework

Climate models are the most useful tools for understanding the climate systems and climate changes. A new set of global coordinated climate model experiments was established following the endorsements of World Climate Research Program (WCRP)'s Working Group on Coupled Modelling (WGCM), which initiated the fifth phase of the Coupled Model Intercomparison Project

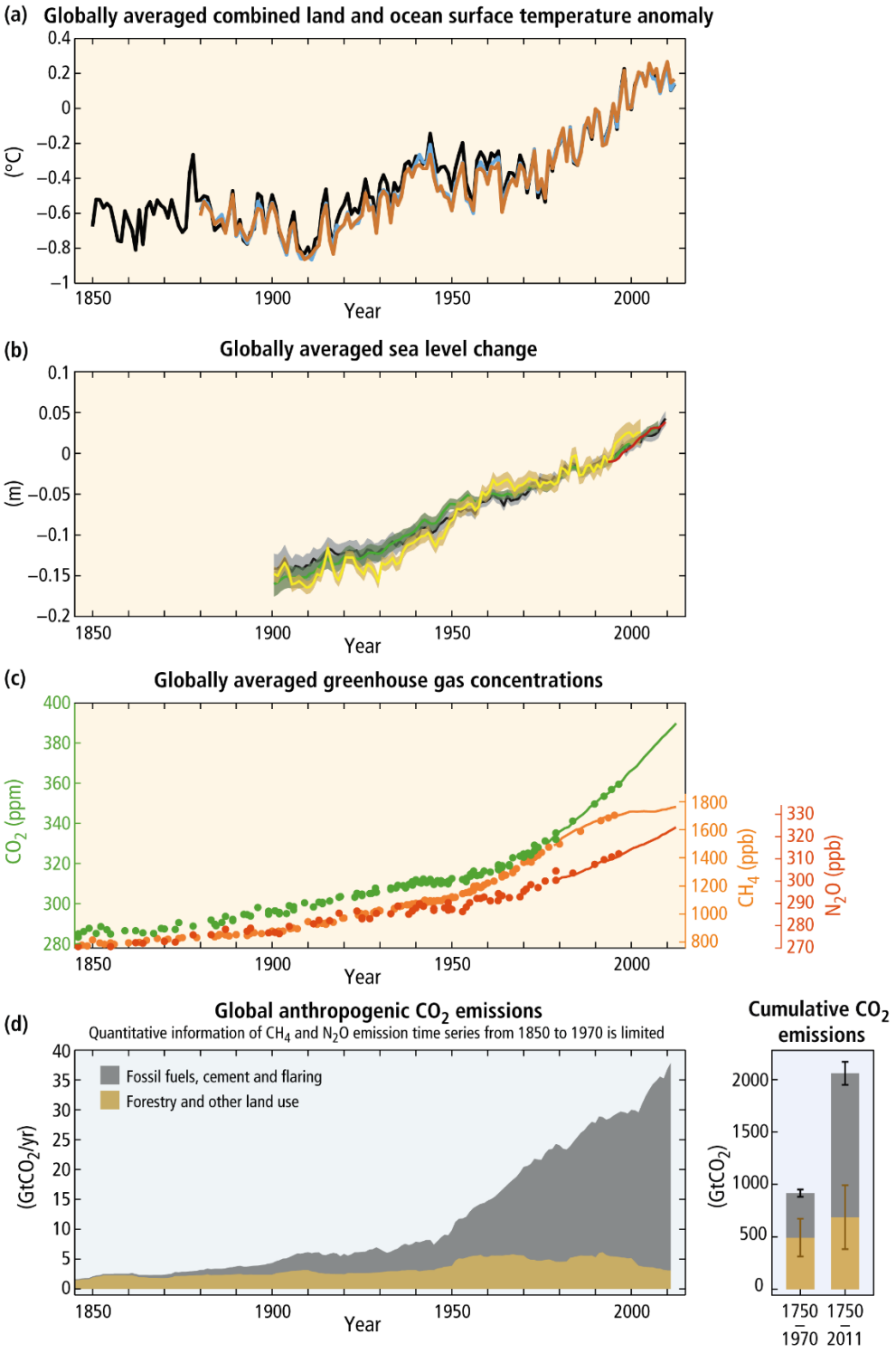

Figure 4 Observed global warming and GHG emissions (colors for different dataset). ***(a)*** Annually and globally averaged combined land-and-ocean surface temperature anomalies relative to the average over 1986–2005. ***(b)*** Annually and globally averaged sea-level change relative to the average of 1986 to 2005. ***(c)*** Evolution of atmospheric CO_2 (green), CH_4 (orange) and N_2O (red). ***(d)*** Global anthropogenic CO_2 emissions from forestry and land use as well as from fossil fuel combustions, cement production, and flaring (the corresponding cumulative CO_2 emission and their uncertainties are shown as bars and whiskers, respectively) (IPCC, 2013; IPCC, 2014).

(CMIP5) (Taylor et al., 2012). In the global coordinated framework of CMIP5, the main tasks consisted of 1) improving the poorly understood processes associated with carbon and cloud cycles, 2) investigating predictive abilities of climate models on decadal to century scales and 3) exploring the cause of underlying differences in the produced range of responses among climate models (Taylor et al., 2012). CMIP5 hence aimed to provide a state-of-art multi-model ensemble context that form the basis for exploring climate change impacts and policy issues of considerable interests, which were used to inform the major assessment activities of IPCC AR5 (IPCC, 2013). The CMIP5 includes two types of model experiments, namely near-term decadal prediction experiments until 2035 and long-term century climate projections until the end of the 21st century and beyond. The entirely new suite of near-term prediction, based on the time-slice approach to integrate recent decadal climate and future climate until 2035, aims to examine the predicative skill of forecast systems on decadal time scales that are still in the exploratory phase (Kirtman et al., 2013; Taylor et al., 2012). For instance, a number of different methods have been tested to assimilate ocean observations into these forecast systems, but no single method has gained widespread acceptance (Taylor et al., 2012). In contrast, the long-term experiments are directly built on the CMIP3 but include additional runs to provide more comprehensive understandings of long-term climate change and variability (Taylor et al., 2012). For these simulations, conventional atmosphere–ocean GCMs and Earth system Models (ESMs) of intermediate complexity are for the first time being joined by more recently developed ESMs in CMIP5, in which a richer set of output fields will be archived (Taylor et al., 2012). These models respond to specified, time-evolving concentration of various atmospheric constituents (e.g. greenhouse gases and aerosols) and land cover changes, producing an interactive representation of the atmosphere, land, ocean and sea ice conditions (Taylor et al., 2012).

2.2.4 Climate change projections and scenarios under CMIP5

For future projections, climate model simulations are performed with pre-defined trajectories of anthropogenic emission and atmospheric concentrations of GHG, aerosols and other drivers, which are the net results of human activities and expressed as climate change scenario (changes in the natural drivers such as volcanic eruptions or solar variations are not included) (IPCC, 2013; IPCC, 2014). The resulting anthropogenic emission scenarios provide crucial emission inputs to climate models for exploring possible responses of our climate system. These scenarios account for a broad

range of evolutions of future population growth, societal-economic development and technological advancement, such as the scenarios developed in the Special Report on Emission Scenarios (SRES) that are used in the IPCC third and fourth assessment reports (Nakicenovic et al., 2000). Future evolution of global GHG emissions and concentrations is highly uncertain, and climate change scenarios are appropriate tools for analyzing the plausible influence of driving forces on emission outcomes that in turn impact climate simulations in GCMs, reflecting our current understandings and knowledge in the existing literature for the underlying uncertainties on how alternative images of future may unfold (Nakicenovic et al., 2000). In the framework of CMIP5, a set of four emission scenarios are formulated, corresponding to the new generation of scenarios, i.e. Representative Concentration Pathways (RCPs) (Moss et al., 2010; van Vuuren et al., 2011). In comparison with SRES scenarios, RCPs do not specify societal-economic changes, but rather assume different pathways to targeting specific Radiative Forcing (RF) in the end of the 21st century, with respect to the pre-industrial level (van Vuuren et al., 2011). The RF corresponds to net changes on the energy fluxes of various well-mixed GHG or other atmospheric constituents: a positive RF leads to a warming surface, whilst a negative value indicates a surface cooling trend (Collins et al., 2006; Shine, 2000). The anthropogenic influences have made a substantial contribution to the GHG emissions, resulting in increased RF and additional energy uptake by surface and ocean (Shine, 2000).

As listed in **Table 1**, RCP8.5 is a business-as-usual high emission scenario, with rapid increases of RF reaching 8.5 W/m^2 in the end of 21st century. Similarly, other assumed emission pathways lead to the target RF of 2.6 W/m^2, 4.5 W/m^2 and 6 W/m^2, corresponding to one mitigation scenario of RCP2.6 and two stabilization scenarios of RCP4.5 and RCP6.0 (Moss et al., 2010) (**Table 1**). In contrast to previous scenarios from SRES (e.g. A1 or A1B), RCPs already represent a range of climate policies for adaptation and mitigation throughout the 21st century undertaken to achieve certain emission targets. These are deemed necessary as extensive uncertainties exist in future forcing of and responses to climate change, necessitating the use of future scenarios to explore the potential consequences of different response options (Moss et al., 2010; Taylor et al., 2012; van Vuuren et al., 2011). It should also be noted though that RCPs span a wide range of total forcing values, they do not cover the full range of emissions in the literature, particularly for aerosols (IPCC, 2014).

Table 1. Overview of four Representative Concentration Pathways (RCPs) (Moss et al., 2010; van Vuuren et al., 2011).

RCP scenarios	Radiative forcing	CO_2 equivalent concentration (ppmv)	Pathway	Scenario category
RCP2.6	Peak at ~3 W/m^2 before 2100 and decline afterwards	Peak at ~490 before 2100 and decline afterwards	Peak and decline	Mitigation
RCP4.5	~4.5 W/m^2 at stabilization after 2100	~650 stabilization after 2100	Stabilization without overshoot	Stabilization
RCP6.0	~6 W/m^2 at stabilization after 2100	~850 stabilization after 2100	Stabilization without overshoot	Stabilization
RCP8.5	>8.5 W/m^2 in 2100	>1370 in 2100	Continuous rising	High-emission

Note: The approximate radiative forcing levels were defined as ±5% of the stated level relative to pre-industrial levels. The radiative forcing are net effects of all anthropogenic GHG and other forcing agents

2.2.5 Regional climate projections and EURO-CORDEX

A new generation of more complex GCMs employed in CMIP5 are expected to provide more detailed and accurate climate projections, with projected spatial patterns of global temperature and precipitation changes rather consistent among models (Knutti and Sedláček, 2012). However, the exercises of risk assessments of climate change impacts and development of local-to-regional adaptation strategies highlight the need for availability of high-resolution climate projections. It is evident that the relatively coarse spatial resolutions of CMIP5 models, mostly GCMs or ESMs ranging from 0.5° to 4°, are insufficient to meet the research needs for a broad range of climate-related disciplines, such as hydrological modelling at river basins (Yang et al., 2010) or crop modelling at field scales (Yang et al., 2019).

Within the European branch of the global Coordinated Regional Downscaling Experiment (EURO-CORDEX), a number of fine-resolution RCMs, implemented over an European domain at 50 km (EUR-44) or 12.5 km (EUR-11), were employed to dynamically downscale the corresponding GCMs simulations from CMIP5 under four RCP scenarios (Jacob et al., 2014). More emphasis are placed on EUR-11 as it stands for the finest spatial resolutions of climate projections to date. The added value of using RCMs can be reflected by better representations of present-day climates and more relevant and accurate projections of future climate, resulting from more detailed descriptions of geographic features and sub-grid scale parameterization schemes (IPCC, 2015; Jacob et al., 2014). It is also frequently noted that the added value are more likely to occur for precipitation than for temperature, as regional precipitation change signals simulated by

RCMs tend to show substantial orographically-induced fine scale structure that is absent in GCMs (Di Luca et al., 2012; Giorgi and Lionello, 2008).

2.2.6 Bias Correction and Delta Change

There are growing demands for regional climate information to be used in impact models that provide crucial downstream inputs for decision-making. However, despite the fine-resolution climate data generated by GCMs-RCMs, such information still contains a number of uncertainties that cannot be directly used by impact models, as the latter often require high resolution unbiased inputs (Maraun, 2016). For instance, there is often a historical control period defined for GCMs-RCMs simulations using measured atmospheric concentrations of GHG, but some limitations should be expected regarding the estimated climate statistical properties of important meteorological variables (e.g. temperature and precipitation), such as sub-daily, daily, monthly and seasonal means or standard deviations (Yang et al., 2010). Regardless, all climate models are an approximation and simplification of the real climate system, applying different physical parameterization schemes and numerical approaches (IPCC, 2015). Alternatively, Empirical Statistical Downscaling (ESD) can be used to provide statistical downscaling of GCMs outputs, which calibrate model simulations against observations according to the exploited dependencies between large and small scales of different climate variables, such as temperature and precipitation (Maraun et al., 2015). But some of these statistical approaches do not provide reliable climate change trends (Maraun, 2016).

Bias correction (BC) has become an integral part of pre-processing of climate model simulations prior to being used by impact models. The correction factors are derived by comparing RCMs simulations during the reference (baseline) period with observations, which are then applied to projections for a future period, a technique in meteorology known as model output statistics that has been extensively used to correct weather forecasts (Yang et al., 2010). As future climate change is expected not only to influence mean climates, but also to modify the frequency and intensity of extreme weather events (Moriondo et al., 2011), BC is known to better preserve future climate variability produced by individual RCMs and to take into account the covariance between temperature and precipitation, resulting in improved usability by climate change impact studies (IPCC, 2015; Yang et al., 2010). It should be noted that BC is generally a post-statistical approach absence of any physical arguments, but it could potentially alter climate change signals compared

to non-adjusted climate projections (Maraun, 2016; Maurer and Pierce, 2014). Various BC methods, such as quantile mapping (Piani et al., 2010) or distribution-based scaling (Yang et al., 2010), are yet to be thoroughly assessed by climate science communities. Guidance on BC availability, use, interpretation, limitation and uncertainty in the broad context of other possible post-processing techniques, shall be well elaborated in the upcoming 6th assessment report of IPCC (IPCC, 2015).

Similarly, future time series of climate data can also be constructed by perturbing observational records of reference period with projected long-term mean changes (or changes factors) simulated by RCMs, an approach conventionally called Delta Change (DC) (Hay et al., 2000; Ruiter, 2012). The long-term differences (e.g. temperature) or ratios (e.g. precipitation and radiation) between mean values in the historical run and future periods, are calculated on monthly or seasonal basis by individual GCMs-RCMs chains and added to the observed weather records (Ruiter, 2012). Clearly, one major flaw of DC is the rough assumption that variance of future climate has kept the same as in the historical period, which is unlikely true (Hay et al., 2000; Yang et al., 2010). The covariance between weather variables (e.g. temperature, radiation and precipitation) is artificially weakened when DC is implemented separately (Yang et al., 2010).

2.2.7 Observed climate and climate change projections in Portugal

Situated in southern Europe, Portugal is a Mediterranean country, with typically mild and rainy winters and warm and dry summers. The mean annual temperature varies between 2°C in the inner highlands of central Portugal and 18°C in the southern coast, whilst the mean annual precipitation is around 900 mm, with a strong northwest–southeast gradient (e.g. 3000 mm in the northwestern mountains and below 400 mm in the southernmost parts) (Carvalho et al., 2014).

The observed climate conditions in the second half of the twentieth century show a warming and drying trend over mainland Portugal, with increases in both maximum and minimum temperatures (Espírito Santo et al., 2014; Páscoa et al., 2017). The analysis of the temperature trend shows a cooling period over 1945–1975, followed by a significant and widespread warming during 1976–2006 (Espírito Santo et al., 2014). The annual mean temperature increased by 0.52°C per decade during 1976–2006, which is more than double the rate of mean annual global temperature increase (Carvalho et al., 2014; Ramos et al., 2011). Heat waves have become more frequent since the beginning of this century (e.g. occurred in 1981, 1991, 2003, 2006, 2009 and 2010), and eight of

the ten warmest years occurred in the last 20 years (e.g. 1997 is the warmest year since 1941) (Carvalho et al., 2014). The precipitation distribution in Portugal shows strong seasonality and inter-annual variability (Mourato et al., 2010), mostly concentrating in winter from December to February, with ~7% in summer from June to August (Carvalho et al., 2014). There is evidence of a generalized decrease of spring precipitation since 1970, with an opposite wetting trend for autumn precipitation (Santo et al., 2014). In the last 30 years, the drying trend has become particularly pronounced in mainland Portugal (e.g. 2005 was the driest in the last 78 years, followed by 2007 and 2004), with severe droughts occurring in 2004–2005 and 2011–2012 (Carvalho et al., 2014). This observed drying trend is more noticeable in southern Portugal, where prolonged dry spells and a tendency toward arid climatic conditions during 1955–1999 are detected (Costa and Soares, 2009; Mourato et al., 2010). Consequently, decreased precipitation, coupled with increased atmospheric evaporative demand caused by rising temperature, has been widely associated to the observed increase in drought severity in Portugal and the Iberian Peninsula (IP), which might be aggravated in future climate (Páscoa et al., 2017; Vicente-Serrano et al., 2014). Numerous independent studies using outputs from a broad range of climate models, indicate a robust climate change signal for continuous warming and drying trend, accompanied by greater frequency and intensity of extreme weather events, such as number of hot days >35°C and severe drought (Carvalho et al., 2014; Costa et al., 2012; Fraga et al., 2012; Miranda et al., 2002; Ramos et al., 2011; Santos and Miranda, 2006). However, these studies differ in terms of the extent of the increase in temperature and of the decrease in precipitation. To contribute to a reduction of these uncertainties, we have recently developed climate change projections over 2021-2080 in southern Portugal (Alentejo) (Yang et al., 2019) (**Fig. 5**), based on the multiple bias-corrected outputs of fine-resolution GCMs-RCMs simulations (~12.5 km) within the framework of EURO-CORDEX (Jacob et al., 2014). The multi-model ensemble mean simulations in Alentejo show that average annual mean temperature is projected to increase by 0.6–1.5°C in 2021–2050 and by 1.5–2.7°C in 2051–2080 in comparison to mean baseline temperature over 1981–2010, with a more pronounced increase under RCP8.5 than in RCP4.5 (**Fig. 5a**). Similarly, average annual precipitation is projected to decrease by –12% to –3% in 2021–2050 and by –18% to –12% in 2051–2080, depending on the RCP (**Fig. 5b**).

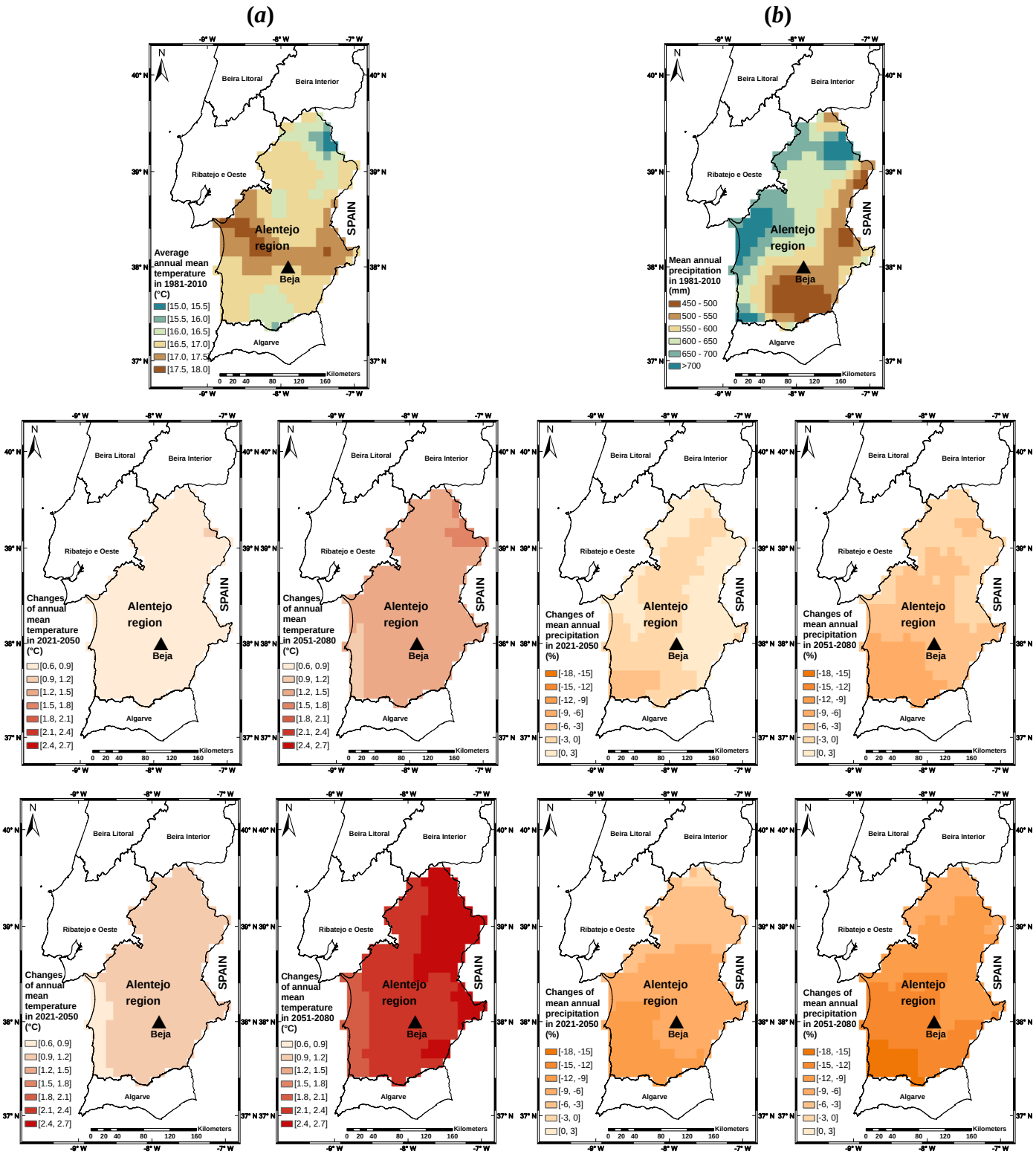

Figure 5 Simulated average annual ***(a)*** mean temperature (°C) and ***(b)*** precipitation (mm) over baseline along with their corresponding changes by climate projections over 2021-2080 under RCP4.5 (middle panels) and RCP8.5 (bottom panels) in Alentejo region (Southern Portugal) as represented by multi-model ensemble means of bias-corrected GCM-RCM outputs from EURO-CORDEX (Jacob et al., 2014; Yang et al., 2019).

2.3 Modelling crop response to climate change and adaptation exploration

2.3.1 Statistical crop models (SCMs) vs dynamic crop models (DCMs)

Traditional agricultural research has focused on pot, glasshouse trials or field experiments, where crop production functions in relation to environment factors were derived from statistical analysis, without referring to the underlying detailed biophysical processes (Oteng-Darko et al., 2013). The application of correlation and regression analysis into field data has provided some qualitative understandings of cropping systems that help advance the agriculture science. One practical example is to summarize observed relationship between weather input and crop yield outputs, which is frequently used in Statistical Crop Models (SCMs) for predicting crop yield response to changes in the seasonal weather and examining projections for future yields (Challinor et al., 2014; Lobell and Burke, 2010; Shi et al., 2013). However, the quantitative information obtained from SCMs are site-specific and very limited, in which the corresponding findings are only relevant for other sites with similar range of weather variations (e.g. usually required more than 10 years of weather data to capture inherent variability) and agronomic conditions (Oteng-Darko et al., 2013). Further, in analysing crop yield response to climate change, SCMs do not properly resolve the covariance between weather variables (e.g. temperature and radiation). In addition, they are not able to explicitly incorporate adaptation effects for more comprehensive evaluations (Shi et al., 2013). These identified limitations greatly hinder the quantitative applicability of regression-based SCMs for decision-making.

The process-based crop models or Dynamic Crop models (DCMs), based on ecophysiology knowledge and a wide range of empirical relationships, have proven to be useful tools to simulate the complex interactions between Genotypes, Management and Environment (G × M × E), which are difficult to be captured by site-specific field trials (Rotter et al., 2018; Rotter et al., 2015). These models are frequently used to assess the impacts of G × M × E interactions on crop yield potential, phenology and crop water use in response to environment changes (Rotter et al., 2015). In agricultural research, they have been proposed as possible tools for multiple practical applications, including the potential to develop and optimize agronomic practices for sustainable intensification of agriculture systems (Debaeke, 2004; Urruty et al., 2017), support for aiding in ideotype design and breeding of future cultivars (Batley and Edwards, 2016; Rotter et al., 2015), as well as use of multi-model ensemble for climate change risk assessment and explore adaptation options to better inform farmers and decision-makers (Asseng et al., 2014; Asseng et al., 2013;

Challinor et al., 2014; Ewert et al., 2015; Rosenzweig et al., 2013; Seidel et al., 2018). In particular, recent research efforts for modelling adaptations to multiple climate-induced risks (Challinor et al., 2018) have focused on integrated strategies by modifying cultivar traits with management adjustment, in order to deal with potentially enhanced heat and drought stress during sensitive crop growing cycles (e.g. anthesis and grain-filling), associated with projected increases of climate variability and frequency and severity of adverse extreme weather events (Moriondo et al., 2011; Rotter et al., 2015; Ruiz-Ramos et al., 2018). For instance, for wheat production in the Mediterranean South Environment zone of Spain, an ensemble of 17 dynamic crop models are used to build up the adaption response surface, concluding that effective local adaptions should be based on the combination of supplementary irrigation, early sowing date and spring wheat cultivars without vernalization requirement (Ruiz-Ramos et al., 2018).

DCMs are an integration of our current knowledge on crop growth and development originating from various disciplines, including crop physiology, agronomy, agrometeorology and soil science, which are structured in a consistent, quantitative and process-oriented manner (Oteng-Darko et al., 2013). In particular, DCMs contain a set of mathematical equations to characterize the influence of various explanatory variables on several outputs of agronomic interest (e.g. grain yield and N content, total biomass and water drainage) (Seidel et al., 2018), enable quantitatively combining climate, crop, soil and management practices to simulate or imitate the real crop behaviour. As for SCMs, they are largely constrained by availability of adequate, representative yield data, and lack information on the crucial interaction derived from weather-management-soils (Rotter et al., 2018). In contrast, DCMs not only predict the final state of crop production or harvestable yields, but also contain quantitative information about underlying biophysical processes occurring in the cropping system (Brisson et al., 2009; Oteng-Darko et al., 2013; Rotter et al., 2018). Moreover, the restricted applicability only to the historical range of weather variations where statistical models are trained, are not reflected in dynamic modelling, given the robust empirical relations between crop behaviours and environment variables (depending on model structures, formalisms and parameterizations). This capability warrants a more consistent and reliable climate change impact assessment with respect to the uncertainties of changes in climate variability.

However, in no way should we determine that dynamic crop models perform better than statistical models, but comparative analysis of both approaches will surely stimulate the discussions and improve the understandings of major yield limitations at higher aggregation level (Rotter et al.,

2018). As such, SCMs continue to play a prominent role in hinting at the mechanisms and relationships that are not sufficiently covered in DCMs. By attributing observed yield variability to a few simplified measurement of climatic variables (e.g. mean temperature or precipitation), SCMs inherently integrate yield limiting factors that DCMs largely have ignored, namely pest and disease damages and weed infestation (as the actual yield might include impacts of these factors), thus possibly leading to inaccurate estimation of crop yields by DCMs in regions where biotic stress are significant (Rotter et al., 2018). On the other hand, DCMs are able to entangle and quantify contributions of more important yield-limiting factors at some certain environments (such as the heat and drought stress during critical growth stages), which could in turn help to improve SCMs. In one rare example, it has demonstrated that combined use of both SCMs and DCMs would enhance the reliability of evaluation results by complementing each other in estimating yield response to climate changes: SCMs were firstly trained on the simulated historical maize yield variability by DCMs of CERES-Maize model at nearly 200 sites in Sub-Saharan Africa, before estimating the yield response to changes in mean temperature and precipitation (Lobell and Burke, 2010).

2.3.2 Uncertainties in dynamic crop model predictions

Despite the well-known advantages of process-based crop models, uncertainties in model simulation have been identified (Asseng et al., 2013; Seidel et al., 2018; Wallach and Thorburn, 2017). The DCMs prediction uncertainty is defined as the distribution of prediction errors that is written as the sum of prediction bias between simulation and observations, plus a predictor error term that represents the random variations due to uncertainties in model structure, input values and parameter sets (Seidel et al., 2018; van Oijen and Ewert, 1999; Wallach and Thorburn, 2017). The structural uncertainty mainly arises from the fact that no single model could include all relevant explanatory variables and describe all underlying bio-physical processes within a defined cropping system, or the formalisations (mathematic equations) and parameterization schemes are not robust enough in reproducing observations (Seidel et al., 2018). Input uncertainty is largely caused by sampling errors of observed variables or limitation in data availability (Seidel et al., 2018; Wallach and Thorburn, 2017). Similarly, measurement errors and insufficient data are also the source of uncertainties in the estimation of parameter values, plus a source of variability due to different methods and approaches chosen in calibrating the models (Wallach et al., 2011; Wallach et al.,

2012). Complex mathematic structures in the model, such as non-linearity, discontinuity and intricate correlation among numerous outputs, lead to the fact that no standard statistical method or software exist to crop model calibration procedures (Wallach et al., 2018).

Consequently, different models differ substantially in the way they simulate the dynamic processes, resulting in large disparities about evaluated climate change impacts with even the same conditions (Asseng et al., 2013; White et al., 2011). In the context of modelling crop yield response to climate change, a landmark study published in nature using 27 different DCMs and 16 climate models at four contrasting wheat growing environments, concluded that a great proportion of uncertainties in projected climate change impacts was due to variations of crop models than to variations among downscaled GCMs (Asseng et al., 2013). Asseng et al. (2013) further suggested that uncertainties could be reduced by continuous improvement of models, particularly for improving the relationship between temperature and CO_2 functions. However, Wang et al. (2018) argues that climate projections in their study were based on the Delta Change (DC) approach using downscaled GCM outputs, without accounting for the potential changes in climate variability, thus possibly narrowing the wide range of uncertainty that potentially exists in climate projections.

2.3.3 Categories of process-based crop models

The relevance of DCMs (hereafter crop models) in agronomy research was once doubted, as considerable debates exist as to whether the mathematic descriptions of complex physical, physiological, morphological processes within a cropping system would be accurate and reliable enough (Oteng-Darko et al., 2013). However, the practice of crop modelling has undergone an important evolution in recent years, with growing practical applications in decision support and risk assessment, of which the improvement also contribute to the progress of agriculture research (Challinor et al., 2018). Much of this progress has been undertaken by several pioneering research projects, such as the Agricultural Model Intercomparison and Improvement Project (AgMIP) (Rosenzweig et al., 2013), Inter-Sectoral Impact Model Intercomparison Project (ISIMIP) (Warszawski et al., 2014) and European knowledge hub on Modelling European Agriculture with Climate Change for Food Security (MACSUR) (Bindi et al., 2015). These projects consistently highlight the need for the use of multi-model ensembles to quantify the uncertainties among crop models and make the predictions more robust and reliable. Although the major goal is to have a more balanced viewpoint on prediction error and the predictor uncertainty (Wallach and Thorburn,

2017), the coordinated, standardized and objective multi-model ensemble simulations are enormously challenged when undertaken by a single research team.

No one universal crop model exists in the agriculture field, and it is always necessary to adapt the system definitions, simulation processes and model formalisations to specific problems or situations (Brisson et al., 2003). In general, a crop model simulates the crop development and growth process, as well as the water and nitrogen (some models do not consider the N effects) balance of the cropping system on a daily time-step. It can estimate both agricultural variables (e.g. crop grain yields and N content, biomass) and environmental variables (e.g, soil water and drainage, N leaching amount, not available in some models), by taking into account the interactions from weather-crop-soil-management practices (Coucheney et al., 2015). The upper boundary of the system is the atmosphere, which is characterized by several relevant weather variables (e.g. temperature, radiation, rainfall, wind speed, relative humidity or other forms of humidity), whereas the lower boundary corresponds to the soil/sub-soil interface (Brisson et al., 2009). Crops are generally perceived in terms of phenology stages, Leaf Area Index (LAI), above-ground biomass and biomass of harvest organs (such as grains or fruits). Many models have conducted a sequential simulation process where temperature drives phenology development rate, which in turns determine LAI development that influence biomass formations and followed by its partitions into various organs (e.g. grains) (Brisson et al., 2009; Jamieson et al., 1998; Jones et al., 1991; Jones et al., 2003; Keating et al., 2003; Ritchie et al., 1985; Stöckle et al., 2003; van Diepen et al., 1989). Different modelling approaches in parameterization are adopted among these models, and could possibly lead to different sensitivity of climate change impacts (Challinor et al., 2018). As a generic framework and listed in **Table 2**, the most frequently used process-based DCMs are distinguished and organized into three categories depending on how these growth models estimate net photosynthesis and biomass production rate from captured source, such as carbon dioxide, radiation and water (and nutrients) (Abedinpour et al., 2012). Surely, there are other classification methods depending on how these model simulate several important growth processes (LAI development or yield formations) according to their objectives (Asseng et al., 2013), but net photosynthesis is widespread perceived as the most important crop growth process that is also the basis for final yield determination. In fact, the simulation of yield formation process is very different among models (Abedinpour et al., 2012). Accordingly, the first category corresponds to the (i) carbon-driven models, where a traditional net photosynthesis concept is prescribed for

biomass accumulations, computing the balance between gross photosynthesis and respiration; (ii) water-driven models, where models associate net photosynthesis with water uptake, by assuming a near-linear relationship between transpiration rate and biomass growth rate (an overall small number of models in this category); (iii) radiation-driven models (highest number of existing models fall within this category), where net photosynthesis and corresponding daily biomass production rate are estimated from canopy intercepted radiation, following a radiation (light) use efficiency approach (**Table 2,** note some models adopt mixed simulation strategies).

Table 2. Categories of crop models based on their net photosynthesis growth engines (asterisks indicate models with mixed approaches).

Model class	Modelling approaches for net photosynthesis	Categorized crop growth models
Carbon-driven models	Balance between gross photosynthesis and respiration	*GECROS** (Stenger et al., 1999) *HERMES* (Kersebaum, 2007) *LPJmL* (BONDEAU et al., 2007) *MCWLA* (Tao et al., 2009) *SUCROS* (Goudriaan and Van Laar, 2012) *WOFOST* (van Diepen et al., 1989)
Water-driven models	Associations of net photosynthesis with water uptake, i.e. transpiration	*AquaCrop* (Steduto et al., 2009) *CropSyst* (Stöckle et al., 2003) *GECROS** (Stenger et al., 1999) *GLAM** (Challinor et al., 2004) *OLEARY* (O'Leary et al., 1985)
Radiation-driven models	Transformation of canopy intercepted photosynthetic active radiation into biomass prescribed by Radiation Use Efficiency (RUE)	*APSIM* (Keating et al., 2003) *DSSAT* (Jones et al., 2003) *Expert-N-CERES* (Biernath et al., 2011) *EPIC* (Jones et al., 1991) *GLAM** (Challinor et al., 2004) *InfoCrop* (Aggarwal et al., 2006) *LINTUL4* (Spitters and Schapendonk, 1990) *MONICA* (Nendel et al., 2011) *SALUS* (Basso et al., 2010) *Sirius* (Jamieson et al., 1998) *STICS* (Brisson et al., 2009)

2.3.4 A brief overview of STICS model

As previously mentioned, my PhD research is committed to using the STICS (Simulateur mulTIdisciplinaire pour les Cultures Standard) crop model. Therefore, a brief description of STICS model, in terms of how the model simulates important development and growth processes, is presented in this section. This is important for model users to understand the mechanisms behind the simulated outputs and carry out the sensitivity analysis accordingly. More detailed information

is available in Brisson et al. (1998); Brisson et al. (2002); Brisson et al. (2003); (Brisson et al., 2009). In particular, please refer to Brisson et al. (2009) for a thorough and more comprehensive documentation of theory, system definitions, underlying formalizations and parameterization schemes. The whole model software platform and a list of relevant documentations are freely available at http://www6.paca.inra.fr/stics_eng/.

STICS is a soil-crop model developed by the French National Institute for Agricultural Research (INRA) since 1996 in collaboration with many other research institutions worldwide (Brisson et al., 2003). It was initially parameterized for cereal crops such as wheat and maize (Brisson et al., 1998; Brisson et al., 2002), but soon adapted to many other crops such as grassland and other perennial crops (e.g. grapevine) (Brisson et al., 2003). Compared to other crop models, STICS is made up of a number of original parts, which include the use of iteratively calculated crop temperature and enable considerations of many special farming management techniques (e.g. plastic or crop residue mulching, various forms of forage cuttings, winter pruning for woody crops) (Brisson et al., 2009). However, the remaining parts, especially with respect to ecophysiology principles, are taken from conventional formalizations of many other preceding crop models. The three strong points are (i) model generic, adaptability to a wide range of crops according to whether crops have determinate (vegetative and reproductive growth occurs successively, e.g. wheat, maize, soybean and sorghum) or indeterminate growth pattern (vegetative and reproductive growth occurs simultaneously or partly, e.g. tomato, potato, forage grass and grapevine); (ii) modularity that enable adding new modules to complement system descriptions to facilitate subsequent model development; (iii) its robustness, with the ability to simulate various agro-climatic conditions (including Mediterranean climate) without significant biases using its standard parameters. This aspect has been recently re-affirmed, exhibiting particularly high performance for soil water content (10%), followed by plant biomass (35%) and N content (33%) in terms of normalized Root Means Square Error (nRMSE) (Coucheney et al., 2015).

2.3.5 Key mathematic equations used in STICS model parameterization

The STICS model is organized into modules: a first set of three modules deals with the ecophysiology of above-ground parts (phenology, shoot growth, yield formation), while the second set of four modules tackles soil water and nitrogen transfer and balance together with the function of root growth and distribution (i.e. water and N absorber) (**Fig. 6**). In addition, the

microclimate module simulate the combined effects of climate and soil water balance on crop canopy temperature and humidity that in turn drive the phenology development (**Fig. 6**). Lastly, the crop management module specifically handles the interaction between the applied techniques and the soil-crop-microclimate system (**Fig. 6**). Within each module, there are submodule and options that can be used to extend the scope of applicability of STICS to various cropping system. The following section will focus on the aboveground growth modules only, as they directly relate to crop growth and development processes and offer a quick look at the underlying ecophysiology principles.

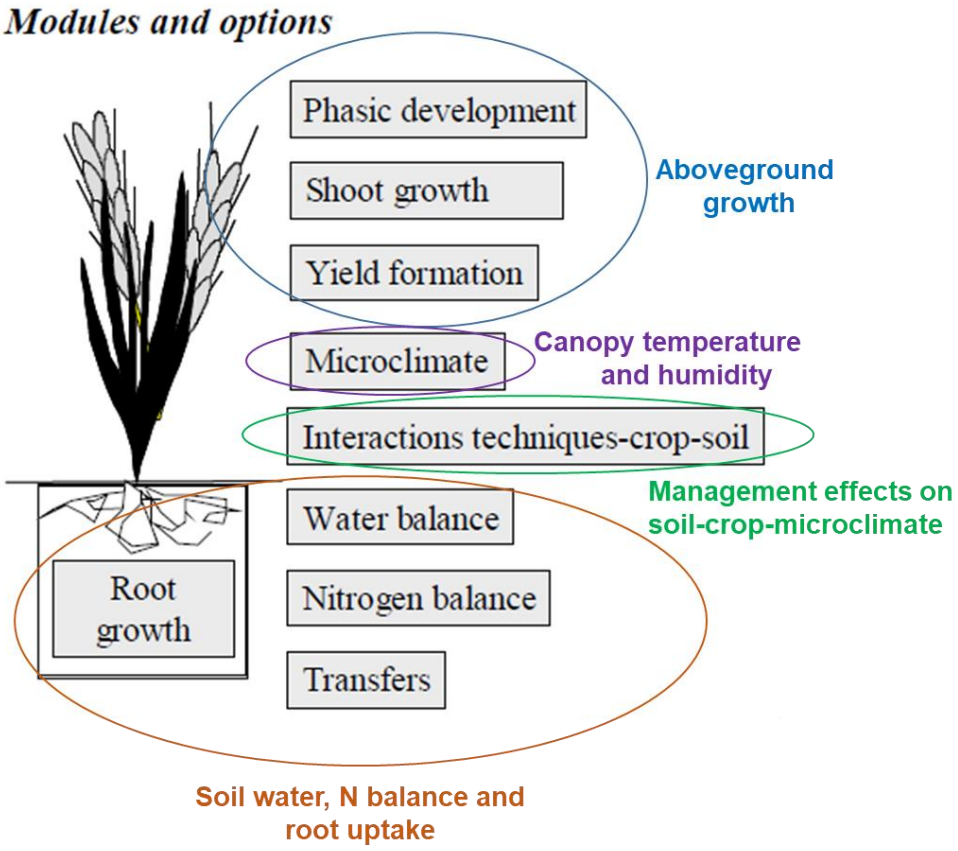

Figure 6 Main modules of STICS soil-crop model.

In **equation 1**, calculations of crop phenology development rate is given. The crop development is mainly driven by accumulation of effective temperature using the thermal index of Growing Degree Days (GDDs) with different base temperatures depending on the crop species. Depending on the plant type, it is also possible to consider influences of photo-thermal index (photoperiod

and vernalization) on the phasic course. Besides, crop development progress can be delayed in case of water and nitrogen stresses. It is also noteworthy that for more detailed descriptions on functions of individual component with each equation, please refer to Brisson et al. (2009).

Equation (1)-Phenology: $UPVT\ (I) = UDEVCULT(I) \times RFPI(I) \times RFVI(I) \times (STRESSDEV \times \min(TURFAC(I), INNLAI(I)) + 1 - STRESSDEV)$.

Where *I* within the parentheses refer to a given day of the growing season, *UDEVCULT* stands for the triangular function of GDD, *RFPI* and *RFVI* are the photoperiod and vernalization index respectively, varying from 0 (completely halt of development) to 1 (no effects). *TURFAC* and *INNLAI* are water and nitrogen stress respectively, which are specifically used for development dynamics. *STRESSDEV* is an optional parameter that represents active or inactive for water and nitrogen stress effects. It should be noted this function is only applicable after crop emergence, whereas a different function is used for development rate during germination and emergence.

Phenology development rate subsequently drives leaf growth and LAI dynamics, but the net leaf growth rate is the product of gross growth (**equation 2)** and leaf senescence (**equation 3)**. **Equation 2** reveals how simulated LAI evolution in canopy scale responds to development progression, influence of canopy temperature (or incidentally thermal stress damages), inter-plant competition to decrease surface leaf area and environment conditions (water and nitrogen stress).

Equation (2)-LAI dynamics (gross growth): $DELTAI(I) = DELTAI_{dev}(I) \times DELTAI_{T}(I) \times DELTAI_{dens}(I) \times DELTAI_{stress}(I)$.

Where $DELTAI_{dev}$ describes a logistic curve with prescribed asymptote and inflexion point of dynamics that can be modified, which is driven by *UPVT* from the development module. $DELTAI_{T}$ corresponds to the effective crop temperature accumulated in the canopy. $DELTAI_{dens}$ represents the empirical plant density-dependent function. $DELTAI_{stress}$ adopts the relatively severer effect between water and nitrogen stress from involved *TURFAC* or *INNLAI*. Note that a maximum threshold of LAI growth rate per unit of biomass accumulation is introduced to associate leaf expansion with shoot biomass accumulation rate, aiming to account for trophic effects and avoid unrealistic simulations.

In **equation 3**, leaf senescence is described. In STICS, shoot senescence only concerns leaf where the LAI and the part of accumulated dry matter amount starts to disappear once the senescence is elapsed. To calculate the onset of senescence, the concept of lifespan is employed to explicitly distinguish natural senescence due to aging and senescence accelerated by stress (e.g. water and nitrogen stress and frost damages) (**equation 3)**. The natural leaf lifespan is calculated from the date that leafs are emitted and it is assumed to linearly increase from the end of juvenile phase until a constant value at the stage of maximum LAI, which is specified as a genotype-dependent parameter. The natural lifespan, however, could be possibly reduced in the events of water and nitrogen stress or frost damages (consider the interaction by adopting the severest effect). The resulting calculated dynamic threshold (considered as the plant vigour limit) of leaf lifespan will then be directly compared to the actual accumulation of lifespan (thermal-time) by crops. In this comparative analysis scheme, if the accumulated lifespan exceeds the dynamic lifespan threshold, senescence occurs and the LAI and part of biomass produced on a given senescence day will be lost. However, senescent losses of LAI and biomass are reversible if the lifespan threshold on a given day becomes higher than the accumulated lifespan (this is possible when stresses are relieved during a period of time when crop lifespan accumulation is very close to this threshold).

Equation (3)-LAI dynamics (leaf senescence): $DURVIE\ (I) = f(DURAGE_0) + f(SENTRESS);\ SOMSEN(I) = 2\hat{}(UPVT(I)/10);\ If \sum_{I0}^{I} SOMSEN(I) > DURVIE,\ DELTAI\ and\ DLTAMS$ on a given day made disappear and reduced, respectively.

Where *DURVIE* represent the dynamic lifespan threshold combining $f(DURAGE_0)$ corresponding to the natural leaf aging function involving a cultivar dependent parameter, with $f(SENTRESS)$ corresponding to the stress function involving water and nitrogen stress effect, and frost damage. *SOMSEN* refers to the actual accumulated life span associated with phenology development module (*UPVT),* but expressed as an exponential function (cumulative Q10 units). *DELTAI and DLTAMS* are LAI and biomass growth rate, respectively.

Leaf growth and expansion make possible the calculations of canopy intercepted photosynthetic active radiation, forming the basis for biomass production calculations. In **equation 4**, canopy interception of radiation available for biomass transformation is presented. Crop canopy is

assumed to be a homogeneous environment with random distributions of leaves, thus allowing the direct use of Beer´s law.

Equation (4)-Radiation interception: $RAINT\ (I) = 0.95 \times PARSURRG \times TRG\ (I) \times (1-exp\hat{}(-EXTIN \times LAI\ (I))$

Where *PARSURRG* represents the classic astronomic ratio of surface photosynthetic active radiation to global radiation (default of 0.48 subject to modification). The *TRG(I)* represents the surface shortwave radiation coming from weather variable input. The *EXTIN* is the extinction coefficient used in the Beer´s law: the more erect the plant, the smaller is the extinction coefficient. Transformation of canopy intercepted radiation into aerial biomass is achieved using **equation 5**. The linear relationship between biomass accumulation rate in the plant and radiation intercepted by foliage leads to the definition of Radiation Use Efficiency (RUE) as the slope of this relationship. RUE has been widely used in many crop models for its simplified approach to synthesize gross photosynthesis and respiration, while exhibiting its robust relationship over a wide range of environments. However, RUE is likely to vary with different growth stages and environmental conditions. To account for this aspect, RUE is proposed as a physiologic function in STICS model that varies depending on the stages, taking into account various factors known to influence the elementary photosynthesis and respiration processes (temperature, water, nutrients and CO_2 concentrations) (**equation 5)**.

Equation 5-Biomass growth: $DLTAMS = [EBMAX\ (I) \times RAINT\ (I) - COEFB \times RAINT\ (I)^2] \times FTEMP\ (I) \times SWFAC\ (I-1) \times INNS\ (I-1) \times EXOBIOM\ (I-1) \times FCO2 + DLTAREMOBIL\ (I)$

Where *DLTAMS* is the daily biomass production rate, calculated as the function of intercepted photosynthetic active radiation (*RAINT*), maximal RUE (*EBMAX*) of a crop species on the given stage, which could be reduced in the case of sub-optimal temperature conditions (*FTEMP*), water stress (*SWFAC*) and water-logging effect (*EXOBIOM*) as well as nitrogen stress (*INNS*). The *COEFB* stands for the radiation saturation effect that can be observed on individual leaf scale when calculations are made on daily scale. Higher atmospheric CO_2 concentrations can stimulate photosynthesis and result in higher biomass production, which is expressed using an exponential

relationship within *FCO2*. In perennial woody crops, such as grapevine, daily biomass accumulation can be complemented by remobilized perennial reserve (*DLTAREMOBIL*).
During the period of grain filling, the accumulated biomass begins to partition into harvest organs (grains or fruits). Between the onset of grain filling and maturity, the amount of carbon assimilates allocated to grains is calculated by applying the progressively increased Harvest Index (HI), in analogous to a dynamic partition coefficient (**equation 6)**. However, a translocation temperature threshold could potentially halt the grain-filling process.

Equation 6-Grain yield formation: $DLTAGS(I) = (IRCARB(I+1) \times MASEC(I+1) - IRCARB(I) \times MASEC(I)) \times FTEMPREMP(I)$

Where *DLTAGS* denotes daily grain filling rate, which is determined by the cumulative above-ground biomass (*MASEC*) and the progressively increased HI (*IRCARB*). The grain filling dynamics could be inhibited by extreme high temperature effects (*FTEMPREMP*). The cumulative *DLTAGS* over grain filling period eventually gives the final harvest yield at maturity.

2.3.6 Modelling climate change impacts on crop productivity in Mediterranean region

The Mediterranean basin is one of the most prominent climate change hotspot due to its unique transitional zone between the arid climate of North Africa and the temperate and rainy climate of central Europe, which is sensitive to the interactions between mid-latitude and tropical processes (Giorgi and Lionello, 2008). Climate trends observed in recent decades suggest that climate conditions in the Mediterranean basin are moving towards a more arid climate type with increased annual mean temperature and decreased annual rainfall (Ruiz-Ramos et al., 2018). Projections from a wide range of global and regional climate models confirm a robust climate change signal of an overall warming and drying trend for Mediterranean region, accompanied by greater frequency and intensity of extreme events (Diffenbaugh and Giorgi, 2012; Giorgi and Lionello, 2008; IPCC, 2013). The state-of-the-art multi-model ensemble median projections for the Mediterranean region, indicates a long-term mean increase of annual mean temperature by ~5°C and a decrease of annual precipitation by about 15% until the end of 21st century under RCP8.5 (IPCC, 2013). Associated with these changes, an increase in the frequency and intensity of extreme

daily maximum temperature is projected, particularly for the Iberian Peninsula (Giorgi and Lionello, 2008; Sánchez et al., 2004).

Modelling studies integrating future climate change impacts (net effect of projected changes in temperature, precipitation and CO_2) on crop yields in the Mediterranean region or under Mediterranean-type climates, reveal overall negative impacts, most of which are driven by heat and drought stresses that differently affect maize (Guereña et al., 2001; Meza and Silva, 2009; Meza et al., 2008; Rosenzweig and Tubiello, 1997; Tubiello et al., 2000), wheat (Iglesias et al., 2010; Mínguez et al., 2007; Moriondo et al., 2011; Olesen et al., 2007; Ruiz-Ramos et al., 2018; Tubiello et al., 2000), and grassland (Chang et al., 2017; Cullen et al., 2009; Keller et al., 2014; Ruget et al., 2010).

Impacts on irrigated maize production systems

For maize production (mainly irrigated) in the Mediterranean region, the negative impacts are relatively consistent, which mainly derive from the early maturity and reduction of crop growing season caused by higher temperature (Guereña et al., 2001; Meza et al., 2008; Tubiello et al., 2000). Increased temperature accelerates the crop development rate and advances crop phenological stages, resulting in a shortening of crop growing season, with less time available for photosynthesis and captured resources (water, nutrients and light), consequently lowering crop productivity. These negative impacts are expected not to be compensated by elevated atmospheric CO_2 concentrations for C4 crops like maize, leading to net yield reductions under irrigation (Gabaldón-Leal et al., 2015; Meza et al., 2008; Rosenzweig and Tubiello, 1997; Tubiello et al., 2000). For instance, Tubiello et al. (2000) indicate that maize yield under irrigated conditions is reduced by 20% in response to combined effects of temperature increase and doubled CO_2 level at Modena (Italy), resulting from the shortened growth duration by 16 days and diminished seasonal evapotranspiration by 70 mm. Similarly, in the south of the Iberian Peninsula, the irrigated maize productivity is projected to decrease by 6 to 20% (depending on the locations), in response to rising temperature and CO_2 level (Gabaldón-Leal et al., 2015; Guereña et al., 2001). In the central part of Chile with Mediterranean-type climate, climate change diminished irrigated maize yield by 10–30% (Meza et al., 2008). For C4 crops, elevated CO_2 is more likely to stimulate the intercellular leaf CO_2 assimilation rate only when crop is under water stress, through which stomatal conductance is reduced (combined effects of water stress and increasing CO_2), and resultantly soil

water was conserved (Ghannoum et al., 2000; Kimball, 2016). Moreover, water availability for irrigation is facing increasingly intense competition in the Mediterranean region due to growing water demand from the non-food sector (e.g. household, sanitation and entertainment utilizations) and climate-driven decreased and more variable precipitation (Rosenzweig and Tubiello, 1997). The irrigation requirement of maize is under complex interactions of higher potential evapotranspiration caused by rising temperature, smaller stomatal conductance rate and seasonal transpiration induced by higher CO_2 level, as well as by shortened growth duration (Tubiello et al., 2000). The net results of this interaction differed in literatures, where projections showed either reduced water use and irrigation requirement with improved WUE (Gabaldón-Leal et al., 2015; Meza et al., 2008), or sharply increased irrigation demand by 60–90% to maintain current yield level (Tubiello et al., 2000).

Impacts on rainfed wheat production systems

Global wheat grain yield is estimated to decline between 4.1% and 6.4% with 1ºC global temperature increase (Liu et al., 2016), and yield reductions can amount to 28% if temperature increase reaches 2ºC and to 55% for a 4ºC increase (Asseng et al., 2014). Wheat yield potentials under rainfed Mediterranean conditions have been long constrained by late season occurrences of enhanced water deficits and high temperature events, primarily overlapped with the critical reproductive stages, which has been identified as the main vulnerability facing climate change (Asseng et al., 2011; Moriondo et al., 2010; Ruiz-Ramos et al., 2018; Shavrukov et al., 2017). In particular, the projected increases of frequency and severity of extreme climatic events during sensitive wheat growth stages are expected to dominate the negative impacts, during which high-temperature episodes may intensify the adverse effects of water scarcity, which are hardly compensated by CO_2 fertilization effects (Moriondo et al., 2011; Ruiz-Ramos et al., 2018). In a European-wide study, Moriondo et al. (2010) explicitly show that the wheat yields respond negatively to projected 2°C warming scenario, including changes in both climate mean state and variability, which are more pronounced in southern Mediterranean areas than in Northern Europe, as a consequence of higher frequency of both heat and drought stresses at anthesis. Specifically for the "Mediterranean south environment zone" of Spain, where an ensemble of 17 crop models are built to simulate winter wheat yield response to perturbed temperature and precipitation, CO_2 under different soil types, the multi-model ensemble median shows a wide range of mean yield

response from 3000 to 7000 kg/ha, demonstrating that temperature tends to be the yield limiting factor at high precipitation increment, whereas precipitation will dominate the yield variations at low temperature increase (Ruiz-Ramos et al., 2018). At national scale, a 21% mean yield decrease is projected until the end of 21st century (Olesen et al., 2007) across Spain, while the yield response becomes more variable in Northern Spain with decreased yield linked to low elevation area and increased yield link to high elevation area (Mínguez et al., 2007). At another Mediterranean site of Italy, where wheat crops already suffer severe water stress during baseline conditions, projected wheat yields could be significantly reduced by 30%–50% (Tubiello et al., 2000).

Impacts on perennial grassland production systems

In total, the effects of climate change on the productivity or seasonal Dry Matter Yield (DMY) of perennial grassland in the Mediterranean region from available studies are summarized as follow: early shift of phenology stages with an earlier onset of winter and spring growth, increased DMY during cooler and wetter season (e.g. autumn and winter), with a clear decrease in DMY during summer (Chang et al., 2017; Cullen et al., 2009; Ergon et al., 2018; Graux et al., 2013; Keller et al., 2014; Ruget et al., 2010). Annual DMY of established semi-intensive Mediterranean grassland is analysed as the sum of accumulated DMY during two distinguished seasonal growing patterns: September–April (autumn regrowth and favourable growth during winter and spring) and May–August (unfavourable summer growth with drought and high temperature) (Lelievre and Volaire, 2009). For the first period, with cool and wet season, water supply is generally optimal and forage growth rate mainly depends on temperature, being proportional to thermal time (Lelievre and Volaire, 2009). Climate warmings, depending on the local magnitude, could help alleviate the cold stress and promote production during this period. In the second period, during the warm and dry summer season, the major agronomic goal in the Mediterranean region is to use forage germplasm with high drought tolerance so as to ensure sufficient surviving plant density throughout the long, dry summer, without active growth, but that can regrow rapidly at the onset of the wet autumn, a cultivar trait known as summer dormancy (Lelievre and Volaire, 2009). More severe and frequent summer droughts reducing forage productivity and persistence (standing density), is considered the major challenge for forage production in the Mediterranean region (Ergon et al., 2018; Lelievre and Volaire, 2009). In France, a study using STICS model to simulate the semi-natural grassland system for 34 locations, shows consistently enhanced winter production in future climate, whereas

summer DMY accumulation remarkably decreases as a result of aggravated water deficits (Ruget et al., 2010). Similarly, for another modelling study conducted in France, grass summer DMY accumulation is shown to be markedly reduced until the end of 21st century, but with higher DMY production during autumn, winter and spring due to combined effects of higher temperature and CO_2 level, leading to an overall increased annual productivity (Graux et al., 2013). At a study site in Australia with Mediterranean-type climate, the mean annual DMY is projected to be slightly higher than the baseline under 2030s but declined by 18% until 2070s in a high emission scenario, resulting from progressively decreased summer growth rate and shortening of spring growing season (Cullen et al., 2009).

Overall, it is clear that the magnitudes of climate change impacts depend on the selected crop models, climate models (including downscaling methods), emission scenarios, time period chosen for analysis (baseline and future) and intensity of current management systems, while the source of these variations in turn will vary substantially from region to region globally (Asseng et al., 2013; Challinor et al., 2014; Kang et al., 2009). As a general framework of modelling climate changes impacts on agriculture, Rosenzweig and Tubiello (1997) propose that a particular analysis should (i) clearly define the study area, analyse cropping systems and summarize current climate and farming practices; (ii) properly calibrated crop models using locally relevant observational data and test the calibrated parameters; (iii) develop local-relevant climate change scenarios for both short-term and long-term future.

2.3.7 Modelling adaptation response to climate change in Mediterranean region

Adaptations on cropping systems have shown great potential to alleviate or counteract the projected adverse climate change impacts (Challinor et al., 2018; Challinor et al., 2014; Howden et al., 2007; Moriondo et al., 2010). Adaptation options explored using process-based crop models are typically field-scale or crop-level adaptations, such as changes of cultivated crop varieties from a genetic breeding perspective (e.g. longer or shorter cycle, better drought and heat tolerance etc.) and from a management perspective by adjusting sowing dates, irrigation and fertilization strategies (organic and mineral fertilization) (Challinor et al., 2014). These relatively marginal changes and variations of cropping systems are highly contrasting with a more systemic change, e.g. by choosing different growing crops and grazing integration or to the transformational approach, e.g. with crop relocations and complete changes of farming systems (Challinor et al.,

2014; Rickards and Howden, 2012). However, the effectiveness of these adaptation options shows substantial benefits on some cropping systems only under moderate climate changes (e.g. moderate perturbations of temperature and precipitation), whereas the adaptive responses can be constrained under severe climate changes (Howden et al., 2007). Therefore, the development of appropriate and targeted adaptations should particularly address previously identified vulnerabilities of cropping systems facing climate changes (e.g. the increasing risks of crop exposure to heat stress at anthesis) and test solutions to improve resilience. Besides, a single adaptation option might not be enough to cope with the projected climate change impacts over the Mediterranean region with conditions of high uncertainty, whereas combined adaptation measures could be more effective in mitigating yield decline (Gabaldón-Leal et al., 2015; Ruiz-Ramos et al., 2018).

Adaptations on irrigated maize production systems

Of evaluated crop-level adaptation strategies for irrigated maize system, several studies agree on the need to incorporate the longer cycle cultivars to counterbalance the effects of accelerated phenology and shortened growing duration due to warmer climates (Gabaldón-Leal et al., 2015; Meza et al., 2008; Rosenzweig and Tubiello, 1997; Tubiello et al., 2000). Moreover, benefiting from projected temperature increase in spring, early planting for spring-sown crops (maize), is also widely suggested to be helpful and a potentially effective adaptation option by minimizing or reducing the risks of exposure to enhanced drought and heat stresses during the hotter and drier summer months (Gabaldón-Leal et al., 2015; Meza et al., 2008; Tubiello et al., 2000). However, extended growing season under warmer climate to maintain or increase crop yield will in turn cause higher irrigation requirements and resulting in decreased irrigation WUE. Tubiello et al. (2000) explicitly show that though combination of longer growth duration with early planting succeed in maintaining crop yields at current level, irrigation requirement is increased significantly by 60–90% for maize, along with a concomitant decrease of irrigation WUE. Another study conducted for the south of Iberia, coupling the CERES-Maize model with a bias-corrected high resolution RCM, highlight that combined adaptation options of early sowing dates and use of a longer cycle maize cultivar are able to fully compensate, and even reverse the projected yield reductions, resulting in up to 14% higher yield relative to baseline, with a concomitant reduction of irrigation requirement and irrigation WUE (Gabaldón-Leal et al., 2015). In addition, Meza et al. (2008) propose an innovative adaptation strategy based on double cropping (i.e. two harvests of

maize cultivation successively in the same land and in a single year) to cope with extreme climate change scenarios. This strategy is likely to have better yield and economic gains than other adaptation alternatives based on agronomic decisions, being able to mitigate economic impacts of climate change or generate additional monetary return (Meza et al., 2008).

Adaptations on rainfed wheat production systems

Model-based adaptation studies for rainfed wheat in the Mediterranean basin have primarily focused on a combined adaptation strategy by introducing adaptive cultivars with efficient management practices, to alleviate the detrimental impacts of pronounced terminal drought and heat stresses, partially coinciding with the sensitive growth cycle (e.g. anthesis and grain-filling) (Moriondo et al., 2010; Ruiz-Ramos et al., 2018; Shavrukov et al., 2017). For targeted cultivar traits, early flowering cultivars, associated with rapid crop development and quick transition to reproductive phase, represent a successful stress escaping strategy for wheat production under typical Mediterranean environments, by minimizing the risk of crop exposure to terminal drought/heat stress during reproductive stages (Debaeke, 2004; Shavrukov et al., 2017). Early flowering varieties follow short vegetative phases, resulting in an early completion of growth cycle prior to enhanced terminal stresses, in a process that usually correlates with short season genotypes. Under favourable conditions, early flowering/maturity trait can limit grain yield potential as growth duration becomes shorter with less time for capturing light, nutrients and water. Despite such trade-off, gradual shift toward using early flowering wheat genotypes and overall yield benefits are observed over the last century in countries with Mediterranean-type climate (Shavrukov et al., 2017). For the Mediterranean basin, previous studies consistently demonstrate earlier occurrence of anthesis and shift of grain filling towards a cooler and wetter period induced by the use of early flowering wheat cultivars, which partially offset the increasing temperature trends on grain-filling duration under warmer future climates (Moriondo et al., 2010; Moriondo et al., 2011). This successfully reduces the frequency of stress occurrences of drought by 12% and heat by 14% on average, during sensitive reproductive stages (Moriondo et al., 2010). Early sowing date, is also widely recommended for wheat adaptation to the impacts of projected higher frequency of terminal heat stress and longer dry spell in the Mediterranean basin, as it allows anticipation of the crop cycle to advance the anthesis and grain-filling periods (resemble early flowering adaptation) (Moriondo et al., 2010; Moriondo et al., 2011; Ruiz-Ramos et al., 2018).

Supplemental irrigation that supply additional water for rainfed crop during the drought-sensitive period, has also been suggested to be a very promising strategy for wheat production in the Mediterranean region (Oweis et al., 2003; Saadi et al., 2015). As it helps mitigating the negative effects on critical assimilate partition processes, while minimizing the water losses through evaporation, aiming to stabilize crop yield and maximize water use efficiency (Oweis et al., 2003). A single supplemental irrigation is sufficient to develop high yield adaptive potential in wheat cultivation zone in north-eastern Spain, allowing to overcome most of the detrimental effects of complex interactions among a wide range of temperature, precipitation and CO_2 perturbations (Ruiz-Ramos et al., 2018).

Adaptations on perennial grassland production systems

In the Mediterranean region, water availability will often be the limiting factor for photosynthesis and forage DMY accumulation, and severe water deficits, such as Mediterranean summer drought will have marked impacts on standing density and cause plant mortality (Ergon et al., 2018; Porqueddu et al., 2016). In contrast, the direct effect of heat stress is unlikely to be equally important for grassland, probably because the effect is masked by the strong dominance of water scarcity. The development of adaptation strategies for grassland-based forage production in the Mediterranean region needs to address the challenge and opportunities arising from the climatic changes. Climate change is likely to alter grass seasonal growth patterns, which will shift towards cooler and wetter winter season due to warmer winters and drier summers (Ergon et al., 2018). To take advantage of this emerging opportunity, breeding efforts are required to develop forage varieties or select species with growth pattern that increase production during the favourable part of the year (e.g. winter), while conferring an balance between growth potential, nutritive values and responsiveness to the CO_2 fertilization effect (Ergon et al., 2018). Likewise, defoliation and fertilization regimes, representing crucial management practices, also need adaptations to optimize forage growth pattern (e.g. more frequent grazing and early fertilization to increase winter and spring growth rate) (Ergon et al., 2018; Lelievre and Volaire, 2009). On the other hand, diversity among responses to critical weather factors improves resilience at both sward and farm level. Thus, design and utilization of species and variety mixture composition is generally considered a key strategy to maintain production and meet the challenges of climate change (Lüscher et al., 2004). Under dry Mediterranean conditions, grass-legume mixtures including both annuals and perennials,

as compared to monocultures or simple mixture, are widely suggested to achieve higher and stable yield, as well as providing greater flexibility in forage utilization and ecosystem services in future climate (Ergon et al., 2018; Lelievre and Volaire, 2009; Porqueddu et al., 2016). For improving drought persistence and survival rate, breeding programs should be prioritized at continuous improvement of summer dormancy traits that is associated with growth cessation at the onset of successive drought with dehydration avoidance and tolerance of basal meristematic tissues, rather than targeting maintenance of growth under moderate drought (Ergon et al., 2018; Lelievre and Volaire, 2009; Porqueddu et al., 2016). Moreover, inclusion of forage legumes has several advantages including nitrogen fixation, better utilization and exploitation of elected CO_2 level and improvement of forage quality (Ergon et al., 2018). Other adaptive recommendation consists of using perennial grassland species with deep root system to enhance water uptake and resilience of grassland community (Cullen et al., 2014; Ergon et al., 2018). However, modelling adaptation strategy for grassland should further explicitly account for plant drought persistence, e.g. involving increased mortality response to successive summer droughts but regrow rapidly after wet autumn onset (depending on the number of survival basal tissues), as well as integrating the interaction effects of botanic composition with seasonal climatic variations (Cullen et al., 2009; Ergon et al., 2018; Graux et al., 2013). These factors are not well simulated currently in many grassland models (including STICS) and their improvement should represent a necessary step for building a more robust and reliable analytic framework in the future.

References

Abedinpour, M. et al., 2012. Performance evaluation of AquaCrop model for maize crop in a semi-arid environment. Agricultural Water Management, 110: 55-66.

Aggarwal, P.K., Kalra, N., Chander, S. and Pathak, H., 2006. InfoCrop: A dynamic simulation model for the assessment of crop yields, losses due to pests, and environmental impact of agro-ecosystems in tropical environments. I. Model description. Agr Syst, 89(1): 1-25.

Aires, L.M., Pio, C.A. and Pereira, J.S., 2008. The effect of drought on energy and water vapour exchange above a mediterranean C3/C4 grassland in Southern Portugal. Agr Forest Meteorol, 148(4): 565-579.

Alexandratos, N. and Bruinsma, J., 2012. World agriculture towards 2030/2050: the 2012 revision, ESA Working paper No. 12-03, Rome, FAO.

Almeida, A., Maçãs, B., Luís Gaspar Rodrigues, V. and Manuel Torrão, M., 2016. The History of Wheat Breeding in Portugal, The world wheat book: a history of wheat breeding, pp. 93-125.

Araus, J., 2004. problems of sustainable water use in the Mediterranean and research requirements for agriculture. Annals of applied biology.

Arguez, A. and Vose, R.S., 2011. The Definition of the Standard WMO Climate Normal: The Key to Deriving Alternative Climate Normals. Bulletin of the American Meteorological Society, 92(6): 699-704.

Asseng, S. et al., 2014. Rising temperatures reduce global wheat production. Nature Climate Change, 5: 143.

Asseng, S. et al., 2013. Uncertainty in simulating wheat yields under climate change. Nature Climate Change, 3(9): 827-832.

Asseng, S., Foster, I. and Turner, N.C., 2011. The impact of temperature variability on wheat yields. Global Change Biol, 17(2): 997-1012.

Basso, B., Cammarano, D., Troccoli, A., Chen, D. and Ritchie, J.T., 2010. Long-term wheat response to nitrogen in a rainfed Mediterranean environment: Field data and simulation analysis. European Journal of Agronomy, 33(2): 132-138.

Batley, J. and Edwards, D., 2016. The application of genomics and bioinformatics to accelerate crop improvement in a changing climate. Curr Opin Plant Biol, 30: 78-81.

Biernath, C. et al., 2011. Evaluating the ability of four crop models to predict different environmental impacts on spring wheat grown in open-top chambers. European Journal of Agronomy, 35(2): 71-82.

Bindi, M., Palosuo, T., Trnka, M. and Semenov, M.A., 2015. Modelling climate change impacts on crop production for food security. Clim Res, 65: 3-5.

BONDEAU, A. et al., 2007. Modelling the role of agriculture for the 20th century global terrestrial carbon balance. Global Change Biol, 13(3): 679-706.

Brisson, N. et al., 2003. An overview of the crop model STICS. European Journal of Agronomy, 18(3-4): 309-332.

Brisson, N. et al., 2010. Why are wheat yields stagnating in Europe? A comprehensive data analysis for France. Field Crops Research, 119(1): 201-212.

Brisson, N., Launay, M., Mary, B. and Beaudoin, N., 2009. Conceptual basis, formalisations and parameterization of the STICS crop model. Editions Quae, Versailles, France, 297 pp.

Brisson, N. et al., 1998. STICS: a generic model for the simulation of crops and their water and nitrogen balances. I. Theory and parameterization applied to wheat and corn. Agronomie, 18(5-6): 311-346.

Brisson, N. et al., 2002. STICS: a generic model for simulating crops and their water and nitrogen balances. II. Model validation for wheat and maize. Agronomie, 22(1): 69-92.

Carvalho, A., Schmidt, L., Santos, F.D. and Delicado, A., 2014. Climate change research and policy in Portugal. Wires Clim Change, 5(2): 199-217.

Challinor, A.J. et al., 2018. Improving the use of crop models for risk assessment and climate change adaptation. Agr Syst, 159: 296-306.

Challinor, A.J. et al., 2014. A meta-analysis of crop yield under climate change and adaptation. Nature Climate Change, 4: 287.

Challinor, A.J., Wheeler, T.R., Craufurd, P.Q., Slingo, J.M. and Grimes, D.I.F., 2004. Design and optimisation of a large-area process-based model for annual crops. Agr Forest Meteorol, 124(1): 99-120.

Chang, J. et al., 2017. Future productivity and phenology changes in European grasslands for different warming levels: implications for grassland management and carbon balance. Carbon Balance and Management, 12(1): 11.

Charlier, H. and de Gasperi, R.A., 2007. The EU farm structure surveys from 2010 onwards, Proceedings of the Fourth International Conference on Agricultural Statistics (ICAS-IV).

Collins, W.D. et al., 2006. Radiative forcing by well-mixed greenhouse gases: Estimates from climate models in the Intergovernmental Panel on Climate Change (IPCC) Fourth Assessment Report (AR4). Journal of Geophysical Research: Atmospheres, 111(D14).

Costa, A.C., Santos, J.A. and Pinto, J.G., 2012. Climate change scenarios for precipitation extremes in Portugal. Theor Appl Climatol, 108(1): 217-234.

Costa, A.C. and Soares, A., 2009. Trends in extreme precipitation indices derived from a daily rainfall database for the South of Portugal. Int J Climatol, 29(13): 1956-1975.

Costa, R. et al., 2013. Effect of sowing date and seeding rate on bread wheat yield and test weight under Mediterranean conditions. Emir J Food Agr, 25(12): 951-961.

Coucheney, E. et al., 2015. Accuracy, robustness and behavior of the STICS soil–crop model for plant, water and nitrogen outputs: Evaluation over a wide range of agro-environmental conditions in France. Environ Modell Softw, 64: 177-190.

Cullen, B.R. et al., 2009. Climate change effects on pasture systems in south-eastern Australia. Crop and Pasture Science, 60(10): 933-942.

Cullen, B.R., Rawnsley, R.P., Eckard, R.J., Christie, K.M. and Bell, M.J., 2014. Use of modelling to identify perennial ryegrass plant traits for future warmer and drier climates. Crop Pasture Sci, 65(8): 758-766.

Debaeke, P., 2004. Scenario analysis for cereal management in water-limited conditions by the means of a crop simulation model (STICS). Agronomie, 24(6-7): 315-326.

Deser, C., Knutti, R., Solomon, S. and Phillips, A.S., 2012. Communication of the role of natural variability in future North American climate. Nature Climate Change, 2: 775.

Di Luca, A., de Elía, R. and Laprise, R., 2012. Potential for added value in precipitation simulated by high-resolution nested Regional Climate Models and observations. Clim Dynam, 38(5): 1229-1247.

Diffenbaugh, N.S. and Giorgi, F., 2012. Climate change hotspots in the CMIP5 global climate model ensemble. Climatic Change, 114(3): 813-822.

Ergon, Å. et al., 2018. How can forage production in Nordic and Mediterranean Europe adapt to the challenges and opportunities arising from climate change? European Journal of Agronomy, 92: 97-106.

Espírito Santo, F., de Lima, M.I.P., Ramos, A.M. and Trigo, R.M., 2014. Trends in seasonal surface air temperature in mainland Portugal, since 1941. Int J Climatol, 34(6): 1814-1837.

Evenson, R.E. and Gollin, D., 2003. Assessing the Impact of the Green Revolution, 1960 to 2000. Science, 300(5620): 758-762.

Ewert, F. et al., 2015. Crop modelling for integrated assessment of risk to food production from climate change. Environ Modell Softw, 72: 287-303.

FAO, 2003. Food and Agriculture Organization.

Fraga, H., Santos, J.A., Malheiro, A.C. and Moutinho-Pereira, J., 2012. Climate change projections for the Portuguese viticulture using a multi-model ensemble. Ciência e Técnica Vitivinícola, 27: 39-48.

Fraga, H. et al., 2016. Climatic suitability of Portuguese grapevine varieties and climate change adaptation. Int J Climatol, 36(1): 1-12.

Frankcombe, L.M., England, M.H., Mann, M.E. and Steinman, B.A., 2015. Separating Internal Variability from the Externally Forced Climate Response. J Climate, 28(20): 8184-8202.

Gabaldón-Leal, C. et al., 2015. Strategies for adapting maize to climate change and extreme temperatures in Andalusia, Spain. Clim Res, 65: 159-173.

Geerts, S. and Raes, D., 2009. Deficit irrigation as an on-farm strategy to maximize crop water productivity in dry areas. Agricultural Water Management, 96(9): 1275-1284.

Ghannoum, O., Caemmerer, S.V., Ziska, L.H. and Conroy, J.P., 2000. The growth response of C4 plants to rising atmospheric CO2 partial pressure: a reassessment. Plant, Cell & Environment, 23(9): 931-942.

Giorgi, F. and Lionello, P., 2008. Climate change projections for the Mediterranean region. Global Planet Change, 63(2): 90-104.

Godfray, H.C.J. et al., 2010. Food Security: The Challenge of Feeding 9 Billion People. Science, 327(5967): 812-818.

Goudriaan, J. and Van Laar, H., 2012. Modelling potential crop growth processes: textbook with exercises, 2. Springer Science & Business Media.

Gouveia, C. and Trigo, R.M., 2008. Influence of Climate Variability on Wheat Production in Portugal. In: A. Soares, M.J. Pereira and R. Dimitrakopoulos (Editors), geoENV VI – Geostatistics for Environmental Applications: Proceedings of the Sixth European

Conference on Geostatistics for Environmental Applications. Springer Netherlands, Dordrecht, pp. 335-345.

Graux, A.-I., Bellocchi, G., Lardy, R. and Soussana, J.-F., 2013. Ensemble modelling of climate change risks and opportunities for managed grasslands in France. Agr Forest Meteorol, 170: 114-131.

Guereña, A., Ruiz-Ramos, M., Díaz-Ambrona, C.H., Conde, J.R. and Mínguez, M.I., 2001. Assessment of Climate Change and Agriculture in Spain Using Climate Models. Agron J, 93(1): 237-249.

Hamdy, A., Abu-Zeid, M. and Lacirignola, C., 1995. Water Crisis in the Mediterranean: Agricultural Water Demand Management. Water International, 20(4): 176-187.

Harrould-Kolieb, E.R. and Herr, D., 2012. Ocean acidification and climate change: synergies and challenges of addressing both under the UNFCCC. Climate Policy, 12(3): 378-389.

Hawkins, E. and Sutton, R., 2011. The potential to narrow uncertainty in projections of regional precipitation change. Clim Dynam, 37(1): 407-418.

Hay, L.E., Wilby, R.L. and Leavesley, G.H., 2000. A COMPARISON OF DELTA CHANGE AND DOWNSCALED GCM SCENARIOS FOR THREE MOUNTAINOUS BASINS IN THE UNITED STATES1. JAWRA Journal of the American Water Resources Association, 36(2): 387-397.

Howden, S.M. et al., 2007. Adapting agriculture to climate change. Proceedings of the National Academy of Sciences, 104(50): 19691-19696.

Iglesias, A., Garrote, L., Flores, F. and Moneo, M., 2007. Challenges to manage the risk of water scarcity and climate change in the Mediterranean. Water Resources Management, 21(5): 775-788.

Iglesias, A., Quiroga, S. and Schlickenrieder, J., 2010. Climate change and agricultural adaptation: assessing management uncertainty for four crop types in Spain. Clim Res, 44(1): 83-94.

INE, 2015. Main crops surface (ha) by Geographic localization (Agricultural census), Instituto Nacional de Estatística (INE), Lisbon, Portugal.

INE, 2019. Main crops surface (ha) and production (t) by Geographic localization (Agrarian region) and Specie. Instituto Nacional de Estatística (INE), Lisbon, Portugal.

IPCC, 2013. The physical science basis. Contribution of working group I to the fifth assessment report of the intergovernmental panel on climate change [Stocker, T.F., D. Qin, G.-K. Plattner, M. Tignor, S.K. Allen, J. Boschung, A. Nauels, Y. Xia, V. Bex and P.M. Midgley (eds.)]. Cambridge University Press, Cambridge, United Kingdom and New York, NY, USA, 1-1535 pp.

IPCC, 2014. Climate Change 2014: Synthesis Report. Contribution of Working Groups I, II and III to the Fifth Assessment Report of the Intergovernmental Panel on Climate Change, Geneva, Switzerland.

IPCC, 2015. Workshop Report of the Intergovernmental Panel on Climate Change Workshop on Regional Climate Projections and their Use in Impacts and Risk Analysis Studies [Stocker, T.F., D. Qin, G.-K. Plattner, and M. Tignor (eds.)], IPCC Working Group I Technical Support Unit, University of Bern, Bern, Switzerland.

IPCC, 2018. Global warming of 1.5°C. An IPCC Special Report on the Impacts of Global Warming of 1.5°C Above Pre-Industrial Levels and Related Global Greenhouse Gas Emission Pathways, in the Context Of Strengthening the Global Response to the Threat of Climate Change, Sustainable Development, and Efforts to Eradicate Poverty.

Jacob, D. et al., 2014. EURO-CORDEX: new high-resolution climate change projections for European impact research. Regional Environmental Change, 14(2): 563-578.

Jamieson, P.D., Semenov, M.A., Brooking, I.R. and Francis, G.S., 1998. Sirius: a mechanistic model of wheat response to environmental variation. European Journal of Agronomy, 8(3): 161-179.

Jones, C.A. et al., 1991. EPIC: An operational model for evaluation of agricultural sustainability. Agr Syst, 37(4): 341-350.

Jones, J.W. et al., 2003. The DSSAT cropping system model. European Journal of Agronomy, 18(3): 235-265.

Jongen, M., Pereira, J.S., Aires, L.M.I. and Pio, C.A., 2011. The effects of drought and timing of precipitation on the inter-annual variation in ecosystem-atmosphere exchange in a Mediterranean grassland. Agr Forest Meteorol, 151(5): 595-606.

Kang, Y., Khan, S. and Ma, X., 2009. Climate change impacts on crop yield, crop water productivity and food security – A review. Progress in Natural Science, 19(12): 1665-1674.

Kassie, B.T. et al., 2015. Exploring climate change impacts and adaptation options for maize production in the Central Rift Valley of Ethiopia using different climate change scenarios and crop models. Climatic Change, 129(1): 145-158.

Keating, B.A. et al., 2003. An overview of APSIM, a model designed for farming systems simulation. European Journal of Agronomy, 18(3): 267-288.

Keller, E.D., Baisden, W.T., Timar, L., Mullan, B. and Clark, A., 2014. Grassland production under global change scenarios for New Zealand pastoral agriculture. Geosci. Model Dev., 7(5): 2359-2391.

Kersebaum, K.C., 2007. Modelling nitrogen dynamics in soil–crop systems with HERMES. Nutr Cycl Agroecosys, 77(1): 39-52.

Kimball, B.A., 2016. Crop responses to elevated CO2 and interactions with H2O, N, and temperature. Curr Opin Plant Biol, 31: 36-43.

Kirtman, B. et al., 2013. Near-term climate change: projections and predictability.

Knutti, R. and Sedláček, J., 2012. Robustness and uncertainties in the new CMIP5 climate model projections. Nature Climate Change, 3: 369.

Lelievre, F. and Volaire, F., 2009. Current and Potential Development of Perennial Grasses in Rainfed Mediterranean Farming Systems. Crop Sci, 49(6): 2371-2378.

Lesk, C., Rowhani, P. and Ramankutty, N., 2016. Influence of extreme weather disasters on global crop production. Nature, 529: 84.

Liu, B. et al., 2016. Similar estimates of temperature impacts on global wheat yield by three independent methods. Nature Climate Change, 6: 1130.

Lobell, D.B. and Burke, M.B., 2010. On the use of statistical models to predict crop yield responses to climate change. Agr Forest Meteorol, 150(11): 1443-1452.

Lüscher, A., Daepp, M., Blum, H., Hartwig, U.A. and Nösberger, J., 2004. Fertile temperate grassland under elevated atmospheric CO2—role of feed-back mechanisms and availability of growth resources. European Journal of Agronomy, 21(3): 379-398.

Maraun, D., 2016. Bias Correcting Climate Change Simulations - a Critical Review. Current Climate Change Reports, 2(4): 211-220.

Maraun, D. et al., 2015. VALUE: A framework to validate downscaling approaches for climate change studies. Earth's Future, 3(1): 1-14.

Maurer, E.P. and Pierce, D.W., 2014. Bias correction can modify climate model simulated precipitation changes without adverse effect on the ensemble mean. Hydrol. Earth Syst. Sci., 18(3): 915-925.

Meza, F.J. and Silva, D., 2009. Dynamic adaptation of maize and wheat production to climate change. Climatic Change, 94(1): 143-156.

Meza, F.J., Silva, D. and Vigil, H., 2008. Climate change impacts on irrigated maize in Mediterranean climates: Evaluation of double cropping as an emerging adaptation alternative. Agr Syst, 98(1): 21-30.

Mínguez, M.I., Ruiz-Ramos, M., Díaz-Ambrona, C.H., Quemada, M. and Sau, F., 2007. First-order impacts on winter and summer crops assessed with various high-resolution climate models in the Iberian Peninsula. Climatic Change, 81(1): 343-355.

Miranda, P. et al., 2002. 20th century Portuguese climate and climate scenarios. Climate Change in Portugal. Scenarios, Impacts and Adaptation Measures—SIAM Project (Santos FD, Forbes K, Moita R, eds). Lisbon: Gradiva Publishers: 23-83.

Moriondo, M. et al., 2010. Impact and adaptation opportunities for European agriculture in response to climatic change and variability. Mitig Adapt Strat Gl, 15(7): 657-679.

Moriondo, M., Giannakopoulos, C. and Bindi, M., 2011. Climate change impact assessment: the role of climate extremes in crop yield simulation. Climatic Change, 104(3): 679-701.

Moss, R.H. et al., 2010. The next generation of scenarios for climate change research and assessment. Nature, 463: 747.

Mourato, S., Moreira, M. and Corte-Real, J., 2010. Interannual variability of precipitation distribution patterns in Southern Portugal. Int J Climatol, 30(12): 1784-1794.

Nakicenovic, N. et al., 2000. Special report on emissions scenarios (SRES), a special report of Working Group III of the intergovernmental panel on climate change. Cambridge University Press.

Nendel, C. et al., 2011. The MONICA model: Testing predictability for crop growth, soil moisture and nitrogen dynamics. Ecological Modelling, 222(9): 1614-1625.

O'Leary, G.J., Connor, D.J. and White, D.H., 1985. A simulation model of the development, growth and yield of the wheat crop. Agr Syst, 17(1): 1-26.

Olesen, J.E. et al., 2007. Uncertainties in projected impacts of climate change on European agriculture and terrestrial ecosystems based on scenarios from regional climate models. Climatic Change, 81(1): 123-143.

Olesen, J.E. et al., 2011. Impacts and adaptation of European crop production systems to climate change. European Journal of Agronomy, 34(2): 96-112.

Oteng-Darko, P., Yeboah, S., Addy, S., Amponsah, S. and Danquah, E.O., 2013. Crop modeling: A tool for agricultural research–A. J. Agricultural Res. Develop., 2(1): 001-006.

Oweis, T., Rodrigues, P.N. and Pereira, L.S., 2003. Simulation of Supplemental Irrigation Strategies for Wheat in Near East to Cope with Water Scarcity. In: G. Rossi et al. (Editors), Water Trans. Springer Netherlands, Dordrecht, pp. 259-272.

Páscoa, P., Gouveia, C.M., Russo, A. and Trigo, R.M., 2017. The role of drought on wheat yield interannual variability in the Iberian Peninsula from 1929 to 2012. Int J Biometeorol, 61(3): 439-451.

Pereira, H., Domingos, T. and Vicente, L., 2004. Portugal millennium ecosystem assessment: state of the assessment report, Centro de Biologia Ambiental, Faculdade de Ciências da Universidade de Lisboa, Universidade de Lisboa.

Piani, C., Haerter, J.O. and Coppola, E., 2010. Statistical bias correction for daily precipitation in regional climate models over Europe. Theor Appl Climatol, 99(1): 187-192.

Porqueddu, C. et al., 2016. Grasslands in 'Old World' and 'New World' Mediterranean-climate zones: past trends, current status and future research priorities. Grass Forage Sci, 71(1): 1-35.

Porter, J.R. and Semenov, M.A., 2005. Crop responses to climatic variation. Philos Trans R Soc Lond B Biol Sci, 360(1463): 2021-2035.

Ramos, A.M., Trigo, R.M. and Santo, F.E., 2011. Evolution of extreme temperatures over Portugal: recent changes and future scenarios. Clim Res, 48(2-3): 177-192.

Ramos, T.B., Simionesei, L., Jauch, E., Almeida, C. and Neves, R., 2017. Modelling soil water and maize growth dynamics influenced by shallow groundwater conditions in the Sorraia Valley region, Portugal. Agricultural Water Management, 185: 27-42.

Rickards, L. and Howden, S.M., 2012. Transformational adaptation: agriculture and climate change. Crop and Pasture Science, 63(3): 240-250.

Ritchie, J., Godwin, D. and Otter-Nacke, S., 1985. CERES-Wheat. A simulation model of wheat growth and development. ARS (1985).(págs. 159-175). US Department of Agriculture.

Rosenzweig, C. et al., 2013. The Agricultural Model Intercomparison and Improvement Project (AgMIP): Protocols and pilot studies. Agr Forest Meteorol, 170: 166-182.

Rosenzweig, C. and Tubiello, F.N., 1997. Impacts of Global Climate Change on Mediterranean Agrigulture: Current Methodologies and Future Directions. An Introductory Essay. Mitig Adapt Strat Gl, 1(3): 219-232.

Rotter, R.P., Hoffmann, M.P., Koch, M. and Muller, C., 2018. Progress in modelling agricultural impacts of and adaptations to climate change. Curr Opin Plant Biol, 45: 255-261.

Rotter, R.P., Tao, F., Hohn, J.G. and Palosuo, T., 2015. Use of crop simulation modelling to aid ideotype design of future cereal cultivars. J Exp Bot, 66(12): 3463-3476.

Ruget, F., Moreau, J., Cloppet, E. and Souverain, F., 2010. Effect of climate change on grassland production for herbivorous livestock systems in France, 23rd General Meeting of the EGF Grassland in a changing world, Kiel (Germany), Aug 29th-Sept 2th 2010, pp. 75-77.

Ruiter, A., 2012. Delta-change approach for CMIP5 GCMs. Trainee report, Royal Netherlands Meteorological Institute.

Ruiz-Ramos, M. et al., 2018. Adaptation response surfaces for managing wheat under perturbed climate and CO2 in a Mediterranean environment. Agr Syst, 159: 260-274.

Saadi, S. et al., 2015. Climate change and Mediterranean agriculture: Impacts on winter wheat and tomato crop evapotranspiration, irrigation requirements and yield. Agricultural Water Management, 147: 103-115.

Sánchez, E., Gallardo, C., Gaertner, M.A., Arribas, A. and Castro, M., 2004. Future climate extreme events in the Mediterranean simulated by a regional climate model: a first approach. Global Planet Change, 44(1): 163-180.

Santo, F.E., Ramos, A.M., de Lima, M.I.P. and Trigo, R.M., 2014. Seasonal changes in daily precipitation extremes in mainland Portugal from 1941 to 2007. Regional Environmental Change, 14(5): 1765-1788.

Santos, F.D. and Miranda, P., 2006. Climate Change in Portugal: Scenarios, Impacts and Adaptation Measures - SIAM II Project. Gradiva, Lisbon.

Schär, C. et al., 2004. The role of increasing temperature variability in European summer heatwaves. Nature, 427(6972): 332-336.

Seidel, S.J., Palosuo, T., Thorburn, P. and Wallach, D., 2018. Towards improved calibration of crop models – Where are we now and where should we go? European Journal of Agronomy, 94: 25-35.

Semenov, M.A. and Porter, J.R., 1995. Climatic variability and the modelling of crop yields. Agr Forest Meteorol, 73(3): 265-283.

Shavrukov, Y. et al., 2017. Early Flowering as a Drought Escape Mechanism in Plants: How Can It Aid Wheat Production? Front Plant Sci, 8.

Shi, W., Tao, F. and Zhang, Z., 2013. A review on statistical models for identifying climate contributions to crop yields. J Geogr Sci, 23(3): 567-576.

Shine, K.P., 2000. Radiative Forcing of Climate Change. Space Science Reviews, 94(1): 363-373.

Spitters, C.J.T. and Schapendonk, A.H.C.M., 1990. Evaluation of breeding strategies for drought tolerance in potato by means of crop growth simulation. Plant Soil, 123(2): 193-203.

Steduto, P., Hsiao, T.C., Raes, D. and Fereres, E., 2009. AquaCrop—The FAO Crop Model to Simulate Yield Response to Water: I. Concepts and Underlying Principles. Agron J, 101(3): 426-437.

Stenger, R., Priesack, E., Barkle, G. and Sperr, G., 1999. A tool for simulating nitrogen and carbon dynamics in the soil-plant atmosphere system, Proceedings of the technical session, pp. 19-28.

Stöckle, C.O., Donatelli, M. and Nelson, R., 2003. CropSyst, a cropping systems simulation model. European Journal of Agronomy, 18(3): 289-307.

Tao, F., Yokozawa, M. and Zhang, Z., 2009. Modelling the impacts of weather and climate variability on crop productivity over a large area: A new process-based model development, optimization, and uncertainties analysis. Agr Forest Meteorol, 149(5): 831-850.

Taylor, K.E., Stouffer, R.J. and Meehl, G.A., 2012. An Overview of CMIP5 and the Experiment Design. Bulletin of the American Meteorological Society, 93(4): 485-498.

Teixeira, R.F.M. et al., 2011. Soil organic matter dynamics in Portuguese natural and sown rainfed grasslands. Ecological Modelling, 222(4): 993-1001.

Trindade, H., 2015. Portuguese dairy farming systems, Grassland and forages in high output dairy farming systems. Proceedings of the 18th Symposium of the European Grassland Federation, Wageningen, The Netherlands, 15-17 June 2015, pp. 21-25.

Tubiello, F.N., Donatelli, M., Rosenzweig, C. and Stockle, C.O., 2000. Effects of climate change and elevated CO2 on cropping systems: model predictions at two Italian locations. European Journal of Agronomy, 13(2): 179-189.

Urruty, N., Guyomard, H., Tailliez-Lefebvre, D. and Huyghe, C., 2017. Factors of winter wheat yield robustness in France under unfavourable weather conditions. European Journal of Agronomy, 90: 174-183.

Valverde, P. et al., 2015. Climate change impacts on rainfed agriculture in the Guadiana river basin (Portugal). Agricultural Water Management, 150: 35-45.

van Diepen, C.A., Wolf, J., van Keulen, H. and Rappoldt, C., 1989. WOFOST: a simulation model of crop production. Soil Use and Management, 5(1): 16-24.

van Oijen, M. and Ewert, F., 1999. The effects of climatic variation in Europe on the yield response of spring wheat cv. Minaret to elevated CO2 and O3: an analysis of open-top chamber experiments by means of two crop growth simulation models. European Journal of Agronomy, 10(3): 249-264.

van Vuuren, D.P. et al., 2011. The representative concentration pathways: an overview. Climatic Change, 109(1-2): 5-31.

Vicente-Serrano, S.M. et al., 2014. Evidence of increasing drought severity caused by temperature rise in southern Europe. Environ Res Lett, 9(4).

Wallach, D. et al., 2011. A package of parameter estimation methods and implementation for the STICS crop-soil model. Environ Modell Softw, 26(4): 386-394.

Wallach, D., Keussayan, N., Brun, F., Lacroix, B. and Bergez, J.-E., 2012. Assessing the Uncertainty when Using a Model to Compare Irrigation Strategies. Agron J, 104(5): 1274-1283.

Wallach, D., Makowski, D., Jones, J.W. and Brun, F., 2018. Working with dynamic crop models: methods, tools and examples for agriculture and environment. Academic Press.

Wallach, D. and Thorburn, P.J., 2017. Estimating uncertainty in crop model predictions: Current situation and future prospects. European Journal of Agronomy, 88: A1-A7.

Wang, B., Liu, D.L., Waters, C. and Yu, Q., 2018. Quantifying sources of uncertainty in projected wheat yield changes under climate change in eastern Australia. Climatic Change, 151(2): 259-273.

Warszawski, L. et al., 2014. The Inter-Sectoral Impact Model Intercomparison Project (ISI–MIP): Project framework. Proceedings of the National Academy of Sciences, 111(9): 3228-3232.

White, J.W., Hoogenboom, G., Kimball, B.A. and Wall, G.W., 2011. Methodologies for simulating impacts of climate change on crop production. Field Crops Research, 124(3): 357-368.

WMO, 1983. Guide to climatological practices. World Meteorological Organization Geneva.

Yang, C., Fraga, H., van Ieperen, W., Trindade, H. and Santos, J.A., 2019. Effects of climate change and adaptation options on winter wheat yield under rainfed Mediterranean conditions in southern Portugal. Climatic Change, 154(1): 159-178.

Yang, C.Y., Fraga, H., Van Ieperen, W. and Santos, J.A., 2017. Assessment of irrigated maize yield response to climate change scenarios in Portugal. Agr Water Manage, 184: 178-190.

Yang, W. et al., 2010. Distribution-based scaling to improve usability of regional climate model projections for hydrological climate change impacts studies. Hydrology Research, 41(3-4): 211-229.

Zhang, H. and Oweis, T., 1999. Water–yield relations and optimal irrigation scheduling of wheat in the Mediterranean region. Agricultural Water Management, 38(3): 195-211.

CHAPTER 3

Assessment of irrigated maize responses to climate change scenarios in Portugal

Briefing notes:

Grain maize production plays a dominant social-economic role in Portugal, amounting to about 7 million tons per year with a huge gross economic volume of around 120 million euros/year. The principal growing area is located in Ribatejo region, having ~30,000 ha of concentrated maize fields. Irrigation is essential to sustain the maize growth and successful grain yield production during the hot, dry summer under Mediterranean climate. However, water is a scarce resource across Mediterranean basin, and water allocation for agricultural purpose is rapidly declining due to growing competition from non-food sector (e.g. urban sanitation and entertainment purposes), as well as being driven by projected warming and drying trends under future climate change. Thus, climate change is expected to intensify existing risks, particularly in regions where water scarcity is already a concern. Taken together, it highlights the need to develop adaptation strategies for appropriate and integrated agricultural water management, by promoting sustainable practices and methods to improve crop and irrigation water productivity while maintaining crop yields in a changing climate.

In this context, we have developed a study concerning the projections of climate change impacts on several important aspects (e.g. grain yield, irrigation water use and productivity) of irrigated maize system at three sites in Ribatejo (Portugal), as well as exploring appropriate adaptation strategies based on examining the water-yield relations and their variations under different climate change projections. Two dynamic crop models (STICS and AquaCrop) are used to simulate the maize growth and yield responses to climate projections using the fine-resolution regional climate model. The ensemble mean over two models and three sites is used to represent the simulations at regional scale for a specific climatic period and scenario. Inter-model comparison and uncertainty analysis are also performed.

This chapter specifically covers this developed study, which has been published as a research article entitled "*Assessment of irrigated maize yield response to climate change scenarios in Portugal*" in an international journal of *Agricultural Water Management*. The works correspond to task 1 and 2 undertaken, aiming to provide insights and crucial information for stakeholders and policymakers to explore regional food security prospects, as well as aiding in enacting a sustainable and long-term agricultural policy (specifically for maize production and irrigation water management), preferably taking into account the need for adaptation response to forthcoming climate changes in the following decades.

Title: Assessment of irrigated maize responses to climate change scenarios in Portugal

Chenyao Yang[a,*], Helder Fraga[a], Wim van Ieperen[b] and João A. santos[a]

[a]*Centre for the Research and Technology of Agro-environmental and Biological Sciences, CITAB, Universidade de Trás-os-Montes e Alto Douro, UTAD, 5000-801, Vila Real, Portugal*

[b]*Group Horticulture and Product Physiology, 6700 AA Wageningen University, the Netherlands*

*****Corresponding author. E-mail: cyang@utad.pt

Refer to https://doi.org/10.1016/j.agwat.2017.02.004 for online published version.

Abstract

Maize is an important crop for the Portuguese agricultural sector. Future climate change, with warmer and dryer conditions in this Mediterranean environment, will challenge this high-water demanding crop. The present study aims at assessing the response of maize yield, growth cycle, seasonal water input and daily water productivity (DWP) to climate change, and analyse water-yield relations. For this purpose, two process-based crop models are used (STICS and AquaCrop) and were validated in simulating irrigated maize yields in Central Portugal (Ribatejo) by using regional statistics (1986–2005). Both models show an overall agreement in their outputs. The 2-model mean outputs are considered under future climate projections (2021–2080; RCP4.5 and 8.5), using the global/regional climate model chain M-MPI-ESM-LR/SMHI-RCA4. The most significant reductions on maize yield (–17%), growth cycle (–12%) and DWP (–19%) are observed for 2061–2080 under RCP8.5, with a noticeable decrease of seasonal water input (–9%) during 2041–2060. Decreased DWP is largely due to significant yield reduction, with limited benefit of atmospheric CO_2 enrichment. A water-yield relation analysis highlights that an increase of 2–14% in irrigation for future scenarios (compared to 1986–2005) might be a suitable strategy to mitigate yield reduction, despite substantially lower DWP (down to –23%). These findings demonstrate that our model approach can be used as a decision support tool by Portuguese farmers, particularly in optimizing maize production under changing climates.

Keywords: Maize Irrigation, Water Use Efficiency, STICS, AquaCrop, Climate Change Projections, Adaptation Strategies

3.1 Introduction

Crop production systems are often largely controlled by environmental factors, thus being vulnerable to climate change (IPCC, 2013). Anthropogenic forcing, leading to continuous rise of greenhouse gas (GHG) atmospheric concentrations, is expected to alter regional temperature and precipitation patterns, also contributing to higher risks of extreme weather events and climate irregularity (IPCC, 2013), with obvious implications on crops (Porter and Semenov, 2005). Maize (*Zea mays* L.) is a main food crop in the world and Europe is one of the most productive regions (Olesen et al., 2011). Assessments of maize responses to past changing climatic conditions generally point to an increased risk of yield reduction for Southern Europe and Mediterranean regions (Olesen et al., 2011; Supit et al., 2010; Wolf and Vandiepen, 1995). In the recent-past, irrigation strategies has been critical to stabilize/maximize yields in many regions worldwide, such as in Mediterranean-type climatic regions, where precipitation is scarce during the maize growing season. Crop water stress hampering physiologic processes (e.g. canopy cover expansion and stomatal functions) is expected to be enhanced by future warmer and drier climates, requiring more irrigation to mitigate potential yield reductions (Doll, 2002; Fischer et al., 2007; Wolf and Vandiepen, 1995).

Portugal, located in Southwestern Europe, features typical Mediterranean conditions. Maize has the largest area amongst annual crops, playing a key role in the Portuguese agri-food sector (Nóbrega, 2006). One of the most important maize growing regions is Ribatejo-Oeste (in Central Portugal, hereafter Ribatejo) **(Figure 1)**, having approximately ~30,000 ha of maize fields (ca. 35% of the total maize area in Portugal) (INE, 2015). The Ribatejo climate, characterized by very dry summers, does not naturally provide optimal conditions for a high water-demanding crop like maize, with a spring-summer growing season. Hence, almost all of the maize cultivated area (94%) is currently irrigated (INE, 2015).

According to the IPCC latest report (IPCC, 2013), southern Iberia (where Ribatejo is located) is projected to experience higher temperatures and lower precipitation in the future, which may bring new challenges for the regional sustainability of this crop. Furthermore, water availability for agricultural purposes is decreasing rapidly, as water demand by other socioeconomic sectors is also growing (Iglesias and Garrote, 2015; Iglesias et al., 2007). Maximizing water use efficiency (WUE) or water productivity (WP), i.e. the ratio of crop yield to transpiration-driven water uptake, is a plausible adaptation measure for stabilizing crop yields in the future (Zhang and Oweis, 1999).

WP can also be defined based on the ratio of yield to the sum of precipitation and irrigation (Howell, 2001).

Therefore, it becomes necessary to analyze maize yield response to varying water supply in order to identify the most efficient irrigation scheduling (Afzal et al., 2016; Dagdelen et al., 2006; Farre and Faci, 2009; Katerji and Mastrorilli, 2009). In future climates, the established water-yield relations are susceptible to being changed. The enhanced CO_2 levels may trigger higher maize biomass accumulation and yields, particularly under crop water stress conditions, while it tends to reduce water demand by diminishing crop transpiration (Islam et al., 2012). Rising temperatures may accelerate crop phenological development rates and shorten growing season, along with intensified transpiration rates. The multiple interactions among climatic elements and crops require an integrated analysis. As such, to better evaluate crop responses to climate change, process-based crop models are becoming increasingly used tools (Kang et al., 2009).

Coupling crop models with climate change projections, generated by high resolution regional climate models, is a common approach. Crop models dynamically simulate crop responses to management practices (e.g. irrigation), soil properties (e.g. texture, depth), as well as crop physiological responses to atmospheric conditions (e.g. air temperature, precipitation and CO_2). Some examples of these models are STICS (Simulateur mulTIdisciplinaire pour les Cultures Standard) (Brisson et al., 2003) and AquaCrop (Steduto et al., 2009). These two crop models mainly differ in their growth module: STICS is a radiation-driven model, estimating daily biomass formation from canopy intercepted radiation (Brisson et al., 2009), whereas AquaCrop adopts a water-driven strategy, assuming a linear relationship between crop transpiration and biomass production (Steduto et al., 2007). STICS has been tested and validated in simulating maize yield under deficit irrigation strategies (Katerji et al., 2010), also showing a good accuracy in predicting soil water content under various agro-environments (Constantin et al., 2015; Coucheney et al., 2015). AquaCrop, developed by FAO (Food and Agriculture Organization of the United Nations), also proves to be an effective tool to simulate maize yield response to contrasting irrigation regimes and soil moisture conditions (Abedinpour et al., 2012; Katerji et al., 2013; Paredes et al., 2014).

The present study aims at assessing climate change impacts on maize in Portugal, under recent-past and future scenarios, by coupling crop models with climate models. Particular emphasis will be given to water productivity. Therefore, our objectives are four-fold: 1) to compare the performance of two process-based crop models (STICS and AquaCrop) in simulating important

maize parameters under recent-past conditions; 2) to validate the two models in simulating regional irrigated maize yield; 3) to assess climate change impacts under different scenarios and future periods; 4) to test the effects of a wide range of seasonal water inputs on yield under different future climates.

3.2 Data and methods

3.2.1 Study sites

Three sites in Ribatejo, which have been used for maize cultivation in the past decades, were selected to capture spatial heterogeneities, namely Salvaterra de Magos (39.003°N, 8.793°W, 10 m a.s.l.), Catapereiro (38.822°N, 8.863°W, 20 m a.s.l.) and Coruche (38.960°N, 8.467°W, 30 m a.s.l.) **(Fig. 1)**. In Ribatejo, maize is grown in spring/summer, with conventional tillage and sowing date ranging from March to June. The mostly planted corn cultivars are medium-late varieties (FAO500-FAO600), with growth length around 130 days. A number of regional water reservoirs are critical for crop irrigation (Batista et al., 2001). Sprinkler irrigation is broadly used, with high irrigation efficiency (Nóbrega, 2006).

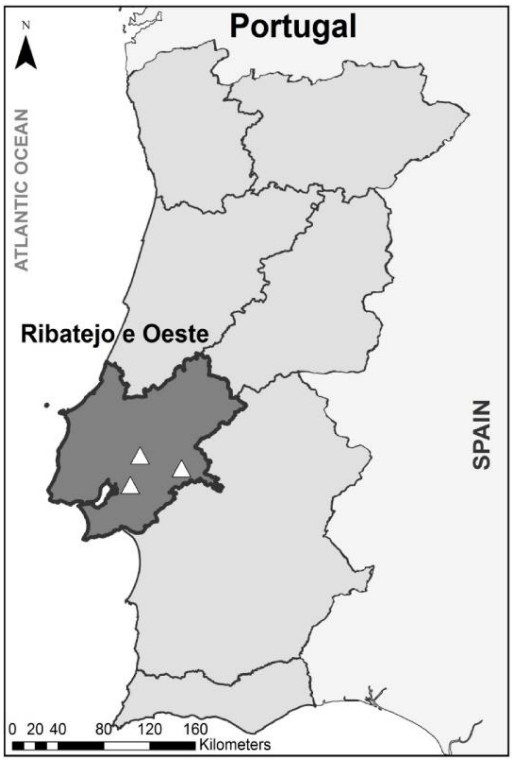

Figure 1 Location of the three selected sites in Ribatejo, Portugal.

3.2.2 Climate parameters and scenario projections

Daily weather data for running the two crop models are: minimum and maximum 2-m air temperature (ºC), solar radiation (MJ m^{-2} day^{-1}), rainfall (mm), wind speed (m s^{-1}), water vapour pressure (hPa), and atmospheric CO_2 concentration (ppmv). Potential evapotranspiration (PET), estimated by the Penman-Monteith method (Penman, 1948), is a climatic parameter also used by both models. In both models, PET was used to estimate maximum ET and, subsequently, the actual ET is obtained as a model output. Based on the selected three sites, daily temperature and precipitation over the historic period of 1986–2005 (baseline) are obtained from the E-OBS dataset (Haylock et al., 2008), v14.0, comprising gridded datasets (0.25° latitude × 0.25° longitude) from observational records (http://eca.knmi.nl/). For each site, wind speed, water vapour pressure and solar radiation are directly obtained from the evaluation run of the Regional Climate Model (RCM) SMHI-RCA4 (Samuelsson et al., 2011), produced within the EURO-CORDEX project at a spatial resolution of 0.125° latitude-longitude (Jacob et al., 2014). This running was forced by ERA-interim reanalysis (Dee et al., 2011). The atmospheric CO_2 concentration varies annually and was obtained from the Mauna Loa Observatory for the baseline and from two Representative Concentration Pathways, RCP4.5 and RCP8.5, for the future period. RCP4.5 is a climate change scenario with a slow rising rate of CO_2 content after 2070, while RCP8.5 is a CO_2 rising scenario until the end of the 21st century, at which the CO_2 concentration almost doubles that in RCP4.5 **(Table 1)**.

Table 1. Mean atmospheric CO_2 equiv. concentration for the three sub-periods of RCP4.5 and RCP8.5. For baseline (1986–2005) the mean value is of 363 ppmv.

Mean CO_2 concentration (ppmv)	**RCP4.5**	**RCP8.5**
2021-2040 (short-term)	460	485
2041-2060 (medium-term)	526	635
2061-2080 (long-term)	568	842

Regarding the climate change projections, the M-MPI-ESM-LR (Global Climate Model, GCM) coupled with the regional climate model (SMHI-RCA4) is used in the current study. The GCM/RCM chain, also obtained from the EURO-CORDEX project (Jacob et al., 2014), is selected due to its high performance in reproducing the observed seasonality in westernmost European

regions (Santos et al., 2016). In EURO-CORDEX, future daily weather data was forced by two scenarios (RCP4.5 and RCP8.5) for the period of 2021–2080. The projected changes on CO_2 are also taken into account by the crop models, allowing the integration of elevated CO_2 effect on maize yield. Moreover, in the present study, model data was submitted to preliminary point-by-point bias corrections on a monthly scale, using E-OBS as a reference for temperatures and precipitation and the evaluation run for the remaining variables.

3.2.3 Soil parameters

The three study sites are selected to represent the predominant agricultural soil texture (USDA) in Ribatejo, which is loamy sand with some distribution of sandy soil **(Table 2)**. The main site-specific soil properties are obtained from the Harmonized World Soil Database (HWSD, v1.2). HWSD is an ensemble of several soil databases, providing worldwide soil data at high grid cell resolution (~1 km), in which 48,148 soil profile tables are presented, including standardized taxonomic classification, soil phases, and chemical-physical properties of topsoil (30 cm) and subsoil (70 cm) (Jones and Thornton, 2015). Site related topographic characteristics, such as slope degree and elevation, are obtained from the GTOPO30 digital elevation model (https://lta.cr.usgs.gov/GTOPO30, **Table 2**). Based on the obtained slope degree, no surface runoff is considered for study sites. The dry soil albedo is only considered in STICS, which plays a significant role in estimating soil temperature (Richard and Cellier, 1998).

Both models require hydrodynamic characteristics (e.g. soil volumetric content at field capacity, wilting point, infiltration rate, cumulative evaporation limit), which are calculated as a function of obtained soil texture class using pedo-transfer functions (Brisson et al., 2009; Wosten et al., 2001) **(Table 2)**. In both models, standard soil layer thicknesses are set as: 0–30 cm for top soil, and 30–100 cm and 100–200 cm for the two subsoil layers. The two models incorporate soil characteristics at different degrees of resolution, i.e. an elementary layer of 1 cm for STICS and of 10 cm for AquaCrop. Soil chemical parameters are also different, with pH and $CaCO_3$ content considered in STICS and salinity level in AquaCrop **(Table 2)**. Since the study sites are irrigated fields (deep capillary rise is ignored), initial soil water content at planting date is set at field capacity.

3.2.4 Agronomic parameters

Table 2. Soil parameters for three study sites in Ribatejo, along with their respective denomination, dataset source or reference literature. Parameters used in pedotransfer functions for soil hydrodynamic property estimations are highlighted by "*".

Soil parameter description	Salvaterra de Magos		Catapereiro		Coruche		Calculation method/Source
	STICS	AquaCrop	STICS	AquaCrop	STICS	AquaCrop	
Limestone content in topsoil (%)	0	-	0	-	0	-	HWSD
Initial soil pH in topsoil	6	-	4.4	-	4.4	-	HWSD
Dominant soil group (FAO)	Arenosols		Podzols		Podzols		HWSD
Topsoil texture*	Coarse		Coarse		Coarse		HWSD
Topsoil USDA texture*	Sand		Loamy Sand		Loamy Sand		HWSD
Subsoil texture*	Coarse		Coarse		Coarse		HWSD
Subsoil USDA texture*	Sand		Sand		Sand		HWSD
Albedo of dry soil	0.25	-	0.25	-	0.25	-	(Richard and Cellier, 1998)
Cumulative evaporation limit (mm)	*q0*=6.65	*REW*=4	*q0*=6.95	*REW*=5	*q0*=6.95	*REW*=5	(Brisson et al., 2009; Ritchie, 1972)
Mean slope classes (%)	0–2		0–2		0–2		GTOPO30
Soil salinity (dS/m)	-	0.1	-	0.1	-	0.1	HWSD

In order to represent the commonly grown varieties in Ribatejo, a medium-late maturation is defined in both STICS and AquaCrop. This is done by adjusting crop model phenological parameters to the thermal forcing requirements (e.g. growing degree day – GDD) for different development stages. A selected medium-late variety with standard settings is used in STICS, while the modification of GDD parameters in crop file is performed for AquaCrop **(Table 3)**. Although the thermal requirements are similar for the selected medium-late varieties, the GDD definition in both models is different, since the corresponding threshold temperatures (T_{base} /T_{max}) are 6/32 ºC in STICS and 8/30 ºC in AquaCrop **(Table 3)**.

In both models, root growth determines crop water availability and water stress level. More sensitive parameters for these processes are modified. In STICS, sensitivity of root deepening rate to soil moisture is defined by parameter *Sensrec* (default=0, indicating root growth is extremely sensitive to soil water deficit), in which an intermediate value of 0.5 would avoid overestimation of soil dryness on hindering roots growth (Jego et al., 2011) **(Table 3)**. As in AquaCrop maize

maximum effective root depth determines root volume and available soil moisture, 1.2 m is specified to represent the medium-deep root system (Abedinpour et al., 2012).

An automatic scheduling of irrigation events is selected for both models. The criterion for activating an irrigation event is based on a pre-defined crop water stress level, for STICS, and based on soil moisture depletion of total available water (TAW) over the root zone, for AquaCrop. However, crop water stress affecting canopy expansion, transpiration rate and biomass growth is determined as a function of root zone water availability and crop water demand in both models. To account for moderate local irrigation input, mild crop water stress before an irrigation event (*ratiol*=0.5 for STICS and 50% decrease in TAW for AquaCrop, **Table 3**) is set for irrigation thresholds (Tardieu and Katerji, 1991). For individual irrigation events, STICS replenishes soil water content to field capacity, whereas AquaCrop supplements small amounts to maintain the pre-defined TAW depletion, following the concept of net irrigation requirement (Raes et al., 2012). These differences imply more frequent irrigation in AquaCrop.

Table 3. Modified crop and management input parameters of STICS and AquaCrop for validation procedure.

Parameters	STICS	AquaCrop
Cultivar phenology characteristics	Embedded cultivar (Pactol) in default value: *Tbase*=6 °C, *Tmax*=32 °C Emergence to end of juvenile (GDD): 253 End of juvenile to max leaf area (GDD): 507 Emergence to grain filling onset (GDD): 1080 Grain filling onset to maturity (GDD): 600 Root lifetime (GDD): 1500 Flowering duration (GDD): 250	*Tbase*=8 °C, *Tmax*=30 °C Sowing to emergence (GDD): 84 Sowing to max Canopy (GDD): 708 Sowing to senescence (GDD): 1260 Sowing to maturity (GDD): 1560 Sowing to max root (GDD): 1260 Sowing to flowering (GDD): 876 Flowering duration (GDD): 192 HI building duration (GDD): 588
Sensitivity parameter of root growth	*Sensrec*=0.5	Effective Root depth =1.2 m
Sowing date	April 20th	April 20th
Sowing density	7.5 plant.m^{-2}	7.5 plant.m^{-2}
Irrigation	*Ratiol*=0.5	Determination of net irrigation requirement= 75%**RAW*=50%**TAW*
Fertilization	160 kg ha^{-1} mineral N fertilizer, equally split between 12 and 30 days after sowing	Near optimal nutrition condition, corresponding to 7% soil fertility stress
Organic residue	*julres*=100, *coderes*= 1, *qres*=9, *Crespc*=42, *CsurNres*=90, *Nminres*=0, *eaures*=7, *jultrav*=100, *profres*=0, *proftrav*=25	-
Harvest method	Physiological maturity	Physiological maturity

Note: *Tbase* – minimum temperature allowing plant development; *Tmax* – maximum temperature allowing plant development; *Sensrec* – index of root sensitivity to drought; *Ratiol* – crop stomatal water stress index below which an irrigation event is triggered; *julres* – Julian day for organic residue addition; *coderes* – type of organic residue; *qres* – organic residue quantity; *Crespc* – organic carbon content; *CsurNres* – C/N ratio of organic residue; *Nminres* – mineral nitrogen fraction; *eaures* – water content of organic residue; *jultrav* – Julian day of tillage; *profres* – upper depth of organic residue; *proftrav* – maximum depth of organic residue incorporation. *RAW* – readily available water for root zone uptake before start of stomatal closure. TAW – total available water between soil field capacity and wilting point.

For both models, sowing date, sowing density and harvest method are empirically obtained from local cultivation practices **(Table 3)**. In STICS, the organic residue provides certain amount of mineral N and helps maintaining soil moisture, being parameter values describing residue attributes retrieved from Brisson et al. (2009), assuming that cereal straw prevails on maize field surface. Organic residue practices are not considered in AquaCrop. Fertilization is the most important source of mineral N, for which fertilization rate and frequencies are input parameters for STICS. For AquaCrop, only qualitative estimation of soil fertility stress on potential biomass reduction is established (Raes et al., 2012). Herein, both models assume near optimal N condition **(Table 3)**.

3.2.5 Model runs and validation

Based on the selected three sites, the two models (STICS v8.41 and AquaCrop v5.0) were run over different periods (i.e. 20 years each) for baseline (1986–2005), for future short-term (2021–2040), medium-term (2041–2060) and long-term (2061–2080) periods under RCP4.5 and RCP8.5. Crop model validation for yield simulation is herein carried out at regional scale over baseline, by comparing modelled with observed yields retrieved from national statistical bureau (*Instituto Nacional de Estatística*, INE). Additionally, a comparative analysis of the performance of the two models is undertaken to examine their agreement in simulating yield and yield-related outputs over baseline. Keeping the same settings (e.g. moderate water supply) as in baseline, impact assessments of the two climate change scenarios on studied variables (described below) are performed.

3.2.6 Water use efficiency

The conventional crop WUE definition is based on the ratio between yield and actual crop ET (Perry, 2011), but the present study aims to assess irrigation requirement during the growing cycle. Therefore, an adapted measure of applied water, Daily Water Productivity (DWP), is proposed as

an efficiency indicator of seasonal water input (irrigation plus precipitation). DWP ($kg.m^{-3}$.day) is the yield divided by daily water input (ratio of seasonal water input to growth cycle length). This metric allows taking into account precipitation seasonal distribution for assessing irrigation scheduling on a daily basis in both STICS and AquaCrop, which enables accurate water accounting and provides guidelines when attempting to optimize irrigation input. The current methodology aims to quantify the role of growth cycle on seasonal water use, under present and future scenarios. In fact, shorter maize growth cycle is likely to occur in the future, thus reducing seasonal water supply, crop transpiration and water demand (Islam et al., 2012; Meza et al., 2008). Conversely, a longer growth cycle is likely to produce larger and deeper root systems that allow extracting more soil moisture and maximizing crop water uptake (Blum, 2009; Debaeke and Aboudrare, 2004). DWP incorporates three components: yield, seasonal water input and growth cycle length, which are the main study variables of agronomic interest for irrigated maize. However, DWP is an adapted water use efficiency indicator, used herein for a specific purpose. For comparison purposes, the conventional WUE was also computed (i.e. yield divided by actual ET), and differences to this new metric were assessed. A more comprehensive analysis of agricultural water use efficiency terminology can be found in Perry (2011).

3.2.7 Adaptation measures: irrigation trials

In order to assess maize yield response to seasonal water supply, with changes in DWP under different climate change scenarios, several seasonal water input in silico trials (crop water stress varying from severe to mild, or to absence) are undertaken. Therefore, possible adaptation measures based on irrigation strategies can be identified to mitigate potential yield losses. This is carried out by implementing a wide range of irrigation thresholds in both crop models, keeping other parameters invariant. Seasonal irrigation is gradually increased: water stress level from 0.00 to 1.00 at 0.02 intervals, for STICS, and soil water depletion level from 100% to 0% at 2% intervals, for AquaCrop. For each seasonal water input trial, the two models are re-run for baseline and for the three future sub-periods under RCP4.5 and RCP8.5. The averages for the two models and three sites are then computed (ensemble means). The corresponding relative changes (%) to the 0%-baseline (i.e. baseline for model comparison and validation) in yield, seasonal water input and DWP are assessed for the different time periods separately.

3.3 Results and Discussions

3.3.1 Historic and future climatic conditions in Ribatejo

Monthly mean temperatures (T_{min}, T_{mean} and T_{max}) and precipitation (Prec) over both baseline (1986–2005) and future long-term period (2061–2080) are firstly investigated across the three selected sites. For the recent-past, T_{mean} varies from approximately 10.0ºC in January to around 23.5ºC in July/August, showing moderate temperature seasonality, while T_{min} remains above 5.0ºC throughout the year and T_{max} ranges from 15.0ºC in January to 31.0ºC in July/August (hot summertime diurnal temperatures) **(Fig. 2a)**. Precipitation is mostly concentrated in autumn and winter (October to February), being summer particularly dry (neglectful rainfall from June to August) **(Fig. 2a)**. For the growing season, T_{mean} rises from ~15.0ºC around seeding (April) to ~23.5ºC during grain filling stage (June to September). Regarding the precipitation regime, it is clearly unfavorable: high water demanding stages (June to September) present monthly rainfall

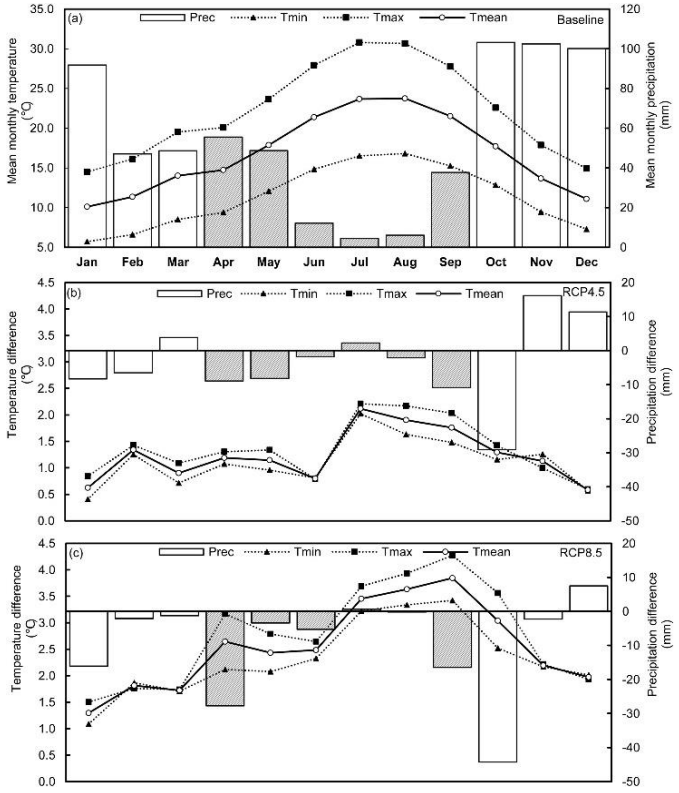

Figure 2 Monthly means of daily minimum (T_{min}), maximum (T_{max}) and mean (T_{mean}), temperatures and mean monthly precipitation totals (Prec) are shown for the three selected sites in Ribatejo over (***a***) baseline (1986–2005). The differences for T_{min}, T_{max}, T_{mean} and Prec between the long-term period (2061–2080) and baseline are shown for (***b***) RCP4.5 and (***c***) RCP8.5. The growing season for local grain maize cultivation is from April to September (filled columns).

varying from 4.4 mm to 37.7 mm, with very low precipitation accumulation from June to August (<10 mm) **(Fig. 2a)**. In fact, the offset between the maize growing season and the precipitation regime subjects maize growth to the dry half of the year, which is unsuitable for rainfed maize.

For the future long-term period in RCP4.5 and RCP8.5, a strong seasonal warming trend and intensified precipitation shortage are observed. Growing season T_{mean} is projected to averagely increase by 1.5ºC and 3.1ºC, under RCP4.5 and RCP8.5 respectively, with significant rise for the warmest months (yield formation stage), where T_{mean} increase by 2.0ºC under RCP4.5 or 3.5ºC under RCP8.5 **(Fig. 2b, c)**. Moreover, the projected changes for T_{min} and T_{max} are very similar to T_{mean} in both scenarios, but with slightly stronger changes for T_{max}. For precipitation in both scenarios, monthly precipitation is projected to decrease for spring and autumn (transitional seasons), while summer remain very dry, thus enhancing overall dryness conditions throughout most of the year **(Fig. 2b, c)**. The extent of reduction is more pronounced in RCP8.5 (6–17 mm) than in RCP4.5 (2–11 mm) over the critical water demanding stage **(Fig. 2b, c)**. It is worth noting that the greatest precipitation reduction occurred in October for both scenarios, but with no direct implications on maize production.

3.3.2 Inter-model comparison

Assessing the coherence between STICS and AquaCrop in simulating the selected maize output variables (yield, growth cycle, irrigation and seasonal water input, maximum leaf area index and cumulative actual evapotranspiration) are analyzed for baseline (0%-baseline) **(Fig. 3)**. Statistically significant correlations (p<0.01, two-tail Spearman method) between models are found for yield (r=0.89), growth cycle (r=0.87), irrigation amount (r=0.60), seasonal water amount (r=0.89), maximum leaf area index (LAI_{max}) (r=0.92) and cumulative actual evapotranspiration (ET) (r=0.81) **(Fig. 3a-f)**. For the 20-year means, STICS shows relatively higher yields than AquaCrop (STICS=10,690.7 kg ha^{-1}, AquaCrop=9,471.8 kg ha^{-1}), i.e. a relative difference of 11.4%. Nonetheless, STICS shows lower values than AquaCrop for the remaining variables, but with small relative differences: growing cycle length (STICS=122.0 days, AquaCrop=126.0 days, –3%), irrigation (STICS=407.5 mm, AquaCrop=418.9.0 mm, –3%), seasonal water input (STICS=495.2 mm, AquaCrop=507.6 mm,–3%), LAI_{max} (STICS=3.0 m^2 m^{-2}, AquaCrop=3.37 m^2 m^{-2}, –12%) and ET (STICS=509.6 mm, AquaCrop=535.9 mm,–5%). Apart from yields, these outputs cannot be validated owing to the lack of observational data at regional scale.

The linear regression slopes also provide an estimate of output sensitivity (value distribution range of each model) to climatic conditions. The LAI_{max} is the variable clearly showing a larger climate sensitivity in AquaCrop than in STICS, while the remaining variables present similar responses **(Fig. 3a-f)**. The high correlation and relatively small differences between the two crop models for these outputs is evident. Hence, the 3-site model ensemble means will be subsequently used for annual simulation.

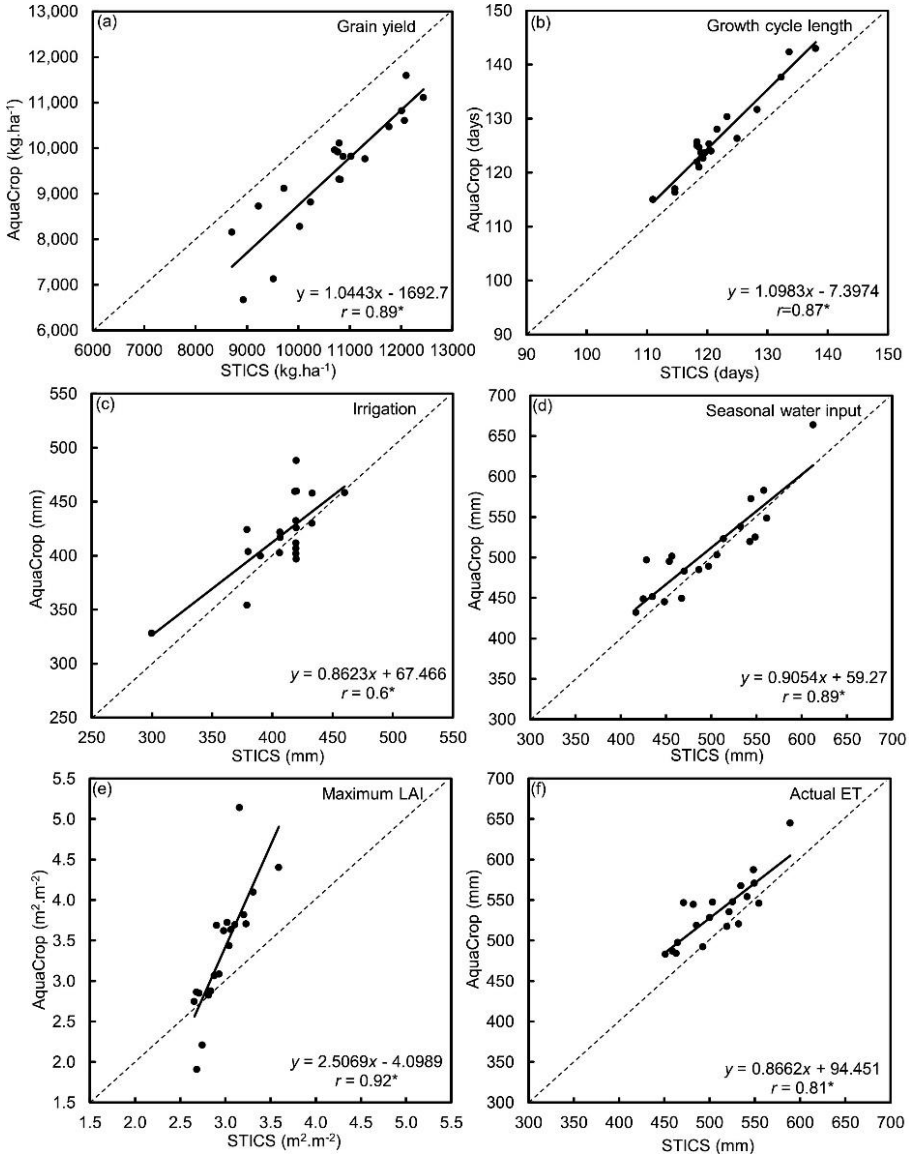

Figure 3 Comparison of STICS and AquaCrop in simulating seasonal (***a***) grain yield, (***b***) growth cycle length, (***c***) irrigation, (***d***) seasonal water input, (***e***) LAI_{max} (maximum LAI) and (***f***) actual ET (evapotranspiration) over the baseline period (1986–2005) and in the study sites. *r* indicates correlation coefficients between the two model outputs ("*" denotes statistically significant correlation at $p<0.01$ by two-tail Spearman analysis).

3.3.3 Regional yields and model validation

In Ribatejo, the mean observational yield has initially fluctuated around 6,300 kg ha^{-1} in the 1986–1991 period, but rose rapidly to 9,500 kg ha^{-1} by the end of the 1990s, despite the reduction to 8,600 kg ha^{-1} in 2005 **(Fig. 4a)**. The anomalously low yield in 2005 can be explained by the extreme 2004/05 drought in Portugal (Santos et al., 2007). The simulated yields show that both models systematically overestimate observational yields, being the bias in their means 2,473.3 kg.ha^{-1} for STICS and 1,254.5 kg.ha^{-1} for AquaCrop **(Fig. 3a, 4a)**. However, this will not significantly compromise the model skills at regional scale, since more emphasis is given to their ability to replicate inter-annual variability of yield (i.e. correlation coefficient between observations and simulations) than to simulate its absolute-values (Li et al., 2011; Xiong et al., 2007). Further, a strong upward linear trend of 236.1 kg ha^{-1} year^{-1} is identified for the observational 20-year time series with the mean yield of 8,217.4 kg ha^{-1}. As the trend may largely reflect gradual changes in technology development and agronomic practices (e.g. land use, fertilization, irrigation and varietal selection), which are difficult to discriminate and are out of the scope of the present study, the linear trend is removed.

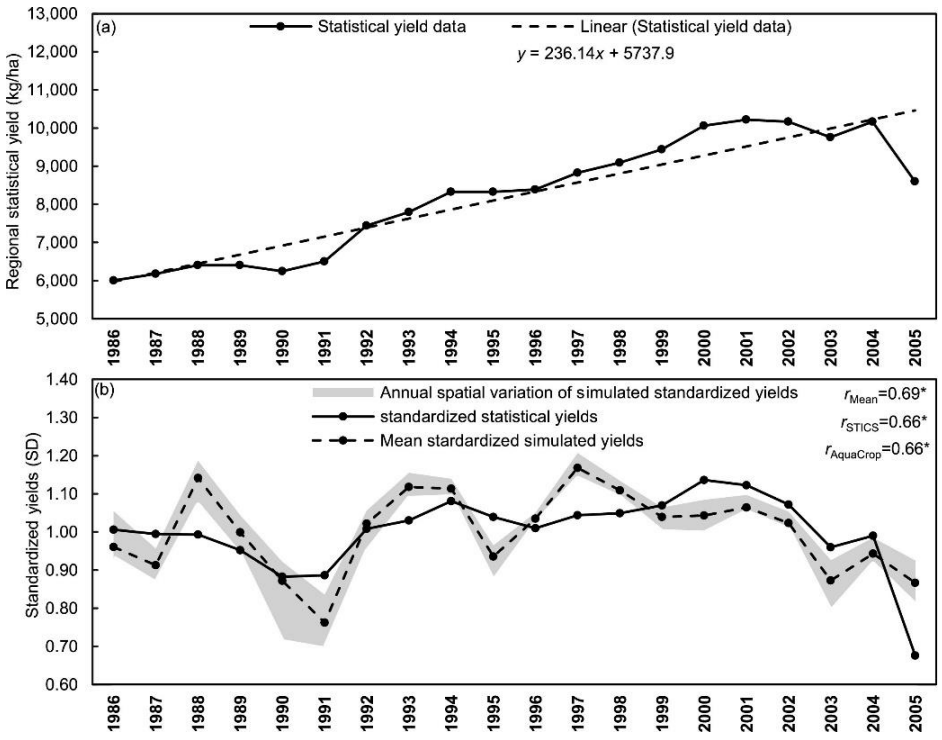

Figure 4 Standardized irrigated maize yields from simulations for the 3 study sites and observed yields over baseline (1986-2005). (***a***) Chronogram of statistical yield series in Ribatejo for baseline, along with the respective linear trend.

(***b***) Comparison of standardized yields between regional statistics and mean simulations by STICS and AquaCrop, along with the corresponding correlation coefficient ("*" denotes statistically significant correlation at $p<0.01$ by two-tail Spearman analysis). The simulated annual yield spatial variation (grey shading) is also displayed.

The agreement for the standardized yields (divided by their corresponding averages) between observation and simulation is clear ($r=0.69$, $p<0.01$ according to the two-tail Spearman test) **(Fig. 4b)**. The two models separately obtain a lower correlation coefficient ($r=0.66$) than the model ensemble average. For baseline period, a low simulated spatial yield variation is observed among three sites (grey shading in **Fig. 4b**). For annual simulation (3-site model ensemble mean), the coefficient of variation (CV) for yield varies from 3% to 16% over the baseline period. A similar study validating crop model simulations (from CERES-Maize) at grid-level and using statistical maize yield, shows the association with $r<0.5$ (Xiong et al., 2007). The overall good agreement suggests that our model approach is able to reproduce temporal and spatial maize yield variations, also allowing climate change impact assessments.

3.3.4 Climate change impacts

A clear strong warming and drying trend under RCP4.5 and RCP8.5 are projected for the study sites **(Fig. 2)**. The projected annual outputs correspond to the ensemble means over the 3 sites and 2 models. An 11-year moving average is firstly applied to filter out high-frequency inter-annual variability, emphasizing a long-term trend over the future period **(Fig. 5a, c, e, g)**. For yield, 60-year linear downward trends are projected, with annual reduction rates of 20 kg ha^{-1} year^{-1} (RCP4.5) or 28.9 kg ha^{-1} year^{-1} (RCP8.5) **(Fig. 5a)**. Similar analysis for growth cycle, seasonal water input and DWP also reveal progressive decline trends, displaying stronger effects for RCP8.5 than for RCP4.5 **(Fig. 5c, e, g)**. The mean and standard deviation (SD) of simulated outputs are now analysed for each specific period.

Impacts on grain yield (kg ha^{-1})

The predicted yields show a continuously decrease from 10,081.3 kg ha^{-1} in the baseline to 9,791.3 kg ha^{-1} (–3%, RCP4.5) or 9,434.4 kg ha^{-1} (–6%, RCP8.5) for 2021–2040 (short-term period), to 9,184.5 kg ha^{-1} (–9%, RCP4.5) or 8,776.1 kg ha^{-1} (–12.9%, RCP8.5) for 2041–2060 (medium-term period), then falling to 9,029.9 kg ha^{-1} (–10%, RCP4.5) and 8,410.6 kg ha^{-1} (–17%, RCP8.5) for 2061–2080 (long-term period) **(Fig. 5b)**. A slight decrease of yield variability is detected from

baseline (SD=1,145.2 kg ha^{-1}) to the long-term period for RCP4.5 (SD=1,042.9 kg ha^{-1}) or RCP8.5 (SD=1,073.6 kg ha^{-1}). However, it is known that crop yield SD simulated using atmospheric datasets derived from climate models tend to be lower than using observational data (Qian et al., 2011). The projected yield reduction in Ribatejo (Portugal) could be compared to other intense irrigated maize fields under Mediterranean-type climates. For instance, the combined effect of CO_2 increase with warmer and drier climates was simulated using CropSyst in two Italy sites, projecting a maize yield reduction of 20% with significant growth cycle reduction (Tubiello et al., 2000). Similar values were found by Guerena et al. (2001) for two Spanish basins, in which maize yield has been projected to decrease by up to 16%.

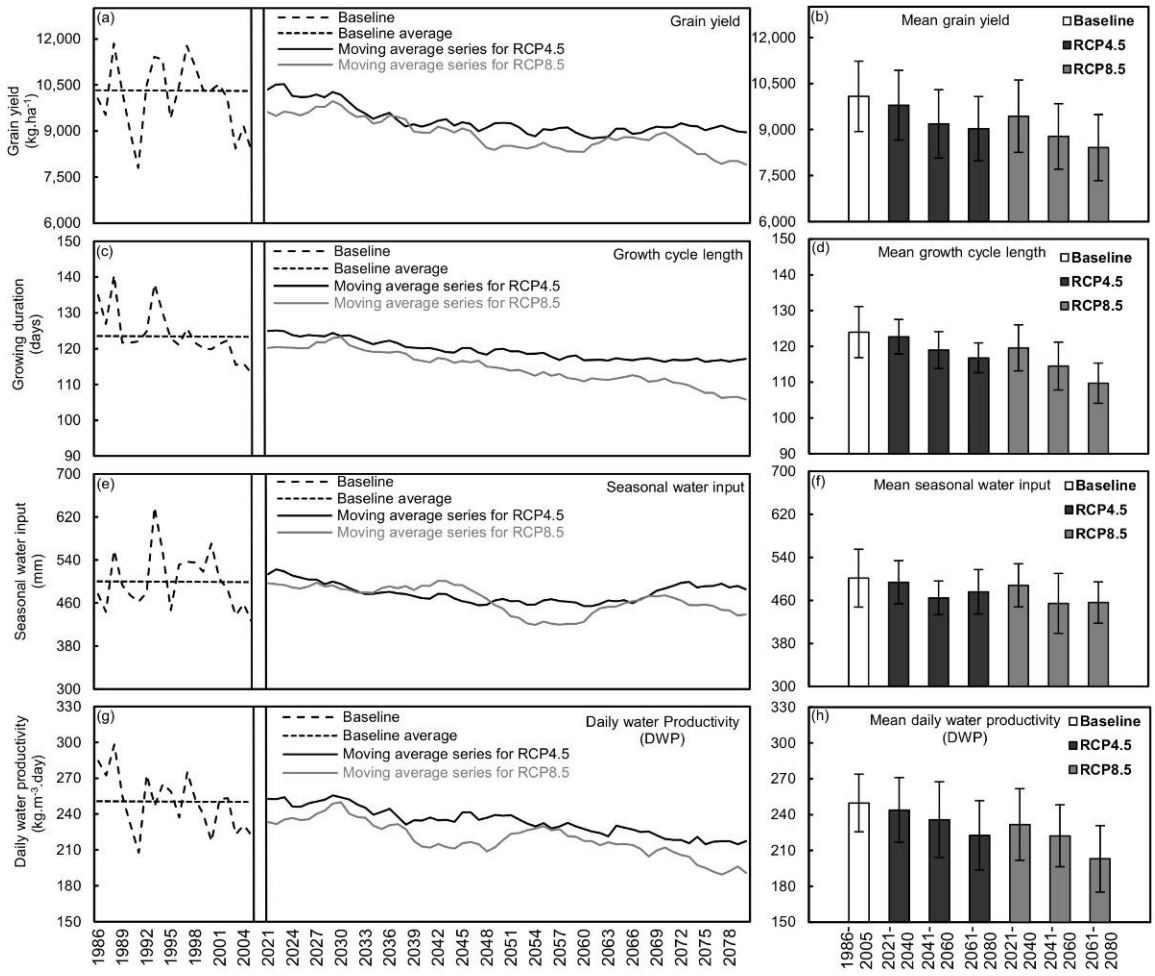

Figure 5 Projected yield, growth cycle length, seasonal water input and daily water productivity (DWP) under climate change scenarios (RCP4.5 and RCP8.5) for the three study sites in Ribatejo: (***a, c, e, g***) corresponding 11-year moving averaged series for RCP4.5 and RCP8.5; (***b, d, f, h***) averages and standard-deviations (error bars) for baseline and future sub-periods (2021–2040, 2041–2060 and 2061–2080) under RCP4.5 and 8.5. The ensemble means for the 2 models and 3 sites are used for annual outputs.

Impacts on seasonal growth duration (days)

The growth cycle length is projected to decline from 124 days (baseline) to 123 (–1%, RCP4.5) or 119 days (–4%, RCP8.5) in the short-term, to 119 (–4%, RCP4.5) or to 114 days (–8%, RCP8.5) for the medium-term, and to 117 days (–6%, RCP4.5) or to 109 days (–12%, RCP8.5) for the long-term period **(Fig. 5d)**. The mean SD over the three periods in RCP4.5 (4 days) or RCP8.5 (6 days) shows shorter ranges than for baseline (8 days). A steady reduction on both yield and growth cycle throughout the future period, mostly for RCP8.5, is observed, including decreasing inter-annual variability. Future higher temperature may facilitate a faster crop development rate, thus shortening growth cycle length, likely with insufficiently long phenological stages (e.g. flowering or grain filling for dry matter and yield formation), subsequently resulting in lower yields, as was already found in field experiments ~100 km away from our study sites (da Silva and Silva, 2008).

Impacts on seasonal water input (mm)

Seasonal water input combines precipitation with irrigation, which are determined by weather conditions and by root zone water deficit. It decreases from 501 mm (baseline) to 494 mm (–1%, RCP4.5) or 488 mm (–3%, RCP8.5) in the short-term period and to 465 mm (–7%, RCP4.5) or 454 mm (–9%, RCP8.5) over the medium-term, then following a slight increase to 476 mm (–5%, RCP4.5) or 456 mm (–9%, RCP8.5) for the long-term period **(Fig. 5f)**. In the same way, the mean SD over the three sub-periods displays longer ranges for RCP8.5 (45 mm) than for RCP4.5 (38 mm), but lower than for the baseline (54 mm).

The general reduction of seasonal water input compared to baseline may be attributed to both decreasing precipitation and shortening growth cycle with less opportunity for receiving irrigation. Similar studies, using the DSSAT crop model and multiple future climate change scenarios, illustrate that the seasonal irrigation water use for corn tends to decrease substantially with diminished crop transpiration (crop water requirement), caused by elevated CO_2 level and shortening of crop maturity duration (Islam et al., 2012; Meza et al., 2008). However, in current study, the higher seasonal water use in the long-term period than in the medium-term under both scenarios is due to more frequent irrigation supply in the former period to guarantee a moderate irrigation input as defined in baseline. As the severest water stress is expected in the long-term period, with decreased growing season, more frequent irrigation applications could be perceived as an adaptation strategy for model to meet the increased occurrence of pre-defined specified water

stress (STICS) or allowable root zone water depletion (AquaCrop). This could also be reflected by the variation of daily water input: 4.04 mm day^{-1} in the baseline, decreased to 3.91 mm day^{-1} (RCP4.5) or 3.94 mm day^{-1} (RCP8.5) over the medium-term period, followed by an increase to 4.06 mm day^{-1} (RCP4.5) or 4.15 mm day^{-1} (RCP8.5) over the long-term period.

Impacts on seasonal water productivity (kg m^{-3} day)

Owing to the projected decrease in yield, growth cycle and seasonal water input, DWP decreases from 249.8 (baseline) to 243.8 (–2%, RCP4.5) or 231.7 kg m^{-3} day (–7%, RCP8.5) in the short-term period **(Fig. 5h)**. The medium-term period shows a reduction to 235.7 (–6%, RCP4.5) or 222.3 (–11%, RCP8.5) kg m^{-3} day, then descending to 222.6 (–11%, RCP4.5) or 203.0 (–19%, RCP8.5) kg m^{-3} day for the long-term period **(Fig. 5h)**. With respect to the conventional WUE (yield per unit of ET), the decrease in RCP4.5 varies from 2.01 kg m^{-3} in baseline to 1.98 (–1.4%), 1.97 (–1.8%) and 1.90 kg m^{-3} (–5.5%), for the short-term, medium-term and long-term period, respectively. The respective reductions of WUE in RCP8.5 over these periods are 1.93 (–4%), 1.94 (–3%) and 1.85 kg m^{-3} (–8%). The larger magnitude of decrease for DWP than for WUE demonstrates that DWP is a more sensitive indicator of water use efficiency under climate change scenarios. Moreover, the decline trend for DWP is more driven by the observed reduction on yield than by the variation of daily water input, since only small differences are detected for daily water input until the long-term period, either for RCP4.5 (4.06 mm day^{-1}) or RCP8.5 (4.15 mm day^{-1}), compared to baseline (4.04 mm day^{-1}). Additionally, in contrast with the previous parameters, the mean SD of the three sub-periods increases from 24.0 in baseline to 29.3 for RCP4.5 or 27.9 kg m^{-3} day for RCP8.5.

Previous findings suggest the increased atmospheric CO_2 concentration generally result in an increase of WUE, owing to enhanced photosynthetic rate and declined stomatal conductance and transpiration (Polley, 2002). However, the interaction between such positive effect and the potential negative impact from the remaining climate elements on WUE has been less addressed. In our study, DWP gradually declines as a result of yield reduction, despite the elevated CO_2 level. It suggests that the beneficial CO_2 effects are not enough to mitigate other negative impacts on yield. As Mo et al. (2009) shows, the simulated detrimental effect of warming is significantly larger than the positive CO_2 enrichment on maize yield in North China Plains, leading to a 25% reduction on WUE.

3.3.5 Adaptation measures: irrigation trials

In view of the projected yield reductions under RCP4.5 and RCP8.5, different irrigation amounts are tested (in silico) as possible climate change adaptation measures to maintain past yields. These trials firstly lead to the relative change (%, relative to 0%-baseline) of seasonal water input from –35% to 35% for the baseline, RCP4.5 and RCP8.5, together with corresponding changes in yield and DWP **(Fig. 6)**. In addition, only changes in seasonal water input are displayed to conform to DWP definition, which directly corresponds to changes in irrigation amount. Although such changes comprise various irrigation timings, only seasonal totals are considered. Third-order polynomial curves are applied to the outputs of these irrigation trials (fitness measurement by R-square) **(Table 4)** and are then described in the following sections.

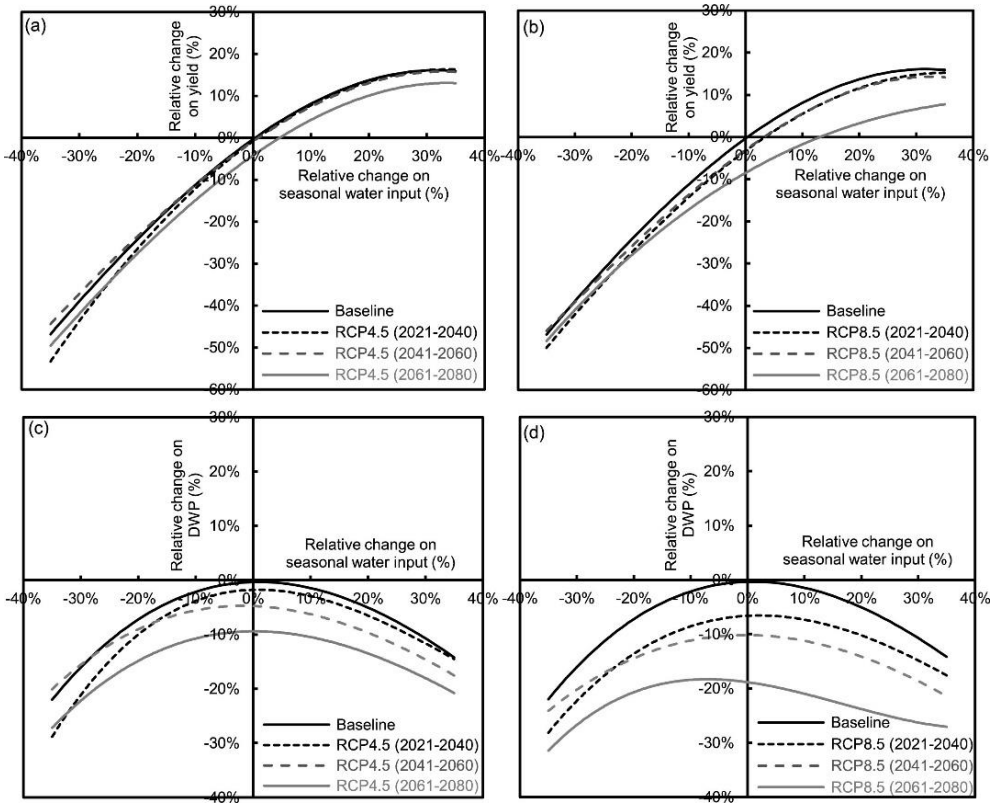

Figure 6 Effects on yields and daily water productivity (DWP) as a function of relative changes (%) in seasonal water input for (***a, c***) baseline and future sub-periods under RCP4.5, and for (***b, d***) baseline and future sub-periods under RCP8.5.

In comparison with the 0%-baseline (i.e. 0% change in irrigation, yield and DWP), 35% less seasonal irrigation (i.e. severe water stress) corresponds to a 47% yield reduction, while 35% more

(i.e. absence of water stress) leads to a 16% yield increase (potential yield) over baseline period **(Fig. 6a-b)**. At higher irrigation levels (>20%), yield stabilizes thereafter. These results highlight the non-linear relationship between yield and irrigation, which is taken into account by the crop models. In accordance with WUE evolution suggested by Geerts and Raes (2009), DWP of all studied periods is firstly very low for limited water supply, following a linear increase with additional water application, until a range of optimal water supply is achieved with maximum DWP **(Fig. 6c-d)**. DWP then decreases owing to excessive water supply that will slow yield increase rate and increase seasonal water input. For all baseline irrigation trials, the maximum obtained DWP (249.8±1.3 kg m^{-3} day) is achieved by a range of irrigation from –7% to 9%, including the 0%-baseline trial **(Fig. 6c-d)**.

Table 4. Equations of three-order polynomial curves for relative changes (in %) in yield or daily water productivity (DWP) (dependent variables) as a function of the relative changes (in %) in seasonal water input (independent variable) for the outlined periods. The corresponding R-square measures fitting these relations are also outlined.

Periods		**Yield change (*y*) vs. Seasonal water change (*x*)**	**DWP change (*y*) vs. Seasonal water change (*x*)**	**R^2 (yield/DWP)**
Baseline (1986-2005)		$y = -0.6424x^3 - 1.2363x^2 + 0.975x - 0.0032$	$y = 0.6868x^3 - 1.4505x^2 + 0.0272x - 0.0035$	0.98/0.93
RCP 4.5	2021-2040	$y = -0.0236x^3 - 1.4471x^2 + 0.9979x - 0.0078$	$y = 1.4173x^3 - 1.6249x^2 + 0.0305x - 0.0177$	0.91/0.87
	2041-2060	$y = -0.6701x^3 - 1.1047x^2 + 0.9405x - 0.0082$	$y = 0.6396x^3 - 1.1467x^2 - 0.0419x - 0.0477$	0.87/0.82
	2061-2080	$y = -0.5844x^3 - 1.1494x^2 + 0.9657x - 0.0419$	$y = 0.6999x^3 - 1.189x^2 + 0.0061x - 0.0942$	0.89/0.83
RCP 8.5	2021-2040	$y = -0.5156x^3 - 1.154x^2 + 0.995x - 0.0325$	$y = 0.7911x^3 - 1.3271x^2 + 0.0531x - 0.0662$	0.82/0.89
	2041-2060	$y = -0.9207x^3 - 1.0523x^2 + 0.972x - 0.0301$	$y = 0.3683x^3 - 1.0299x^2 - 0.0068x - 0.1017$	0.83/0.84
	2061-2080	$y = 0.2572x^3 - 0.9675x^2 + 0.7713x - 0.0848$	$y = 1.7006x^3 - 0.8496x^2 - 0.1454x - 0.1884$	0.72/0.69

For RCP4.5, the necessary increase of irrigation (relative to the 0%-baseline) to mitigate the projected yield reduction of both the short/medium-term is ~2% and ~5% for the long-term (**Fig. 6a** intercept of x-axis). However, this adaptation strategy will still lead to a DWP decrease from –3% and –9%, compared to the DWP for the 0%-baseline (**Fig. 6c** intercept of y-axis). For RCP8.5, the yield response in the first two sub-periods is very similar, showing ~4% more irrigation to

maintain past yield, while DWP decreases from –6% to –10% for the short- and medium-term, respectively **(Fig. 6b, d)**. For the long-term period, the projected irrigation increment to maintain yield is of ~14%, leading to a DWP reduction of –23% **(Fig. 6b, d)**. Our results show that 2–14% more irrigation than for baseline (1986–2005) might be a robust strategy to counteract future yield reduction, though the maximum DWP is substantially lower than for baseline (up to –23%).

3.3.6 Uncertainties

Crop model uncertainty

Apart from the ensemble mean shown before for climate change impact assessment **(Fig. 5)**, uncertainty arises for STICS and AquaCrop in simulating yield under a higher atmospheric CO_2 concentration (i.e. long-term period of RCP8.5). The mean yield relative difference for STICS minus AquaCrop over the long-term period of RCP8.5 reaches –1,865.5 kg ha^{-1} (–25%), compared to –174.3 kg ha^{-1} (–2%) in the short-term period, with lower CO_2 level **(Fig. 7a, b)**. In comparison with baseline, where CO_2 level is the lowest, the long-term period of RCP8.5 shows significant mean yield reduction in STICS (7477.9 kg ha^{-1}, –30%), with the highest CO_2 level **(Fig. 7a)**. Conversely, the mean yield in AquaCrop remains almost the same (9,343.4 kg ha^{-1}, –1%) for the long-term period in RCP8.5 relative to the baseline **(Fig. 7b)**. These results suggest that AquaCrop may be more sensitive to the CO_2 fertilization effect than STICS, notably offsetting the detrimental climate change impacts on yields. The CO_2–biomass effect sub-modules in each crop model are indeed different: adapted from Stockle et al. (1992) for STICS and from Steduto et al. (2007) for AquaCrop. Besides, each model simulation of DWP tends to follow the yield trend, highlighting again that yield plays a central role in DWP response to climate change scenarios **(Fig. 7c, d)**. However, the agreement between STICS and AquaCrop is quite clear in simulating seasonal water input and growth cycle with increased CO_2 level **(Fig. 7e, f, g, h)**. In general, the two-model ensemble means of each variable may be more statistically robust measures than single-model variables.

Pedo-climatic uncertainties

Our projected climate change impacts heavily rely on the coupled GCM/RCM outputs (M-MPI-ESM-LR/SMHI-RCA4) in the study sites and in RCP uncertainties (Wilcke and Barring, 2016). Furthermore, the HWSD minimal mapping unit ranges from 1 to 10 km, which can affect soil

properties at each site (Fraga et al., 2016). The simplified management (e.g. sowing date and density and fertilization rate) and limited number of representative maize cultivars, without considering their changes in the future, is another source of uncertainty.

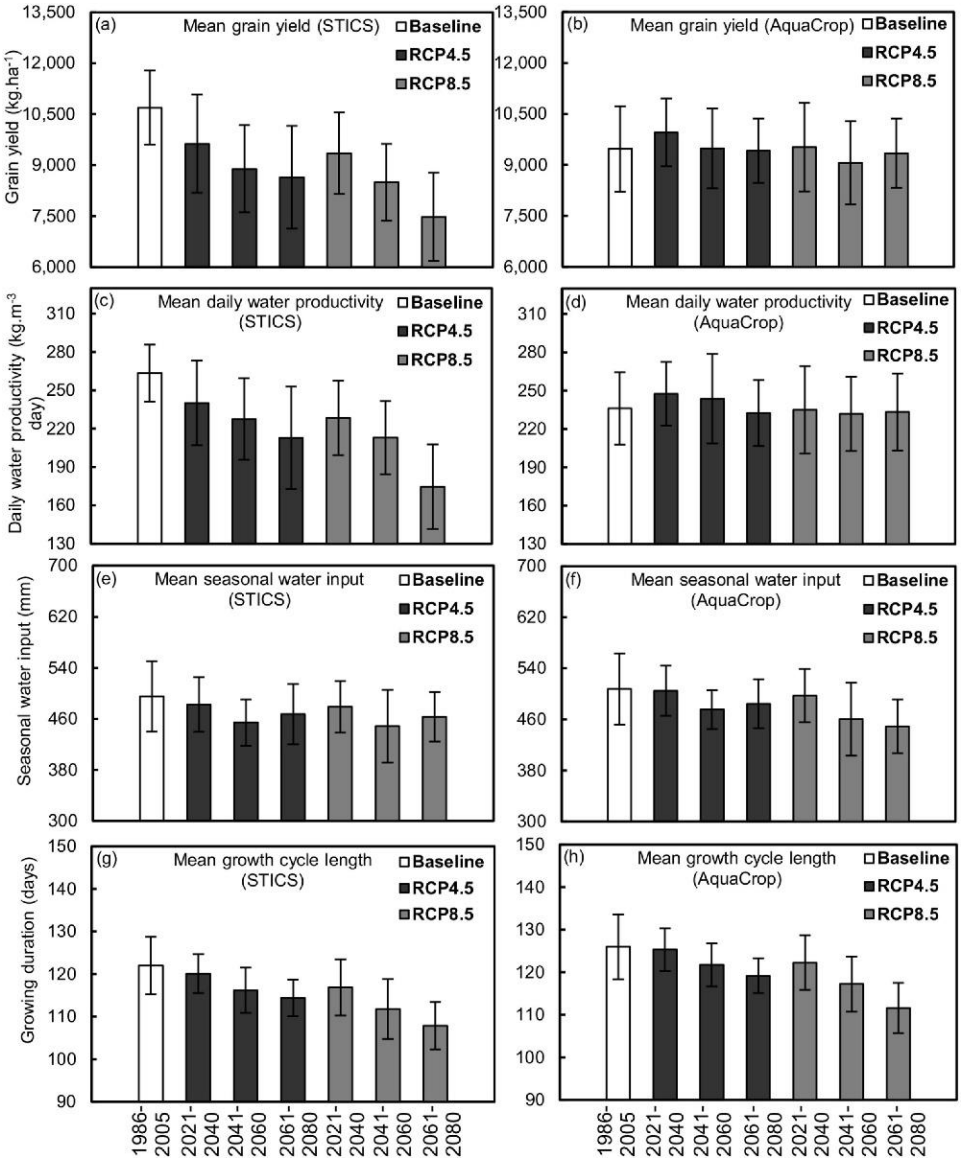

Figure 7 Individual model simulations (STICS and AquaCrop) under climate change scenarios (RCP4.5 and 8.5) for the three selected sites in Ribatejo. Averages and corresponding standard-deviations from STICS (***a, c, e, g***) and AquaCrop (***b, d, f, h***) are shown for yield, daily water productivity (DWP), seasonal water input and growth cycle length over baseline (1986–2005), RCP4.5 (2021–2080) and RCP8.5 (2021–2080).

3.4 Conclusion

The present study hints at the close behavior of two process-based crop models (STICS and AquaCrop) in simulating several maize yield-related outputs, as well as the good agreement between normalized statistical yields and regional simulations over the past period (1986–2005) in Ribatejo (Portugal). An adapted daily water productivity (DWP) measure, i.e. yield divided by daily water input (ratio of seasonal water input to growth cycle length), allows integrating the effect of shortened growing periods on seasonal water input. Future climate change projections show warmer and drier climate change scenarios. The impact of RCP4.5 and RCP8.5 on maize growth reveals a progressive decrease effect, with the most significant reduction on maize yield (–17%), growth cycle (–12%) and DWP (–19%) for 2061–2080 under RCP8.5, associated with a decrease of seasonal water input (–9%) during 2041–2060. The decreased DWP is largely due to the significant yield reduction, for which the positive CO_2 enrichment effect on crop yield increment is not enough to mitigate other unfavorable climate-driven processes (e.g. excessive warming).

By testing different irrigation amounts as possible adaptation measures to mitigate the projected yield reductions, the required water supply increment by irrigation is higher in RCP8.5 than in RCP4.5, despite lower water use efficiency. The required irrigation increments are of 2–14% than for baseline (1986–2005), with substantially lower DWP than for baseline (down to –23%). Overall, these findings provide scientific knowledge for stakeholders and decision-makers within the Portuguese maize sector when planning suitable regional irrigation strategies under future climate change.

Acknowledgments

This work was supported by European Investment Funds by FEDER/COMPETE/POCI–Operational Competitiveness and Internationalization Programme, POCI-01-0145-FEDER-006958, and by FCT - Portuguese Foundation for Science and Technology, UID/AGR/04033/2013. The authors also acknowledge the FCT scholarship given to Chenyao Yang, PD/BD/113617/2015, under the Doctoral Programme "Agricultural Production Chains – from fork to farm" (PD/00122/2012).

References

Abedinpour, M. et al., 2012. Performance evaluation of AquaCrop model for maize crop in a semi-arid environment. Agr Water Manage, 110: 55-66.

Afzal, M., Battilani, A., Solimando, D. and Ragab, R., 2016. Improving water resources management using different irrigation strategies and water qualities: Field and modelling study. Agr Water Manage, 176: 40-54.

Batista, S., Silva, E., Cerejeira, M. and Silva‐Fernandes, A., 2001. Exposure of ground water to alachlor, atrazine and metolachlor in maize areas of Ribatejo and Oeste (Portugal). Toxicological & Environmental Chemistry, 79(3-4): 223-232.

Blum, A., 2009. Effective use of water (EUW) and not water-use efficiency (WUE) is the target of crop yield improvement under drought stress. Field Crops Research, 112(2): 119-123.

Brisson, N. et al., 2003. An overview of the crop model STICS. Eur J Agron, 18(3-4): 309-332.

Brisson, N., Launay, M., Mary, B. and Beaudoin, N., 2009. Conceptual basis, formalisations and parameterization of the STICS crop model. Editions Quae, 297 pp.

Constantin, J., Willaume, M., Murgue, C., Lacroix, B. and Therond, O., 2015. The soil-crop models STICS and AqYield predict yield and soil water content for irrigated crops equally well with limited data. Agric. For. Meteorol., 206: 55-68.

Coucheney, E. et al., 2015. Accuracy, robustness and behavior of the STICS soil–crop model for plant, water and nitrogen outputs: evaluation over a wide range of agro-environmental conditions in France. Environ Modell Softw, 64: 177-190.

da Silva, J.R.M. and Silva, L.L., 2008. Evaluation of the relationship between maize yield spatial and temporal variability and different topographic attributes. Biosyst Eng, 101(2): 183-190.

Dagdelen, N., Yilmaz, E., Sezgin, F. and Gurbuz, T., 2006. Water-yield relation and water use efficiency of cotton (Gossypium hirsutum L.) and second crop corn (Zea mays L.) in western Turkey. Agricultural Water Management, 82(1-2): 63-85.

Debaeke, P. and Aboudrare, A., 2004. Adaptation of crop management to water-limited environments. Eur J Agron, 21(4): 433-446.

Dee, D.P. et al., 2011. The ERA-Interim reanalysis: configuration and performance of the data assimilation system. Q J Roy Meteor Soc, 137(656): 553-597.

Doll, P., 2002. Impact of climate change and variability on irrigation requirements: A global perspective. Climatic Change, 54(3): 269-293.

Farre, I. and Faci, J.M., 2009. Deficit irrigation in maize for reducing agricultural water use in a Mediterranean environment. Agr Water Manage, 96(3): 383-394.

Fischer, G., Tubiello, F.N., Van Velthuizen, H. and Wiberg, D.A., 2007. Climate change impacts on irrigation water requirements: Effects of mitigation, 1990-2080. Technol Forecast Soc, 74(7): 1083-1107.

Fraga, H., García de Cortázar Atauri, I., Malheiro, A.C. and Santos, J.A., 2016. Modelling climate change impacts on viticultural yield, phenology and stress conditions in Europe. Global Change Biol, 22(11): 3774–3788.

Geerts, S. and Raes, D., 2009. Deficit irrigation as an on-farm strategy to maximize crop water productivity in dry areas. Agr Water Manage, 96(9): 1275-1284.

Guerena, A., Ruiz-Ramos, M., Diaz-Ambrona, C.H., Conde, J.R. and Minguez, M.I., 2001. Assessment of climate change and agriculture in Spain using climate models. Agron J, 93(1): 237-249.

Haylock, M.R. et al., 2008. A European daily high-resolution gridded data set of surface temperature and precipitation for 1950–2006. J. Geophys. Res., 113(D20): D20119.

Howell, T.A., 2001. Enhancing water use efficiency in irrigated agriculture. Agron J, 93(2): 281-289.

Iglesias, A. and Garrote, L., 2015. Adaptation strategies for agricultural water management under climate change in Europe. Agr Water Manage, 155: 113-124.

Iglesias, A., Garrote, L., Flores, F. and Moneo, M., 2007. Challenges to manage the risk of water scarcity and climate change in the Mediterranean. Water Resources Management, 21(5): 775-788.

INE, 2015. Main crops surface (ha) by Geographic localization (Agricultural census), Instituto Nacional de Estatística (INE), Lisbon, Portugal.

IPCC, 2013. The physical science basis. Contribution of working group I to the fifth assessment report of the intergovernmental panel on climate change. K., Tignor, M., Allen, SK, Boschung, J., Nauels, A., Xia, Y., Bex, V., Midgley, PM, Eds: 1535.

Islam, A. et al., 2012. Modeling the impacts of climate change on irrigated corn production in the Central Great Plains. Agr Water Manage, 110: 94-108.

Jacob, D. et al., 2014. EURO-CORDEX: new high-resolution climate change projections for European impact research. Regional Environmental Change, 14(2): 563-578.

Jego, G., Pattey, E., Bourgeois, G., Drury, C.F. and Tremblay, N., 2011. Evaluation of the STICS crop growth model with maize cultivar parameters calibrated for Eastern Canada. Agron Sustain Dev, 31(3): 557-570.

Jones, P.G. and Thornton, P.K., 2015. Representative soil profiles for the Harmonized World Soil Database at different spatial resolutions for agricultural modelling applications. Agr Syst, 139: 93-99.

Kang, Y.H., Khan, S. and Ma, X.Y., 2009. Climate change impacts on crop yield, crop water productivity and food security - A review. Prog Nat Sci-Mater, 19(12): 1665-1674.

Katerji, N., Campi, P. and Mastrorilli, M., 2013. Productivity, evapotranspiration, and water use efficiency of corn and tomato crops simulated by AquaCrop under contrasting water stress conditions in the Mediterranean region. Agricultural water management, 130: 14-26.

Katerji, N. and Mastrorilli, M., 2009. The effect of soil texture on the water use efficiency of irrigated crops: Results of a multi-year experiment carried out in the Mediterranean region. Eur J Agron, 30(2): 95-100.

Katerji, N., Mastrorilli, M. and Cherni, H.E., 2010. Effects of corn deficit irrigation and soil properties on water use efficiency. A 25-year analysis of a Mediterranean environment using the STICS model. Eur J Agron, 32(2): 177-185.

Li, X., Takahashi, T., Suzuki, N. and Kaiser, H.M., 2011. The impact of climate change on maize yields in the United States and China. Agr Syst, 104(4): 348-353.

Meza, F.J., Silva, D. and Vigil, H., 2008. Climate change impacts on irrigated maize in Mediterranean climates: Evaluation of double cropping as an emerging adaptation alternative. Agr Syst, 98(1): 21-30.

Mo, X.G., Liu, S.X., Lin, Z.H. and Guo, R.P., 2009. Regional crop yield, water consumption and water use efficiency and their responses to climate change in the North China Plain. Agr Ecosyst Environ, 134(1-2): 67-78.

Nóbrega, C.M., 2006. Climate Change in Portugal. Scenarios, Impacts and Adaptation Measures. SIAM Project-1ª edição. Silva Lusitana, 14(1): 130-131.

Olesen, J.E. et al., 2011. Impacts and adaptation of European crop production systems to climate change. Eur J Agron, 34(2): 96-112.

Paredes, P., de Melo-Abreu, J.P., Alves, I. and Pereira, L.S., 2014. Assessing the performance of the FAO AquaCrop model to estimate maize yields and water use under full and deficit irrigation with focus on model parameterization. Agr Water Manage, 144: 81-97.

Penman, H.L., 1948. Natural evaporation from open water, bare soil and grass, Proceedings of the Royal Society of London A: Mathematical, Physical and Engineering Sciences. The Royal Society, pp. 120-145.

Perry, C., 2011. Accounting for water use: Terminology and implications for saving water and increasing production. Agricultural Water Management, 98(12): 1840-1846.

Polley, H.W., 2002. Implications of atmospheric and climatic change for crop yield and water use efficiency. Crop Sci, 42(1): 131-140.

Porter, J.R. and Semenov, M.A., 2005. Crop responses to climatic variation. Philos T R Soc B, 360(1463): 2021-2035.

Qian, B.D., De Jong, R., Yang, J.Y., Wang, H. and Gameda, S., 2011. Comparing simulated crop yields with observed and synthetic weather data. Agr Forest Meteorol, 151(12): 1781-1791.

Raes, D., Steduto, P., Hsiao, T. and Fereres, E., 2012. Reference Manual AquaCrop (Version 4.0). AquaCrop website http://www.fao.org/nr/water/aquacrop.html.

Richard, G. and Cellier, P., 1998. Effect of tillage on bare soil energy balance and thermal regime: an experimental study. Agronomie, 18(3): 163-180.

Ritchie, J.T., 1972. Model for predicting evaporation from a row crop with incomplete cover. Water Resour Res, 8(5): 1204-1213.

Samuelsson, P. et al., 2011. The Rossby Centre Regional Climate model RCA3: model description and performance. Tellus A, 63(1): 4-23.

Santos, J., Corte-real, J. and Leite, S., 2007. Atmospheric large-scale dynamics during the 2004/2005 winter drought in Portugal. Int J Climatol, 27(5): 571-586.

Santos, J.A., Belo-Pereira, M., Fraga, H. and Pinto, J.G., 2016. Understanding climate change projections for precipitation over western Europe with a weather typing approach. Journal of Geophysical Research: Atmospheres, 121(3): 1170-1189.

Steduto, P., Hsiao, T.C. and Fereres, E., 2007. On the conservative behavior of biomass water productivity. Irrigation Sci, 25(3): 189-207.

Steduto, P., Hsiao, T.C., Raes, D. and Fereres, E., 2009. AquaCrop-The FAO Crop Model to Simulate Yield Response to Water: I. Concepts and Underlying Principles. Agron J, 101(3): 426-437.

Stockle, C.O., Williams, J.R., Rosenberg, N.J. and Jones, C.A., 1992. A Method for Estimating the Direct and Climatic Effects of Rising Atmospheric Carbon-Dioxide on Growth and Yield of Crops .1. Modification of the Epic Model for Climate Change Analysis. Agr Syst, 38(3): 225-238.

Supit, I. et al., 2010. Recent changes in the climatic yield potential of various crops in Europe. Agr Syst, 103(9): 683-694.

Tardieu, F. and Katerji, N., 1991. Plant-Response to the Soil-Water Reserve - Consequences of the Root-System Environment. Irrigation Sci, 12(3): 145-152.

Tubiello, F.N., Donatelli, M., Rosenzweig, C. and Stockle, C.O., 2000. Effects of climate change and elevated CO2 on cropping systems: model predictions at two Italian locations. Eur J Agron, 13(2-3): 179-189.

Wilcke, R.A.I. and Barring, L., 2016. Selecting regional climate scenarios for impact modelling studies. Environ Modell Softw, 78: 191-201.

Wolf, J. and Vandiepen, C.A., 1995. Effects of Climate-Change on Grain Maize Yield Potential in the European-Community. Climatic Change, 29(3): 299-331.

Wosten, J.H.M., Pachepsky, Y.A. and Rawls, W.J., 2001. Pedotransfer functions: bridging the gap between available basic soil data and missing soil hydraulic characteristics. J Hydrol, 251(3-4): 123-150.

Xiong, W., Matthews, R., Holman, I., Lin, E. and Xu, Y.L., 2007. Modelling China's potential maize production at regional scale under climate change. Climatic Change, 85(3-4): 433-451.

Zhang, H.P. and Oweis, T., 1999. Water-yield relations and optimal irrigation scheduling of wheat in the Mediterranean region. Agricultural Water Management, 38(3): 195-211.

CHAPTER 4

Climate change impacts and adaptation options for winter wheat under rainfed Mediterranean conditions in southern Portugal

Briefing notes:

Wheat (*Triticum aestivum* L.) is a traditionally important crop in Portugal, but insufficient domestic production leads to high dependency on wheat importation for satisfying its internal demand. The principal wheat growing area is situated in the Alentejo region in southern Portugal, where the prevalence of dryland farming system in this region, with typical Mediterranean climate, leads to wheat cultivation mostly under rainfed conditions. It plays an important social-economic role and represents essential source of livelihood for local smallholder famers. However, the observed warmer and drier climate trends in the last decades imply an exacerbation of crop water deficit and high temperature episodes, especially during sensitive crop growth stage (anthesis and grain-filling), that is typical of wheat cropping system in this region. This climatic trend is likely to continue under global warming, thus expect to aggravate the identified vulnerability with higher frequency and severity of extreme weather events, adding serious concerns over yield returns and its economic viability. Therefore, development, planning and guiding target and appropriate adaptation strategies are strongly needed.

In this context, we have developed a study on evaluating impacts of a wide range of climate change projections (derived from 10 bias-corrected dynamically downscaled climate model outputs), on winter wheat yield using STICS crop model at one representative site in Alentejo, as well as exploring field-level adaptation options. The proposed and tested adaptation options are using early-flowering cultivars and early sowing dates, aiming to minimize the risk of crop exposure to enhanced terminal drought and heat stresses during grain filling period. STICS is calibrated using independently published wheat yield data from a 5-year local field trial with meteorological conditions ranging from anomalous dry to anomalous wet (each year encompasses combined treatment of three different N fertilization and two sowing dates).

This chapter specifically covers aforementioned content and has been previously published as a research article by *Climatic Change*, entitled as "*Effects of climate change and adaptation options on winter wheat yield under rainfed Mediterranean conditions in southern Portugal*". The works correspond to task 3 and 4 undertaken, aiming for a better understanding of crop yield response to climate changes under Mediterranean environment, as well as aiding in designing target adaptation strategies for policymakers by providing valuable information on guiding breeding efforts.

Title: Climate change impacts and adaptation options for winter wheat under rainfed Mediterranean conditions in southern Portugal

Chenyao Yang[a,*], Helder Fraga[a], Wim van Ieperen[b], Henrique Trindade[a] and João A. santos[a]

[a]*Centre for the Research and Technology of Agro-environmental and Biological Sciences, CITAB, Universidade de Trás-os-Montes e Alto Douro, UTAD, 5000-801, Vila Real, Portugal*

[b]*Group Horticulture and Product Physiology, 6700 AA Wageningen University, the Netherlands*

*****Corresponding author. E-mail: cyang@utad.pt

Refer to https://doi.org/10.1007/s10584-019-02419-4 for online published version.

Abstract

Projected warming and drying trend over Mediterranean region represent a substantial threat for wheat production. The present study assesses winter wheat yield response to potential climate change and estimate the quantitative effectiveness of proposed adaptation options for the major wheat production region of Portugal. A crop model STICS is used for this purpose, which is calibrated for yield simulations before projecting yields. Climate projections over 2021–2050 and 2051–2080 under two emission scenarios (RCP4.5 and RCP8.5), are retrieved from bias adjusted datasets, generated by a 10-member climate model ensemble. Projected intensification of water deficits and more frequent high temperature events during late spring (April–June), coinciding with the sensitive grain filling stage, primarily result in continuous mean yield losses (relative to 1981–2010) by –14% (both scenarios) during 2021–2050 and by –17% (RCP4.5) or –27% (RCP8.5) during 2051–2080, also accompanied by increased yield variabilities. Of evaluated adaptation options at various levels, using earlier flowering cultivars reveal higher yield gains (26–38%) than that of early sowings (6–10%), which are able to reverse the yield reductions. The adopted early flowering cultivars successfully advances the anthesis onset and grain-filling period, which reduces or avoids the risks of exposure to enhanced drought and heat stresses in late spring. In contrast, winter warming during early sowing window could affect vernalization fulfilment with prolonged pre-anthesis growth, thus with limited effects on advancing reproductive stage. Crop yield projections and explored adaptation options are essential to assess food security prospects (availability and stability) of dry Mediterranean areas, providing crucial insights for policymaking.

Keywords: Dryland Environment, Crop Modelling, STICS, Regional Climate Projections, Multi-model ensemble, EURO-CORDEX

4.1 Introduction

How to improve agricultural production to meet projected increasing demand of global food products by around 60% until 2050, due to growing population and economic development, represents a substantial challenge, particularly in the context of climate change (Alexandratos and Bruinsma, 2012). Projected anthropogenic-driven climate change, with elevated atmospheric CO_2 level, rising surface air temperatures and changes in local precipitation regimes are expected to adversely affect crop growth and yields in many parts of the world (IPCC, 2013), bringing numerous uncertainties and risks for agricultural production and food security (Schmidhuber and Tubiello, 2007).

Wheat (*Triticum aestivum* L.) is the staple food crop throughout the world, and Portugal is a country that still highly depends on the importation of wheat, e.g. used as fodder crop in many dairy farms. In this context, satisfying internal demands via increased domestic production may play a vital social-economic role (Páscoa et al., 2017). Wheat production is mainly concentrated in southern Portugal, namely in the Alentejo region, which contributes to more than 75% of national wheat production (Eurostat, 2015). In Alentejo, the prevalence of dryland farming systems leads to wheat cultivation under rainfed conditions (Valverde et al., 2015). Approximately, 95% of wheat growing areas in Alentejo are devoted to bread wheat production (Gouveia and Trigo, 2008). The typical Mediterranean climate in this region causes a high evaporative demand in late spring (ca. April–June) when precipitation is low, considerably enhancing the risks of occurrence of severe water deficit during the most susceptible growth stage of winter wheat, i.e. flowering and post-anthesis grain filling period (Costa et al., 2013; Páscoa et al., 2017). A previous analysis for this region revealed climatic water deficits in May and June, largely coinciding with the grain filling and ripening stages, could impose strong limitation on wheat yields (Páscoa et al., 2017). Moreover, such a critical growing period is also frequently exposed to extremely high temperatures, with clear detrimental effects on final grain yield (Dias and Lidon, 2009; Scotti-Campos et al., 2014). For instance, post-anthesis high temperature (>30°C), which is common in Alentejo (Scotti-Campos et al., 2014), can cause significant grain yield reductions, resulting from a shortened grain-filling phase and increased leaf senescence (Asseng et al., 2011; Dias and Lidon, 2009). A modelling study in major wheat growing regions of Australia suggested that variations in mean growing season temperature by ± 2°C could impose a substantial reduction on wheat grain production by up to 50% (Asseng et al., 2011). Observed climate conditions in southern Portugal

have shown a clear trend towards a more arid climate, with increased mean temperature and decreased annual precipitation, particularly spring precipitation (Páscoa et al., 2017; Rolim et al., 2017; Valverde et al., 2015). The observed warming and drying trends are likely to be strengthened in future climates (Páscoa et al., 2017; Rolim et al., 2017), with a concomitant increase in the frequency and intensity of extreme weather events, e.g. droughts (Santos et al., 2016).

Adaptation measures on cropping systems have shown great potential to reduce or counteract the negative climate change impacts (Howden et al., 2007). For instance, a meta-analysis reviewing numerous studies revealed that the projected wheat yield losses, in both tropical and temperate regions, can be avoided or even reversed by implementing crop-level adaptation options, such as cultivar changes, adjusting planting date, irrigation and residue management (Challinor et al., 2014). However, analysis of effects of these adaption options will rely on a contextual approach (Challinor et al., 2014; Howden et al., 2007), which requires incorporating local characteristics, such as local soil properties, climatic projections, crop behavior and common agronomic practices. Process-based crop models are efficient tools for simulating interactions amongst weather, soil, crop and management practices, and are increasingly used to project future crop yield and explore adaptation options in different regions worldwide (Asseng et al., 2013; Kassie et al., 2015; Wang et al., 2017). STICS is such a model, initially parameterized and validated for cereal crops (Brisson et al., 2003; Brisson et al., 1998; Brisson et al., 2002), and has been thoroughly evaluated over a wide range of agro-environmental conditions (including Mediterranean-type climates), showing a satisfactory and robust performance in simulating growth and yield of winter wheat (Coucheney et al., 2015).

Although future climate projections are often carried out by global climate models (GCMs), their coarse spatial resolutions (100–500 km) often constrain the direct use of GCM outputs in crop models (often operated on a one hectare-basis). Dynamical downscaling is a common approach to obtain appropriate regional climate information, in which higher resolution regional climate models (RCMs) are applied within limited areas, with boundary conditions provided by coupled GCMs (IPCC, 2015). Within the European branch of the global Coordinated Regional Downscaling Experiment (EURO–CORDEX) initiative, a number of RCMs, driven by large-scale outputs of GCMs under different Representative Concentration Pathways (RCPs), were used to carry out high resolution RCM simulations (~12.5 to 50 km) throughout Europe (Jacob et al., 2014). Nevertheless, raw outputs from GCM–RCM model chains still tend to have systemic errors (bias)

as compared to observations, because either GCMs or RCMs are just an approximation of the earth climate system, which highlights the need for bias-adjustments towards observed climatology (IPCC, 2015; Yang et al., 2010). While multiple climate models are increasingly used for a comprehensive understanding of potential climate change, few studies have applied bias-corrected multi-model ensembles from high-resolution RCMs, to assess climate change impacts on crop yields.

Previous studies on potential climate change influences on wheat production in Portugal were either focused on assessing crop water deficits (Rolim et al., 2017) or using climate change projections without accounting for the potential changes in climate variabilities and associated extreme events (Valverde et al., 2015). Besides, neither of these studies attempt to explore adaptation strategies. In the present study, ten bias-corrected GCM–RCM pairs and two RCPs are used to cover both model and anthropogenic forcing uncertainties for future climate projections (IPCC, 2015). STICS is calibrated using local wheat yield data before projecting future yields. We aim to (i) assess impacts of a range of climate change projections on winter wheat yield for the major wheat production region (Alentejo) of Portugal and (ii) explore consistent and suitable adaptation strategies to cope with potential climate change.

4.2 Data and methods

4.2.1 Study region and representative site

The study was performed within the Alentejo region (southern Portugal), featuring vast open areas of rolling plains, with some mountainous areas in the northeast (**Fig. 1a**). The area was characterized as a dry (sub-humid to semi-arid) Mediterranean climate, with extensive development of dryland farming systems, occupying ~63400 ha (Valverde et al., 2015). Rainfed winter wheat was typically sown in November, with a flexible sowing window, and harvested in June of next year (Gouveia and Trigo, 2008). Pests/diseases damages and weed infestation were generally well managed and controlled (Costa et al., 2013). Owing to the relatively homogeneous regional climate, the study site was chosen at Beja district (38.0°N, 7.9°W, 192 m a.s.l., **Fig. 1a**) to represent the dominant soil type (vertisol), where a weather station is also located <10 km away. Standard soil physical properties were primarily obtained from local measurements (Carvalho and Basch, 1995), complemented by information from the global SoilGrids dataset at 250 m resolution (Hengl et al., 2017) and Harmonized World Soil Database (~1 km resolution)

(FAO/IIASA/ISRIC/ISSCAS/JRC, 2012), which are summarized in **Online Resource (OR) 1**. Required soil hydraulic properties were directly obtained from EU–SoilHydroGrids (**OR1**), a newly developed fine-resolution (1 km) multiplayer soil hydraulic database (Brigitta et al., 2017).

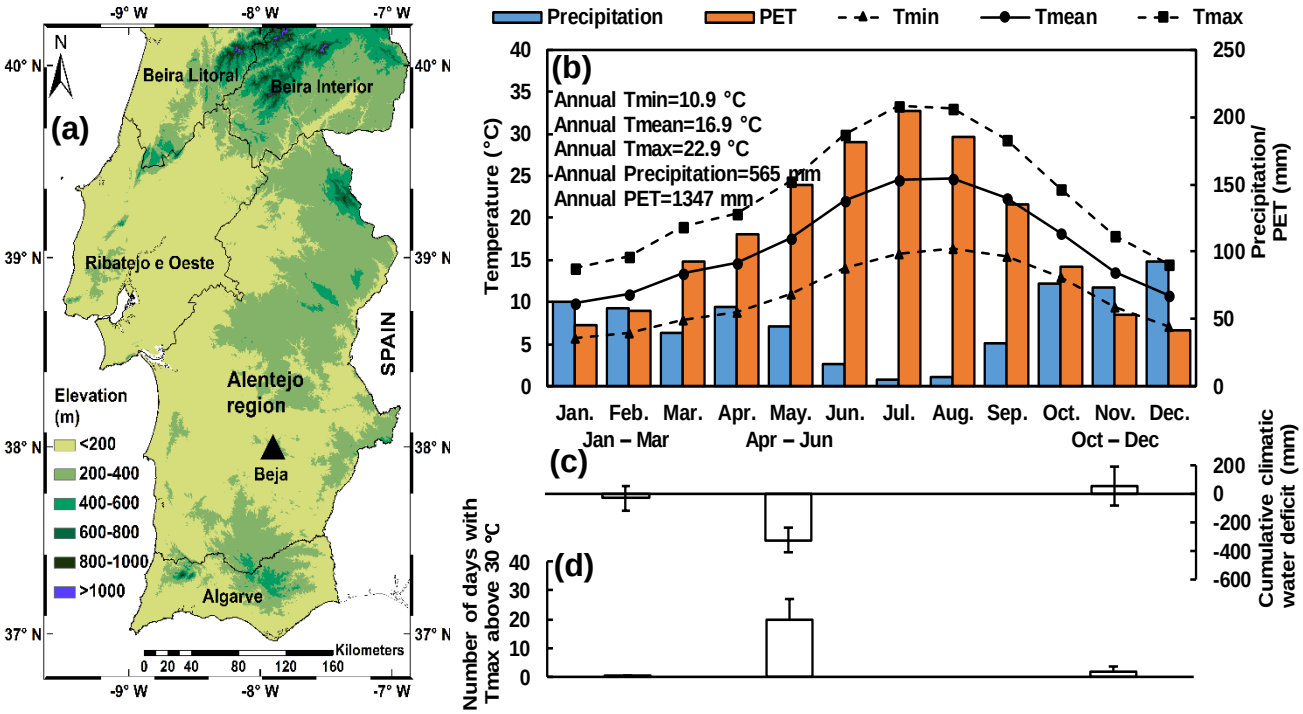

Figure 1 Study site and characterization of historical climate conditions. (***a***) Geographic location of the Beja district in southern Portugal (Alentejo region) with (***b***) average annual and monthly minimum (Tmin, °C), maximum (Tmax, °C) and mean (Tmean, °C) temperatures, precipitation sum (mm) and potential evapotranspiration (PET, mm) over the baseline period (1981–2010). Mean and standard deviation of (***c***) cumulative water deficit (precipitation minus PET, mm) and of (***d***) days (only positive error bars are plotted) with maximum temperature >30 °C in three wheat growing phases during baseline.

4.2.2 STICS description and calibration

In STICS, simulations for crop development and growth processes mainly involve phenological stages, leaf growth and senescence, transformation of intercepted photosynthetic radiation into aerial biomass, followed by its partition into various organs (e.g. grain). These processes were simultaneously governed by simulated stress factors, such as water shortage or waterlogging, N deficiency and thermal stresses. Furthermore, for winter wheat, the phenology development could also be slowed either by the sub-optimal photoperiod conditions or by non-compliance with vernalization requirement. Detailed model parameters, formalizations and modelling approaches are available at Brisson et al. (2009).

STICS was calibrated for simulating local grain yield (15% grain moisture) of winter wheat, using available published yield data for consecutive five growing seasons (1981–1986) at Beja (Carvalho and Basch, 1995) (**OR2**). Yield data were averaged over two experimental cultivars (Etoile and Mara) to facilitate comparison with our simulations, as no significant differences were found between them (**OR2**). Detailed information on experimental design and relevant inputs, such as common seeding date and rate as well as N fertilization practices, were documented by Carvalho and Basch (1995) and summarized in **OR 2**.

For calibration, the performance of nine built-in cultivars of winter wheat were firstly examined. As only yield data was available, no attempt was made to calibrate default cultivar parameters, such as phenology and leaf area index (LAI) dynamics, but focusing only on the cultivar choice (No.1 to No.9). Subsequently, the general plant parameters, i.e. radiation use efficiency (RUE) that represented how the crop net photosynthesis was modelled (Brisson et al., 2009), were adjusted by testing a wide range of predefined values (2.25–4.25 with 0.25 interval). Various combinations of RUE with cultivar choice were thus investigated. The pair providing the best goodness-of-fit between observed and simulated yields was eventually selected. The overall approach was in agreement with standard procedures proposed by Jégo et al. (2010). The calibrated crop parameters and agronomic input values were kept invariant in the following climate change impact analysis.

4.2.3 Climate data

For the historical period of 1981–2010 (hereafter "baseline"), observed daily minimum and maximum air temperatures (°C) and precipitation (mm) were directly obtained from the Beja weather station, available at European Climate Assessment & Dataset (ECA&D, www.ecad.eu) (Klein Tank et al., 2002). Daily surface solar radiation data (MJ m^{-2} day^{-1}) were extracted from both the coarse-resolution (0.75° × 0.75°) ERA-Interim reanalysis (Dee et al., 2011) and the finer-resolution (0.05° × 0.05°) satellite-based observations (CM SAF) (Pfeifroth et al., 2018). A good linear agreement was found within their overlap period (1983–2010) and the corresponding linear function was then applied to calibrate ERA-Interim data for the entire baseline period (**OR3**). Potential evapotranspiration (PET) was externally calculated using the FAO ET0 (v3.2) calculator. Annual records of atmospheric CO_2 concentration (ppm) for baseline were retrieved from NOAA (www.esrl.noaa.gov/gmd/) and supplied as input in STICS.

The future periods of 2021–2050 (near-future) and 2051–2080 (distant-future) were selected. High-resolution (~12.5 km) projections for temperature (minimum and maximum) and precipitation were retrieved from ten bias-adjusted GCM–RCM simulations, produced by the EURO–CORDEX project and under RCP4.5 and RCP8.5, and for each period (10 models × 2 scenarios) (Jacob et al., 2014). RCP4.5 corresponds to an anthropogenic radiative forcing reaching 4.5 W/m^2 by 2100 relative to the pre-industrial level, whereas RCP8.5 is a high-emission scenario, with a radiative forcing of 8.5 W/m^2 by 2100 (van Vuuren et al., 2011). The ten GCM–RCM pairs combine five RCMs, three GCMs and four initializations (**OR4**). The bias adjustment was based on distribution-based scaling approach, where corrected distribution parameters were obtained by comparing model simulations and observations during the control period (1989–2010), and then applied to adjust the frequency distribution of raw model future projections (Yang et al., 2010). Such an approach was known to better preserve projected climate variability generated by individual RCM, as well as being able to realistically consider the covariance between temperature and precipitation (Yang et al., 2010). The observation source for bias-adjustments was the MESoscale ANalysis (MESAN) dataset at 3–12 km resolution throughout Europe, which was extensively used for regional reanalysis of a number of surface parameters (e.g. temperature and precipitation) (Dahlgren et al., 2016; Landelius et al., 2016). Moreover, as recommended from IPCC (2015), it is also essential to verify the performance of the bias adjustment using independent (additional) observational data (IPCC, 2015). Hence, the cumulative distribution functions of monthly mean temperature and precipitation sum between local weather station data and model simulations were thus compared for the control period (**OR5**). An overall agreement was found, particularly for monthly precipitation (**OR5**), suggesting sufficient bias adjustment for individual model outputs, as well as demonstrating the relevance of regional climate projections for the local impact study.

Radiation projections were not directly retrievable from bias-adjusted model outputs, but from raw outputs of each GCM–RCM pair within EURO-CORDEX (Jacob et al., 2014). Nonetheless, the bias adjustment was still performed by firstly deriving the ratios of mean monthly radiation sum between observations and model simulations over baseline. These monthly ratios were then applied as multiplicative correction factors to the raw projections of daily radiation of the respective month. The projected radiation sum eventually shows no significant differences at monthly scale compared to baseline data (not shown). Furthermore, to account for elevated CO_2

effect on crop growth and yield, the pre-defined future atmospheric CO_2 concentrations for each scenario were considered (RCP4.5 or RCP8.5).

4.2.4 Exploration of adaptation strategies

Two potentially suitable adaptation strategies were proposed in an attempt to minimize exposure of the most sensitive grain-filling phase (i.e. anthesis to grain maturity) to the typical unfavourable spring (April–June) conditions that were expected to be exacerbated in future climate. The first adaptation strategy assumed the genotypic development and use of earlier flowering wheat cultivar, which was suggested to be useful in avoiding critical/terminal stress conditions during reproductive stages for winter wheat under Mediterranean-type climates (Debaeke, 2004; Wang et al., 2017). Simulation of a future early flowering cultivar was achieved by reducing the growing degree days (GDD) requirement between emergence and anthesis, without altering other cultivar parameters (e.g. GDD for grain filling duration) in STICS (**OR2**). Three different adaptation levels were set, corresponding to 10%, 20% and 30% GDD reductions. Note that 30% reduction represents about the maximum extent of earliness to ensure no prior occurrence of anthesis over heading onset, while it still remains practical for cultivar breeding efforts. In general, this adaptation strategy tends to explore the trade-off effect between lower risk of yield limitation by drought/heat stress and higher risk of potential yield reduction with shorter growth duration (because of GDD reductions). Nevertheless, early flowering cultivars could be subject to the risk of spring frost damage with yield losses. In view of predictable climate warming, occurrence of spring frost is expected to be markedly reduced, such as the projections obtained for the wheat belt of Eastern Australia (Wang et al., 2015), thus likely being a lesser concern for yield threat under a warmer climate. The second adaptation strategy, namely early sowings, hypothesized that similar avoiding effects could be equally achieved from a management perspective, resulting from an anticipation of the growth cycle. Range of sowing dates (three different levels) were tested, namely 10, 20 and 30 days early sowing (i.e. early sowing window from Oct_30 to Nov_20 with 10-day interval) relative to the baseline adopted average sowing date of Nov_30 (**OR2**), without changing other parameters. Late sowings are not considered as sowing in the late December or early January were expected to notably increase the crop exposure to frequent drought and heat stresses during the sensitive grain filling period, thus leading to more yield reductions (Dias and Lidon, 2009).

4.2.5 Statistical analysis

Comparison of STICS simulations with local observed wheat yields was statistically assessed using the following complementary metrics: normalized Root Mean Square Error (nRMSE, %), Mean Absolute Error (MAE, kg ha^{-1}) and Correlation Coefficient (*r*). Regarding future yield projections, Student´s independent sample *t*-test was applied for assessing the significance of differences in means between baseline and each future period. Yield inter-annual variability of each period was expressed using the coefficient of variation (CV).

4.3 Results

4.3.1 Calibration for simulating wheat yield

Prediction errors (nRMSE and MAE) reveal a gradual increase as a function of RUE for individual cultivars, while differences of errors among cultivars tend to enlarge (**Fig. 2a, b**). The lowest nRMSE (stabilized at 20%) and MAE (432–476 kg ha^{-1}) are consistently found for cultivar No.7 with RUE ranging from 2.75 to 3, though 2.75 should be preferentially selected to minimize cultivar differences (**Fig. 2a, b**). Furthermore, a robust model performance is found, i.e. simulated yields are highly correlated with observations (r>0.75), irrespective of RUE and cultivar (**Fig. 2c**). Highest *r* is also obtained using cultivar No.7, for which *r* tends to stabilize with RUE>2.75 (**Fig. 2c**). Hence, for the combination of cultivar No.7 and RUE=2.75 (**OR2**), the simulations explain 90% of observed variance, with nRMSE of 20% and MAE of 464 kg ha^{-1} (**Fig. 2d**), which are chosen henceforth for following analysis.

4.3.2 Baseline and projected climates

Baseline average annual mean temperature is of 16.9°C, with monthly mean temperature varying from 9.9°C in January to 24.7°C in August (**Fig. 1b**). For the growing season, mild winter temperatures (typically>10°C) are followed by a steadily increase from 14.7°C in April to 22.0°C in June (end of the growing season), with average maximum temperature reaching 30.0°C in June (**Fig. 1b**). The rainy season concentrates in October–March, with baseline average precipitation of 403 mm and low evaporative demand (**Fig. 1b**), leading to a negligible climatic water deficit (**Fig. 1c**). In contrast, lower spring precipitation with rising temperature results in a mean baseline climatic water deficit of –324 mm for April–June (**Fig. 1b, c**). High temperature events (daily

maximum temperature >30°C) are also frequent during these months, with an average occurrence of 20 days in baseline (**Fig. 1d**).

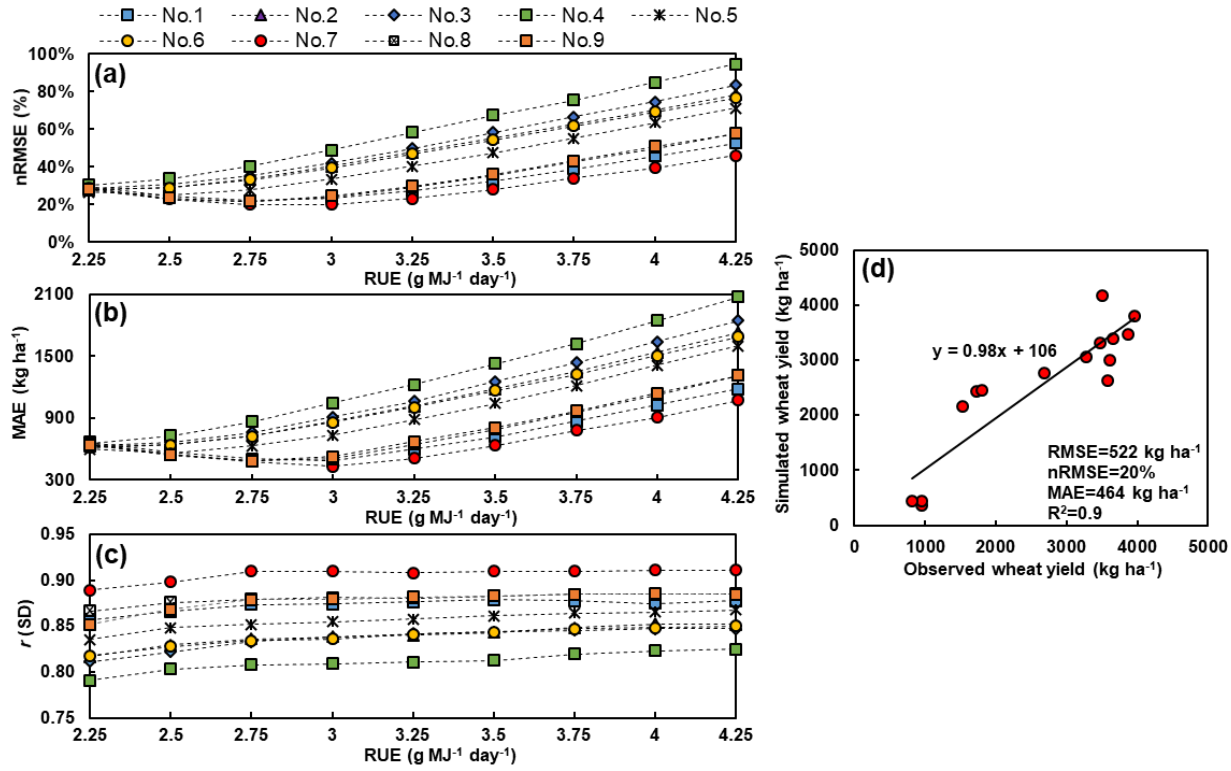

Figure 2 Comparison between observed yield data and simulations, with inputs from different combinations of a general plant parameter (RUE, radiation use efficiency) and STICS built-in cultivar choice (No.1 to No.9). The following evaluation metrics are considered: (***a***) nRMSE (normalized root mean square error), (***b***) MAE (mean absolute error) and (***c***) correlation coefficient (*r*), together with (***d***) the results from the selected combination of RUE (approximation of 2.75 to 2.8 g MJ^{-1} day^{-1}) and cultivar choice (cultivar No.7–*Thetalent*). Refer to online resource 2 for summarized input parameters used for calibration.

Climate projections for the selected models and scenarios show increased annual mean temperature by an average (among models) of 0.8°C (0.6–1.0°C) in RCP4.5 or 1.0°C (0.8–1.2°C) in RCP8.5 for 2021–2050, and of 1.3°C (1.0–1.7°C) in RCP4.5 or 2.3°C (2.2–2.5°C) in RCP8.5 for 2051–2080, with respect to baseline (**OR6**). Projected warming rates show a remarkable asymmetry at the monthly scale, with highest mean temperature increase (by model-average) in May (up to 2.9°C) and lowest increase in March (up to 1.7°C) over the growing season (**OR6**). Further, higher temperature increases in RCP8.5 than in RCP4.5 are clearly discernible in 2051–2080 (**OR6**). As a result of temperature increase, mean annual PET are also increased, depending on RCP4.5 or RCP8.5, by an average of 30 or 44 mm in 2021–2050 and of 56 or 105 mm in 2051–

2080, respectively (**OR6**). Precipitation projections indicate that annual precipitation reductions are very likely, in which projected mean precipitation changes vary from –8% to +7% (excluding outlier) in RCP4.5 or from –24% to –2% in RCP8.5 during 2021–2050, and from –19% to –4% (RCP4.5) or –28% to –6% (RCP8.5) during 2051–2080 (**OR6**). However, monthly precipitation projections are more uncertain, e.g. varying widely from –78% to 39% (RCP4.5) in June during 2021–2050 and from –29% to 42% in March (RCP8.5) during 2051–2080 (**OR6**). Climate projections over the whole Alentejo region (as indicated by multi-model ensemble mean) also show increased annual mean temperature (up to 2.7°C) and decreased annual precipitation (up to –18%), revealing a regional homogeneity of climate signals for a given scenario and period (**OR7**).

4.3.3 Impacts of climate change projections on wheat yield

The simulated 30-year baseline yield (inter-quartile) ranges from 1409 to 2848 kg ha^{-1}, with an average of 2045 kg ha^{-1} and a strong inter-annual variability (CV=47%) (**Fig. 3a**). Future projections tend to show an overall decrease in mean yield, accompanied by enhanced variability. For RCP4.5, ensemble mean yield is of 1427–2109 kg ha^{-1} for 2021–2050 and of 1310–1962 kg ha^{-1} for 2051–2080, with mean yield reductions (relative to baseline) of –14% and–17%, respectively (**Fig. 3a, b**). Increased yield variability (CV>47%) is projected in 2021–2050 by 50% of climate model projections and by 70% in 2051–2080 (**Fig. 3a**). Under RCP4.5, mean yield change under individual model projection ranges from –25% to –5% in 2021–2050 and –33% to 6% (including significant reductions from –33% to –24%) in 2051–2080 (**Fig. 3b**). For RCP8.5, ensemble mean yield shows a range of 1471–2119 kg ha^{-1} in 2021–2050, with decreased mean yield by –14%, and of 1180–1804 kg ha^{-1} in 2051–2080, with significant mean yield reduction of –27% (**Fig. 3c**). Increased yield variability is also projected in 2021–2050 by 50% of climate projections, whereas it is projected by all models in 2051–2080 (RCP8.5) (**Fig. 3c**). The range of mean yield changes vary from –22% to 5% in 2021–2050, while significant mean yield reductions are consistently projected in 2051–2080 (RCP8.5), ranging from –39% to –22% (**Fig. 3d**). Uncertainties are higher among climate models than between scenarios, in which mean yield reductions are of –18% to 0% for models (averaged over scenarios) and –13% to –11% for scenarios (averaged over models) during 2021–2050, and of –36% to –8% for models and –28% to –17% for scenarios during 2051–2080 (**Fig. 3**). Elevated atmospheric CO_2 levels reveal limited

benefits on crop yield, mitigating mean yield reductions by an average of 4% for RCP4.5 or 5% for RCP8.5 during 2021–2050 and 7% for RCP4.5 or 10% for RCP8.5 during 2051–2080 (**OR8**).

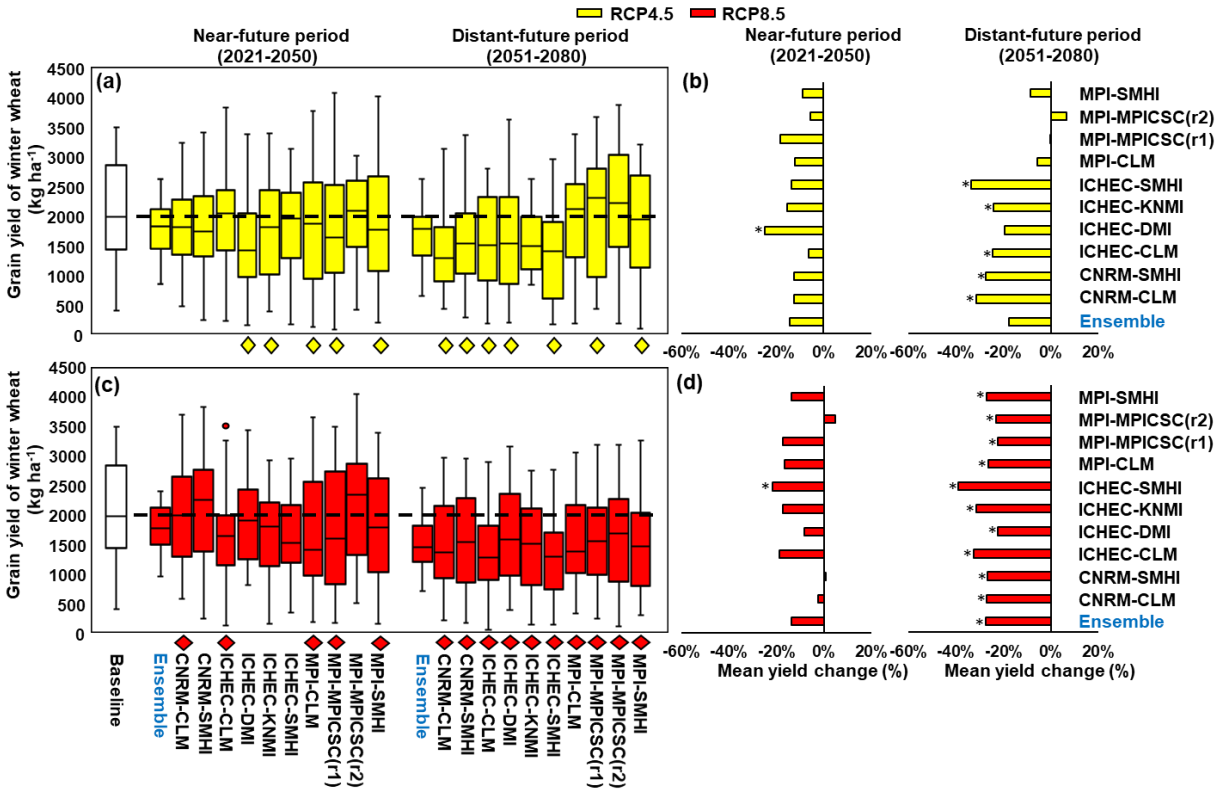

Figure 3 Projections of wheat yield under (***a, b***) RCP4.5 and (***c, d***) RCP8.5 over the near-future (2021–2050) and distant-future periods (2051–2080) under climate projections from 10 models (GCM-RCM). Refer to online resource 4 for detailed information of individual climate models. Dash lines indicate the median value of baseline yield and the diamond symbols denote increased yield inter-annual variability under respective climate model projection (left segments). Statistically significant changes (p<0.05) of mean yield with respect to baseline are highlighted with asterisks (right segments).

4.3.4 Projections of water deficit and high temperature events

Climate projections reveal a high likelihood of increased climatic water deficit and more frequent high temperature events during April–June (**Fig. 4**), which are assumed as the primary drivers of the projected yield reductions and increased variability. In April–June, multi-model ensemble mean indicates significantly enhanced (increased) water deficits by –38 (RCP4.5) or –51 (RCP8.5) mm for 2021–2050, and by –59 (RCP4.5) or –90 (RCP8.5) mm for 2051–2080, with respect to baseline (**Fig. 4a, b**). The projected range of changes of mean water deficit during April–June primarily shows significant intensification, adding up to –65 (RCP4.5) or –76 mm (RCP8.5) deficits in 2021–2050 (**Fig. 4a, b**). Significant increases of mean water deficits are coherently

found in 2051–2080 apart from one model projection, adding up to –89 (RCP4.5) or –107 mm (RCP8.5) deficits for this critical growing period (**Fig. 4a, b**). Regarding high temperature events in April–June, ensemble means indicate significant increases by 3 (RCP4.5) or 6 (RCP8.5) days in 2021–2050, and by 8 (RCP4.5) or 14 (RCP8.5) days in 2051–2080 (**Fig. 4c, d**). There are significant mean increases over 2021–2050, varying from 4 to 8 days (RCP4.5) or 6 to 11 days (RCP8.5) (**Fig. 4c**). Until 2051–2080, 70% of the projections under RCP4.5 suggest significant increases by 7 to 12 days, while significant increases are consistently found under RCP8.5, ranging from 10 to 19 days (**Fig. 4d**). Note that significant mean increases of high temperature occurrences (by up to 6 days) with enhanced water deficits (adding up to –87 mm) are also projected during October–December, particularly over 2051–2080, but the overall effects are much less pronounced for the cool rainy season (October–March) (**Fig. 4b, d**).

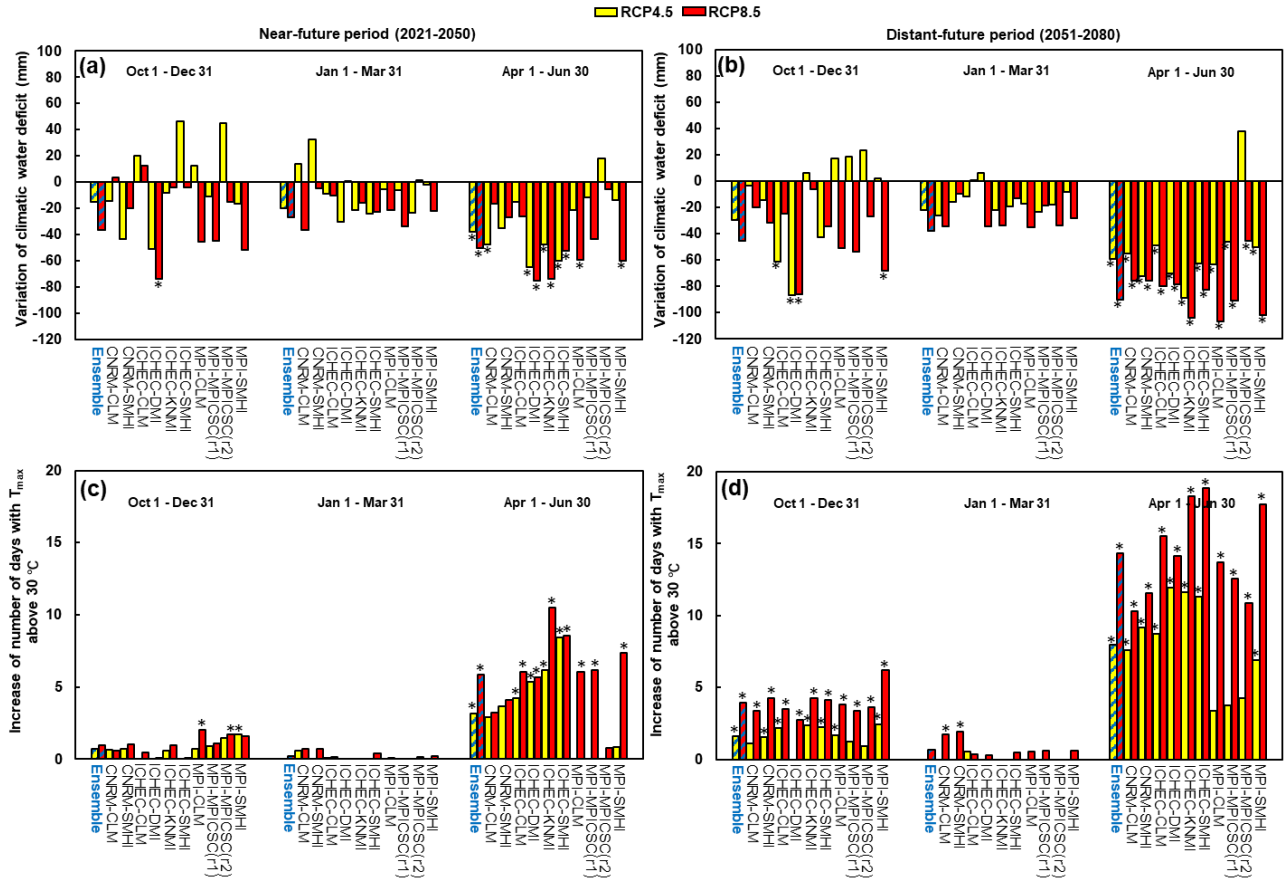

Figure 4 Projected mean changes of (***a, b***) cumulative water deficits (precipitation minus PET, mm) and of (***c, d***) days with maximum temperature >30 °C during three wheat growing phases for future periods with respect to baseline. Statistically significant changes (p<0.05) are highlighted with asterisks.

4.3.5 Adaptation strategies

It is clear that projected negative climate change impacts (**Fig. 3**) are gradually alleviated by using 10%, 20% and 30% earlier flowering cultivars, in which projected yield losses are offset or eventually reversed (**Fig. 5a**). During 2021–2050, ensemble means reveal that projected mean yield reductions of –14% under both scenarios (without cultivar adaptation) (**Fig. 3b**) are mitigated to –7% or –2% (10% early), and are reversed to an increase of 3% or 11% (20% early) and a continuous increase of 12% or 24% (30% early), depending on RCP4.5 or RCP8.5, respectively (**Fig. 5a**). Likewise, during 2051–2080, ensemble means indicate that mean yield reductions of –17% (RCP4.5) or –27% (RCP8.5) (without cultivar adaptation) (**Fig. 3d**) are continuously ameliorated to –8% or –17% (10% early), 3% or –6% (20% early) and 14% or 6% (30% early) (**Fig. 5a**). Hence, mean yield gains from no cultivar adaptation to use of up to 30% earlier flowering cultivar, are of 26% (RCP4.5) or 38% (RCP8.5) for 2021–2050 and 31% (RCP4.5) or 33% (RCP8.5) for 2051–2080. Moreover, the consistent significant mean yield reductions during 2051–2080 under RCP8.5 (**Fig. 3d**) almost disappear by only introducing the 10% early flowering cultivar, while projected yield losses are almost reversed in 2021–2050 with the adoption of the 20% early flowering cultivar (**Fig. 5a**). The use of the 30% early flowering cultivar contributes to a nearly consistent increase in mean yield for both 2021–2050 and 2051–2080, during which potential increases are projected to reach up to 32% and 39%, respectively (**Fig. 5a**).

In contrast, wheat yield seems to be less responsive to early sowings with only slightly yield improvement, in which projected yield losses are unlikely to be fully counteracted under a range of climate projections (**Fig. 5b**). Ensemble means reveal that projected yield losses of –14% during 2021–2050 (without early sowings) (**Fig. 3b**) are slightly reduced to a range of –8% to –4% (RCP4.5) or –7% to –4% (RCP8.5), following 10–30 days early sowing strategies (**Fig. 5b**). Similarly, mean yield reductions of –17% (RCP4.5) or –27% (RCP8.5) in 2051–2080 (**Fig. 3d**) are only marginally alleviated to a range of –13% to –11% (RCP4.5) or –24% to –19% (RCP8.5) (**Fig. 5b**). Thus, maximum mean yield gains by early sowings are projected to be 10% (both scenarios) in 2021–2050 and 6% (RCP4.5) or 8% (RCP8.5) in 2051–2080. There are no increases in yield gains from 10 to 30 days early sowings, particularly during 2051–2080, in which more adverse results (significant reductions up to –27%) are found with 30 days early sowing than that of 20 days (**Fig. 5b**). Less favorable performance of early sowing adaptations can be largely attributed to its limited effects to advance the onset of anthesis and grain filling period to avoid

intensified drought/heat stress late in the season. This could be reflected by increased pre-anthesis growth durations when sowings occur earlier than the prescribed date (Nov 30th). There are robust (small variations of results among climate projections and between scenarios) mean increases of 6, 13 and 21 days (ensemble means) in phenology phase between germination and stem elongation over both 2021–2050 and 2051–2080 periods, with 10, 20 and 30 days early sowings, respectively (**OR9**). The extended early growth duration effectively leads to prolonged vegetative growth, in which days to anthesis are increased by an average of 8, 17 and 26 days for both 2021–2050 and 2051–2080 with 10, 20 and 30 days early sowings, respectively (**OR9**).

4.4 Discussions

4.4.1 Calibration performance

Soil-crop models, such as STICS, has been increasingly used as powerful tools to assess interactive effects of crop growth, climate conditions, soil properties and management practices on yield and environment impacts on agriculture (Coucheney et al., 2015). When the model is applied to address a particular research question at a given site, calibrations of some model parameters are often firstly performed to fit simulations to available observations for better representing local production conditions. Our results indicate that an appropriate adjustment of general plant parameter and built-in cultivar choice could lead to a considerable improvement of prediction accuracy for wheat yield, where nRMSE is reduced from up to 100% to as low as 20% (**Fig. 2a**). In the pilot project of Agricultural Model Intercomparison and Improvement (AgMIP), similar prediction accuracy of wheat yields (nRMSE of 30%) has been achieved using STICS under various environmental conditions, before being applied to project yield response to future climate change (Asseng et al., 2013). Furthermore, the 5-year observed yields are herein obtained under quite different meteorological conditions (including an extremely dry year) and over a wide range of possible yields, i.e. 800–4000 kg ha^{-1} (**Fig. 2d** and **OR2**). The model ability to reproduce observed yield variability, as reflected by a consistently high agreement between simulations and observations (r>0.75, **Fig. 2c**), suggests that inter-annual sensitivity of wheat yield to weather variations could be skilfully captured by the model (in particular from extreme weather events), which may warrant its applicability in climate change impact assessments. Moreover, observed yields are directly obtained from independent field measurements of published data, thus further strengthening the reliability of our model calibrations and outcomes. However, the relevance of

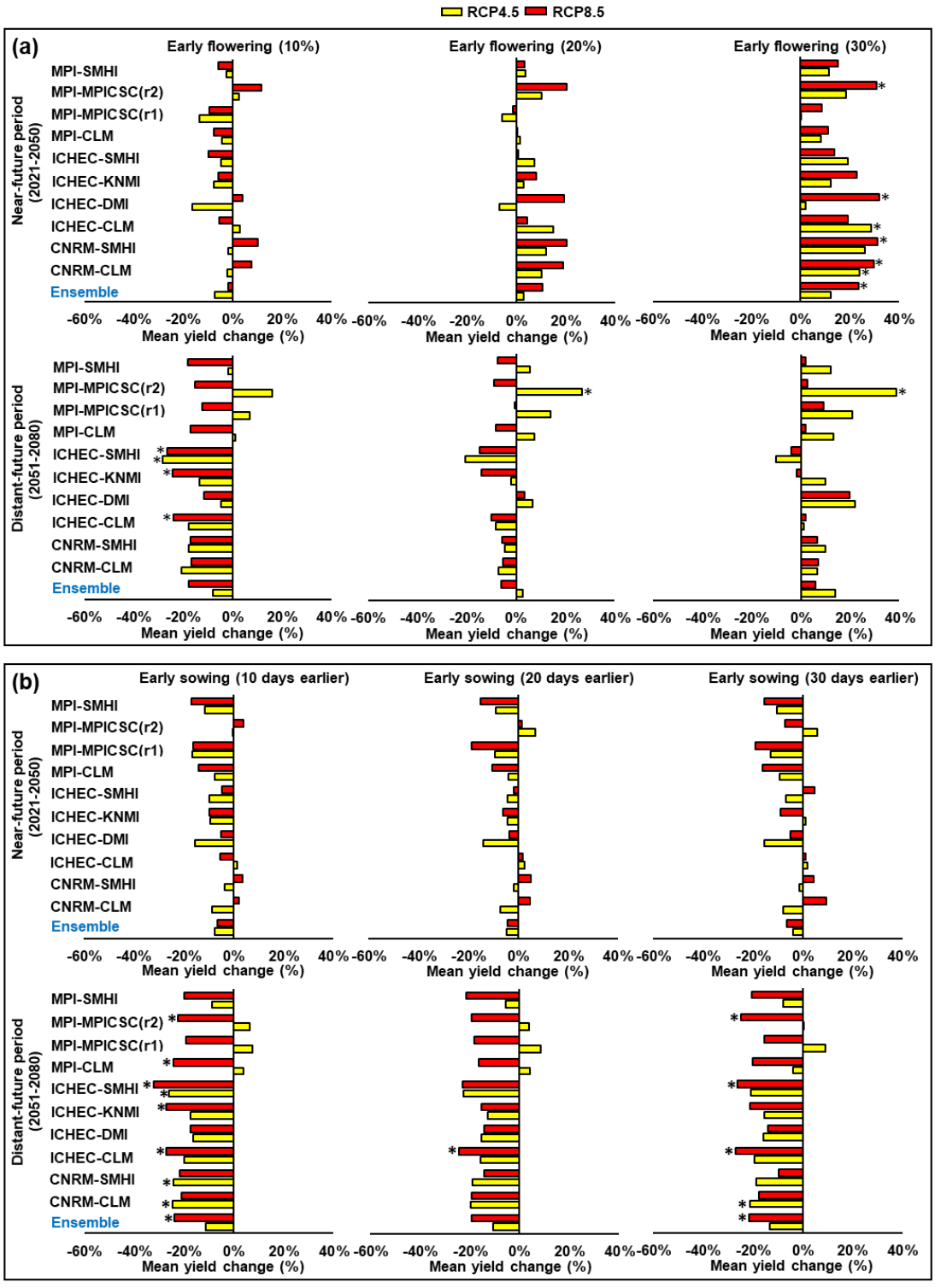

Figure 5 Effects of adaptation measures on wheat yield by using (***a***) early flowering cultivars with three different extent of earliness at anthesis (earlier than the baseline cultivar), and by using (***b***) three early sowing dates (earlier than the baseline adopted average sowing date: Nov_30) for the near-future (2021–2050) and distant-future (2051–2080) periods, under RCP4.5 and RCP8.5. Statistically significant mean yield changes (p<0.05) with respect to baseline are highlighted with asterisks.

newly calibrated parameter values for local conditions (e.g. RUE=2.8) should be further evaluated using additional representative datasets.

4.4.2 Climate projections

Climate models are widely accepted tools to simulate present and future climates. However, climate model projections are inherently uncertain, resulting from simplified representation of the real climate system by climate models with different numerical approaches for describing physical processes (IPCC, 2015), from social-economic uncertainties regarding influences on future trajectories of greenhouse gas emissions (Asseng et al., 2013; van Vuuren et al., 2011) and from model initializations (Deser et al., 2012). Within the EURO-CORDEX initiative, a coordinated bias-adjusted multi-model, multi-scenario and multi-initialization ensemble of downscaled experiments with fine spatial resolution (0.11°) were generated (Jacob et al., 2014). A subset of these model runs are employed in our study to address these uncertainties, in which the diverse ensemble composition (10 models and 4 initializations under 2 forcing scenarios) enables a wide range of probable projections. The resulting climate projections over near- and distant-future period, indeed give a relatively robust climate change signal with small range of variations, e.g. projected annual mean temperature increase by 2.2–2.5°C accompanied by precipitation reductions by up to –28% in 2051–2080 under RCP8.5 (**OR6**). Hence, a reasonable level of confidence for climate projections has been achieved in the current study, despite some uncertainties found at monthly scale (e.g. in June) (**OR6**). It is worth mentioning that these multi-model ensembles of climate projections also account for a broad range of altered climate variabilities, thus the projected yield impacts implicitly integrate the potential changes (increase) in the frequency and intensity of extreme events.

4.4.3 Impacts of climate change and regional food security

The overall climate change projections depict a moderate warming and enhanced dryness with increased magnitudes as a function of time (**OR6**), resulting in continuously decreased mean yield with increased variabilities (**Fig. 3**). During 2021–2050, projected variations of mean yield changes are relatively close between RCP4.5 (–25% to –5%) and RCP8.5 (–22% to 5%), in which both scenarios agree on a mean yield reduction of –14% (by ensemble mean) (**Fig. 3b, d**). The two emission scenarios indeed present relatively smaller differences in the projected trends of

greenhouse gas concentrations (in particular CO_2 concentration) before 2050s, and only begin to diverge substantially in the latter half of the century, with different impacts on climate simulations (van Vuuren et al., 2011). During 2051–2080, significant decreases of mean yields (–39% to –22% with an ensemble mean of –27%) are consistently found under high emission scenarios (RCP8.5), with a strong agreement concerning increased yield variabilities (**Fig. 3c, d**). The stabilization scenario (RCP4.5) is also likely to have a mean yield loss (–33% to 6% with an ensemble mean of –17%) over this period, together with the projected high likelihood (70%) of increased yield inter-annual variabilities (**Fig. 3a, b**).

The overall results are consistent with a meta-analysis of crop yield response to projected climate change, concluding that wheat yield changes are expected to be negatively affected by even moderate warming (by 2°C of local warming), with higher risk of mean yield loss and greater yield variabilities in the second half of the 21st century than in the first one (Challinor et al., 2014). In southern Portugal (Guadiana river basin), a similar study also indicates the susceptibility of rainfed winter wheat to climate change, where projected mean yield reductions range from –8% to –4% for 2011–2040 and from –14% to –7% for 2041–2070, across multiple climate models and different emission scenarios (Valverde et al., 2015). In comparison, these relatively smaller magnitudes of yield losses could be attributed to the lack of introducing climate projections with altered climate variabilities, where variance of projected future climate is kept the same as in the historical baseline period (Valverde et al., 2015), which are unlikely true. In general, our findings indicate that negative yield impacts are very likely (i.e. high agreement in yield reductions with increased variabilities) despite the magnitudes of impacts vary among models and between scenarios, which are particularly emphasized for 2051–2080 (**Fig. 3**). Simulated yield variations among climate model projections represent major source of impact uncertainties when compared to variations between scenarios (**Fig. 3**). In fact, uncertainties in simulating yield impacts among climate model projections tend to dominate regional climate impact assessment (Kassie et al., 2015; Osborne et al., 2013). However, this can also be attributed to the asymmetry between the numbers of models (ten) and of scenarios (two) in our case. On the other hand, the simulated yield benefits from atmospheric CO_2 enrichment, particularly under the high emission scenario of RCP8.5 (i.e. up to 10% mean yield mitigations) (**OR8**), are in contrast to reported average yield increment by about 16–22% (depending on soil water and N availability) for C3 cereals under 190 ppm CO_2 increment (Kimball, 2016). The limited yield response may be explained by the fact that projected

higher temperature above the optimum growth range, could partially offset CO_2 induced stimulation of photosynthesis, in which the similar simulation results were previously obtained by Wang et al. (2017). Interactive effects of temperature and CO_2 on crop photosynthesis and biomass growth are able to be captured by STICS via influences on crop RUE (Brisson et al., 2009).

The projected mean yield decrease with increased variability may undermine the two important dimensions of food security, i.e. availability and stability (Schmidhuber and Tubiello, 2007). Historically, wheat production policies in Portugal encouraged increases in harvest areas, while supporting seed selection and massive use of chemical fertilizers, resulting in an intensification of cropping systems and severe soil degradation on marginal lands (Jones et al., 2011). Following the introduction of afforestation measures and policies favoring meat/milk products since the 1980s, arable crop land (including wheat areas) substantially declined with a concomitant increase of forest land and grassland areas (Jones et al., 2011). On the other hand, wheat yield increased as a result of management and cultivar improvements (Páscoa et al., 2017), as well as by abandonment of less fertile soils. However, recent common agricultural policy promotes integrated management and soil conservation practices (Jones et al., 2011), thus yield improvements by means of intensive resource use (e.g. water and fertilizers) are likely to be more and more constrained. Hence, in the national context of growing environmental concerns on soil degradation, increasing land use competition and restricted resource use, influence of projected wheat yield reductions shall be more pronounced, as the efforts for maintaining or increasing grain production in order to achieve self-sufficiency could be substantially undermined, provided no adaptation measures are implemented.

Annual recorded (winter) wheat yield statistics in Alentejo region over the past three decades has been characterized by a strong variability (~30% of CV), ranging from 566 kg ha^{-1} in 2005 (associated with severe drought) to 2482 kg ha^{-1} in 2016 (national statistics at www.ine.pt). Other than some external factors such as technical trends and growing areas changes, this variability could be largely explained by increased climate variability, particularly by the strong inter-annual variability of seasonal precipitation. During 1986–2012, simultaneous occurrence of dry events and anomalously low wheat yields are consistently found for most of the Iberian Peninsula (Páscoa et al., 2017), showing the vulnerability of rainfed wheat cropping systems to extreme weather conditions, particularly severe drought events. Thus, climate change is expected to further aggravate this vulnerability through increased climate variability with more aridity and frequent

extreme temperature, such as projections shown in **Fig. 4**. As a result, projected increase of yield inter-annual variabilities implies substantial threat to future year-to-year stability of food crop supply with notable impacts to food chain resilience (Challinor et al., 2014).

4.4.4 Adaptation to enhanced water deficits and heat stress

Grain yield production of winter wheat in regions with typical Mediterranean climate is commonly limited by water deficits and heat stress during the flowering and grain filling period and such unfavorable growing conditions are likely to be further worsened in the future climate (Asseng et al., 2011; Páscoa et al., 2017; Wang et al., 2017). Projected negative yield impacts in our study are largely due to the intensified water deficits and more frequent high temperature events during the April–June period, within which grain-filling phase typically occurs (**Fig. 4**). Significant mean increases of water deficits (–38 to –90 mm) and of high temperature events (3 to 14 days) during April–June are coherently projected for the two future periods, along with smaller magnitudes of increases for the early growing season, i.e. October–March (**Fig. 4**). In line with our analysis, Rolim et al. (2017) suggests that average seasonal water deficits of local rainfed winter wheat are projected to increase across three climate models and two scenarios. Moreover, as indicated by Asseng et al. (2011), wheat yield losses owed to high temperatures during the important grain filling phase are likely to be an important constraint for major wheat producing regions worldwide, thus substantially undermining global food security. In particular, our case study illustrates that average hot days (>30°C) during April–June are projected to increase significantly by 14 days over 2051–2080, RCP8.5 (**Fig. 4d**), reaching >34 days (20 days in baseline) for this critical period with enormous detrimental impacts for successful grain production.

Between the adaptation options explored, our study reveals that the use of early flowering cultivars results in more yield gains under a range of climate projections, and thus may outperform the other adaptation measure of early sowings (**Fig. 5**). By adopting early flowering wheat cultivars, crop growing season lengths are expected to markedly decrease under combined effects of reduced thermal requirement and accelerated development rate under warmer climates, resulting in less intercepted nutrients and radiation, with consequently lower biomass accumulation and yield formation (Asseng et al., 2011; Debaeke, 2004; Kassie et al., 2015). Nonetheless, such negative impacts of potential yield reductions with shorter growing duration, are shown to be counterbalanced, with less pronounced effects than the positive effects by advancing anthesis,

where risks of crop exposure to intensified drought and heat stresses during grain filling are reduced or avoided, leading to net seasonal yield gains and mitigations of mean yield reductions (**Fig. 5a**). Besides, a shortened vegetative phase with early flowering cultivar is also likely to result in reduced grain numbers (Farooq et al., 2011), with subsequent detrimental impacts on final grain yields, but this process is currently not incorporated into the model. The projected mean yield reductions (**Fig. 3**) are gradually alleviated and eventually reversed when considering cultivars with progressively early flowering, resulting in maximum yield gains of 26–38% (**Fig. 5a**). In many dry Mediterranean (typical winter-dominant rainfall) environments, earlier flowering has proven to enable shifting the sensitive wheat growth stage (i.e. grain filling) to the cooler and wetter part of the season, thus increasing the harvest index by minimizing the risks of exposure to terminal drought and very high temperatures late in the season (Asseng et al., 2011; Debaeke, 2004; Wang et al., 2015; Wang et al., 2017). Moreover, the nearly consistent increases in the mean yields for both 2021–2050 and 2051–2080 (up to 39%), using 30% early flowering cultivar (**Fig. 5a**), may point out the potential opportunities for local yield improvement despite increasingly unfavorable climate conditions. On the other hand, Wang et al. (2017) projected increased yield of rain-fed winter wheat in the warm and dry sites of Eastern Australia, benefiting from warming-induced early flowering even without cultivar adjustment. Without cultivar adaptation, our results clearly indicate negative yield response, which probably could be attributed to insufficient extent of growth advancement from projected temperature increase alone.

In contrast, 10–30 days early sowing strategy appears to be less favorable with maximum mean yield gains of only 6–10% (**Fig. 5b**), owing to the weak effects of advancing the onset of anthesis and grain filling stage. When sowing occurs 10, 20 and 30 days earlier, duration of pre-anthesis growth increases by an average of 8, 17 and 26 days (**OR9**), respectively, thus largely offsetting the effects of anticipation of the growth cycle. Most of these increases originate from the prolonged seasonal growth duration between germination and stem elongation (**OR9**), corresponding to the main phase for crop vernalization fulfilment (an important prerequisite for the induction of reproductive growth for winter wheat). Climate warming during vernalization period may affect and slow effective chilling accumulation before anthesis, thus increasing the vegetative phase and delaying the onset of anthesis (Rosenzweig and Tubiello, 1996; Wang et al., 2015). The flowering date of winter wheat was previously projected to be delayed by an average of 14 days under RCP8.5 in eastern Australia, resulting from restricted vernalization fulfilment with temperature

increase (Wang et al., 2015). Indeed, the current mean monthly temperature (~15℃) around the early sowing window (i.e. mid of October to early November) at study area, is already close to the defined upper threshold (16.5℃) of effective chilling accumulation (vernalization value) for winter wheat (Brisson et al., 2009). Therefore, early sowing, which allows making use of more winter rainfall, may be compromised by climate warming, resulting from decreased number of effective vernalization days. As such, adopting winter wheat varieties with lower vernalization requirements may be useful to deal with this constraint.

4.5 Conclusion

In summary, among a large range of yield projections, simulations with early flowering cultivars result in higher yield gains than that of early sowings, which successfully mitigate and even reverse the projected mean yield reductions. Therefore, development of early flowering cultivars from breeding programme may help maintain and increase local grain yield productions in future climates for the major wheat production region of Portugal, along with likely effects for regions with similar Mediterranean-type climates. However, the extent of flowering earliness should only reach up to a point where shortened duration of vegetative growth does not constitute significant potential yield reduction. Despite some inherent uncertainties (e.g. climate projection uncertainties) and limitations (e.g. lack of inclusion of other crop models), our findings are expected to contribute to a better understanding of crop yield response to future climate changes under typical Mediterranean environments, as well as aiding in designing suitable adaptation strategies for policy makers, e.g. by providing insights for guiding breeding efforts.

Acknowledgments

This work was supported by European Investment Funds by FEDER/COMPETE/POCI – Operational Competitiveness and Internationalization Programme, under Project POCI-01-0145-FEDER-006958, and National Funds by FCT – Portuguese Foundation for Science and Technology, UID/AGR/04033/2013. The authors acknowledge the FCT scholarship given to the first author, PD/BD/113617/2015, under the Doctoral Programme "Agricultural Production Chains − from fork to farm" (PD/00122/2012). We also thank the FCT for CEECIND/00447/2017.

References

Alexandratos, N. and Bruinsma, J., 2012. World agriculture towards 2030/2050: the 2012 revision, ESA Working paper No. 12-03, Rome, FAO.

Asseng, S. et al., 2013. Uncertainty in simulating wheat yields under climate change. Nature Climate Change, 3(9): 827-832.

Asseng, S., Foster, I. and Turner, N.C., 2011. The impact of temperature variability on wheat yields. Global Change Biol, 17(2): 997-1012.

Brigitta, T., Melanie, W., László, P. and Tomislav, H., 2017. 3D soil hydraulic database of Europe at 250 m resolution. Hydrol Process, 31(14): 2662-2666.

Brisson, N. et al., 2003. An overview of the crop model stics. European Journal of Agronomy, 18(3): 309-332.

Brisson, N., Launay, M., Mary, B. and Beaudoin, N., 2009. Conceptual basis, formalisations and parameterization of the STICS crop model. Editions Quae, Versailles, France, 297 pp.

Brisson, N. et al., 1998. STICS: a generic model for the simulation of crops and their water and nitrogen balances. I. Theory and parameterization applied to wheat and corn. Agronomie, 18(5-6): 311-346.

Brisson, N. et al., 2002. STICS: a generic model for simulating crops and their water and nitrogen balances. II. Model validation for wheat and maize. Agronomie, 22(1): 69-92.

Carvalho, M. and Basch, G., 1995. Optimisation of nitrogen fertilisation. Fert Res, 43(1): 127-130.

Challinor, A.J. et al., 2014. A meta-analysis of crop yield under climate change and adaptation. Nature Climate Change, 4: 287.

Costa, R. et al., 2013. Effect of sowing date and seeding rate on bread wheat yield and test weight under Mediterranean conditions. Emir J Food Agr, 25(12): 951-961.

Coucheney, E. et al., 2015. Accuracy, robustness and behavior of the STICS soil–crop model for plant, water and nitrogen outputs: Evaluation over a wide range of agro-environmental conditions in France. Environ Modell Softw, 64: 177-190.

Dahlgren, P., Landelius, T., Kallberg, P. and Gollvik, S., 2016. A high-resolution regional reanalysis for Europe. Part 1: Three-dimensional reanalysis with the regional HIgh-Resolution Limited-Area Model (HIRLAM). Q J Roy Meteor Soc, 142(698): 2119-2131.

Debaeke, P., 2004. Scenario analysis for cereal management in water-limited conditions by the means of a crop simulation model (STICS). Agronomie, 24(6-7): 315-326.

Dee, D.P. et al., 2011. The ERA-Interim reanalysis: configuration and performance of the data assimilation system. Q J Roy Meteor Soc, 137(656): 553-597.

Deser, C., Knutti, R., Solomon, S. and Phillips, A.S., 2012. Communication of the role of natural variability in future North American climate. Nature Climate Change, 2: 775.

Dias, A.S. and Lidon, F.C., 2009. Evaluation of Grain Filling Rate and Duration in Bread and Durum Wheat, under Heat Stress after Anthesis. J Agron Crop Sci, 195(2): 137-147.

Eurostat, 2015. Annual crop production price and absolute economic value over 2004-2014 in Portugal. Office for Official Publications.

FAO/IIASA/ISRIC/ISSCAS/JRC, 2012. Harmonized World Soil Database (version 1.2), FAO, Rome, Italy and IIASA, Laxenburg, Austria.

Farooq, M., Bramley, H., Palta, J.A. and Siddique, K.H.M., 2011. Heat Stress in Wheat during Reproductive and Grain-Filling Phases. Critical Reviews in Plant Sciences, 30(6): 491-507.

Gouveia, C. and Trigo, R.M., 2008. Influence of Climate Variability on Wheat Production in Portugal. In: A. Soares, M.J. Pereira and R. Dimitrakopoulos (Editors), geoENV VI – Geostatistics for Environmental Applications: Proceedings of the Sixth European Conference on Geostatistics for Environmental Applications. Springer Netherlands, Dordrecht, pp. 335-345.

Hengl, T. et al., 2017. SoilGrids250m: Global gridded soil information based on machine learning. Plos One, 12(2): e0169748.

Howden, S.M. et al., 2007. Adapting agriculture to climate change. Proceedings of the National Academy of Sciences, 104(50): 19691-19696.

IPCC, 2013. The physical science basis. Contribution of working group I to the fifth assessment report of the intergovernmental panel on climate change [Stocker, T.F., D. Qin, G.-K. Plattner, M. Tignor, S.K. Allen, J. Boschung, A. Nauels, Y. Xia, V. Bex and P.M. Midgley (eds.)]. Cambridge University Press, Cambridge, United Kingdom and New York, NY, USA, 1-1535 pp.

IPCC, 2015. Workshop Report of the Intergovernmental Panel on Climate Change Workshop on Regional Climate Projections and their Use in Impacts and Risk Analysis Studies

[Stocker, T.F., D. Qin, G.-K. Plattner, and M. Tignor (eds.)], IPCC Working Group I Technical Support Unit, University of Bern, Bern, Switzerland.

Jacob, D. et al., 2014. EURO-CORDEX: new high-resolution climate change projections for European impact research. Regional Environmental Change, 14(2): 563-578.

Jégo, G. et al., 2010. Calibration and performance evaluation of soybean and spring wheat cultivars using the STICS crop model in Eastern Canada. Field Crops Research, 117(2): 183-196.

Jones, N., de Graaff, J., Rodrigo, I. and Duarte, F., 2011. Historical review of land use changes in Portugal (before and after EU integration in 1986) and their implications for land degradation and conservation, with a focus on Centro and Alentejo regions. Appl Geogr, 31(3): 1036-1048.

Kassie, B.T. et al., 2015. Exploring climate change impacts and adaptation options for maize production in the Central Rift Valley of Ethiopia using different climate change scenarios and crop models. Climatic Change, 129(1): 145-158.

Kimball, B.A., 2016. Crop responses to elevated CO2 and interactions with H2O, N, and temperature. Curr Opin Plant Biol, 31: 36-43.

Klein Tank, A.M.G. et al., 2002. Daily dataset of 20th-century surface air temperature and precipitation series for the European Climate Assessment. Int J Climatol, 22(12): 1441-1453.

Landelius, T., Dahlgren, P., Gollvik, S., Jansson, A. and Olsson, E., 2016. A high-resolution regional reanalysis for Europe. Part 2: 2D analysis of surface temperature, precipitation and wind. Q J Roy Meteor Soc, 142(698): 2132-2142.

Osborne, T., Rose, G. and Wheeler, T., 2013. Variation in the global-scale impacts of climate change on crop productivity due to climate model uncertainty and adaptation. Agr Forest Meteorol, 170: 183-194.

Páscoa, P., Gouveia, C.M., Russo, A. and Trigo, R.M., 2017. The role of drought on wheat yield interannual variability in the Iberian Peninsula from 1929 to 2012. Int J Biometeorol, 61(3): 439-451.

Pfeifroth, U., Sanchez-Lorenzo, A., Manara, V., Trentmann, J. and Hollmann, R., 2018. Trends and Variability of Surface Solar Radiation in Europe Based On Surface- and Satellite-Based Data Records. Journal of Geophysical Research: Atmospheres, 123(3): 1735-1754.

Rolim, J., Teixeira, J.L., Catalao, J. and Shahidian, S., 2017. The Impacts of Climate Change on Irrigated Agriculture in Southern Portugal. Irrig Drain, 66(1): 3-18.

Rosenzweig, C. and Tubiello, F.N., 1996. Effects of changes in minimum and maximum temperature on wheat yields in the central US A simulation study. Agr Forest Meteorol, 80(2): 215-230.

Santos, J.A., Belo-Pereira, M., Fraga, H. and Pinto, J.G., 2016. Understanding climate change projections for precipitation over western Europe with a weather typing approach. J Geophys Res-Atmos, 121(3): 1170-1189.

Schmidhuber, J. and Tubiello, F.N., 2007. Global food security under climate change. Proceedings of the National Academy of Sciences, 104(50): 19703-19708.

Scotti-Campos, P. et al., 2014. Heat tolerance of Portuguese old bread wheat varieties. Emir J Food Agr, 26(2): 170-179.

Valverde, P. et al., 2015. Climate change impacts on rainfed agriculture in the Guadiana river basin (Portugal). Agricultural Water Management, 150: 35-45.

van Vuuren, D.P. et al., 2011. The representative concentration pathways: an overview. Climatic Change, 109(1-2): 5-31.

Wang, B., Liu, D.L., Asseng, S., Macadam, I. and Yu, Q., 2015. Impact of climate change on wheat flowering time in eastern Australia. Agr Forest Meteorol, 209-210: 11-21.

Wang, B., Liu, D.L., Asseng, S., Macadam, I. and Yu, Q., 2017. Modelling wheat yield change under CO2 increase, heat and water stress in relation to plant available water capacity in eastern Australia. European Journal of Agronomy, 90: 152-161.

Yang, W. et al., 2010. Distribution-based scaling to improve usability of regional climate model projections for hydrological climate change impacts studies. Hydrology Research, 41(3-4): 211-229.

CHAPTER 5

Modelling climate change impacts on perennial forage grassland with contrasted growth duration in Portugal

Briefing notes:

Grassland utilization or harvest, through extensive animal grazing or forage conservation as hay and silage production, represent essential source of livelihood for smallholder farmers scattered across the Mediterranean region. However, the projected warming and drying trends, along with higher frequency and intensity of extreme weather events, particularly during summer, are expected to substantially challenge grassland forage production. While it is foreseen that forage production will be increasingly limited by prolonged summer drought, with negative impacts on both productivity and persistence, direct effects of summer heat stress, with detrimental impacts on growth and productivity, has been largely ignored in previous studies. On the other hand, the growing season will likely shift towards winter due to warmer winter and drier summer, leading to modified annual growth pattern of grassland species, with a distinguished seasonal growth pattern. Moreover, the elevated atmospheric CO_2 level may, to some extent, help alleviating drought limitations on photosynthesis and growth, particularly during the cooler winter period. Taken together, changes in CO_2 level, temperature and precipitation are likely to affect productivity of perennial grassland in a complex manner, requiring an integration of local growing conditions. In this context, we have developed a study to evaluate the overall climate change impacts on forage dry matter yield production, under contrasting growing seasons by considering different cutting regimes (early cut for winter-spring growing season only or late cut for winter-spring-summer). For that purpose, the STICS crop model at three different grassland sites across Portugal was used. Simulations are performed under conditions of restricted irrigation in order to avoid simulating drought persistence or mortality rate during hot and dry summer. The findings reveal the development of targeted adaptation strategies should take advantage of emerging opportunity (increase growth potential during the increasingly favorable winter season) and minimize risks to tackle challenges (enhance summer dormancy plant traits to avoid summer heat and drought impacts) arising from climate change.

This chapter thus devotes to fully cover this study, which has been published as a research article "*Modelling climate change impacts on early and late harvest grassland systems in Portugal"* in an international journal of *Crop&Pasture science*. This research corresponds to tasks 5 and 6, aiming to improve our understanding of perennial forage species behavior under climate change, and provide valuable insights for guiding and prioritizing breeding and research efforts to improve the climate resilience of grassland production system.

Title: Modelling climate change impacts on perennial forage grassland with contrasted growth duration in Portugal

Chenyao Yang[a,*], Helder Fraga[a], Wim van Ieperen[b] and João A. santos[a]

[a]*Centre for the Research and Technology of Agro-environmental and Biological Sciences, CITAB, Universidade de Trás-os-Montes e Alto Douro, UTAD, 5000-801, Vila Real, Portugal*

[b]*Group Horticulture and Product Physiology, 6700 AA Wageningen University, the Netherlands*

*****Corresponding author. E-mail: cyang@utad.pt

Refer to https://doi.org/10.1071/CP17428 for online published version.

Abstract

Climate change projections for Portugal showed warming and drying trends, representing a substantial threat for the sustainability of forage production in perennial grassland. The objective of current study was to assess climate change impacts on seasonal dry matter yield (DMY) in three locations (Northwest-, Central-inner and South-Portugal) with different climatic conditions, for two grassland production systems deviating in growing season length, either early cuts in spring (ES) or late cuts in summer (LS). Impacts were estimated using the STICS crop model, by comparing a historical baseline period (1985–2006) with simulated projections over future periods (2021–2080). For this purpose, the STICS crop model was driven by high-resolution climate data from a coupled Global Climate Model / Regional Climate Model chain. As a result, we obtained that, during the baseline period, DMY of LS was consistently much higher than that of ES in all three locations. For LS, significant reductions in mean DMY were forecasted during 2061–2080, ranging from mild (–13%) in the north to severe (–31%) in the south of Portugal. In contrast, seasonal DMY was largely maintained for ES among sites until 2080, benefiting from low water deficits, the expected atmospheric CO_2 rise and the forecasted temperature increase during cool season. Thus, the yield gap was projected to gradually decrease between the two regimes, in which mean DMY for ES was foreseen to exceed that of LS over 2061–2080 in the southern site. Moreover, ES was projected to have very low exposure to extreme heat and severe water stresses. Conversely, LS, subjected to high summer water deficit and irrigation needs, was projected to experience increased summertime water stress (9–11%) and drastically increased heat stress (33–57%) in 2061–2080, with more pronounced heat stress occurring in the south. Frequency of occurrence of extreme heat stress was projected to gradually increase in summer over successive

study periods, with a concomitant increased intensity of DMY response to inter-annual variability of heat stress during 2061–2080. Heat stress tended to be more important than water stress under the prescribed irrigation strategy for LS, potentially being the main limiting factor for summertime DMY production under climate change scenario.

Keywords: Mediterranean Grassland, Dry Matter Production, Seasonal Water Consumption, STICS, Climate Change Scenarios, Summer Heat Stress

5.1 Introduction

Under the Mediterranean environment, permanent grassland was a primary forage source to sustain extensive animal grazing activities crucial to rural economy. Perennial grassland was typically exposed to two distinct growing seasons: from September to April (cool season: autumn–winter–spring period with cool and rainy conditions) and from May to August (warm season: hot dry summers). Thus, Mediterranean grasslands often suffered from regular, and sometimes severe, water deficit, thus leading to a shortage of forage grass, particularly during the dry summertime period. The lack of natural feedstuff over a certain period was incompatible with constant nutritional needs of livestock, which highlights the role of forage production conserved as hay or silage (Courault et al., 2010; Lourenco and Palma, 2001). Given the important role of forage conservation, suitable growing season length represented the key factor for defining a proper cutting regime as seasonal cumulative herbage yield was often subject to various uncertainties, including heterogeneous botanic composition, different fertilization strategies and soil characteristics, as well as climatic variability and change (Belesky and Fedders, 1995; Casella et al., 1996; Cop et al., 2009).

Portugal was characterized by a Mediterranean-type climate, in which the typical irregularity and high inter-annual variability of the precipitation regime was aggravated by warming trends and increased frequencies of temperature extremes over recent decades (Andrade et al., 2014; Andrade et al., 2011). Future climate change in broad Mediterranean areas, manifested by temperature increases and precipitation reductions (IPCC, 2013), was expected to negatively influence forage yields. The lengthening of drought episodes, with a concomitant increase of frequency of their extremes, may not be offset by higher growth rates in the cool season and by the CO_2 fertilization effect (Lelievre and Volaire, 2009). Moreover, heat stress was far from negligible at inhibiting plant growth and yield (Dumont et al., 2015).

There were around 2.3 million hectares of grasslands in Portugal, covering approximately 25% of its territory (Jongen et al., 2011), mainly in northwestern, central-inner and southern regions (Carneiro et al., 2005; Lopes and Reis, 1998; Teixeira et al., 2011). In the northwest, large areas were devoted to intensive dairy farms, which contribute to more than 50% of national milk production (Trindade, 2015). Success of these dairy farms was largely dependent on self-sufficient forage supply from zero-grazing permanent grassland (Trindade, 2015). In the central-inner region, grassland utilization was generally concentrated in a few farms, in which irrigated pasture provided principal forage supply to the integrated livestock production (Pereira et al., 2004). Natural and semi-natural grasslands were the main vegetation cover in southern Portugal (Aires et al., 2008a). Currently, they were critical to sustain extensive animal production, but recent trends showed a gradual replacement by managed sown biodiverse permanent pasture (Teixeira et al., 2011). Across Portugal, there were two prevailing cutting regimes: 1) early cutting in late spring, which may result in insufficient growing periods and low herbage yields; 2) late cutting in the end of summer for a longer growing season, but exposing grassland to potential summer water deficit and heat stress. Under future climate change, there were increasing uncertainties for sustainable and stable production of both grassland systems.

Process-based crop models were widely recognized as efficient tools to simulate crop behaviour under various environmental conditions. In particular, STICS (Simulateur mulTIdisciplinaire pour les Cultures Standard) was a generic model for simulating a wide range of crops (Brisson et al., 2003). STICS was particularly useful in modelling perennial grasslands, being used to monitor and map real-time status of forage growth over France, namely Information and Objective Follow-up of Pastures (ISOP) (Ruget et al., 2006; Ruget et al., 2009). The ISOP system accurately estimated forage production shortage under summer water deficit and hot weather, and thus realistically quantified the impact of drought and heat stresses, which helped mobilizing forage reserves to affected areas (Ruget et al., 2009).

To assess climate change impacts on agricultural yields, coupling crop models with climate models was a common approach. The European Coordinated Regional Downscaling Experiments (EURO-CORDEX) initiative was established to provide daily high-resolution (12.5 km) regional climate change simulations (Jacob et al., 2014), using Regional Climate Models (RCM) to dynamically downscale Global Climate Models (GCM) outputs from the Coupled Model Intercomparison Project Phase 5 (CMIP5) (Samuelsson et al., 2011). Furthermore, these models also provided

simulations driven by different climate change scenarios, i.e. Representative Concentration Pathways (RCP) (Jacob et al., 2014; van Vuuren et al., 2011). The climate model adopted in present study was MPI-ESM-LR/SMHI-RCA4 from EURO-CORDEX (Jacob et al., 2014). This model has previously shown similar mean temporal patterns as the full EURO-CORDEX ensemble mean (Fraga et al., 2016), making it suitable to assess climate change impacts.

Studies coupling STICS with climate models have already been carried out in France, with general findings highlighting that summertime forage production drastically decreased in the distant future, contrasting with enhanced production during winter, though the magnitude of climate effects on grassland varied among regions and future periods (Ruget et al., 2012; Ruget et al., 2013). In Portugal, a few studies have been devoted to assessing climate change impacts on perennial grasslands (Nóbrega, 2006; Valverde et al., 2015). However, those studies neither distinguished forage growing seasons nor operated crop models using climate data at high temporal and spatial resolution. Hence, our objectives were to evaluate the overall impacts of high-resolution climate change projections on grassland dry matter yield (DMY), in association with water and thermal stress conditions, for both short and long growing seasons. For the methods, STICS was run in three locations across Portugal (Northwest-, Central-inner and South-Portugal) and projected changes in temperature, precipitation and atmospheric CO_2 concentration were retrieved from EURO-CORDEX projections. The impacts were quantified by comparing the differences between a historical baseline period (1985–2006) and future period (2021–2080).

5.2 Data and methods

5.2.1 Study sites

The selected three study sites were: "Vilar" (41.29°N, 8.68°W, 42 m a.s.l.) in northwestern Portugal (NP), "Quinta da Franca" (40.27°N, 7.43°W, 436m a.s.l.) in central-inner Portugal (CP) and "Monte do Tojal" (38.47°N, 8.01°W, 186m a.s.l.) in southern Portugal (SP) **(Fig. 1a)**. In NP, the herbaceous community of local hay meadowlands were dominated by *Dactylis* genus (cocksfoot grass) over a wide geographic distribution, from coast to mountains (Lopes and Reis, 1998). Some intensive non-grazing forage cropping systems received enhanced fertilization (organic slurry and mineral fertilizers) and irrigation (Trindade et al., 1997). In CP, permanent pasture (co-existence of natural and sown biodiverse grassland), managed by both grazing and cutting, covered approximately 60% of farm surface with frequent irrigation, which benefits from

the installed irrigation project of "Cova da Beira" (Pereira et al., 2004). The dominant grass species consisted of *Vulpia spp* (subset of fescue genus), genera *Lolium* (ryegrass), *Chamaemelum spp* (chamomiles genus), *bromus spp* (brome genus) (Carneiro et al., 2005). In SP, a study site was chosen to represent a semi-natural grassland type subject to sheep grazing or cutting for hay production. The local grassland was dominated by cool season C3 grass species and drought tolerant perennial C4 grass, including *Vulpia bromoides* and *geniculate* (subsets of fescue genus), *Dactylis glomerata*, *Cynodon dactylon* (Vilfa stellata) (Aires et al., 2008a; Aires et al., 2008b; Serrano et al., 2011).

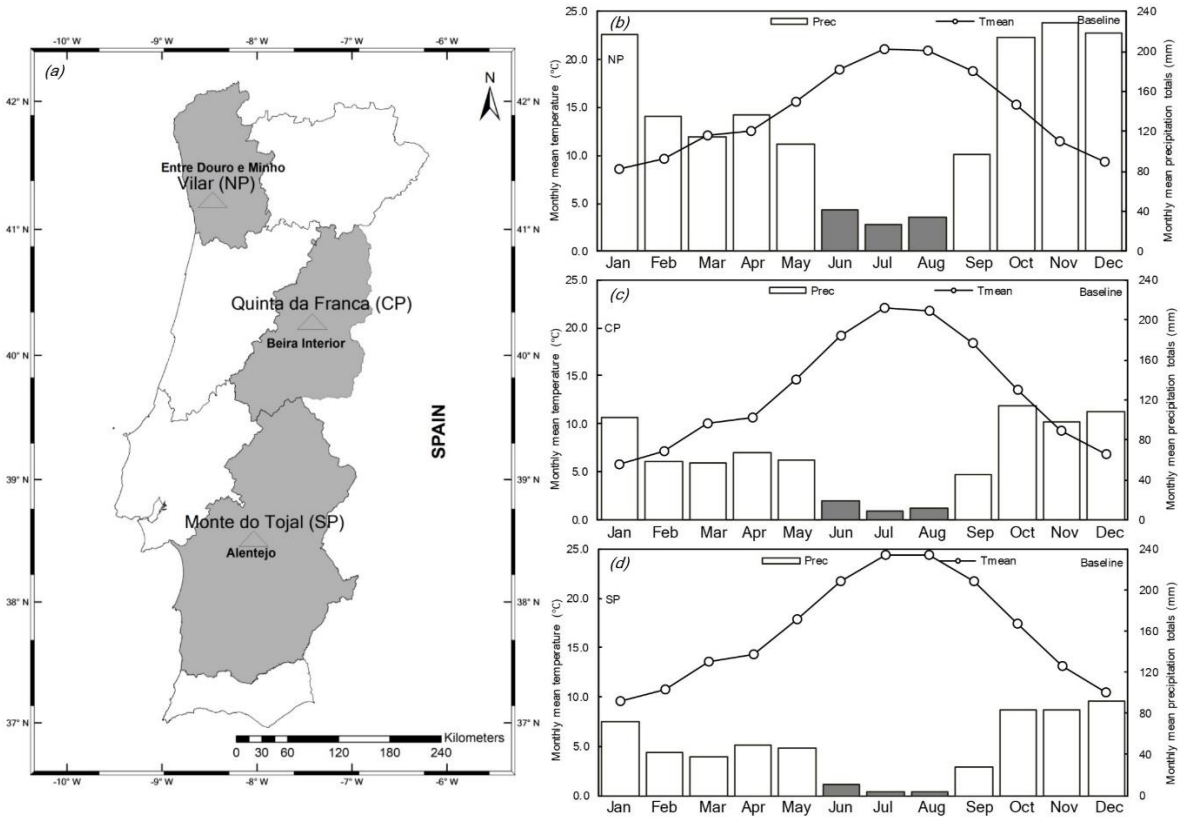

Figure 1 ***(a)*** Indication of three representative study sites of northwestern Portugal (NP), central-inner Portugal (CP), southern Portugal (SP). Monthly mean temperature (T_{mean}) and precipitation sum (P_{rec}) were shown for sites of ***(b)*** NP; ***(c)*** CP; ***(d)*** SP over baseline (1985–2006). Dry season was highlighted with filled bar.

5.2.2 Soil parameters

Information on soil characteristics at each site was mainly obtained from the Harmonized World Soil Database (HWSD), which incorporates the latest updates of soil information worldwide. HWSD provided high-resolution (30 arc-second, ~1 km near equator) soil profile data connected

to each mapping unit, in which chemical-physical properties of topsoil (0-30 cm) and subsoil (30-100 cm) were available (FAO/IIASA/ISRIC/ISSCAS/JRC, 2012). Based on soil profiles, soil hydraulic properties (e.g. water retention capacity) were estimated as a function of soil texture and organic matter, adjusted by the influence of soil structure and salinity level (**Table S1**), which were calculated using soil hydraulic property calculator (Saxton and Rawls, 2006). The soil cumulative evaporation limit, a crucial model parameter for soil evaporation, was calculated as a function of clay or sand content (Brisson et al., 2009) (**Table S1**). Concerning topography, the GTOPO30 digital elevation model, distributed by U.S. Geological Survey, was employed to estimate the surface slope degree, essential for the calculation of surface runoff parameters in STICS (Brisson et al., 2009) (**Table S1**).

5.2.3 Climate data

The input daily weather variables consisted of 2 m minimum and maximum air temperatures (ºC), solar radiation (MJ m^{-2} day^{-1}), precipitation (mm), wind speed (m s^{-1}), water vapour pressure (hPa), potential evapotranspiration (PET, mm) and atmospheric CO_2 concentration (ppmv). Simulations were performed for the baseline period (1985–2006) and for three future periods (short-term: 2021–2040; medium-term: 2041–2060; long-term: 2061–2080). For the baseline, temperatures and precipitation were obtained from the daily observational gridded dataset E-OBS (Haylock et al., 2008), while solar radiation, wind speed and water vapour pressure were obtained from the evaluation run of SMHI- RCA4 (RCM), developed by the Rossby Centre at the Swedish Meteorological and Hydrological Institute (Strandberg et al., 2015). The evaluation run was forced by ERA-Interim, a high-resolution daily observational gridded dataset of global atmosphere reanalysis (Dee et al., 2011). PET calculation was based on the Penman method (Penman, 1948). Atmospheric CO_2 concentration was retrieved from the National Oceanic and Atmospheric Administration (NOAA) global records (https://www.esrl.noaa.gov/gmd/ccgg/trends/global.html, **Table S2**).

Regarding climate change projections (**Table S2)**, SMHI-RCA4 was driven by MPI-ESM-LR (GCM) and retrieved from EURO-CORDEX (Jacob et al., 2014). The projections under RCP8.5 were used herein, tending to incorporate the most noticeable climate change signal (van Vuuren et al., 2011). This scenario projected a continuous rise in atmospheric CO_2 concentration until the end of 21st century (**Table S2)**. Furthermore, the projected daily climate data was subjected to bias

corrections, i.e. differences (ratios) between observed and simulated monthly mean temperatures (precipitation, net solar radiation, wind speed and water vapour pressure) were calculated over baseline and applied as additive (multiplicative) correction factors to the full future period (2021–2080).

5.2.4 Historical characteristics of climate

Air temperatures and precipitation in the three study sites were shown for baseline **(Fig. 1b–d)**. All sites showed typical Mediterranean climate features. NP presented a rainy and mild climate, CP showed relatively cool climate with intermediate precipitation level, and SP had the lowest precipitation with the highest temperatures. Monthly mean temperature varied from around 8ºC, 6ºC and 9ºC, in January (coldest month), to 21ºC, 22ºC and 25 ºC, in July (warmest month), for NP, CP, SP, respectively **(Fig. 1b–d)**. Annual mean temperatures were of 14.5ºC, 13.3ºC and 16.6ºC for NP, CP, SP, respectively **(Fig. 1b–d)**. Precipitation generally concentrated in autumn, winter and spring (September–April), with around 1500 in NP, 710 in CP and 540 mm in SP **(Fig. 1b–d)**. In contrast, summertime (June to August) precipitation were of 100, 40 and 20 mm for NP, CP, SP, respectively **(Fig. 1b–d)**.

5.2.5 Application of STICS to grassland

STICS can run at field, regional and national scales, with inputs from weather variables, soil characteristics and farming practices running at a daily time-step (Brisson et al., 2009). A brief description of the general model scheme was presented herein. More details were available in Brisson et al. (2003) and Brisson et al. (2009). Phenological development rate was calculated as a function of thermal accumulation (i.e. growing degree days – GDD). Note that the temperature thresholds that were used to define the thermal stress effect on plants varied among different processes: phenology, leaf growth and dry matter growth. In addition to water and nutritional stresses, the development rate may be slowed by non-compliance with vernalization requirement or sub-optimal photoperiodic effect. Subsequent phenology-driven leaf area growth determined photosynthetic active radiation, which was directly transformed into above-ground biomass, following a light utilization efficiency approach. In the model, plant roots acted as water and mineral N absorber, according to the growth dynamic of root length and efficient density profile. Additionally, soil water and nitrogen uptakes were simultaneously calculated, by comparing the

balance between crop requirements (considering functions of root growth) and soil water and mineral N availability of root zone. The resulting comparison leaded to the simulation of crop water and nitrogen stresses that inhibited canopy expansion, dry matter growth and plant transpiration (water uptake). For plant water requirement, if the modified effects of reduced stomatal conductance and transpiration by rising atmospheric CO_2 level need to be incorporated, the option of resistance approach must be chosen inside the model to directly calculate water demand at plant level (Shuttleworth and Wallace, 1985), instead of choosing the Penman method to calculate PET for STICS.

For grassland, STICS was able to simulate both annual (e.g. ryegrass) and perennial grass species managed by cutting or grazing for forage dry matter production, taking into account irrigation and fertilization practices (Ruget et al., 2009). Note that the current case was a simulation of established perennial grassland without considering the seeding year. At the beginning of each growing cycle, the model was initialized with plant characteristics (leaf area index, dry matter and root depth) and soil moisture status. Over the growing period, dry matter was accumulated as harvestable and the cutting date was determined by a given developmental stage, by pre-defined dates or by thermal accumulation (Ruget et al., 2009). In the present study, the choice of pre-defined cutting date was selected in order to represent locally existed harvest timings. Consequently, the estimation of associated residue dry matter and LAI after cutting was required to start a regrowth cycle. Following established simulation cycles, multi-year variation of growing seasonal outputs could be analysed.

5.2.6 Parameters of grassland systems

Simulations were initialized at the first day of each year to account for active growth after the winter rest period (October to December), in compliance with overall observed growth conditions (Aires et al., 2008a; Carneiro et al., 2005). In addition, parameters linked to initial plant characteristics were defined according to standard literature values (Courault et al., 2010; Ruget et al., 2009) (**Table S3**). Initial soil water content was set at field capacity to represent soil moisture status after winter precipitation, which was common given the Portuguese winter-dominant precipitation.

To reflect local heterogeneous botanic composition and community functions, the plant file (*grass-prairiep*), which characterized average functional attributes (mainly phenology traits) of groups of

species (Ruget et al., 2008), was chosen to represent sward heterogeneity across study sites (**Table S3**). The plant parameters were sufficiently tested and validated using measured features of permanent grassland in France (mainly composed of a mixture of tall fescue and cocksfoot), and integrated into the ISOP system for widespread application (Ruget et al., 2006). To mimic local available practice and avoid potentially extreme water deficit under climate change scenarios (e.g. may cause numerous zero-production years with high uncertainties), the automatic irrigation strategy was assumed by the model equally among sites and periods. Whenever simulated plant water stress for stomatal function reduced actual transpiration to less than 25% of maximum transpiration requirement, corresponding to model parameter of *ratiol*=0.25, an irrigation event was automatically triggered to replenish depleted soil water content to field capacity down to the rooting depth, without exceeding the maximum daily allowable dose of 40 mm. The process attempted to follow the irrigation strategy with restrained water use.

Two prescribed harvest regimes, including specific cutting dates with respective N fertilization rate, were primarily derived from available regional practices (Aires et al., 2008a; Carneiro et al., 2005; Lopes and Reis, 1998; Lourenco and Palma, 2001; Trindade et al., 1997) (**Table S3**). For each site, the main difference between these two regimes was in cutting dates, leading to two grassland systems with contrasting growing season length:

– Early spring cut system (ES): annual dry matter yield was obtained before June (winter and spring seasons), generally with one cut in the mid-season and another cut in the end of spring, thus corresponding to a short growing season aiming to avoid summer stress.

– Late summer cut system (LS): annual dry matter yield was obtained in the end of May and in mid-September (winter, spring and summer seasons), generally with one cut in the end of spring and another one in the end of summer, thus having a long growing season for dry matter accumulation, but with higher senescence rate.

Immediately following autumn rehydration (after second cut in LS), a pre-growth period (October to December) typically occurred, in which the growth rate of adapted C3 species in Portugal was indeed very small, largely owing to the low temperature (Aires et al., 2008a). Active growth for the following cycle mainly occurred in the beginning of next year. Parameters associated with residue dry matter and LAI after cutting were estimated combining field observations with standard literature values (Aires et al., 2008b; Ruget et al., 2009) (**Table S3**).

5.2.7 Simulation setup

After running STICS with the aforementioned input parameters, variations of seasonal cumulative DMY and associated stress conditions were analysed. Specific emphasis was given to the effects of warming and drought stresses on DMY growth, which were expressed as thermal stress index (FTEMP) and water stress index (SWFAC), respectively. FTEMP and SWFAC varied from 0, for extreme stress, to 1, for no stress, directly affecting daily DMY growth rate (Brisson et al., 2009). Additionally, it was important to analyse grassland response to extreme stress events under future climates (Cullen et al., 2012; Dumont et al., 2015; Zwicke et al., 2013).

Thermal stress (FTEMP) was calculated as a function of daily mean crop temperature, with defined optimal temperature range, taking into account extreme thermal thresholds for halting growth progression (FTEMP=0.01: > 25ºC for extreme heat stress and < 0ºC for extreme cold stress) (Brisson et al., 2009). Crop water stress (SWFAC), was calculated as the ratio of root zone soil water content (cm^3 cm^{-3}), relying on a soil water balance approach, to a threshold of soil water requirement (cm^3 cm^{-3}). Such threshold was computed daily, depending on atmospheric evaporative demand, surface cover status (e.g. LAI and soil surface mulch), plant stomatal function and root distribution in the soil profile (Brisson et al., 2009). Since simulations were under irrigation, the occurrence of severe water stress was defined at the instant when irrigation was needed, for which the effect of severe water stress (0.25) was weaker than that of extreme thermal stress.

5.2.8 Statistical analysis

Student's t-test was applied for assessing the significance of differences in mean between baseline and each future period, as well as for assessing significance of correlation coefficients. The F-test was applied for the significance of linear trends.

5.3 Results

5.3.1 Climate change projections

Regarding climate change projections, a progressive and very significant increase of mean annual temperature up to 2.3, 2.8 and 2.7ºC until 2061–2080, were projected for NP, CP and SP, respectively **(Table S4)**. With respect to mean annual precipitation in comparison to baseline period, NP presented a variable precipitation regime, while a sharp decrease with significant

reductions occurred for CP and SP during 2021–2040, followed by an increase (CP) or a continuous decrease (SP) in 2041–2060, before further significant reductions of 17–20% for both sites over 2061–2080 **(Table S4)**. The inter-annual variability of annual precipitation, expressed as coefficient of variation (CV), ranged from 21% to 28% for NP, 23% to 28% for CP, and 26% to 30% for SP throughout all periods. CV of mean annual temperature generally varied from 3% to 5%.

5.3.2 Dry matter yield in baseline period (1985–2006)

The simulated cumulative seasonal DMY showed differences among the three sites for baseline. For NP, DMY ranged from 7000 to 9500 kg ha^{-1} (mean of 8505 kg ha^{-1}) for ES, while it varied from 8800 to 11300 kg ha^{-1} (mean of 10037 kg ha^{-1}) for LS **(Fig. 2)**. For CP, DMY varied from 4500 to 6900 kg ha^{-1} (mean of 6097 kg ha^{-1}) for ES, while it ranged from 8000 to 9300 kg ha^{-1} (mean of 8539 kg ha^{-1}) for LS **(Fig. 2)**. Lastly, for SP, DMY varied from 5500 to 6300 kg ha^{-1} (mean of 5888 kg ha^{-1}) for ES and from 6000 to 8000 kg ha^{-1} (mean of 7021 kg ha^{-1}) for LS **(Fig. 2)**. Overall, LS consistently exhibited higher DMY than ES across study sites in baseline, owing to the longer growing season and adequate irrigation.

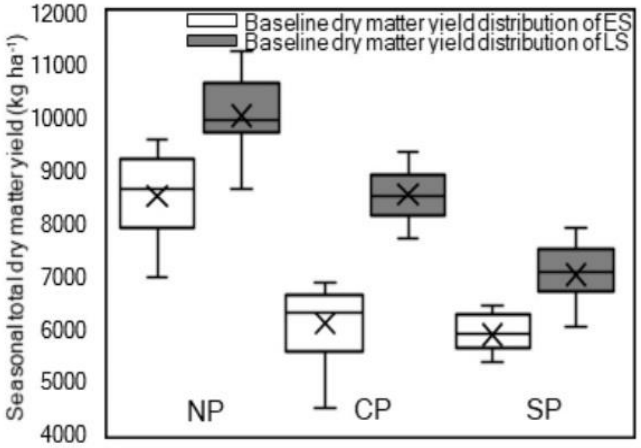

Figure 2 Box-plot analysis for simulated seasonal cumulative DMY of two grassland systems for three study sites (NP, CP, SP) over baseline (1985–2006). Minimum, 25th percentile, 50th percentile, 75th percentile and maximum values were respectively shown (horizon lines from bottom to top) in the box with indicated average mark (symbol of X). ES: early spring cut system; LS: late summer cut system.

5.3.3 Climate change impacts on dry matter yield

Apart from directly presenting changes in the mean (right panels), simulated seasonal total DMY for 2021–2080 under RCP8.5 was firstly shown in 11-year moving average series (smoothed curve) (left panels) to filter out high frequent inter-annual variability, thus emphasizing the inter-decadal variability **(Fig. 3)**. In NP, no statistically significant trend was projected for ES regime, whereas a significant downward trend (–190 kg ha^{-1} $decade^{-1}$**)** was found for LS regime **(Fig. 3a)**. Mean seasonal DMY for ES fluctuated between 8243 and 8852 kg ha^{-1} throughout baseline and future periods, without significant changes, and inter-annual variability (CV) was maintained at around 9% (**Fig. 3b)**. In contrast, mean DMY of LS showed continuous and significant reductions of 506 (–5%), 1233 (–12%) and 1325 kg ha^{-1} (–13%) over successive periods, in relative to baseline **(Fig. 3b)**. The CV increased from 8% in baseline to 10% during 2061–2080.

In CP, a significant upward trend of seasonal DMY at 110 kg ha^{-1} $decade^{-1}$ was projected for ES until 2080, whereas a significant declining trend at –330 kg ha^{-1} $decade^{-1}$ was found in LS **(Fig. 3c)**. Mean DMY of ES maintained within the 5926–6406 kg ha^{-1} range, without significant changes throughout the periods, while CV was stable at 10% **(Fig. 3d)**. Compared to baseline, mean DMY of LS showed progressive and significant decrease by 1165 (–14%), 1542 (–18%) and 2447 kg ha^{-1} (–29%) over successive periods **(Fig. 3d)**. CV increased from 5% in baseline to 14% in 2061–2080.

In SP, a weak rising trend was projected for ES, while a significant downward trend (–240 kg ha^{-1} $decade^{-1}$) was projected for LS (**Fig. 3e)**. For ES, no significant changes were also identified for mean DMY over successive future periods, through which CV remained at about 7% **(Fig. 3f)**. For LS, mean DMY displayed gradual and significant reductions of 1322 (–19%), 1590 (–23%) and 2188 kg ha^{-1} (–31%) for successive periods **(Fig. 3f)**. The CV increased from 9% in baseline to 16% in 2061–2080.

Projected mean seasonal DMY under ES was essentially maintained, whereas progressive reductions were obtained under LS, with a remarkable effect during 2061–2080. Therefore, the yield gap of ES regime from that of LS was gradually diminished, for which higher productivity of ES was projected in SP until 2061–2080 **(Fig. 3f)**.

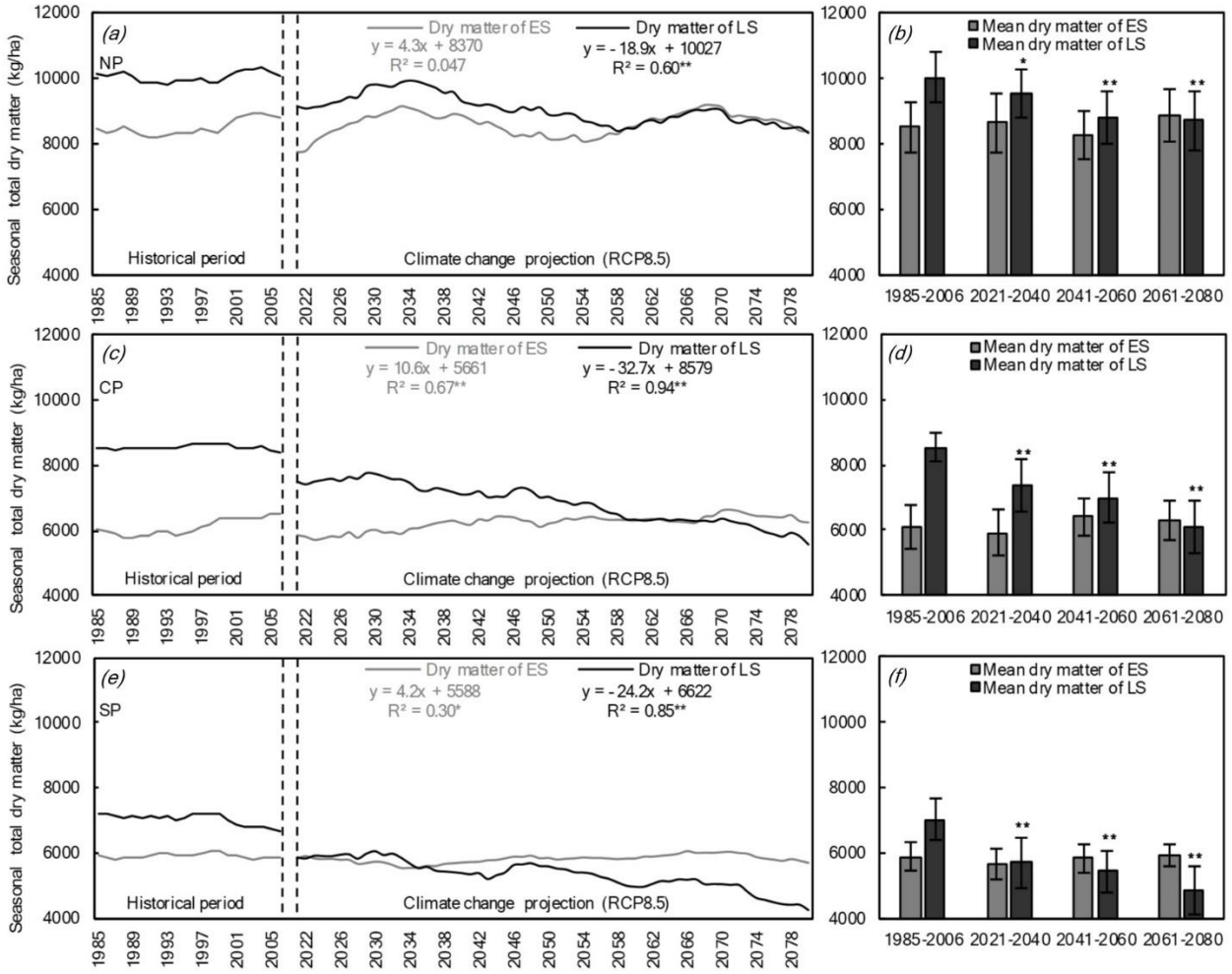

Figure 3 Projection of seasonal cumulative DMY for two grassland systems in (***a,b***) NP, (***c,d***) CP, (***e,f***) SP. Left panels: 11-year moving average of DMY series with Fisher´s test on significance of linearity for trend analysis. Right panels: mean and standard deviation for successive study periods, with independent sample *t*-test performed between baseline and each future period means. Significance levels at p<0.05 (*) and p<0.01 (**) were labelled, respectively.

5.3.4 Variations of seasonal water use from baseline to future climate

No statistically significant difference was discovered for winter-spring (ES) precipitation between baseline and each future period, featuring an overall high inter-annual variability **(Fig. S1a–c)**. However, significantly increased seasonal irrigation requirement by 32% was projected for ES in SP during 2061–2080 **(Fig. S1f)**. For LS (winter + spring + summer), seasonal precipitation was projected to decrease significantly in NP (–19%) and in SP (–19%) **(Fig. S1a, c)**. As a result, seasonal irrigation of LS was projected to increase significantly by 6–30% during 2061–2080 among sites **(Fig. S1d–f)**. Over 2061–2080, significant increases were consistently projected in seasonal cumulative PET among sites, i.e. 30–57 mm increase in ES and 102–149 mm in LS **(Fig. S1g–i)**. Consequently, small but significant increases by 3%–9% for actual ET were projected

among sites and regimes over 2061–2080 **(Fig. S1j–l**). The ratio of actual ET to PET, averaged over all the periods, were 0.94, 0.75 and 0.72 for ES in NP, CP and SP, respectively, which were consistently higher than that for LS (0.73, 0.64 and 0.63).

5.3.5 Enhancement of climatic water deficit under LS

Fig. 4 presented the linear regression analysis between seasonal total DMY and cumulative climatic water deficit (Water supply – PET, expressed as positive values) during dry period under LS regime (1st May to 31st August). In comparison to baseline, the mean cumulative water deficit increased significantly by up to 31%, 28% and 28% in 2061–2080 for NP, CP and SP, respectively (**Fig. 4)**. The gradually increased water deficit under climate change, could partially explain the significant DMY reductions of LS, i.e. decrease of 300, 1200, 1300 kg ha^{-1} for every 100 mm increase in dry period water deficit for NP, CP and SP, respectively (**Fig. 4)**.

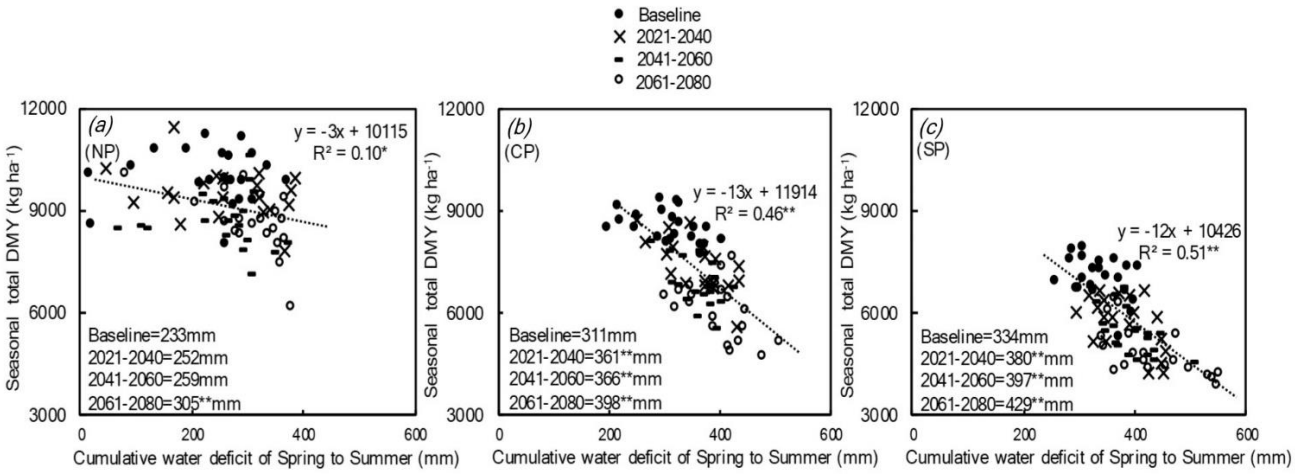

Figure 4 Simulated seasonal total dry matter yield (DMY) as a function of cumulative climatic water deficit (Precipitation + Irrigation – Potential Evapotranspiration) during spring-summer dry period under LS regime for (***a***) NP, (***b***) CP, (***c***) SP. Student´s *t*-test was performed for examining correlation coefficient and for changes in mean water deficits of each future period compared to baseline. Significance levels at $p<0.05$ (*) and $p<0.01$ (**) were labelled, respectively.

5.3.6 Seasonal dynamics between baseline and the long-term period (2061–2080)

For winter and spring seasons under ES, DMY growth rate progressively increased with two cuts imposed. Seasonal average growth rates for baseline were 66, 42 and 46 kg ha^{-1} day^{-1} for NP, CP and SP respectively, which were projected to increase significantly (paired sample *t*-test) by 10%, 7% and 6% for the respective three sites over 2061–2080 **(Fig. 5a**–**c)**. DMY growth rate was

initially inhibited by cold stress (FTEMP), but gradually relieved with subsequent seasonal shift, in which seasonal average FTEMP effects were quantified as negligible for NP (0.89) and SP (0.92), mild (0.80) in CP over baseline **(Fig. 5d**–**f)**. As a result of climate warming, cold stress was alleviated and average FTEMP effects were significantly decreased by 5%, 9% and 2% for NP, CP and SP, respectively, over 2061–2080 **(Fig. 5d**–**f)**. Due to initial maximum soil water reserve, water stress only occurred in the mid of the season, followed by stress variation and intensification until the end of spring, resulting from enhanced soil moisture depletion **(Fig. 5d**–**f)**. In baseline, seasonal average SWFAC effects were negligible for NP (0.97) and CP (0.85) and mild for SP (0.81), which were projected to increase significantly by 4% and 2% for CP and SP respectively over 2061–2080, and remained unchanged for NP **(Fig. 5d**–**f)**. Until the first cut in LS with primarily the same winter-spring season, average DMY growth rate was consistent lower than that of ES, owing to occurrence of senescence that approximately begun since April **(Fig. 5g**–**i)**. However, the overall FTEMP and SWFAC effects for LS were similar to ES among sites and periods, largely due to the shared identical cool and wet seasons, despite different harvest intervals **(Fig. 5d**–**f** and **Fig. 5j**–**l)**.

Consider only summer in LS (between two successive cuts), baseline DMY growth rate in average was 71, 68 and 52 kg ha^{-1} day^{-1} for NP, CP and SP respectively, and was subject to significant decreases by 34%, 53% and 57% with strong day-to-day fluctuations during 2061–2080 **(Fig. 5g**–**i)**. Average summertime FTEMP effect, in the form of heat stress, was clearly more intense in SP (0.64) than in NP (0.89) and CP (0.84) for baseline **(Fig. 5j**–**l)**. Subsequently, during 2061–2080, the significant increases of heat stress by 33%, 52% and 57% for NP, CP and SP respectively, were primarily associated with the markedly decreased growth rate in summer **(Fig. 5j**–**l)**. Due to irrigation, average SWFAC effects over summer were generally moderate (~0.6) among sites during baseline **(Fig. 5j**–**l)**. The reduced summertime DMY rate could be also explained by significantly increased SWFAC, i.e. 11%, 11% and 9% during 2061–2080 for NP, CP and SP, respectively **(Fig. 5j**–**l)**.

Moreover, the influence of the inter-annual variability of daily FTEMP and SWFAC in baseline and for 2061–2080 on daily DMY growth was also analysed by calculating the correlation coefficient (r) between seasonal anomalies (deviation from period mean) of two stress indices and anomalies of DMY growth rate for individual years in both periods **(Fig. 6)**. Accordingly, a greater

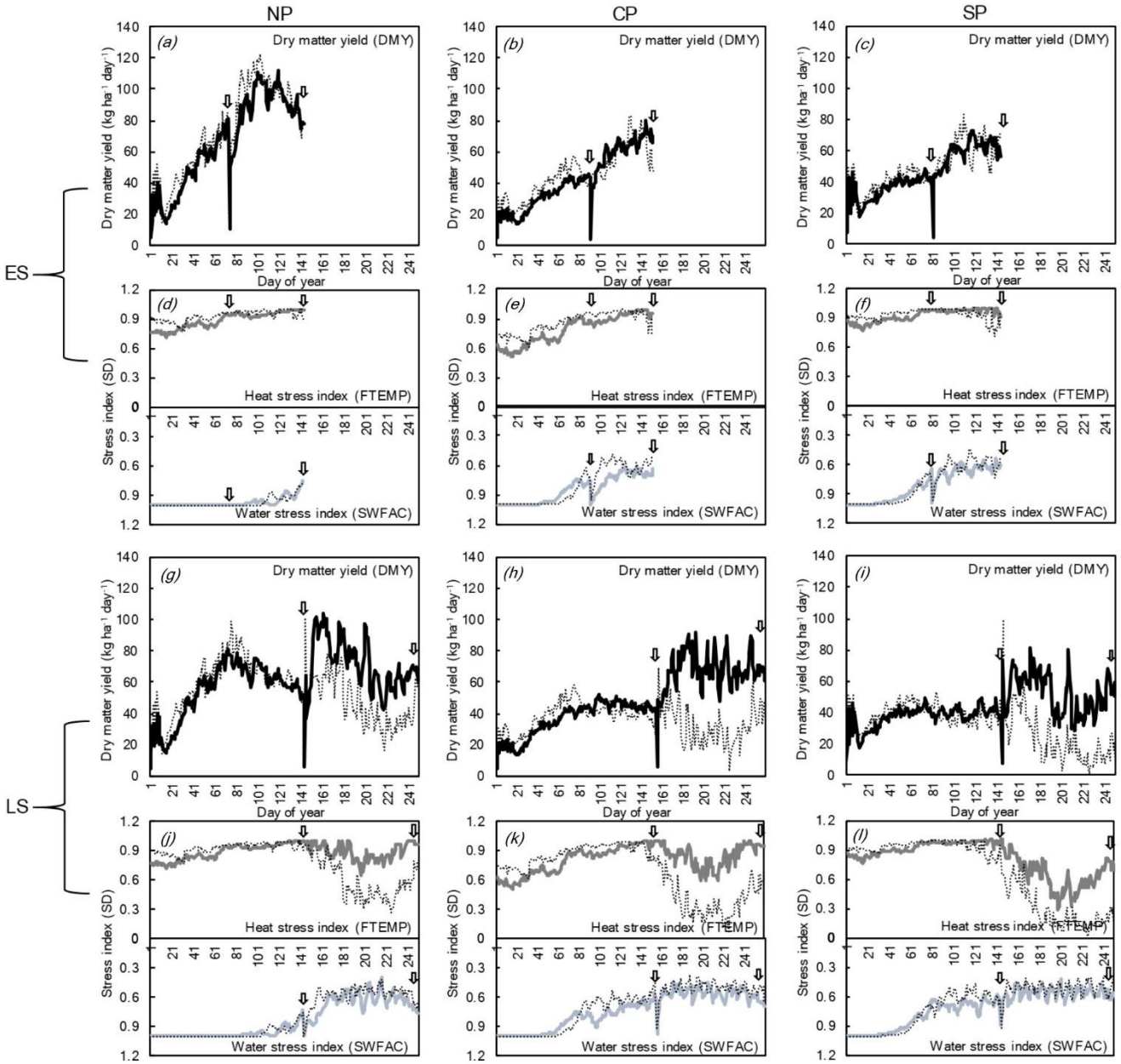

Figure 5 Illustration of seasonal dynamics of daily mean thermal (FTEMP) and water stress (SWFAC) indices along with daily mean DMY in baseline (solid line) and long-term period of 2061–2080 (dash line) for ***(a–f)*** ES and ***(g–l)*** LS regime among study sites. Cutting dates were indicated by arrow symbols.

positive *r* indicated that anomalously lower/higher stress value (stronger/weaker stress effect) was correlated to lower/higher seasonal DMY, and vice-versa. For ES, DMY growth tended to be less responsive to variations of FTEMP during baseline, but consistently subject to stronger effects of inter-annual variability of SWFAC, despite the large uncertainty in NP **(Fig. 6a–c)**. During 2061–

2080, DMY growth rate of ES revealed a similar response, except for SP where magnitude of response to FTEMP became stronger **(Fig. 6d**–**f)**. In contrast, seasonal DMY growth rate under LS was clearly governed by variations of both FTEMP and SWFAC during baseline **(Fig. 6a**–**c)**. During 2061–2080, seasonal DMY rate of LS shifted to be less responsive to variability of SWFAC, but consistently dominated by the factor of FTEMP **(Fig. 6d**–**f).**

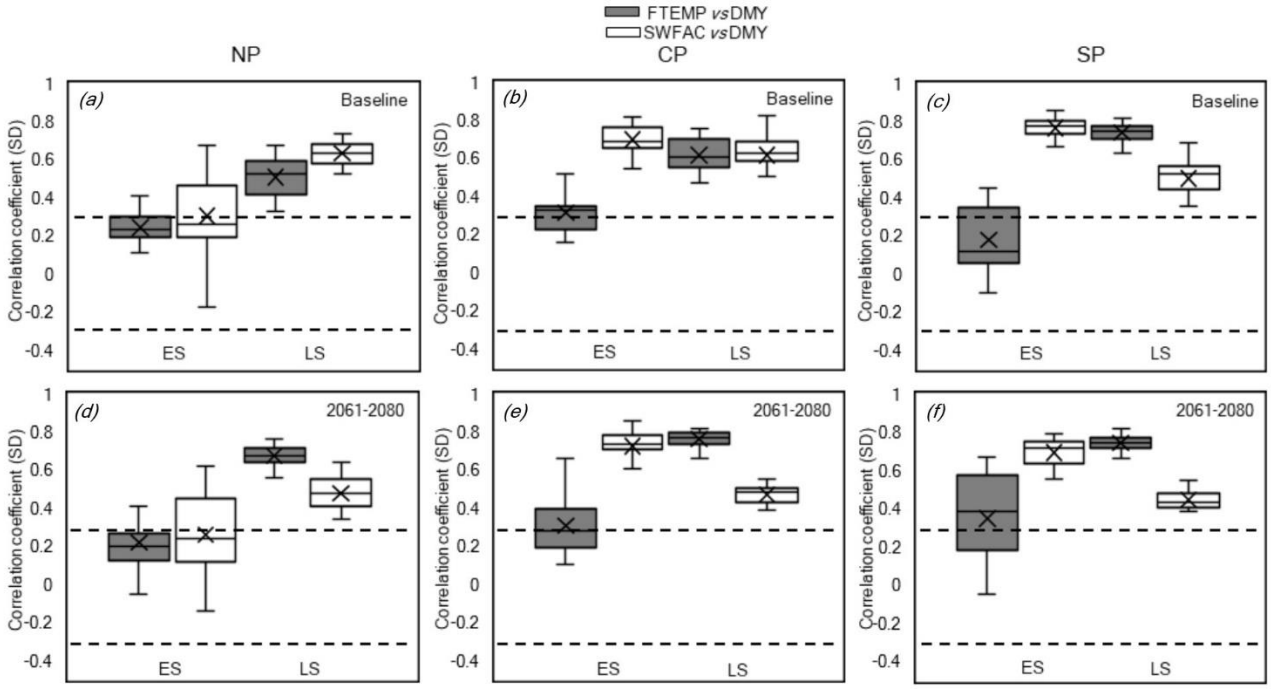

Figure 6 Statistical distribution of correlation coefficients between seasonal anomalies of daily dry matter yield (DMY) and anomalies of daily thermal (FTEMP) or water stress (SWFAC) indices for the ***(a–c)*** baseline and ***(d–f)*** long-term period of 2061–2080. Statistically significant correlations were highlighted outside the ±0.3 dashed lines.

5.3.7 Extreme thermal stress and severe water stress

For winter and spring seasons, extreme FTEMP in the form of winter cold stress seemed unlikely to occur for NP and SP, but emerged for CP (mountainous terrain) over short time and low frequency (no greater than 14%) (**Fig. 7a**–**c)**. Extreme heat stress generally occurred between April and May with low frequency level for all sites (no greater than 25%) (**Fig. 7a**–**c)**.

For summer season under LS regime, continuously increasing frequency of occurrence of extreme FTEMP in the form of heat stress over successive periods, accompanied by gradually prolonged seasonal duration, were consistently found for all sites (**Fig. 7d**–**f)**. Extreme heat stress generally occurred at low frequency below 30% in NP and CP for baseline (**Fig. 7d, e)**. Seasonal frequency

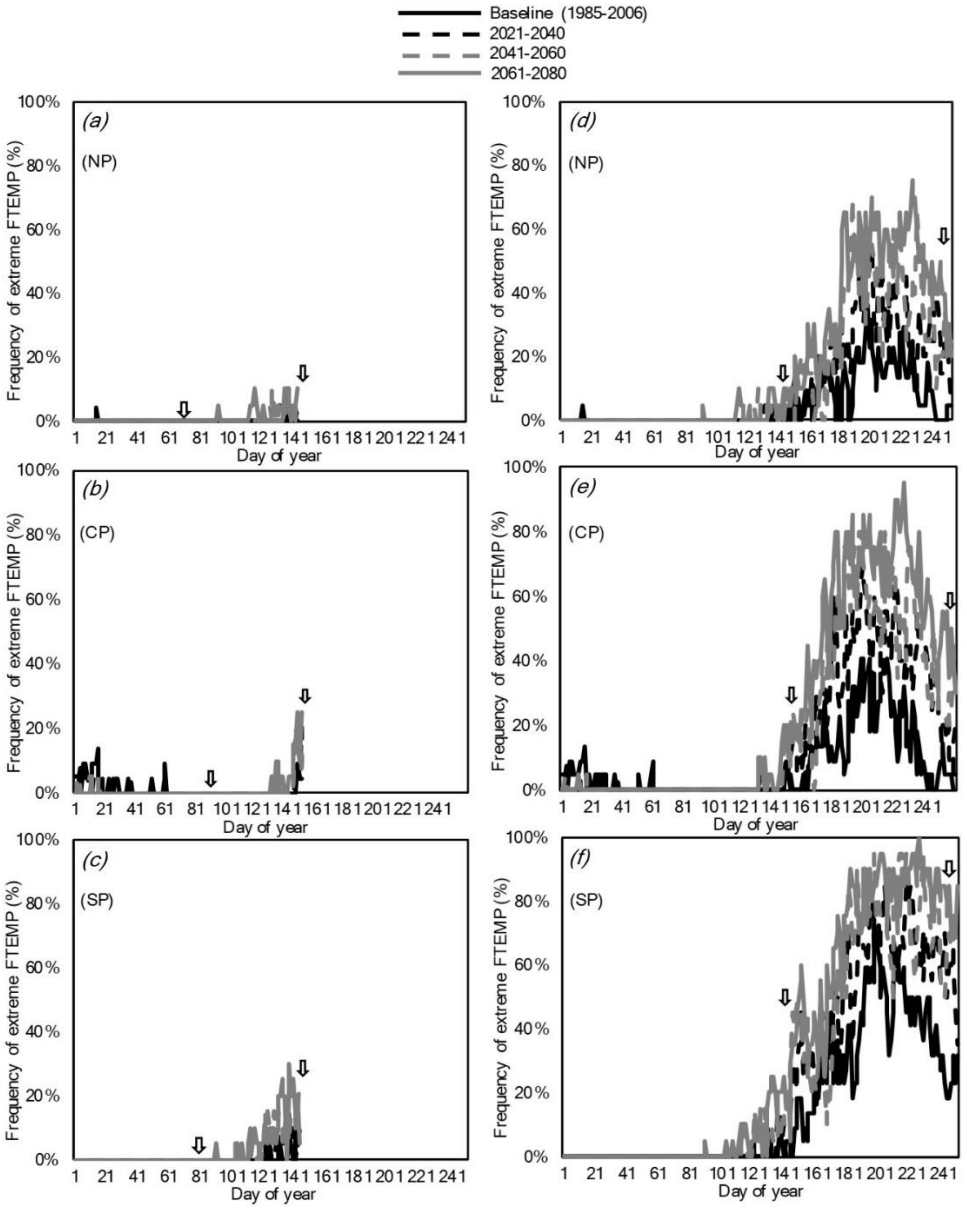

Figure 7 Daily frequency of occurrence of extreme thermal stress (FTEMP) over successive periods across study sites for ***(a–c)*** early spring (ES) and ***(d–f)*** late summer (LS) cut grassland systems. Cutting dates were indicated by arrow symbols.

level was the highest in SP, with majority of summer already subject to probability of extreme heat stress between 30% and 60% in baseline (**Fig. 7f)**. In contrast, extreme heat stress with high seasonal frequency of occurrence above 50% were consistently found for all sites during 2061–2080 (**Fig. 7d**–**f)**. Moreover, the number of days with high probability or frequency of occurrence (above 50%) for extreme temperatures also continuously increased from baseline to the 2061–2080 (**Fig. 7d**–**f** and **Table S5)**. The projected extension of days in summer that were subject to

high probability of extreme heat stress was greater in SP than the other two sites, with the most significant increase of 48 days during 2021–2040 (**Table S5)**. In 2061–2080, these days were projected to cover most of the summer period in CP and SP (**Table S5)**.

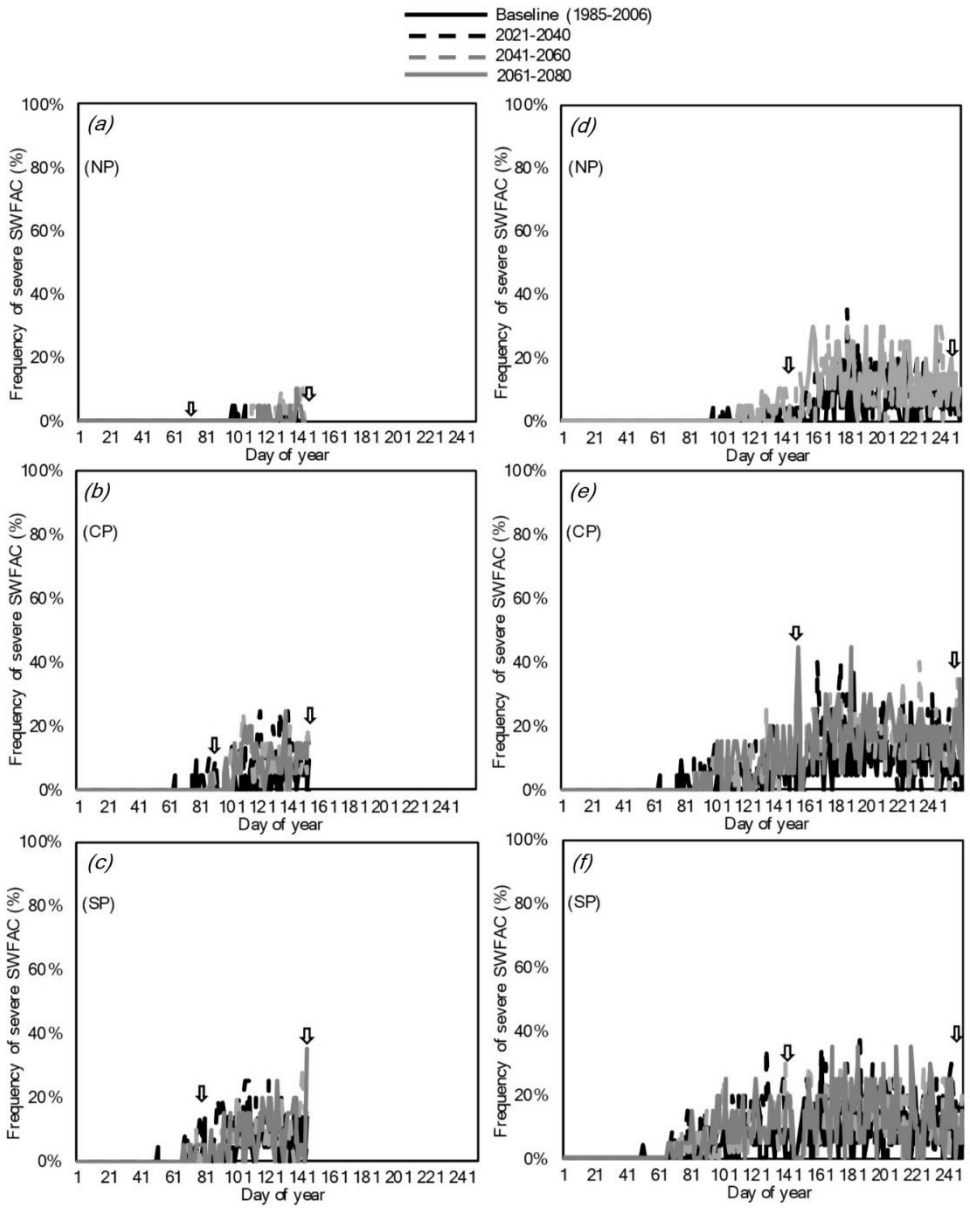

Figure 8 Daily frequency of occurrence of severe water stress (SWFAC) over successive periods across study sites for ***(a–c)*** early spring (ES) and ***(d–f)*** late summer (LS) cut grassland systems. Cutting dates were indicated by arrow symbols.

Concerning the defined extent of severe SWFAC (the day required for irrigation), NP presented negligible seasonal distribution with daily frequency well below 10% throughout each period for

the winter and spring seasons (**Fig. 8a**). Both CP and SP showed moderate stress conditions, in which daily frequency of occurrence of severe SWFAC throughout the growing season generally varied from 5% to 25% without significant changes from baseline to 2061–2080 period (**Fig. 8b, c**). Likewise, severe water stress also tended to occur more often in the summer under LS regime than winter and spring seasons under ES regime (**Fig. 8d–f**). Severe SWFAC mainly occurred at low frequency level (10% to 30%) in baseline, for all sites, without increase over successive periods in summer (**Fig. 8d–f**). This showed that severe water stress was clearly less intense than projected extreme heat stress, in terms of frequency. Nonetheless, an extension of summer days with severe water stress (low probability between 10% and 30%) was still projected (**Table S6**). The number of days markedly increased from baseline to 2021–2040 period over all sites, and stabilizes thereafter until 2061–2080 (**Table S6**).

5.4 Discussion

5.4.1 Examination of DMY simulation and projection

For baseline, higher mean seasonal DMY was simulated in NP, followed by intermediate values in CP and lower values in SP. In NP, higher DMY was a direct response to the exceptionally high N fertilization level used for intensive dairy farming and to the relatively high regional precipitation amount. The documented irrigated forage yield varied from 7500 to 10400 kg ha^{-1} (Trindade et al., 1997), roughly in agreement with the simulated range from 7000 to 11300 kg ha^{-1} **(Fig. 2)**. With respect to CP, the simulated range (4500 to 9300 kg ha^{-1}) **(Fig. 2)** were also in agreement with previous studies (5500 to 9000 kg ha^{-1}) (Carneiro et al., 2005). In SP, a direct comparison between observed and simulated seasonal DMY was not available, as the forage DMY was only obtained under rainfed conditions, being 1570 kg ha^{-1} in a dry year and 5120 kg ha^{-1} in a normal year (Aires et al., 2008a; Aires et al., 2008b). However, our simulated irrigated forage DMY varied from 5500 to 8000 kg ha^{-1} **(Fig. 2)**, showing a reasonable performance relative to rainfed condition. Therefore, the present study simulations were considered to roughly represent local grassland growth and herbage yield. A comprehensive analysis between observed and simulated data required more field data, which were not currently available.

The winter-spring ES regime was projected to have a long-term increasing trend of seasonal DMY for CP and SP, though the mean DMY remained largely unchanged until 2061-2080 relative to

baseline (**Fig. 3c-f)**. Conversely, consistent and significant reductions of mean seasonal DMY were projected in LS extended with summer season, mostly during 2061–2080 **(Fig. 3b, d, f)**. The results were in close agreement with a similar study using STICS throughout France, which concluded that grassland winter production was consistently enhanced under projected future climate, while it decreased in summer (Ruget et al., 2010). Likewise, another modelling study, using a pasture system model under the Mediterranean-type climatic region of Australia, projected an increased biomass growth rate in winter and spring, in spite of a reduction on annual pasture production by up to 18% until 2070 (Cullen et al., 2009). Moreover, a simulation study conducted for a range of agro-climatic conditions in New Zealand, using a different grassland model, explicitly highlighted the contrasted response to the overall effects of climate change between growing seasons, i.e. increased biomass production in winter and decrease in summer (Keller et al., 2014). However, it should be noted that in the present study local standard practises were maintained in time, such as cutting dates for forage conservation. Such fixed management encompassed important uncertainties, since other possible adaptation measures, e.g. taken by local farmers, were not considered in the present modelling approach.

5.4.2 Resilience of winter-spring season to climate change

Both regimes had the same seasonal length of winter and spring periods. The designed cool and wet seasons for ES benefited from low atmospheric evaporative demand, for which mean seasonal precipitation was largely adequate to meet the demand, with very little irrigation, particularly in NP **(Fig. S1a–i)**. The simulations of overall stress conditions for ES regime in baseline **(Fig. 5d–f)** reproduced the general recognition that forage growth of Mediterranean grassland during the winter-spring season, was mainly determined by temperature and, to a lower extent, limited by cold stress, when water supply was generally optimal (Lelièvre et al., 2010; Lelièvre et al., 2011; Lelievre and Volaire, 2009). Additionally, seasonal DMY growth rate in ES with two cuts were consistently higher than that in LS with one cut over the same winter-spring season **(Fig. 5a–c** and **Fig. 5g–i)**. This may imply that early cut grassland for a quick re-establishment and regrowth, could be more preferable to a single late cut with which cumulative herbage yield was influenced by slowed growth rate late in the season (Belesky and Fedders, 1995; Oomes and Mooi, 1981).

For the study sites during the long-term period of 2061–2080, beneficial effects of less cold stress by 2–9%, together with atmospheric CO_2 enrichment, were expected to overcompensate the

negative effect of increased mean water stress up to 4% **(Fig. 5d–f)**. Climate warming favoured biomass production during cool and wet periods by lowering cold stress, as well as by stimulating N mineralization with high soil N availability (Dumont et al., 2015; Wu et al., 2011). The enhanced production response by CO_2 fertilization was calculated as a function of the exponential increase of atmospheric CO_2 concentration, based on the relationship proposed by Stockle et al. (1992). Besides, only marginally increased water stress for ES mainly attributed to the lack of a significant difference of mean winter-spring precipitation between baseline and the future period **(Fig. S1a–c)**. However, even relatively small and short-term alterations to rainfall distribution can reduce productivity of grassland (Walter et al., 2012), hence highlighting the importance of significantly increased irrigation in SP to maintain the production **(Fig. S1f)**. In effect, mean seasonal DMY growth rate of ES significantly increased by 6–10% **(Fig. 5a–c)**. A review study concluded climate warming and CO_2 fertilization effects could contribute to 10–25% increase in DMY production during winter and spring (Lee et al., 2013). Our findings also revealed that seasonal DMY growth over winter-spring season tended to be consistently more sensitive to the inter-annual variability of water stress effect than that of thermal stress effect, despite a larger uncertainty range in NP was identified **(Fig. 6a–f)**. Mediterranean climate featured strong inter-annual variability of precipitation amount and distribution, which had direct impact on soil moisture and plant water stress and had been interpreted as the primary forcing factor to grassland´s forage production variation (Cullen et al., 2009; McKeon et al., 2009; Walter et al., 2012). Moreover, winter-spring season was projected to experience low frequent extreme thermal (cold and heat) stress with short seasonal span (**Fig. 7a–c)**, together with low risk of exposure to severe water stress (**Fig. 8a–c)**, which highlighted additional advantages of the ES regime as a potentially suitable adaptation measure.

5.4.3 Summer water deficits and stress

The warm and dry summer in Portugal, with very high evaporative demand and scarce precipitation, required frequent and high amounts of irrigation (**Fig. S1a–i**) to alleviate the impact of climatic water deficit on LS regime. The accumulated water deficit during this dry period was previously shown to have a great negative impact on persistence and productivity of perennial forage species (Poirier et al., 2012). The calculated water deficits (**Fig. 4)** were less intense than the experimentally established water deficit (436–707 mm) at a Mediterranean site (Poirier et al.,

2012), as comparatively more irrigation was applied in our simulation. On the other hand, the water deficits were generally lower (particularly in NP) than the identified critical threshold of 450 mm, below which autumn tiller survival rate was little affected (80%–100%) (Poirier et al., 2012), which may avoid the risk of significant tiller mortality in the present study. Provided under rainfed conditions, drought impact was more pronounced in summer, for which adaptive traits shifted to ensure tiller survival rate without active growth before autumn rehydration (Lelievre et al., 2011; Lelievre and Volaire, 2009). Substantial summertime DMY production under LS were thus expected in baseline with weak to moderate intensities of drought and heat stresses (**Fig. 5g–l).**

For Portugal, projections pointed to a decrease in summer precipitation, resulting in a continuously enhanced water deficit and summer aridity (Santos et al., 2016). This was clearly reflected by aggravated climatic water deficit during the dry period with LS (increased by up to 30% until 2061–2080), in which SP presented moderate to severe drought conditions even with irrigation (337 to 547 mm, average of 429 mm) (**Fig. 4c)**. Significantly increased seasonal irrigation by 6–30% (**Fig. S1d–f)** was projected to cope with overall enhanced summer dryness, in agreement with projected increase of irrigation for permanent pasture by 11–19% in Guadiana River basin (encompassing CP and SP) until 2041-2070 (Valverde et al., 2015). Nonetheless, it was still not enough to counterbalance the impacts, as mean summertime water stress still increased by 9–11% **(Fig. 5j–l)**. The enhanced climatic water deficit, and the resulting increased summer water stress among sites, should partially explain the significant decrease in DMY of LS during 2061–2080. Besides, the projected increase of irrigation requirements is likely to be constrained by low local water availability, driven by higher temperatures and lower precipitation in future climates (Mourato et al., 2015), as well as by growing economic competitions for water allocation to industry and domestic use (Wimmer et al., 2015). Should this occur, irrigated pastures may become less profitable, as production costs significantly increase with soaring water prices and with higher investment needs for better on-farm water management practices and facilities (Turral et al., 2011). Consequently, this may determine important land use changes through a conversion of irrigated grassland areas into more economically viable crops, e.g. bioenergy crops (Gomez-Casanovasa et al., 2018; Rounsevell et al., 2005).

Further analysis revealed that no significant increases in the frequency of occurrence of severe water stress were projected (severe water stress was defined at the day that irrigation was required). Although irrigation was triggered more frequently throughout the drier growing season in the

future period, it was distributed randomly, leading to an overall similar frequency for a 20-year period **(Fig. 8d–f)**, which also occurred in our previous study using STICS (Yang et al., 2017). Besides, an extension of the severe water stress period was still found in summer **(Fig. 8d–f)**. This extension might be associated with earlier onset of spring growth in the future climate with earlier occurrence of soil moisture depletion. Shift in phenology of grass growth under future climate had been pointed out by multiple studies (Chang et al., 2017; Cullen et al., 2009; Ruget et al., 2010). Consequently, forage grass growth was predominantly governed by water consumption, for which the actual ET/PET ratio was highly and linearly correlated to actual/potential DMY ratio (Lelievre and Volaire, 2009). Actual ET/PET ratio was constantly higher in ES than in LS for the study sites and periods, suggesting the overall seasonal DMY production was less optimal in LS than in ES.

5.4.4 Vulnerability of summer season to heat stress

In baseline, under LS, heat stress during the summer was more emphasized in SP **(Fig. 5l),** in which DMY growth rate was strongly governed by year-to-year changes of heat stress **(Fig. 6c)**. A meta-analysis study based on numerous climate manipulation experiments confirmed the generally positive sensitivity of aboveground biomass to warming effect in herbaceous ecosystems (Wu et al., 2011). During 2061–2080, summer heat stress was significantly increased by 33–57% across sites **(Fig. 5j–l)**, resulting from occurrence of many days with canopy temperature higher than the critical upper threshold (25 ºC). This largely leaded to markedly decreased growth rate by 34–57% **(Fig. 5g–i)**, which appeared to be the main reason for the significant reductions of DMY under LS **(Fig. 3a–f)**. Seasonal DMY growth of LS became more vulnerable to heat stress than water stress variations in 2061–2080 **(Fig. 6d–f)**, which should be related to increased frequency of extreme heat stress with extended time span **(Fig. 7d–f)**. Projected summer warming was largest for the broad Mediterranean area, with enhanced inter-annual variability, leading to more frequent temperature extremes (Giorgi and Lionello, 2008; Kjellstrom et al., 2007; Strandberg et al., 2015). Heat stress was expected to play a more important role than water stress with prescribed irrigation strategy, in terms of both frequency of extremes and seasonal span **(Fig. 7d–f) (Fig. 8d–f)**, thus being the main limiting factor for halting growth progression in summer. The upper temperature threshold of plant functional range used herein was 25ºC, above which extreme heat stress occurred and instantly stopped growth progression. Lee et al. (2013) referred that photosynthesis rate in C3 plants generally rose from 5 ºC to 25ºC, beyond which activity of photosynthesis enzyme

rapidly declined with severe function losses. In SP, where temperature already approached the upper limit conditions in summer of current conditions, our findings showed high temperature extremes were projected to dominate over the whole summer until 2061–2080 **(Fig. 7f)**, which presented an enormous constrain for forage production. Nonetheless, as emphasized by a simulation study (Siebert et al., 2017), surface cooling effect by irrigation should be explicitly considered for reducing heat stress, which was not integrated into current study and may result in its overestimation. On the other hand, given the generally conservative behaviour of the upper temperature threshold for perennial grass growth (Lee et al., 2013; Zaka et al., 2017), the risk of heat stress could still be substantial in the context of particularly accentuated summer warming over the broad Mediterranean area. Therefore, suggested possible adaptation option include selection and breeding efforts for plant traits with increased heat tolerance, which enabled plant to grow under high temperature and rapid recovery following exposure to heat stress (Cullen et al., 2014). For C3 grass species, plant traits with increased rooting depth and greater yield response to increased atmospheric CO_2 concentrations were also shown to be effective adaptation options under projected warmer and drier climates (Cullen et al., 2014).

5.5 Conclusion

Our study aimed at simulating dry matter yield response of early spring (ES) and late summer cutting grassland systems (LS) to projected climate change at three study sites in Portugal. Under historical climate with mild stress conditions, LS, with extended growing season and irrigation requirement, seemed to be more productive and more profitable than ES (balance between production and irrigation water resource). However, the ES option, minimizing exposure to dry and warm summer, was more prone to meet potential dry matter yield with low irrigation demand. Under climate change projections, warmer climate for cool season together with CO_2 fertilization effect were expected to overcompensate slightly increased water stress for ES, leading to significantly increased DMY growth rate. In contrast, continuous and significant productivity reductions were consistently found for LS, due to combined effects of summertime warming and drying. Besides, forage yield of LS was projected to be particularly vulnerable to heat stress variation, which was primarily linked to increased frequencies of high temperature extremes. Extreme heat stress may constitute a substantial threat and may outperform the impacts of severe

water stress, as the latter could be partially controlled under prescribed irrigation strategy. Improved heat tolerance of grass species for Mediterranean grassland deserved further attention and may represent the necessary step towards sustainability and resilience of grassland systems under climate change.

Acknowledgments

This work was supported by European Investment Funds by FEDER/COMPETE/POCI–Operational Competitiveness and Internationalization Programme, POCI-01-0145-FEDER-006958, and by FCT - Portuguese Foundation for Science and Technology, UID/AGR/04033/2013. The authors also acknowledge the FCT scholarship given to Chenyao Yang, PD/BD/113617/2015, under the Doctoral Programme "Agricultural Production Chains – from fork to farm" (PD/00122/2012). The authors would like to thank Dr. Françoise Ruget, whose perspectives and advices shared on STICS-forum greatly help us completing this work.

References

Aires, L.M., Pio, C.A. and Pereira, J.S., 2008a. The effect of drought on energy and water vapour exchange above a mediterranean C3/C4 grassland in Southern Portugal. Agr Forest Meteorol, 148(4): 565-579.

Aires, L.M.I., Pio, C.A. and Pereira, J.S., 2008b. Carbon dioxide exchange above a Mediterranean C3/C4 grassland during two climatologically contrasting years. Global Change Biol, 14(3): 539-555.

Andrade, C., Fraga, H. and Santos, J.A., 2014. Climate change multi-model projections for temperature extremes in Portugal. Atmos Sci Lett, 15(2): 149-156.

Andrade, C., Santos, J.A., Pinto, J.G. and Corte-Real, J., 2011. Large-scale atmospheric dynamics of the wet winter 2009-2010 and its impact on hydrology in Portugal. Clim Res, 46(1): 29-41.

Belesky, D.P. and Fedders, J.M., 1995. Warm-Season Grass Productivity and Growth-Rate as Influenced by Canopy Management. Agron J, 87(1): 42-48.

Brisson, N. et al., 2003. An overview of the crop model STICS. European Journal of Agronomy, 18(3-4): 309-332.

Brisson, N., Launay, M., Mary, B. and Beaudoin, N., 2009. Conceptual basis, formalisations and parameterization of the STICS crop model. Editions Quae, Versailles, France, 297 pp.

Carneiro, J. et al., 2005. Relatório Final do Projecto AGRO 87. Estação Nacional de Melhoramento de Plantas, Universidade de Évora, Instituto Superior de Agronomia, Direcção Regional de Agricultura do Alentejo, Fertiprado, Laboratório Químico Agrícola Rebelo da Silva.

Casella, E., Soussana, J.F. and Loiseau, P., 1996. Long-term effects of CO2 enrichment and temperature increase on a temperate grass sward .1. Productivity and water use. Plant Soil, 182(1): 83-99.

Chang, J. et al., 2017. Future productivity and phenology changes in European grasslands for different warming levels: implications for grassland management and carbon balance. Carbon Balance and Management, 12(1): 11.

Cop, J., Vidrih, M. and Hacin, J., 2009. Influence of cutting regime and fertilizer application on the botanical composition, yield and nutritive value of herbage of wet grasslands in Central Europe. Grass Forage Sci, 64(4): 454-465.

Courault, D. et al., 2010. Combined use of FORMOSAT-2 images with a crop model for biomass and water monitoring of permanent grassland in Mediterranean region. Hydrol Earth Syst Sc, 14(9): 1731-1744.

Cullen, B.R., Eckard, R.J. and Rawnsley, R.P., 2012. Resistance of pasture production to projected climate changes in south-eastern Australia. Crop Pasture Sci, 63(1): 77-86.

Cullen, B.R. et al., 2009. Climate change effects on pasture systems in south-eastern Australia. Crop Pasture Sci, 60(10): 933-942.

Cullen, B.R., Rawnsley, R.P., Eckard, R.J., Christie, K.M. and Bell, M.J., 2014. Use of modelling to identify perennial ryegrass plant traits for future warmer and drier climates. Crop Pasture Sci, 65(8): 758-766.

Dee, D.P. et al., 2011. The ERA-Interim reanalysis: configuration and performance of the data assimilation system. Q J Roy Meteor Soc, 137(656): 553-597.

Dumont, B. et al., 2015. A meta-analysis of climate change effects on forage quality in grasslands: specificities of mountain and Mediterranean areas. Grass Forage Sci, 70(2): 239-254.

FAO/IIASA/ISRIC/ISSCAS/JRC, 2012. Harmonized World Soil Database (version 1.2), FAO, Rome, Italy and IIASA, Laxenburg, Austria.

Fraga, H., García de Cortázar Atauri, I., Malheiro, A.C. and Santos, J.A., 2016. Modelling climate change impacts on viticultural yield, phenology and stress conditions in Europe. Global Change Biol, 22(11): doi:10.1111/gcb.13382.

Giorgi, F. and Lionello, P., 2008. Climate change projections for the Mediterranean region. Global Planet Change, 63(2-3): 90-104.

Gomez-Casanovasa, N., DeLucia, N.J., Hudiburg, T.W., Bernacchi, C.J. and DeLucia, E.H., 2018. Conversion of grazed pastures to energy cane as a biofuel feedstock alters the emission of GHGs from soils in Southeastern United States. Biomass Bioenerg, 108: 312-322.

Haylock, M.R. et al., 2008. A European daily high-resolution gridded data set of surface temperature and precipitation for 1950-2006. J Geophys Res-Atmos, 113(D20).

IPCC, 2013. The physical science basis. Contribution of working group I to the fifth assessment report of the intergovernmental panel on climate change [Stocker, T.F., D. Qin, G.-K. Plattner, M. Tignor, S.K. Allen, J. Boschung, A. Nauels, Y. Xia, V. Bex and P.M.

Midgley (eds.)]. Cambridge University Press, Cambridge, United Kingdom and New York, NY, USA, 1-1535 pp.

Jacob, D. et al., 2014. EURO-CORDEX: new high-resolution climate change projections for European impact research. Regional Environmental Change, 14(2): 563-578.

Jongen, M., Pereira, J.S., Aires, L.M.I. and Pio, C.A., 2011. The effects of drought and timing of precipitation on the inter-annual variation in ecosystem-atmosphere exchange in a Mediterranean grassland. Agr Forest Meteorol, 151(5): 595-606.

Keller, E.D., Baisden, W.T., Timar, L., Mullan, B. and Clark, A., 2014. Grassland production under global change scenarios for New Zealand pastoral agriculture. Geosci. Model Dev., 7(5): 2359-2391.

Kjellstrom, E. et al., 2007. Modelling daily temperature extremes: recent climate and future changes over Europe. Climatic Change, 81: 249-265.

Lee, J.M., Clark, A.J. and Roche, J.R., 2013. Climate-change effects and adaptation options for temperate pasture-based dairy farming systems: a review. Grass Forage Sci, 68(4): 485-503.

Lelièvre, F., Sala, S. and Volaire, F., 2010. Climate change at the temperate-Mediterranean interface in southern France and impacts on grasslands production. Option Méditerranéennes: 187-192.

Lelievre, F., Seddaiu, G., Ledda, L., Porqueddu, C. and Volaire, F., 2011. Water use efficiency and drought survival in Mediterranean perennial forage grasses. Field Crops Research, 121(3): 333-342.

Lelièvre, F., Seddaiu, G., Ledda, L., Porqueddu, C. and Volaire, F., 2011. Water use efficiency and drought survival in Mediterranean perennial forage grasses. Field Crops Research, 121(3): 333-342.

Lelievre, F. and Volaire, F., 2009. Current and Potential Development of Perennial Grasses in Rainfed Mediterranean Farming Systems. Crop Sci, 49(6): 2371-2378.

Lopes, V. and Reis, A., 1998. Altitude related agronomical traits among Dactylis glomerata germplasm. Pastagens e Forragens, 19: 5-17.

Lourenco, M.E.V. and Palma, P.M.M., 2001. The effect of plant population on the yield and quality of annual rye-grass. Proceedings of the Xix International Grassland Congress: 416-417.

McKeon, G.M. et al., 2009. Climate change impacts on northern Australian rangeland livestock carrying capacity: a review of issues. Rangeland J, 31(1): 1-29.

Mourato, S., Moreira, M. and Corte-Real, J., 2015. Water Resources Impact Assessment Under Climate Change Scenarios in Mediterranean Watersheds. Water Resources Management, 29(7): 2377-2391.

Nóbrega, C.M., 2006. Alterações climáticas em Portugal. Cenários, impactos e medidas de adaptação: Projecto SIAM II - 1ª edição. Silva Lusitana, 14: 281-281.

Oomes, M.J.M. and Mooi, H., 1981. The Effect of Cutting and Fertilizing on the Floristic Composition and Production of an Arrhenatherion-Elatioris Grassland. Vegetatio, 46-7(Nov): 233-239.

Penman, H.L., 1948. Natural Evaporation from Open Water, Bare Soil and Grass. Proceedings of the Royal Society of London. Series A. Mathematical and Physical Sciences, 193(1032): 120-145.

Pereira, H., Domingos, T. and Vicente, L., 2004. Portugal millennium ecosystem assessment: state of the assessment report, Centro de Biologia Ambiental, Faculdade de Ciências da Universidade de Lisboa, Universidade de Lisboa.

Poirier, M., Durand, J.L. and Volaire, F., 2012. Persistence and production of perennial grasses under water deficits and extreme temperatures: importance of intraspecific vs. interspecific variability. Global Change Biol, 18(12): 3632-3646.

Rounsevell, M.D.A., Ewert, F., Reginster, I., Leemans, R. and Carter, T.R., 2005. Future scenarios of European agricultural land use II. Projecting changes in cropland and grassland. Agr Ecosyst Environ, 107(2-3): 117-135.

Ruget, F. et al., 2012. Conséquences possibles des changements climatiques sur la production fourragère en France. I. Estimation par modélisation et analyse critique. Fourrages, 210: 87-98.

Ruget, F. et al., 2013. Impacts des changements climatiques sur les productions de fourrages (prairies, luzerne, maïs): variabilité selon les régions et les saisons. Fourrages, 214: 99-109.

Ruget, F., Godfroy, M. and Plantureux, S., 2008. Improved estimation of mountain grassland production by using local input data in a crop model, Biodiversity and animal feed: future

challenges for grassland production. Proceedings of the 22nd General Meeting of the European Grassland Federation, Uppsala, Sweden, 9-12 June 2008, pp. 305-307.

Ruget, F., Moreau, J., Cloppet, E. and Souverain, F., 2010. Effect of climate change on grassland production for herbivorous livestock systems in France, 23rd General Meeting of the EGF Grassland in a changing world, Kiel (Germany), Aug 29th-Sept 2th 2010, pp. 75-77.

Ruget, F., Novak, S. and Granger, S., 2006. Du modèle STICS au système ISOP pour estimer la production fourragère. Adaptation à la prairie, application spatialisée. Fourrages, 186(241): 256.

Ruget, F., Satger, S., Volaire, F. and Lelievre, F., 2009. Modeling Tiller Density, Growth, and Yield of Mediterranean Perennial Grasslands with STICS. Crop Sci, 49(6): 2379-2385.

Samuelsson, P. et al., 2011. The Rossby Centre Regional Climate model RCA3: model description and performance. Tellus A, 63(1): 4-23.

Santos, J.A., Belo-Pereira, M., Fraga, H. and Pinto, J.G., 2016. Understanding climate change projections for precipitation over western Europe with a weather typing approach. J Geophys Res-Atmos, 121(3): 1170-1189.

Saxton, K.E. and Rawls, W.J., 2006. Soil water characteristic estimates by texture and organic matter for hydrologic solutions. Soil Sci Soc Am J, 70(5): 1569-1578.

Serrano, J.M., Peca, J.O., da Silva, J.M. and Shahidian, S., 2011. Calibration of a capacitance probe for measurement and mapping of dry matter yield in Mediterranean pastures. Precis Agric, 12(6): 860-875.

Shuttleworth, W.J. and Wallace, J.S., 1985. Evaporation from sparse crops-an energy combination theory. Q J Roy Meteor Soc, 111(469): 839-855.

Siebert, S., Webber, H., Zhao, G. and Ewert, F., 2017. Heat stress is overestimated in climate impact studies for irrigated agriculture. Environ Res Lett, 12(5).

Stockle, C.O., Williams, J.R., Rosenberg, N.J. and Jones, C.A., 1992. A Method for Estimating the Direct and Climatic Effects of Rising Atmospheric Carbon-Dioxide on Growth and Yield of Crops .1. Modification of the Epic Model for Climate Change Analysis. Agr Syst, 38(3): 225-238.

Strandberg, G. et al., 2015. CORDEX scenarios for Europe from the Rossby Centre regional climate model RCA4, SMHI, Norrköping, Sweden.

Teixeira, R.F.M. et al., 2011. Soil organic matter dynamics in Portuguese natural and sown rainfed grasslands. Ecological Modelling, 222(4): 993-1001.

Trindade, H., 2015. Portuguese dairy farming systems, Grassland and forages in high output dairy farming systems. Proceedings of the 18th Symposium of the European Grassland Federation, Wageningen, The Netherlands, 15-17 June 2015, pp. 21-25.

Trindade, H., Coutinho, J., VanBeusichem, M.L., Scholefield, D. and Moreira, N., 1997. Nitrate leaching from sandy loam soils under a double-cropping forage system estimated from suction-probe measurements. Plant Soil, 195(2): 247-256.

Turral, H., Burke, J.J. and Faurès, J.-M., 2011. Climate change, water and food security, FAO, Rome, FAO Water Reports 36.

Valverde, P. et al., 2015. Climate change impacts on irrigated agriculture in the Guadiana river basin (Portugal). Agr Water Manage, 152: 17-30.

van Vuuren, D.P. et al., 2011. The representative concentration pathways: an overview. Climatic Change, 109(1-2): 5-31.

Walter, J. et al., 2012. Increased rainfall variability reduces biomass and forage quality of temperate grassland largely independent of mowing frequency. Agr Ecosyst Environ, 148: 1-10.

Wimmer, F. et al., 2015. Modelling the effects of cross-sectoral water allocation schemes in Europe. Climatic Change, 128(3-4): 229-244.

Wu, Z.T., Dijkstra, P., Koch, G.W., Penuelas, J. and Hungate, B.A., 2011. Responses of terrestrial ecosystems to temperature and precipitation change: a meta-analysis of experimental manipulation. Global Change Biol, 17(2): 927-942.

Yang, C.Y., Fraga, H., Van Ieperen, W. and Santos, J.A., 2017. Assessment of irrigated maize yield response to climate change scenarios in Portugal. Agr Water Manage, 184: 178-190.

Zaka, S. et al., 2017. How variable are non-linear developmental responses to temperature in two perennial forage species? Agr Forest Meteorol, 232: 433-442.

Zwicke, M. et al., 2013. Lasting effects of climate disturbance on perennial grassland above-ground biomass production under two cutting frequencies. Global Change Biol, 19(11): 3435-3448.

CHAPTER 6

General Discussion

6.1 Summary of outcomes and implications

6.1.1 Climate change projections, vulnerabilities, impacts and associated uncertainties

The Mediterranean basin has been widely identified as one of the most prominent climate change hotspots due to ongoing and projected changes in both climate means and variabilities, consisting of a robust climate change signal of annual mean temperature increase and precipitation reduction, accompanied by more frequent occurrence of extremely high temperature events and severe droughts (Diffenbaugh and Giorgi, 2012; Giorgi and Lionello, 2008; Mariotti et al., 2015; Saadi et al., 2015; Strandberg et al., 2015). The projected overall warming and drying trend is particularly pronounced in southern Europe (Giorgi and Lionello, 2008; Strandberg et al., 2015), for example in mainland Portugal, where annual mean temperature increased at a rate more than double the global warming rate over the past decades (Carvalho et al., 2014; Espírito Santo et al., 2014), along with observed decrease in precipitation and its increase of inter-annual variability (Carvalho et al., 2014; Santo et al., 2014). These observed and projected changes suggest that Portugal is a country that is particularly vulnerable to climate change.

Our research results suggest that future climate change (from mid to the end of the 21st century) is very likely (high confidence) to reduce harvestable grain yields of irrigated maize and rainfed wheat production systems in their current principal production regions (Yang et al., 2018; Yang et al., 2017), as well as constituting a threat to the primary productivity of perennial forage grassland across Portugal (Yang et al., 2019). Moderate or severe yield losses are obtained, depending on low or high emission scenarios and near-future or distant-future period, respectively. This suggests the evolution of human activities (e.g. social-economic development, technology trend and land use changes), and the associated pathway of global anthropogenic forcing, are crucial determinants of regional agriculture productivity for many regions worldwide, i.e. more intense global cumulative GHG emissions, more widespread negative impacts on agriculture production (IPCC, 2018). The inter-annual yield variability steadily increased throughout the century as a result of enhanced climate variability, posing threats to future year-to-year stability of regional food crop supply (Asseng et al., 2014; Challinor et al., 2014). Furthermore, enriched atmospheric CO_2 concentration provides some positive effects for crop growth and yield increment for C3 species (C3 grass and wheat), but not enough to offset the yield reductions, whereas almost no positive effects are found for C4 plant, such as maize, except under drought conditions (Yang et al., 2018; Yang et al., 2019; Yang et al., 2017). The simulated magnitude of CO_2 production response across

different species (photosynthesis stimulation and biomass growth) is broadly consistent with Free Air CO_2 Enrichment (FACE) experiments (Kimball, 2016) and within the range of responses represented by a consortium of existing crop models (Vanuytrecht and Thorburn, 2017).

Despite a high likelihood of an overall negative impact on yield, the projected magnitudes of the impacts remain highly uncertain. The identified cause of yield reductions for one cultivated species (irrigated maize) can bring positive effects for other cropping systems (rainfed wheat and perennial grassland). While higher temperature induced rapid development and shortened growth length (less time for photosynthesis and capture resources) clearly represent an adverse aspect for irrigated maize (Gabaldón-Leal et al., 2015; Meza et al., 2008; Tubiello et al., 2000), it brings an advantage for perennial grass species, for which advanced phenology shifting towards the cooler and wetter part of the year favors growth and biomass accumulation (Ergon et al., 2018; Graux et al., 2013; Lelievre and Volaire, 2009). Furthermore, early maturity with shorter growth duration under warmer climate, may allow winter wheat to finish lifecycle earlier prior to impending critical heat/drought stress that is more detrimental under dry Mediterranean conditions (Moriondo et al., 2010; Wang et al., 2017). Although it is argued that the climate warming effect alone may not be enough to ensure the successful terminal stress escaping strategy for rainfed wheat crops, cultivar adjustment using early flowering cultivars/short-cycle genotypes can help achieving the goal (Shavrukov et al., 2017; Yang et al., 2019). In general, it illustrates that quantifying the climate change impact on the productivity of Mediterranean agriculture is complex, not only because the inherent vulnerability of Mediterranean climate but also the impacts are heavily dependent on the choice of cropping options, locations and the adopted management practices (irrigated or rainfed) (Iglesias et al., 2010; Ruiz-Ramos and Minguez, 2010; Saadi et al., 2015). In particular, the choice of analyzed cropping system represents the dominant source of uncertainty in modeling crop yield response to future climate change in Iberian Peninsula (Ruiz-Ramos and Minguez, 2010), which is part of the reason why we have decided at the beginning to study different crop species, with diversified responses and growth patterns, environment constraints and management practices. Other essential source of uncertainty is largely consistent with previous global analysis, arising from different crop models chosen, applied climate models (including the downscaled approaches), selected time periods of analysis and emission pathways (Asseng et al., 2013; Tao et al., 2018; Wang et al., 2018). Quantifying all these uncertainties, and develop methodologies and tools to better sample the range of possible yield response in a more contextual approach (e.g. by

calibrating crop models using local measured representative data), will provide a fundamental basis for reliable climate change impact assessments. Less uncertainty in describing how climate change may affect agriculture productivity will aid in developing, planning and implementing appropriate and target adaptation strategies (Asseng et al., 2013).

6.1.2 Recommended adaptation strategies

Various adaptation measures provide potential to mitigate these negative impacts, but it overall indicates that a single adaptation measure might not be enough for any of the analyzed cropping systems under Mediterranean conditions, with high uncertainty and variability (Yang et al., 2018; Yang et al., 2019; Yang et al., 2017). It thus highlights the necessities to appropriately combine available options across various levels and scales for comprehensive adaptation strategy development (Challinor et al., 2018; Howden et al., 2007; Rotter et al., 2018; Ruiz-Ramos et al., 2018). The primary research outcomes and its implications to support informed decisions on defining agricultural climate adaptation policies in Portugal, are summarized as below:

(**i**) The recommended adaptation strategy for irrigated maize production in southern Portugal (Ribatejo region), should focus on promoting water-saving techniques to maximize crop WUE and stabilize yields (e.g. develop optimized deficit irrigation strategy with efficient irrigation facilities) (Farré and Faci, 2009; Geerts and Raes, 2009; Yang et al., 2017), while introducing longer-cycle maize cultivars and early sowing time to counterbalance the accelerated development and shortened growing season (Gabaldón-Leal et al., 2015; Meza et al., 2008; Tubiello et al., 2000). Although increased seasonal irrigation water amount to mitigate future yield reductions and maintain current yield level is possible (Yang et al., 2017), its implementation will be increasingly limited by the restrictions of water scarcity and decreasing portion of fresh water available for agriculture in the Mediterranean region (Iglesias et al., 2007). Moreover, crop WUE is expected to decline considerably with increased irrigation, as a result of diminished yield responsiveness to seasonal water input driven by reduced growth duration under a warmer climate (Gabaldón-Leal et al., 2015; Yang et al., 2017). However, the integrated adaptation strategy combining these options awaits to be further rigorously examined under Mediterranean conditions;

(**ii**) The recommended adaptation strategy for rainfed winter wheat production in southern Portugal (Alentejo region) should be based on early flowering cultivars, with less or no vernalization requirement (e.g. spring wheat), together with advocating early sowing and supplemental irrigation during the sensitive stages (Moriondo et al., 2010; Ruiz-Ramos et al., 2018; Shavrukov et al., 2017). A stress escaping strategy has been recently proposed to reduce the duration of overlap between occurrence of terminal heat/drought stress and the sensitive anthesis and grain-filling stage (Farooq et al., 2011; Shavrukov et al., 2017; Yang et al., 2019). By using early flowering cultivars (short-cycle genotypes), the trade-off between lower risk of exposure to terminal stress and higher risk of reduced yield potential tends to be positive, leading to net yield gains (Yang et al., 2019). Early sowing is also expected to achieve the same stress escaping goal by anticipated growth cycle, but tends to be limited, to some extent, by slowed vernalization fulfilment with winter warming. Using wheat cultivars with less or no vernalization requirement (e.g. spring wheat) can thus help advocating early sowing practice. It is noteworthy the proposed stress escaping strategy is indeed more useful to avoid enhanced terminal heat stress (>38ºC concentrated over a short period) than prolonged terminal drought stress (Yang et al., 2019), whereas the latter can be alleviated by supplemental irrigation. For instance, Ruiz-Ramos et al. (2018) already demonstrated that effective adaptation for rainfed wheat cultivation in the Mediterranean south environment zone (Spain) is possible, based on the combination of supplementary irrigation, early sowing date and short-cycle spring wheat cultivar;

(**iii**) The recommended adaptation strategy for perennial forage grassland scattered across Portugal should take advantage of the opportunity and tackle the challenge, both arising from climate change (Ergon et al., 2018; Graux et al., 2013; Lelievre and Volaire, 2009; Yang et al., 2018). Benefiting from the opportunity of advanced phenology towards favourable winter-spring period, with alleviated cold stress and enriched ambient CO_2 concentration, adaptation measures should focus on maximizing growth potential for this period, including an optimized early fertilization strategy (balanced between production potential and nitrate leaching) and develop legume-grass mixture for flexible harvest timings and exploiting the stimulated CO_2 responsiveness (Ergon et al., 2018; Lelievre and Volaire, 2009). In contrast, the challenge of exacerbated risks of summer stress highlights the need for continuous improvement of drought persistence and survival, such as introducing summer dormancy trait into plant materials with deeper root system (e.g. more of

tall fescue) (Ergon, 2017; Lelièvre et al., 2011). Nevertheless, the forage quality issue may arise (Dumont et al., 2015). The distinguished growth response patterns require adaptation measures with contrasting strategies (growth promotion *vs* survival), in which utilizing plant diversity is required at all level with inter- and intraspecific variations. Nonetheless, in a less probable scenario where summer drought survival can be sustained with unlimited irrigation, breeding efforts for adapted germplasm of forage species should be more targeted at heat tolerance, especially in southern Portugal (Yang et al., 2018).

6.2 Summary of strengths and novelties

6.2.1 Fine-resolution regional climate projections

Compared to many previous studies, a major strength and novelty of the present study consists in that we have consistently applied dynamically-downscaled and bias-corrected climate models to provide reliable and relevant inputs for impact models. Site-specific climate change impact assessments and development of locally relevant adaptation strategies require availability of high-resolution regional climate simulations (Giorgi et al., 2009; IPCC, 2015; Jacob et al., 2014; Yang et al., 2010).

While CGMs are powerful tools to study the Earth climate system, their coarse horizontal resolution (200–300 km) precludes them from capturing the effects of local forcing (e.g. complex topography and land-surface characteristics) that modulate climate signal at fine scales (Giorgi et al., 2009; Yang et al., 2010). Therefore, GCMs are also unable to provide accurate descriptions of extreme weather events, which are of fundamental importance for assessing impacts of regional climate change and variability (Giorgi et al., 2009). In other words, the mismatch in scale between GCMs and impact model, as well as the significant gap between coarse climate information provided by GCMs and needs of high-resolution unbiased climate input for regional impact assessment, must be addressed (Giorgi et al., 2009). However, these aspects were not well taken into account by the earlier studies, mostly because of limited developments of RCMs at that time (Rosenzweig and Tubiello, 1997; Santos and Miranda, 2006; Tubiello et al., 2000). These include studies in Portugal from the SIAM project, which directly used GCMs outputs as input for crop models (Santo et al., 2014), and in other Mediterranean regions (Italy) that generate climate projections at study sites based on the spatially linear-interpolated GCMs outputs (Tubiello et al., 2000). In contrast, our successive studies have coherently considered a number of RCMs, with the

finest spatial resolution to date (~12.5 km), to dynamically downscale the GCMs outputs under the latest generation of emission scenarios (i.e. RCPs) (Yang et al., 2018; Yang et al., 2019; Yang et al., 2017). RCMs, operating at fine spatial resolution (~12.5–50 km), perform better at representing local climate due to detailed description of geographic features and sub-grid parameterization of underlying physical processes (Hagemann et al., 2009; Jacob et al., 2014; Yang et al., 2010).

6.2.2 Bias-corrected GCMs-RCMs with preserved climate variability

Despite improved spatial resolutions, there are still systematic biases of simulated long-term climate statistics deriving from GCMs-RCMs chain simulations as compared to observations (Yang et al., 2010). This is because all climate models are approximations of real climate systems and contain different simplifications (IPCC, 2015). Therefore, Bias Correction (BC) techniques (*see section 2.2.6*) have been consistently employed in our studies, not only to adjust raw climate projections for obtaining realistic time series of climate inputs, but also to generate future climate change projections with better preserved climate variability produced by RCMs (Giorgi et al., 2009; IPCC, 2015; Yang et al., 2010). This is an important and novel aspect when the downscaled climate change projections at our study sites are able to incorporate the potential changes in climate variability and associated frequency and intensity of extreme weather events, at which the simulate crop yield changes implicitly integrate the effects of such changes (Yang et al., 2018; Yang et al., 2019; Yang et al., 2017). In contrast, very few studies attempt to account for this aspect across the globe, which is critical to assess the economic prospect on regional stability of food crop supply and price fluctuation (Asseng et al., 2014; Challinor et al., 2014). Furthermore, this is expected to be particularly important for Mediterranean region, as changes in the frequency and magnitudes of extreme climatic events are likely to have more influence on yield determination than mean climate changes (Moriondo et al., 2010). Recent crop yield impact (rainfed + irrigated) assessment studies in Portugal applied the Ensemble Delta technique to statistically-downscaled and bias-corrected GCMs outputs, to create climate change projections that replicated in the future the same inter-annual variation patterns as in the historical baseline (Valverde et al., 2015a; Valverde et al., 2015b). Another similar study conducted in southern Portugal explicitly used RCMs to produce regional climate change projections, but no BC approaches have been applied whilst keeping climate variance of future period the same as the reference period (Rolim et al., 2017). Moreover,

in the southern Spain under Mediterranean conditions, Ruiz-Ramos et al. (2018) used an ensemble of 17 process-based crop models to comprehensively calculate wheat yield response under a range of possible climate perturbations with various adaptation options, but the adopted Delta Change technique only allowed assessment of yield response to changes in mean climatic conditions, thus possibly underestimating the magnitude of yield losses.

6.2.3 Utilization of new generation of emission scenarios

Climate models are valuable tools to simulate the processes that determine the response of climate system to anthropogenic forcings, such as increases in GHG concentrations, atmospheric aerosol loadings and land use changes (Giorgi et al., 2009). However, the future trajectory of these forcings cannot be easily projected, as they are strongly influenced by political, demographic, technical and social-economic factors (Asseng et al., 2013). Under the CMIP5 framework, climate change projections are driven by a set of new RCPs emission scenarios (*see section 2.2.4*) that cover a wide range of population growth, technological development and societal responses (Taylor et al., 2012). In contrast to previously used SRES scenarios from CMIP3, without considering policy interventions (Nakicenovic et al., 2000), RCPs are mitigation scenarios that assume policy actions already taken to achieve the target radiative forcing at the end of 21st century (Moss et al., 2010; van Vuuren et al., 2011). These new emission pathways (RCPs) have been consistently adopted in our studies for more comprehensive and reliable assessments (Yang et al., 2018; Yang et al., 2019; Yang et al., 2017), in contrast to many previous studies in Portugal (Rolim et al., 2017; Santos and Miranda, 2006; Valverde et al., 2015a; Valverde et al., 2015b) that used the SRES scenarios, mainly focused on the social-economic changes.

6.2.4 Adapting STICS simulations to local cropping systems

Like climate models, crop model simulations are also intrinsically uncertain (*see section 2.3.2*), with uncertainty sources deriving from variability of model structure among different models (e.g. adopted function forms), measurement errors of input data and eventually calibrated parameter values (Seidel et al., 2018; Wallach and Thorburn, 2017). To account for the structural uncertainty, the choice of crop model (if multi-model ensemble is not possible) is crucial as there is often a large variability between model predictions even when the same input information is used (model structural variations may also result in differently assigned values of input parameters among

models using the same observed variable) (Asseng et al., 2013; Ruiz-Ramos et al., 2018). The STICS model chosen in our studies previously showed satisfactory prediction performance with its standard parameters over a wide range of agro-climatic conditions (including Mediterranean-type climate) for several important output variables of soil-crop system (Brisson et al., 1998; Brisson et al., 2002), measured by nRMSE, including yield (30%), biomass (35%) and soil water content (10%) (Coucheney et al., 2015). However, this feature of robustness will jeopardize prediction accuracy for a specific local study (Brisson et al., 2003). Quite often, when the model is applied to a particular condition in order to address the local research issue, the standard parameters need to be calibrated to improve fitting to available observations, a process used to address the input and parameter uncertainties (Seidel et al., 2018). This local calibration step has been consistently adopted in our studies, by first integrating local growing conditions, including observed weather data, dominant soil characteristics and representative agronomic practices (Yang et al., 2018; Yang et al., 2019; Yang et al., 2017). The trail-and-error approach is then applied to optimize the goodness-of-fit between simulated and observed productivity, by adjusting pertinent parameters in order to justify the representativeness of local cropping systems as simulated by the model. However, this important calibration step has been largely ignored in most previous studies conducted in Portugal (Santos and Miranda, 2006; Valverde et al., 2015a; Valverde et al., 2015b).

6.2.5 Improved adaptation simulations in Portugal

Crop models are able to deal with multiple climatic factors and their interactions on crop growth and yield formation processes that are sensitive to climate (Asseng et al., 2014). Development of adaptation strategies requires understandings of contributions of various climate variables on crop yields, which need to be quantified and separated (Asseng et al., 2014; Asseng et al., 2011). For instance, changes in temperature would require a very different adaptation strategy than changes in precipitation. To explore underlying causes of potential negative climate change impacts (Rötter et al., 2018), particular attention has been given to separate the drought intensity from that of heat during the sensitive graining-filling stage for winter wheat (Yang et al., 2019), or to isolate the drought stress impacts from that of heat stress for perennial grassland during unfavorable summer season (Yang et al., 2018). Moreover, a variety of adaptation options at different levels have been tested in our studies to identify the target adaptation strategies. In contrast, the SIAM project carried out in Portugal, without paying attention to distinguish the impacts between heat and

drought stress, has led to a very different (probably questionable) adaptation recommendation from ours: the SIAM project findings advocate early sowing alone would be enough for maintaining wheat production in future climate (Santos and Miranda, 2006), whereas our study indicates that early sowing benefits are likely to be impeded by slowed vernalization fulfillment during a warmer winter, and effective adaptations should more focus on using early flowering cultivars with less or no vernalization requirement combined with supplemental irrigation during the sensitive grain filling stages (Yang et al., 2019).

6.3 Summary of uncertainties and limitations

6.3.1 Uncertainties in climate change projections

As illustrated before, uncertainties in projections of climate change impacts on future crop yield derive from different sources in modelling (Asseng et al., 2013). Firstly, the evolution of future GHG emissions and other aerosol loadings is highly uncertain, as they are the consequence of potential demographic changes, social-economic development, technological progress and policy interventions (IPCC, 2018). A range of plausible projections are used instead, characterized as different emission scenarios, in an attempt to encompass the anthropogenic forcing uncertainty (Moss et al., 2010; van Vuuren et al., 2011). Secondly, projecting the response of climate systems to potential increases in GHG concentrations, using GCMs and the associated downscaling methods (dynamic or statistical) to generate regional climate change projections, remain highly uncertain, as different models or methods give different results (Asseng et al., 2013). The choice of climate models is recognized as the largest contributor to the total uncertainty of projected climate change impacts in a short-term period (Kassie et al., 2015; Wang et al., 2018). Given the inherent variations of climate projections, a bias-adjusted multi-model, multi-scenario and multi-initialization ensemble of GCMs-RCMs from EURO-CORDEX were employed in one of our study for a wide range of probable projections (Yang et al., 2019). However, this practice had not been applied for studies on irrigated maize (Yang et al., 2017) and perennial grassland systems (Yang et al., 2018), where only one climate model (MPI-ESM-LR – SMHI-RCA4) was considered by assuming its representative role over the westernmost Europe (Strandberg et al., 2015), leading to substantial impact uncertainties (e.g. less confidence about the range of projected yield losses). Moreover, though the new generation of RCPs scenarios are adopted in our analysis, our studies

only focus on two more plausible emission scenarios (i.e. RCP4.5 and RCP8.5), thus narrowing the possible range of potential outcomes on how alternative images of future might unfold.

6.3.2 Uncertainties in crop model structure and limited data availability

Another important source of uncertainty in our studies derives from the lack of considerations for crop model structure uncertainties (*see section 2.3.2*). Using a variety of different crop models helps to make prediction more robust and enables quantifying the uncertainty, where the multi-model ensemble median better reproduces the observed pattern than any single model (Asseng et al., 2014; Martre et al., 2015). Within the AgMIP pilot project, Asseng et al. (2013) explicitly concluded that the dominant source of uncertainty in projecting wheat yield changes arises from the variability among crop models with less uncertainty arising from variability among climate models. However, Wang et al. (2018) argued that the relative contribution of any single source of uncertainty to total uncertainty of yield impacts of projected climate change is heavily dependent on climatic locations (e.g. the dominant source of uncertainty would differ between temperate and Mediterranean climate). Nevertheless, model calibration using local representative measurements, can help greatly reduce structure-related uncertainty due to reduced range of yield response towards observations (Asseng et al., 2013), where a single-model based analysis should be more stimulated towards improved and more accurate calibration outcomes (Seidel et al., 2018). It is noteworthy though we have consistently calibrated the crop models with an overall agreement between simulations and observations, observation data at a more relevant field-scale is only available for rainfed wheat (Yang et al., 2019). For the other two cropping systems, model performance verification has been carried out either using regional averaged yield statistics (Yang et al., 2017) or empirical range of forage productivity (Yang et al., 2018). The limited quality and amount of observational data will add extra uncertainties in the simulated magnitude of impacts.

6.3.3 Uncertainties in assumptions of constant management and soil properties

The response of cropping system to future climate change will depend on site-specific conditions, such as the management practices (e.g. frequency and amount of water and nitrogen) and soil types (e.g. water retention capacity) (Asseng et al., 2013; Folberth et al., 2016; Kassie et al., 2015; Wang et al., 2018). The inter-model uncertainty of simulated average yield response to climate change (i.e. spread in model response in simulated mean yield changes) has proved to vary with different

soil types and management practices irrespective of the study sites, adding to uncertainty in response coming from individual crop models (Asseng et al., 2013). For instance, simulated maize WUE and grain yields respond differently to projected climate change in the Central Great Plains of Colorado under full and deficit irrigation (Islam et al., 2012), as well as in Central Rift Valley of Ethiopia under full and limited N fertilizations (Kassie et al., 2015). In reality, farmers can autonomously respond to climate change by empirically making management decisions (e.g. crop choice, fertilizers, sowing time), based on profitability expectations averaged over the years of their own experience, but might miss substantial gains in favourable years (Rotter et al., 2018). Therefore, it is essential to dynamically consider adaptations assuming changes in management decisions will take place over time with sufficient flexibility to maintain near optimum economic performance (Meza and Silva, 2009). In such context, the constant assumption of local sowing dates and N fertilization strategy for irrigated maize production in Ribatejo (Yang et al., 2017), unadjusted standard cutting dates for grassland forage conservation across Portugal (Yang et al., 2018) and standard cultivation practices for rainfed wheat cultivations in Alentejo (Yang et al., 2019), all of which are defined over a reference historic period and will contribute to important uncertainties in projected impacts under future climatic period. On the other hand, only dominant soil types were considered at our study sites, neglecting a number of secondary important soil profiles, as well as ignoring potential land use changes with different soil types utilized for crop cultivations (Jones et al., 2011). Different soil types affect crop yield differently, as a consequence of differences in water and nutrient usages, acting as a buffer to maintain crop development and growth under various adverse climatic conditions (Wang et al., 2018). In particular, Folberth et al. (2016) revealed the accuracy of soil input has played an important role in determining the magnitude and direction of climate change impacts under extreme scenarios.

6.3.4 Limitations in lack of interactions with pest, disease and weeds

The known deficiencies and limitations in the current studies are the absence of considerations in modelling the pest and disease damages on crop losses and the effect of weed infestations under climate changes. Process-based crop models so far have largely ignored these effects, assuming grown varieties already with pest-disease resistant traits and proper field preparations on weed controls has already been undertaken (e.g. pre-emergence herbicide application) (Rotter et al., 2018). Quantifying the impacts of plant pests and diseases on crop performance still represents

one major challenge for the scientific community, especially the difficulties to define the pathogen dynamics temporally and spatially (Donatelli et al., 2017). This will eventually prevent accurate estimations of crop yields in regions where biotic stress is significant, possibly leading to underestimations of climate change impacts. From a qualitative point of view, drier climates may prompt pest outbreaks, whereas disease occurrence tends to decrease, because it relies on rainfall and humidity to spear, attack and produce damages on crops (uncertainty is high) (Meza et al., 2008). Elevated CO_2 favours growth of C3 weed species over C4, likely resulting in increased herbicide usage (Meza et al., 2008).

6.3.5 Limitations and uncertainties in representing possible adaptations

In practice, the adaptation effects could be smaller or higher than those simulated in many studies. Overestimation is possible as in reality famers (especially smallholder farmers) sometimes lack capacity to fully implement proposed adaptations due to economic constraints or cultural inappropriateness (Challinor et al., 2014). The co-limitations, such as increasingly restricted water resource for agriculture is expected to limit irrigation-based adaptation strategies (Iglesias et al., 2007), are also expected to overestimate adaptation benefits. This has already been illustrated before where optimized water-saving techniques, e.g. deficit (maize) or supplemental (wheat and grassland) irrigation strategy during the sensitive crop growth stages (Yang et al., 2018; Yang et al., 2019; Yang et al., 2017), are essential, but will create additional pressures for water resources. Yet, the positive effects of adaptation could be underestimated, as the array of adaptation options typically investigated is limited by the assessment tools available, in which the tested adaptation options using the crop model could be just a subset of fully available field-level adaptations (Challinor et al., 2014). Moreover, Challinor et al. (2018) suggest new methods are required to explicitly account for technology development to avoid underestimating the effectiveness of available adaptation options. Our studies are clearly unable to incorporate all these external factors, resulting in either over- or underestimations of adaptation benefits. In particular, the adaptation strategies are only qualitatively explored and suggested for perennial grassland systems at the three selected sites across Portugal (Yang et al., 2018). In addition, more systemic (e.g. grazing integration) or transformational adaptations (e.g. crop relocation) (Challinor et al., 2014), have also been omitted. But if small adjustments of management practices are enough to mitigate potential negative climate change impacts, more drastic changes would be unnecessary.

References:

Asseng, S. et al., 2014. Rising temperatures reduce global wheat production. Nature Climate Change, 5: 143.

Asseng, S. et al., 2013. Uncertainty in simulating wheat yields under climate change. Nature Climate Change, 3(9): 827-832.

Asseng, S., Foster, I. and Turner, N.C., 2011. The impact of temperature variability on wheat yields. Global Change Biol, 17(2): 997-1012.

Brisson, N. et al., 2003. An overview of the crop model stics. European Journal of Agronomy, 18(3): 309-332.

Brisson, N. et al., 1998. STICS: a generic model for the simulation of crops and their water and nitrogen balances. I. Theory and parameterization applied to wheat and corn. Agronomie, 18(5-6): 311-346.

Brisson, N. et al., 2002. STICS: a generic model for simulating crops and their water and nitrogen balances. II. Model validation for wheat and maize. Agronomie, 22(1): 69-92.

Carvalho, A., Schmidt, L., Santos, F.D. and Delicado, A., 2014. Climate change research and policy in Portugal. Wires Clim Change, 5(2): 199-217.

Challinor, A.J. et al., 2018. Improving the use of crop models for risk assessment and climate change adaptation. Agr Syst, 159: 296-306.

Challinor, A.J. et al., 2014. A meta-analysis of crop yield under climate change and adaptation. Nature Climate Change, 4: 287.

Coucheney, E. et al., 2015. Accuracy, robustness and behavior of the STICS soil–crop model for plant, water and nitrogen outputs: Evaluation over a wide range of agro-environmental conditions in France. Environ Modell Softw, 64: 177-190.

Diffenbaugh, N.S. and Giorgi, F., 2012. Climate change hotspots in the CMIP5 global climate model ensemble. Climatic Change, 114(3): 813-822.

Donatelli, M. et al., 2017. Modelling the impacts of pests and diseases on agricultural systems. Agr Syst, 155: 213-224.

Dumont, B. et al., 2015. A meta-analysis of climate change effects on forage quality in grasslands: specificities of mountain and Mediterranean areas. Grass Forage Sci, 70(2): 239-254.

Ergon, Å., 2017. Optimal Regulation of the Balance between Productivity and Overwintering of Perennial Grasses in a Warmer Climate. Agronomy, 7(1): 19.

Ergon, Å. et al., 2018. How can forage production in Nordic and Mediterranean Europe adapt to the challenges and opportunities arising from climate change? European Journal of Agronomy, 92: 97-106.

Espírito Santo, F., de Lima, M.I.P., Ramos, A.M. and Trigo, R.M., 2014. Trends in seasonal surface air temperature in mainland Portugal, since 1941. Int J Climatol, 34(6): 1814-1837.

Farooq, M., Bramley, H., Palta, J.A. and Siddique, K.H.M., 2011. Heat Stress in Wheat during Reproductive and Grain-Filling Phases. Critical Reviews in Plant Sciences, 30(6): 491-507.

Farré, I. and Faci, J.M., 2009. Deficit irrigation in maize for reducing agricultural water use in a Mediterranean environment. Agricultural Water Management, 96(3): 383-394.

Folberth, C. et al., 2016. Uncertainty in soil data can outweigh climate impact signals in global crop yield simulations. Nat Commun, 7: 11872.

Gabaldón-Leal, C. et al., 2015. Strategies for adapting maize to climate change and extreme temperatures in Andalusia, Spain. Clim Res, 65: 159-173.

Geerts, S. and Raes, D., 2009. Deficit irrigation as an on-farm strategy to maximize crop water productivity in dry areas. Agricultural Water Management, 96(9): 1275-1284.

Giorgi, F., Jones, C. and Asrar, G., 2009. Addressing climate information needs at the regional level: the CORDEX framework. Bulletin-World Meteorological Organization, 58(3): 175-183.

Giorgi, F. and Lionello, P., 2008. Climate change projections for the Mediterranean region. Global Planet Change, 63(2): 90-104.

Graux, A.-I., Bellocchi, G., Lardy, R. and Soussana, J.-F., 2013. Ensemble modelling of climate change risks and opportunities for managed grasslands in France. Agr Forest Meteorol, 170: 114-131.

Hagemann, S., Göttel, H., Jacob, D., Lorenz, P. and Roeckner, E., 2009. Improved regional scale processes reflected in projected hydrological changes over large European catchments. Clim Dynam, 32(6): 767-781.

Howden, S.M. et al., 2007. Adapting agriculture to climate change. Proceedings of the National Academy of Sciences, 104(50): 19691-19696.

Iglesias, A., Garrote, L., Flores, F. and Moneo, M., 2007. Challenges to Manage the Risk of Water Scarcity and Climate Change in the Mediterranean. Water Resources Management, 21(5): 775-788.

Iglesias, A., Quiroga, S. and Schlickenrieder, J., 2010. Climate change and agricultural adaptation: assessing management uncertainty for four crop types in Spain. Clim Res, 44(1): 83-94.

IPCC, 2015. Workshop Report of the Intergovernmental Panel on Climate Change Workshop on Regional Climate Projections and their Use in Impacts and Risk Analysis Studies [Stocker, T.F., D. Qin, G.-K. Plattner, and M. Tignor (eds.)], IPCC Working Group I Technical Support Unit, University of Bern, Bern, Switzerland.

IPCC, 2018. Global warming of 1.5°C. An IPCC Special Report on the Impacts of Global Warming of 1.5°C Above Pre-Industrial Levels and Related Global Greenhouse Gas Emission Pathways, in the Context Of Strengthening the Global Response to the Threat of Climate Change, Sustainable Development, and Efforts to Eradicate Poverty.

Islam, A. et al., 2012. Modeling the impacts of climate change on irrigated corn production in the Central Great Plains. Agricultural Water Management, 110: 94-108.

Jacob, D. et al., 2014. EURO-CORDEX: new high-resolution climate change projections for European impact research. Regional Environmental Change, 14(2): 563-578.

Jones, N., de Graaff, J., Rodrigo, I. and Duarte, F., 2011. Historical review of land use changes in Portugal (before and after EU integration in 1986) and their implications for land degradation and conservation, with a focus on Centro and Alentejo regions. Appl Geogr, 31(3): 1036-1048.

Kassie, B.T. et al., 2015. Exploring climate change impacts and adaptation options for maize production in the Central Rift Valley of Ethiopia using different climate change scenarios and crop models. Climatic Change, 129(1): 145-158.

Kimball, B.A., 2016. Crop responses to elevated CO2 and interactions with H2O, N, and temperature. Curr Opin Plant Biol, 31: 36-43.

Lelièvre, F., Seddaiu, G., Ledda, L., Porqueddu, C. and Volaire, F., 2011. Water use efficiency and drought survival in Mediterranean perennial forage grasses. Field Crops Research, 121(3): 333-342.

Lelievre, F. and Volaire, F., 2009. Current and Potential Development of Perennial Grasses in Rainfed Mediterranean Farming Systems. Crop Sci, 49(6): 2371-2378.

Mariotti, A., Pan, Y., Zeng, N. and Alessandri, A., 2015. Long-term climate change in the Mediterranean region in the midst of decadal variability. Clim Dynam, 44(5): 1437-1456.

Martre, P. et al., 2015. Multimodel ensembles of wheat growth: many models are better than one. Global Change Biol, 21(2): 911-925.

Meza, F.J. and Silva, D., 2009. Dynamic adaptation of maize and wheat production to climate change. Climatic Change, 94(1): 143-156.

Meza, F.J., Silva, D. and Vigil, H., 2008. Climate change impacts on irrigated maize in Mediterranean climates: Evaluation of double cropping as an emerging adaptation alternative. Agr Syst, 98(1): 21-30.

Moriondo, M. et al., 2010. Impact and adaptation opportunities for European agriculture in response to climatic change and variability. Mitig Adapt Strat Gl, 15(7): 657-679.

Moss, R.H. et al., 2010. The next generation of scenarios for climate change research and assessment. Nature, 463: 747.

Nakicenovic, N. et al., 2000. Special report on emissions scenarios (SRES), a special report of Working Group III of the intergovernmental panel on climate change. Cambridge University Press.

Rolim, J., Teixeira, J.L., Catalao, J. and Shahidian, S., 2017. The Impacts of Climate Change on Irrigated Agriculture in Southern Portugal. Irrig Drain, 66(1): 3-18.

Rosenzweig, C. and Tubiello, F.N., 1997. Impacts of Global Climate Change on Mediterranean Agriculture: Current Methodologies and Future Directions. An Introductory Essay. Mitig Adapt Strat Gl, 1(3): 219-232.

Rotter, R.P., Hoffmann, M.P., Koch, M. and Muller, C., 2018. Progress in modelling agricultural impacts of and adaptations to climate change. Curr Opin Plant Biol, 45: 255-261.

Rötter, R.P., Hoffmann, M.P., Koch, M. and Müller, C., 2018. Progress in modelling agricultural impacts of and adaptations to climate change. Curr Opin Plant Biol, 45: 255-261.

Ruiz-Ramos, M. et al., 2018. Adaptation response surfaces for managing wheat under perturbed climate and CO2 in a Mediterranean environment. Agr Syst, 159: 260-274.

Ruiz-Ramos, M. and Minguez, M.I., 2010. Evaluating uncertainty in climate change impacts on crop productivity in the Iberian Peninsula. Clim Res, 44(1): 69-82.

Saadi, S. et al., 2015. Climate change and Mediterranean agriculture: Impacts on winter wheat and tomato crop evapotranspiration, irrigation requirements and yield. Agricultural Water Management, 147: 103-115.

Santo, F.E., Ramos, A.M., de Lima, M.I.P. and Trigo, R.M., 2014. Seasonal changes in daily precipitation extremes in mainland Portugal from 1941 to 2007. Regional Environmental Change, 14(5): 1765-1788.

Santos, F.D. and Miranda, P., 2006. Climate Change in Portugal: Scenarios, Impacts and Adaptation Measures - SIAM II Project. Gradiva, Lisbon.

Seidel, S.J., Palosuo, T., Thorburn, P. and Wallach, D., 2018. Towards improved calibration of crop models – Where are we now and where should we go? European Journal of Agronomy, 94: 25-35.

Shavrukov, Y. et al., 2017. Early Flowering as a Drought Escape Mechanism in Plants: How Can It Aid Wheat Production? Front Plant Sci, 8.

Strandberg, G. et al., 2015. CORDEX scenarios for Europe from the Rossby Centre regional climate model RCA4, SMHI, Norrköping, Sweden.

Tao, F. et al., 2018. Contribution of crop model structure, parameters and climate projections to uncertainty in climate change impact assessments. Global Change Biol, 24(3): 1291-1307.

Taylor, K.E., Stouffer, R.J. and Meehl, G.A., 2012. An Overview of CMIP5 and the Experiment Design. Bulletin of the American Meteorological Society, 93(4): 485-498.

Tubiello, F.N., Donatelli, M., Rosenzweig, C. and Stockle, C.O., 2000. Effects of climate change and elevated CO2 on cropping systems: model predictions at two Italian locations. European Journal of Agronomy, 13(2): 179-189.

Valverde, P. et al., 2015a. Climate change impacts on rainfed agriculture in the Guadiana river basin (Portugal). Agricultural Water Management, 150: 35-45.

Valverde, P. et al., 2015b. Climate change impacts on irrigated agriculture in the Guadiana river basin (Portugal). Agricultural Water Management, 152: 17-30.

van Vuuren, D.P. et al., 2011. The representative concentration pathways: an overview. Climatic Change, 109(1): 5.

Vanuytrecht, E. and Thorburn, P.J., 2017. Responses to atmospheric CO2 concentrations in crop simulation models: a review of current simple and semicomplex representations and options for model development. Global Change Biol, 23(5): 1806-1820.

Wallach, D. and Thorburn, P.J., 2017. Estimating uncertainty in crop model predictions: Current situation and future prospects. European Journal of Agronomy, 88: A1-A7.

Wang, B., Liu, D.L., Asseng, S., Macadam, I. and Yu, Q., 2017. Modelling wheat yield change under CO2 increase, heat and water stress in relation to plant available water capacity in eastern Australia. European Journal of Agronomy, 90: 152-161.

Wang, B., Liu, D.L., Waters, C. and Yu, Q., 2018. Quantifying sources of uncertainty in projected wheat yield changes under climate change in eastern Australia. Climatic Change, 151(2): 259-273.

Yang, C., Fraga, H., van Ieperen, W. and Santos, J.A., 2018. Modelling climate change impacts on early and late harvest grassland systems in Portugal. Crop and Pasture Science, 69(8): 821-836.

Yang, C., Fraga, H., van Ieperen, W., Trindade, H. and Santos, J.A., 2019. Effects of climate change and adaptation options on winter wheat yield under rainfed Mediterranean conditions in southern Portugal. Climatic Change, 154(1): 159-178.

Yang, C.Y., Fraga, H., Van Ieperen, W. and Santos, J.A., 2017. Assessment of irrigated maize yield response to climate change scenarios in Portugal. Agricultural Water Management, 184: 178-190.

Yang, W. et al., 2010. Distribution-based scaling to improve usability of regional climate model projections for hydrological climate change impacts studies. Hydrology Research, 41(3-4): 211-229.

CHAPTER 7

Conclusion Remarks and Future Outlooks

7.1 Conclusion Remarks

1. Climate change projections show high confidence of continuous warming and drying trend from the mid until the end of 21st century in Portugal. Portugal is a Mediterranean country that is particularly vulnerable to climate change, due to ongoing and projected changes in climate means and variability. The climate change signal of increased annual mean temperature and deceased annual precipitation is robust in Portugal, accompanied by higher frequency and intensity of extreme high temperature events, particularly in the south (e.g. Alentejo region).

2. A high likelihood of an overall negative climate change impact is obtained for the three studied crop production systems in Portugal, creating risks for regional food security. The negative impact comprises moderate-to-severe yield loss with increased year-to-year variability throughout the 21st century. Yield losses are greater in magnitude with higher inter-annual variability, in the second half of the century than in the first half, and in a high emission pathway than in a low emission scenario. Enriched ambient CO_2 concentration help alleviate the yield declines, but not enough to reverse the yield reductions. Majority of these negative impacts are caused either by the shortened growth duration for irrigated maize under a warmer climate, or exacerbated risks of drought and heat stresses during the susceptible growth stages for both rainfed wheat and perennial forage grassland. These aspects correspond to the vulnerabilities of studied cropping systems facing climate change under typical Mediterranean conditions.

3. Simulated magnitudes of impacts remain highly uncertain, varying substantially with different cropping systems (dominant source of uncertainty in Mediterranean region), locations and management practices, applied climate models (including downscaling approaches) and crop models (including partial or full calibration), selected time periods and emission pathways. Research should be continuously directed towards site-specific studies with a locally tailored approach, e.g. using representative measured dataset for model calibrations and verifications, as well as efforts to develop the multi-model ensemble (both crop and climate models) for robust and reliable estimations.

4. Development of appropriate and risk-focused adaptation policies should clearly address the identified vulnerability of cropping systems and prioritize available options. In particular, a

combination of multiple potential adaptation measures analyzed in a local context, should be envisaged to assist in developing integrated and comprehensive adaptation strategies to cope with climate change under Mediterranean conditions. The recommended adaptation strategies for the three crop production systems in Portugal remain uncertain on their quantitative effectiveness, but may represent appropriate opportunities to maintain and improve crop yields under future climate.

7.2 Future Outlooks

1. Research efforts should be directed towards using the ensembles of multiple crop and climate models for simulating climate change impacts and explore adaptations at a detailed local context, however, this would require sustained international collaboration and exchange of high-quality observational data for model testing. Using multi-model ensembles make more robust and reliable the estimations and allow quantifying the uncertainties, which help better conveying the information for evaluating potential risks to gain the trust of general public.

2. Stronger linking of field experimentation with crop modelling to promote mutual understandings and facilitate upscaling of experimental findings. More mechanic understandings of crop response to climate change are required by target field experimentations to propose improved and robust model function forms and parameterization schemes, particularly in dealing with the interactions of CO_2 response with drought and high temperature episodes (i.e. extreme climate events). In turn, improved crop models that applied to grid-based large scale simulations are useful to extrapolate experimental findings to an aggregated (e.g. regional) level that is relevant for policy makings. But this should be assisted by provisions of high-quality and fine-resolution soil and climate datasets.

3. For a more practical relevance to farmers and policymakers to have effective adaptations at various levels, crop modellings should be integrated into economic modelling framework to better reflect the whole farm and complex production systems. A wide array of adaptation options will be available in a more relevant social-economic and environmental context, where the simulated adaptation options based on the biophysical modelling approach, are subject to profitability and environment-friendly considerations.

Supplementary Material I - Chapter 4

Online Resource 1. Characterization of physical and chemical properties of dominant soil type (Vertisol) at Beja

Depth (cm)	Soil texture	Sand (%)	Silt (%)	Clay (%)	*q0* (mm) estimated by sand or clay content (Brisson et al. 2008)	Bulk density (g/cm^3)	Organic carbon (%)	Calcium Carbonate (%)	pH (H_2O)	Soil hydraulic properties				*Ruisolnu* (%) estimated by slope classes (Brisson et al. 2008)
										θ_{FC} (% vol)	θ_{WT} (% vol)	TAW_{soil} (mm)	*SHC* (cm/ day)	
Top soil (0-30)	Clay	29	23	48	8.1	1.56	1.2	0.2	7.3	33	18	122	3.7	0
Subsoil (30-100)		27	28	45		1.60	0.6	-		32	21		3.4	

Note: *q0* is the daily evaporation threshold. θ_{FC}, θ_{WT}, TAW_{soil}, *SHC* respectively denote soil water content at field capacity and wilting point, soil total available water and saturated hydraulic conductivity. Surface slope degree is estimated using GTOPO30 digital elevation model developed by U.S. Geologic Survey. *Ruisolnu* is a STICS parameter describing Hortonian component of runoff, derived from USDA Runoff Curve number method.

Online Resource 2. Summary of observational yield data for model calibration and of input parameters for crop characteristics and local prevailing agronomic practices

Table OR2.1. Observational final grain yields of winter wheat over five consecutive seasons (1981–1986) in the experimental Farm of Almocreva at Beja used for STICS calibration (Carvalho and Basch 1995)

N fertilization (equally split between sowing and beginning of stem elongation)	Years	Yield of cultivar Etoile (kg ha^{-1})	Yield of cultivar Mara (kg ha^{-1})	Analysis of variance (Two-way ANOVA)		Average yield of two cultivars (kg ha^{-1})
				Factors	p-value	
0 kg ha^{-1}	1981–1982	2740	2618	N fertilization	<0.05	2679
	1982–1983	999	916			958
	1983–1984	1712	1747			1730
	1984–1985	2015	1600			1808
	1985–1986	1728	1342			1535
100 kg ha^{-1}	1981–1982	3830	3480	Cultivar	0.77	3655
	1982–1983	906	1003			955
	1983–1984	3254	3691			3473
	1984–1985	3588	2967			3278
	1985–1986	3620	3534			3577
200 kg ha^{-1}	1981–1982	3070	4862	N fertilization X Cultivar	0.64	3966
	1982–1983	741	880			811
	1983–1984	3234	3760			3497
	1984–1985	3969	3760			3865
	1985–1986	3074	4146			3610

Note: measured yield was the average yield obtained between two common sowing dates (Nov 20th and Dec 10th), at which simulations were respectively performed to derive mean yield under individual growing season and N level.

Table OR2.2. Summary of calibrated crop parameters and local prevailing agronomic practices (Carvalho and Basch 1995)

General plant parameter	Cultivar parameters	Initial soil water content at sowing	Sowing dates		Sowing density	Initial soil mineral N amount	N Fertilization strategies		Other assumptions
			Mean	Two common sowing dates			Amount (kg/ha)	Application stages	
RUE_{veg}=RUE_{rep} =2.8 g MJ^{-1}	Built-in cultivar (No.7–*Thetalent*) with standard setting: $GDD_{emg-amf}$=245 °C.d $GDD_{emg-lax}$=505 °C.d $GDD_{emg-drp}$=837 °C.d $GDD_{drp-mat}$=700 °C.d P_{grain}=0.0521 g P_{num}=3000	50% field capacity + supplementary irrigation (20 mm)	Nov 30th	Nov 20th	120 plants m^{-2}	44 kg ha^{-1}	50	Sowing	Not consider influence of pest, disease and weeds
				Dec 10th			50	End of tillering	

Note: RUE_{veg} and RUE_{rep} are radiation use efficiency of winter wheat during vegetative and reproductive phases, respectively. Growing Degree Days (GDD) are calculated with base temperature at 0 C°. $GDD_{emg-amf}$, $GDD_{emg-lax}$, $GDD_{emg-drp}$ and $GDD_{drp-mat}$ are required growing degree days from emergence to beginning of stem elongation, emergence to maximal leaf area index, emergence to beginning of grain-filling and beginning of grain-filling to maturity, respectively. P_{grain} and P_{num} are genetic potential of grain weight and number, respectively. Mean sowing date is used for climate change impact assessment. Settings of initial soil water at sowing is prescribed to mimic common situation and practice for dryland cropping system in Mediterranean region.

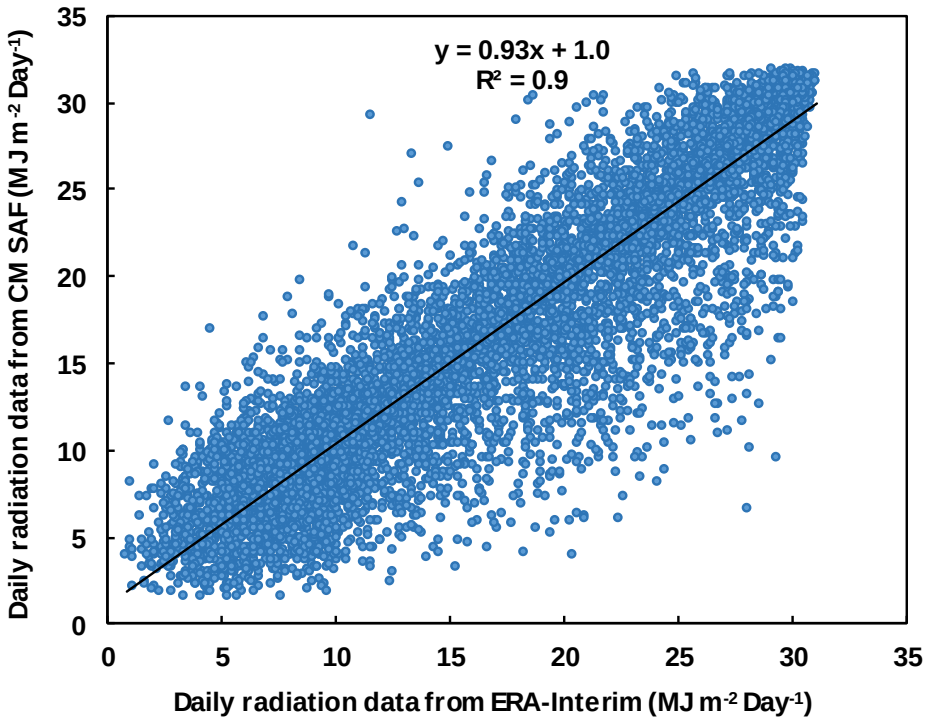

Online Resource 3. Linear regression analysis between daily surface shortwave radiation (MJ m^{-2} day^{-1}) from dataset of ERA–Interim global atmospheric reanalysis (ERA–Interim, X–axis) and from dataset of Satellite Application Facility on Climate Monitoring (CM SAF, Y–axis) in Beja over 1983–2010 period

Online Resource 4. List of employed bias–adjusted Global Climate Model–Regional Climate Model (GCM–RCM) chains from EURO–CORDEX

Short name of GCM–RCM	Driving GCM	Ensemble Group	RCM	Institution (Abbreviation)	Bias Adjustment (BA) method (Abbreviation)	Observational source for BA
CNRM–CLM	CNRM–CERFACS–CNRM–CM5	r1i1p1	CLMcom–CCLM4–8–17	Climate Limited–area Modelling Community (CLMcom)	Distribution–Based Scaling from Swedish Meteorological and Hydrological Institute (SMHI–DBS45) (Yang et al. 2010)	Regional reanalysis of MESoscale ANalysis (MESAN) over 1989–2010 (Dahlgren et al. 2016; Landelius et al. 2016)
ICHEC–CLM	ICHEC–EC–EARTH	r12i1p1				
MPI–CLM	MPI–M–MPI–ESM–LR	r1i1p1				
ICHEC–DMI	ICHEC–EC–EARTH	r3i1p1	DMI–HIRHAM5	Danish Meteorological Institute (DMI)		
ICHEC–KNMI	ICHEC–EC–EARTH	r1i1p1	KNMI–RACMO22E	Royal Netherlands Meteorological Institute (KNMI)		
MPI–MPICSC(r1)	MPI–M–MPI–ESM–LR	r1i1p1	MPI–CSC–REMO2009	Max Planck Institute–Climate Service Centre (MPI–CSC)		
MPI–MPICSC(r2)	MPI–M–MPI–ESM–LR	r2i1p1				
CNRM–SMHI	CNRM–CERFACS–CNRM–CM5	r1i1p1	SMHI–RCA4	Swedish Meteorological and Hydrological Institute (SMHI)		
ICHEC–SMHI	ICHEC–EC–EARTH	r2i1p1				
MPI–SMHI	MPI–M–MPI–ESM–LR	r1i1p1				

Online Resource 5. Cumulative distribution function (CDF) of monthly mean minimum, maximum temperature and precipitation sum between observation and model simulations over 1989–2010 period (during which bias adjustment of model outputs were performed)

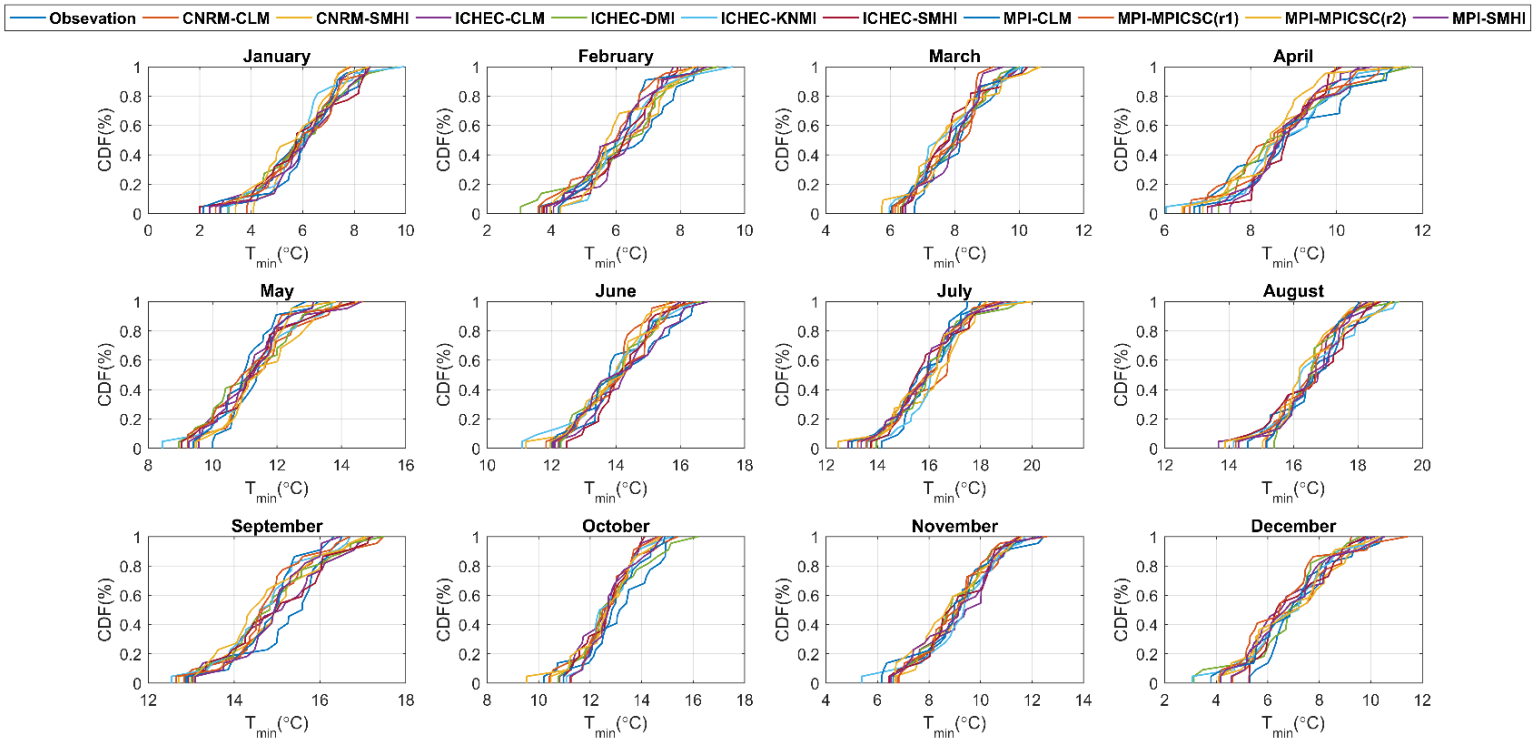

Figure OR5.1. Cumulative distribution function (CDF) of monthly mean minimum temperature (T_{min}) between Beja weather station data (Observation) and outputs of all used GCM–RCM models over 1989–2010 period

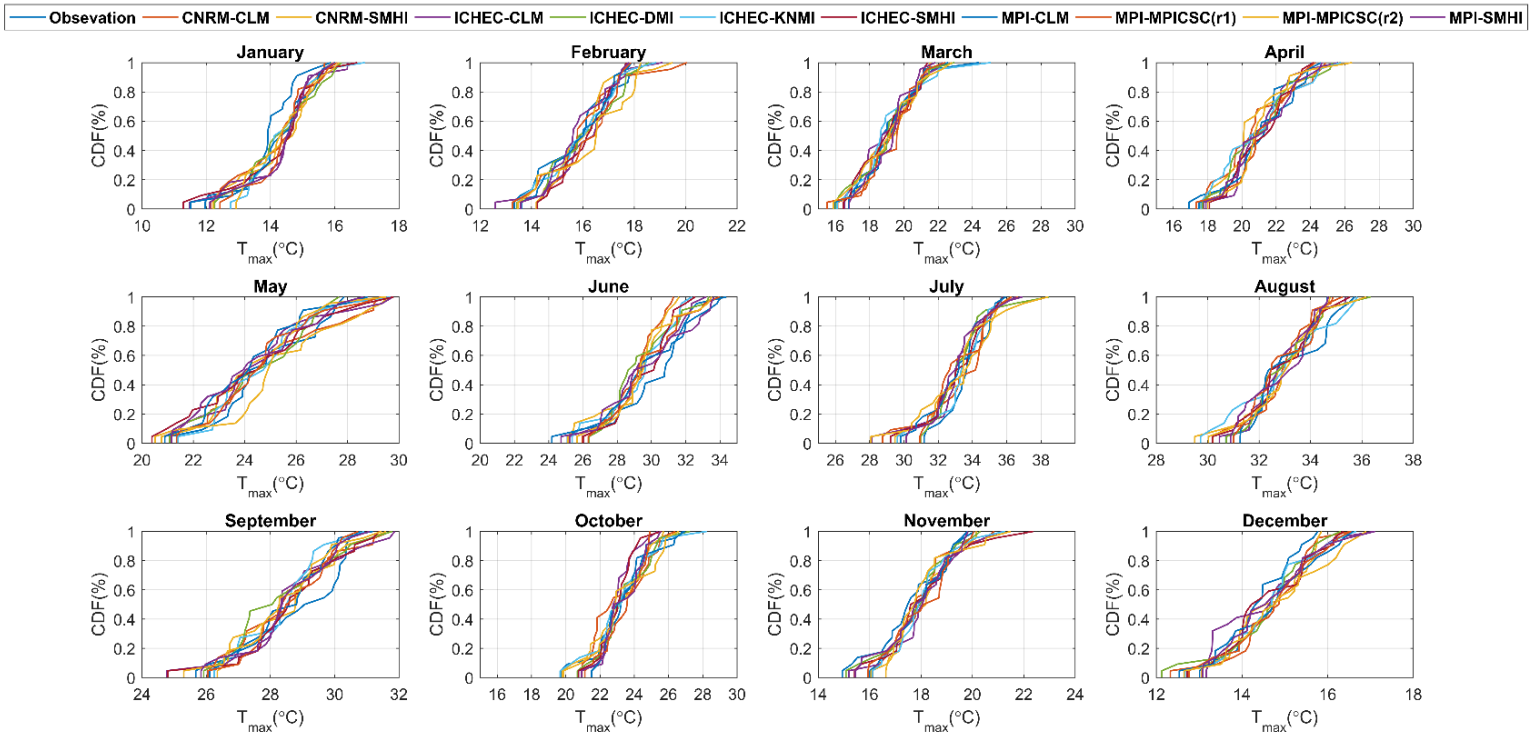

Figure OR5.2. Cumulative distribution function (CDF) of monthly mean maximum temperature (T_{max}) between Beja weather station data (Observation) and outputs of all used GCM–RCM models over 1989–2010 period

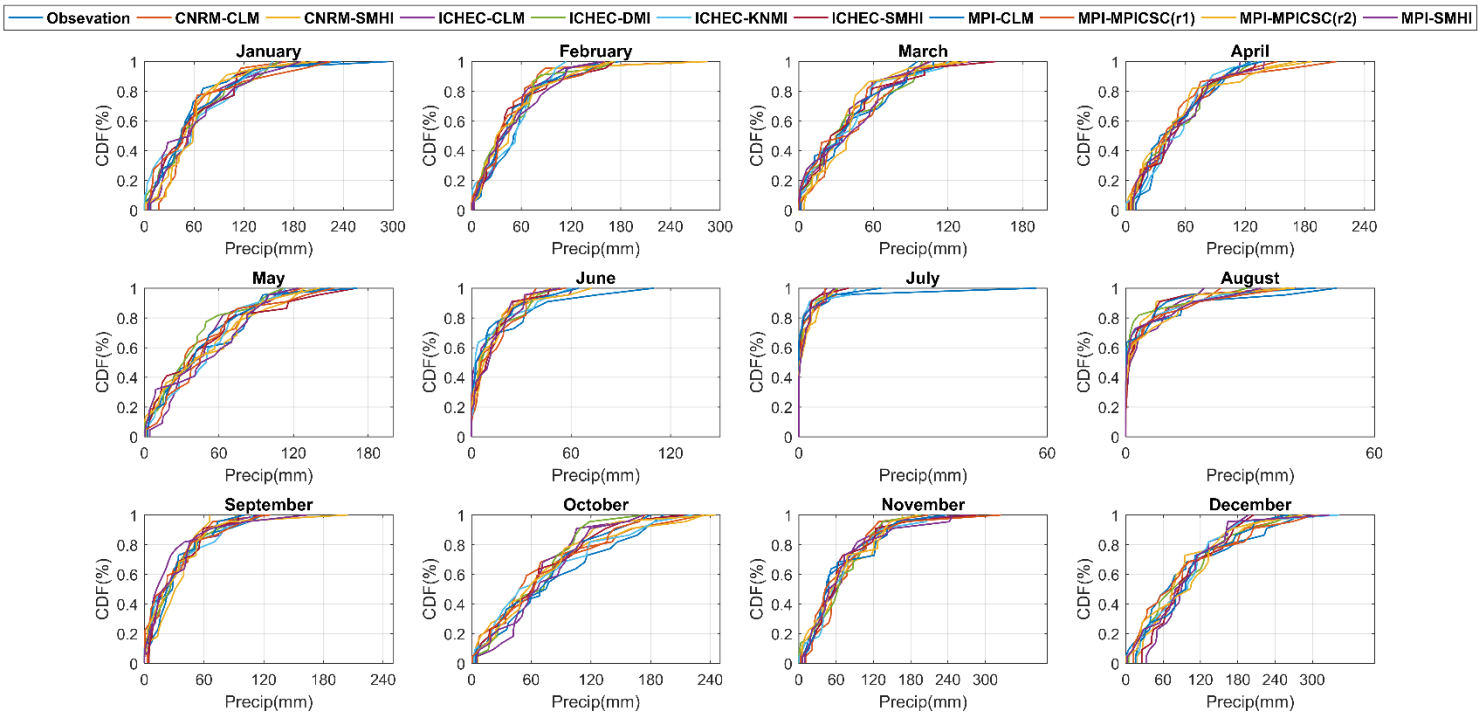

Figure OR5.3. Cumulative distribution function (CDF) of monthly precipitation sum (Precip) between Beja weather station data (Observation) and outputs of all used GCM–RCM models over 1989–2010 period

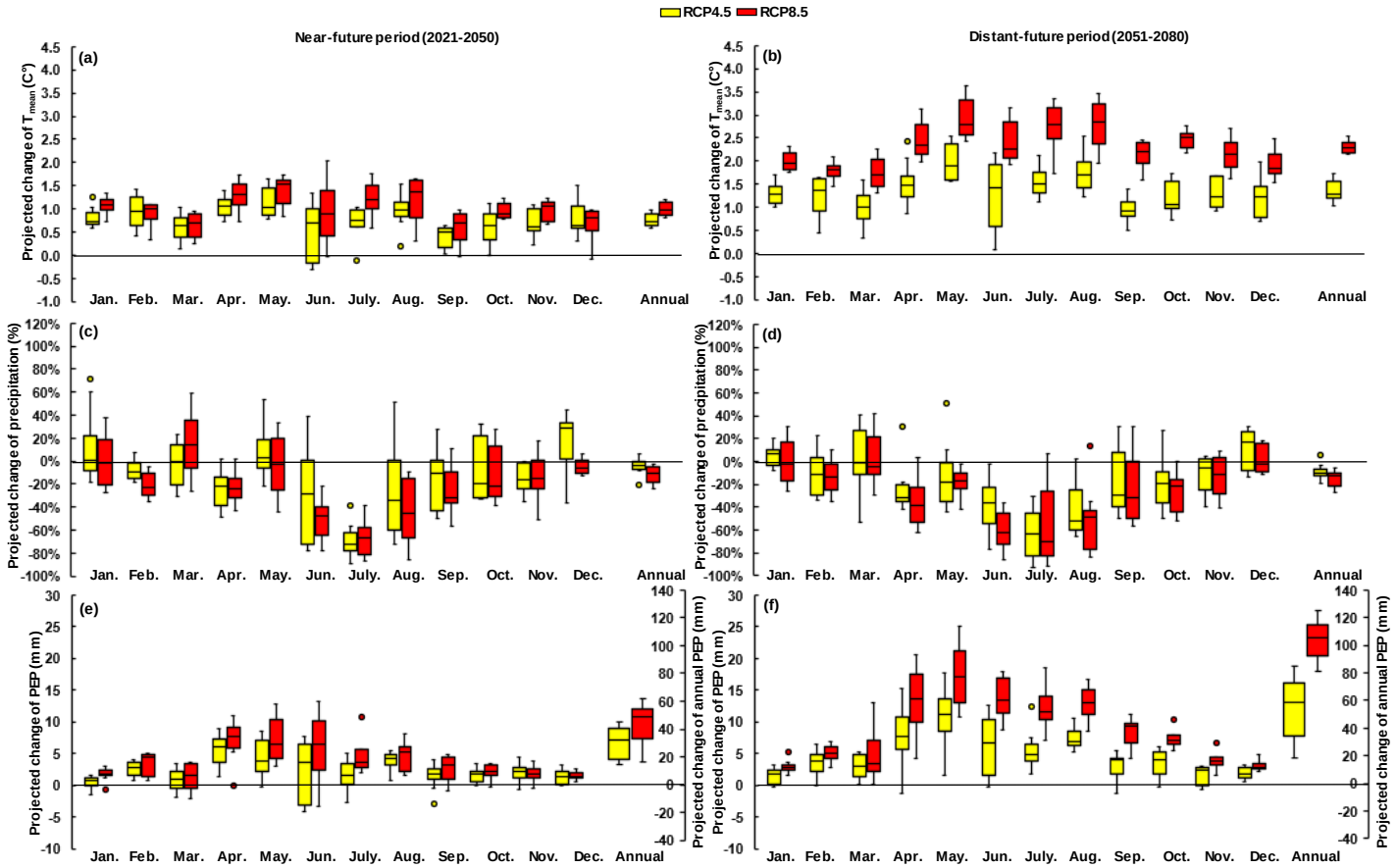

Online Resource 6. Projected range of average changes among all used GCM–RCM models for (***a, b***) mean temperature (T_{mean}, C°), (***c, d***) precipitation sum (%) and (***e, f***) cumulative potential evapotranspiration (PEP, mm) at monthly and annual scales over near-future (2021–2050) and distant-future (2051–2080) periods as compared with weather records over baseline period.

Online Resource 7. Simulated average annual mean temperature and precipitation over baseline along with their corresponding changes by climate projections over Alentejo region (Southern Portugal) as represented by multi-model ensemble means

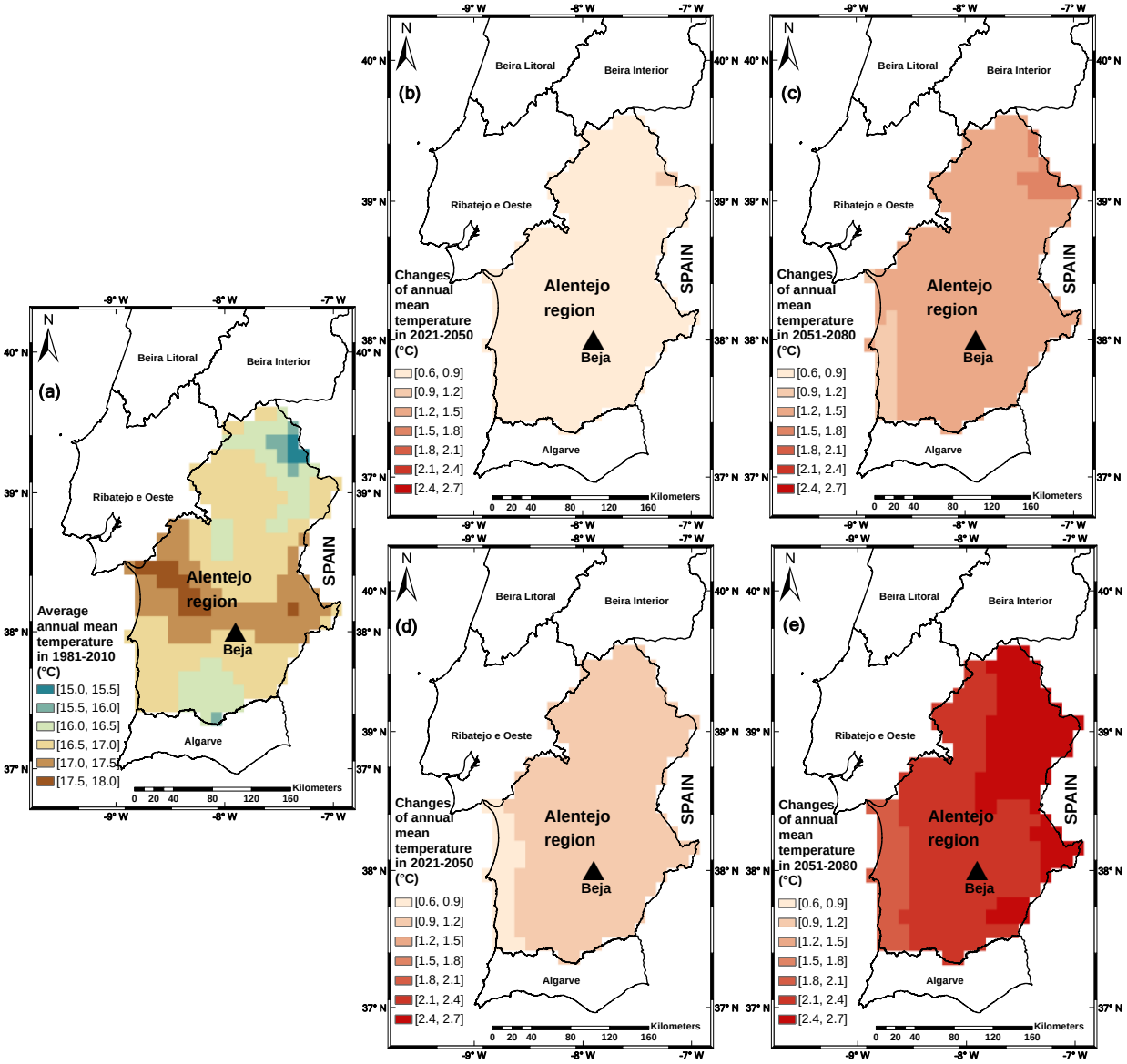

Figure OR7.1. Ensemble mean simulation of average annual mean temperature (°C) for (***a***) baseline period (1981–2010) and for projected corresponding changes (°C) in future periods under (***b,c***) RCP4.5 and (***d,e***) RCP8.5 based on the bias-adjusted outputs of all selected (10) GCM–RCM models

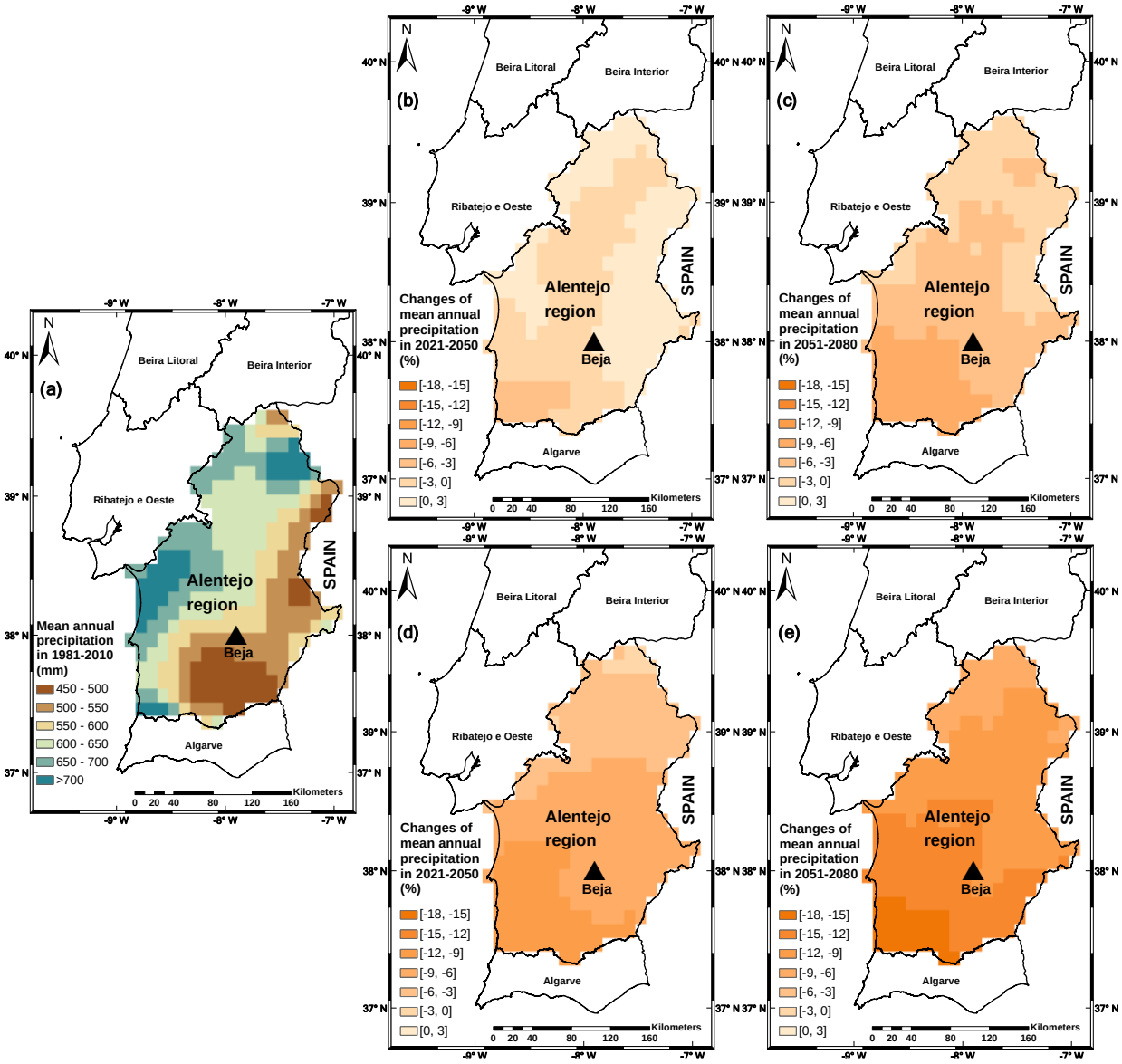

Figure OR7.2. Ensemble mean simulation of average annual precipitation sum (mm) for (***a***) baseline period (1981–2010) and for projected corresponding changes (%) in future periods under (***b,c***) RCP4.5 and (***d,e***) RCP8.5 based on the bias-adjusted outputs of all selected (10) GCM–RCM models

Online Resource 8. Simulated effects of elevated atmospheric CO_2 levels on mitigating mean yield reductions between RCP4.5 and RCP8.5 over near- and distant-future period (mean baseline CO_2 concentration is set to be 362 ppm)

		RCP4.5				RCP8.5			
		Mean yield reductions (%)			Mean increased atmospheric CO_2 concentration relative to baseline (ppm)	Mean yield reductions (%)			Mean increased atmospheric CO_2 concentration relative to baseline (ppm)
	GCMs-RCMs	Without CO_2 effect	With CO_2 effect	Mitigation		Without CO_2 effect	With CO_2 effect	Mitigation	
2021–2050	CNRM-CLM	–17%	–13%	4%	87	–8%	–2%	6%	111
	CNRM-SMHI	–16%	–12%	4%		–5%	1%	6%	
	ICHEC-CLM	–11%	–6%	5%		–24%	–19%	5%	
	ICHEC-DMI	–28%	–25%	3%		–14%	–8%	6%	
	ICHEC-KNMI	–20%	–15%	5%		–22%	–17%	5%	
	ICHEC-SMHI	–16%	–13%	3%		–25%	–22%	3%	
	MPI-CLM	–16%	–12%	4%		–22%	–17%	5%	
	MPI–MPICSC(r1)	–22%	–18%	4%		–23%	–17%	6%	
	MPI–MPICSC(r2)	–11%	–5%	6%		–2%	5%	7%	
	MPI-SMHI	–14%	–9%	5%		–19%	–13%	6%	
	Ensemble mean	–18%	–14%	4%		–19%	–14%	5%	
2051–2080	CNRM-CLM	–37%	–31%	6%	153	–37%	–27%	10%	284
	CNRM-SMHI	–33%	–27%	6%		–36%	–27%	9%	
	ICHEC-CLM	–31%	–25%	6%		–41%	–33%	8%	
	ICHEC-DMI	–26%	–19%	7%		–30%	–22%	8%	
	ICHEC-KNMI	–31%	–24%	7%		–42%	–32%	10%	
	ICHEC-SMHI	–40%	–33%	7%		–46%	–39%	7%	
	MPI-CLM	–13%	–6%	7%		–36%	–26%	10%	
	MPI–MPICSC(r1)	–9%	0%	9%		–33%	–22%	11%	
	MPI–MPICSC(r2)	–2%	6%	8%		–33%	–23%	10%	
	MPI-SMHI	–16%	–9%	7%		–37%	–27%	10%	
	Ensemble mean	–24%	–17%	7%		–37%	–27%	10%	

Online Resource 9. Simulated impacts of adaptation option of early sowings on (increase) the growth duration from germination to beginning of stem elongation or to beginning of grain-filling over future periods

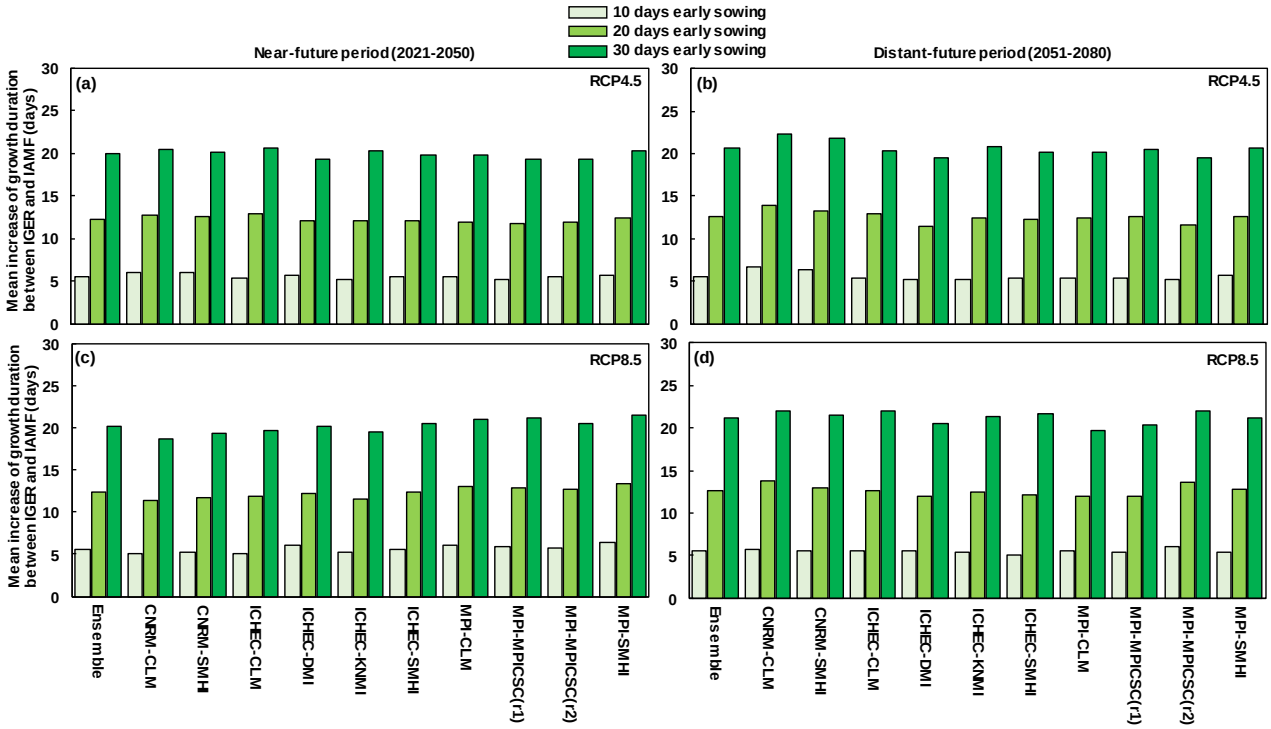

Figure OR9.1. Effects of early sowings (10, 20 and 30 days earlier than the prescribed common sowing date) on extending the growth duration (days) between germination (IGER) and beginning of stem elongation (IAMF) over near–future (2021–2050) and distant–future (2051–2080) periods under (***a, b***) RCP4.5 and (***c, d***) RCP8.5 among all used GCM–RCM models (including ensemble mean) (Developmental process of fulfilling vernalization requirement generally occurs within this development stage)

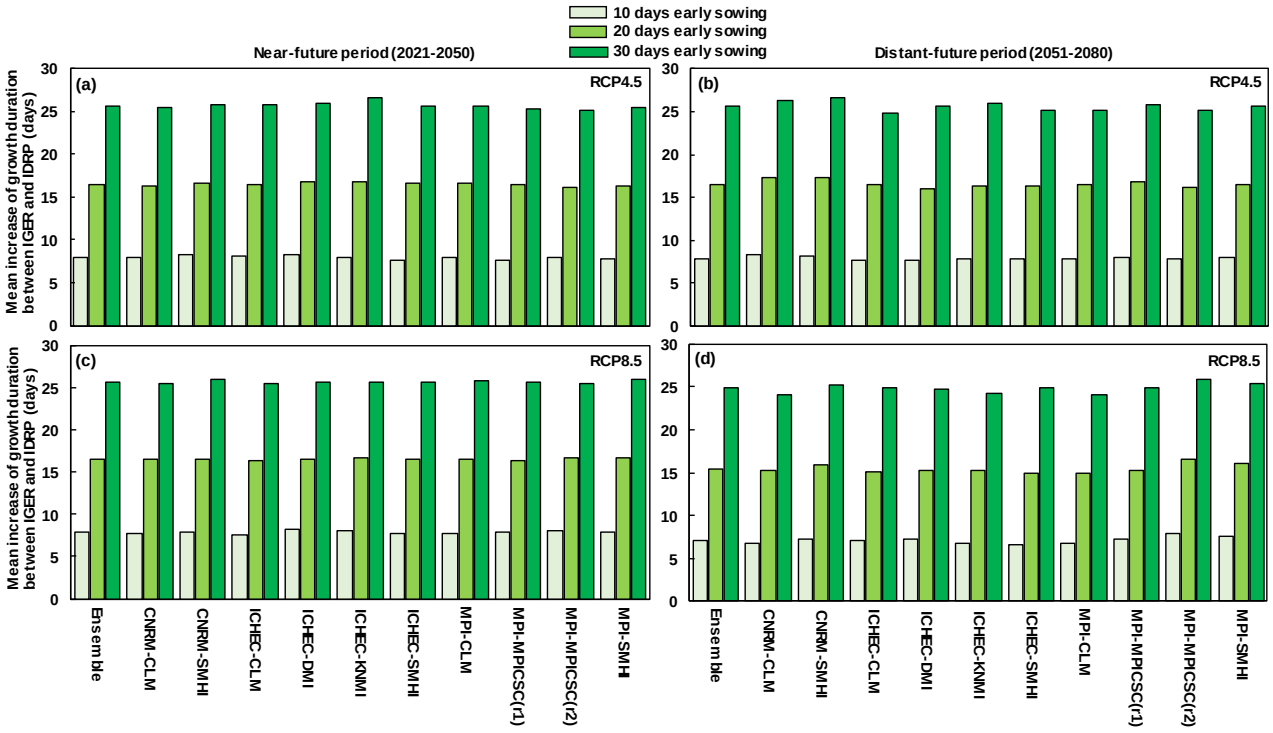

Figure OR9.2. Effects of early sowings (10, 20 and 30 days earlier than the prescribed common sowing date) on extending the growth duration (days) between germination (IGER) and beginning of grain-filling (IDRP) over near–future (2021–2050) and distant–future (2051–2080) periods under (***a, b***) RCP4.5 and (***c, d***) RCP8.5 among all used GCM–RCM models (including ensemble mean)

Supplementary Material II - Chapter 5

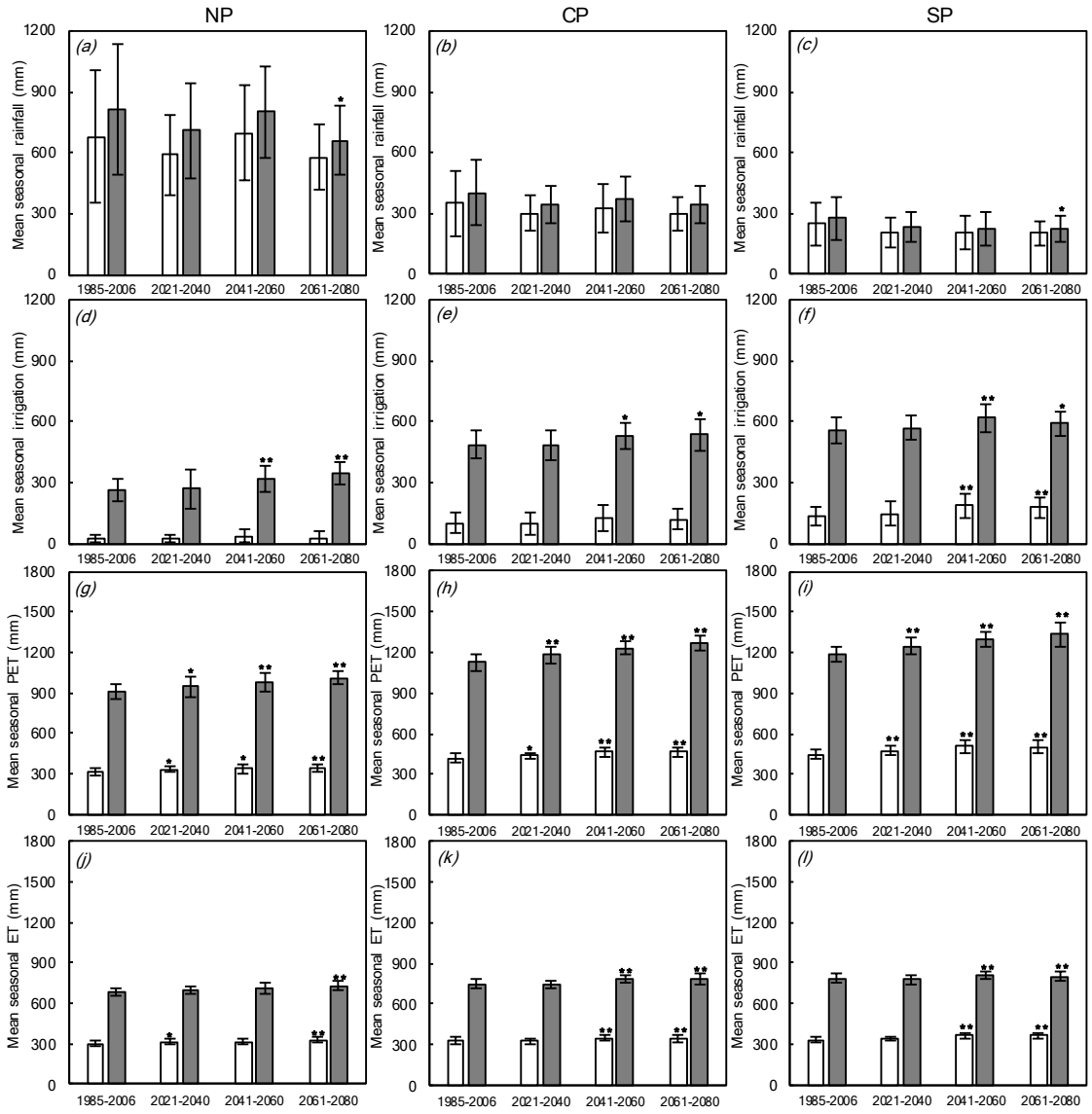

Figure S1. Simulated mean and standard deviation of seasonal quantities (mm) of ***(a–c)*** precipitation, ***(d–f)*** irrigation, ***(g–i)*** potential evapotranspiration (PET) and ***(j–l)*** actual evapotranspiration (ET) over successive periods in study sites. Blank and dark bars were for early spring (ES) and late summer (LS) cut grassland systems, respectively. Independent sample *t*-test was performed in means between baseline and each future period, with significance levels at $p<0.05$ (*) and $p<0.01$ (**) respectively.

Table S1. Summary of soil parameters for three study sites, along with respective dataset source and documented literatures for calculation approach.

Soil parameter description	Locations			Dataset source / Reference literature
	NP	CP	SP	
Soil layer division	30 cm of topsoil and 70 cm of subsoil			HWSD
Soil structure	normal soil compaction and low gravel content			HWSD
Soil salinity level	Extremely low			HWSD
Soil organic matter (% weight)	2.72 topsoil 1.07 subsoil	0.70 topsoil 0.27 subsoil	0.40 topsoil 0.24 subsoil	HWSD
Topsoil pH (H_2O)	5.3	5.1	6.5	HWSD
Topsoil carbonate content (%)	0	0	0	HWSD
Topsoil USDA texture	Loam	Sandy loam	Loamy sand	HWSD
Topsoil fraction (%)	41% sand 36% silt 23% clay	75% sand 15% silt 10% clay	82% sand 8% silt 10% clay	HWSD
Subsoil USDA texture	Loam	Sandy loam	Sandy loam	HWSD
Subsoil fraction (%)	44% sand 32% silt 24% clay	68% sand 17% silt 15% clay	75% sand 8% silt 17% clay	HWSD
Estimation of soil hydraulic parameters	θ_{FC1}= 29% θ_{WP1}= 16% θ_{FC2}= 28% θ_{WP2}= 15% TAW_{soil}= 130 mm	θ_{FC1}= 13% θ_{WP1}= 6% θ_{FC2}= 17% θ_{WP2}= 9% TAW_{soil}= 77 mm	θ_{FC1}= 11% θ_{WP1}= 6% θ_{FC2}= 17% θ_{WP2}= 10% TAW_{soil}= 64 mm	Soil texture and structure, organic matter content, salinity / (Saxton and Rawls 2006)
Estimation of cumulative maximum soil evaporation without energy limit (mm)	q0= 9.84	q0= 8.75	q0= 9.6	Topsoil fraction / (Brisson *et al.* 2009)
Estimation of slope degree (%)	0 – 4.5%	0 – 6.1%	0 – 2.1%	GTOPO30
Estimation of surface runoff coefficient	ruisolnu= 0.03	ruisolnu= 0.03	ruisolnu= 0	Slope degree / (Brisson *et al.* 2009)

Table S2. Mean atmospheric CO_2 concentration for study periods of historical global record and climate change scenario (RCP8.5).

Study Periods	Mean CO_2 concentration (ppm)	Data source
Baseline (1985–2006)	362.6	NOAA
Short term (2021–2040)	451.9	RCP8.5
Medium term (2041–2060)	545.4	
Long term (2061–2080)	682.3	

Table S3. Summary of defined grassland system parameters with supported references.

Grassland system parameters	Parameter values				Relevant references
Initial status	Plant initialization (LAI = 1 m^2m^{-2}, dry matter = 1.5 t ha^{-1}, root depth= 60 cm)				(Ruget *et al.* 2009; Courault *et al.* 2010)
Grass features	*Grass-prairiep* with standard value: *GDD* from emergence to end of juvenile stage = 116 ºC, *GDD* from emergence to end of leaf initialization = 1500 ºC, *GDD* from emergence to grain filling = 1000 ºC				(Ruget *et al.* 2006)
Farming practices	Locations	NP	50 kg/ha mineral N per cut and 216 kg/ha slurry (with 65 kg/ha ammonium nitrogen) applied in winter	Early cut dates (DOY_1=73, DOY_2=143) Late cut dates (DOY_1=143, DOY_2=250)	(Trindade *et al.* 1997; Lopes and Reis 1998)
		CP	25 kg/ha mineral N per cut	Early cut dates (DOY_1=91, DOY_2=152) Late cut dates (DOY_1=155, DOY_2=260)	(Carneiro *et al.* 2005)
		SP	25 kg/ha mineral N per cut	Early cut dates (DOY_1=80, DOY_2=144) Late cut dates (DOY_1=144, DOY_2=250)	(Lourenco and Palma 2001; Aires *et al.* 2008a)
Residue matter	Estimated residue matters after cutting (LAI = 0.2 m^2m^{-2}, dry matter = 1 t ha^{-1})				(Aires *et al.* 2008b; Ruget *et al.* 2009)

Table S4. Summary of variations in mean annual temperature (T_{mean}) and mean annual precipitation sum (P_{rec}) of future periods in relative to baseline. Student's *t*-test was performed for changes in the mean values of each future period compared to baseline (* and ** indicated significance level at $p<0.05$ and $p<0.01$, respectively).

Future periods in RCP8.5	Location of NP		Location of CP		Location of SP	
	T_{mean} (ºC)	P_{rec} (%)	T_{mean} (ºC)	P_{rec} (%)	T_{mean} (ºC)	P_{rec} (%)
2021–2040 (short-term)	+0.7**	–12	+0.9**	–15*	+0.9**	–16*
2041–2060 (medium-term)	+1.4**	–4	+1.8**	–8	+1.7**	–15*
2061–2080 (long-term)	+2.3**	–9	+2.8**	–17*	+2.7**	–20*

Table S5. Summary of number of days in summer with frequency above 50% for the occurrence of defined extreme heat stress in each study period (figures in brackets indicate the increased days).

Periods	Extreme heat stress in summer (days)		
	NP	CP	SP
Baseline	0	0	20
short-term	3 (+3)	19 (+19)	68 (+48)
medium-term	14 (+11)	46 (+27)	71 (+3)
long-term	35 (+21)	71 (+25)	83 (+12)

Table S6. Summary of number of days in summer with frequency between 10% and 30% for the occurrence of defined severe water stress in each study period (figures in brackets indicate the variations of days).

Periods	Severe water stress in summer (days)		
	NP	CP	SP
Baseline	22	34	42
short-term	36 (+14)	64 (+30)	51 (+9)
medium-term	44 (+8)	69 (+5)	57 (+6)
long-term	47 (+3)	73 (+4)	48 (–9)

The End of PhD Thesis